Iterative Learning Control design for uncertain and time-windowed systems

Iterative Learning Control design for uncertain and time-windowed systems

PROEFSCHRIFT

ter verkrijging van de graad van doctor
aan de Technische Universiteit Eindhoven,
op gezag van de Rector Magnificus, prof.dr.ir. C.J. van Duijn,
voor een commissie aangewezen door het College voor Promoties
in het openbaar te verdedigen
op woensdag 12 november 2008 om 16.00 uur

door

Jeroen Johan Maarten van de Wijdeven

geboren te Veghel

Dit proefschrift is goedgekeurd door de promotoren:

prof.ir. O.H. Bosgra
en
prof.dr.ir. M. Steinbuch

disc

Contents

Nomenclature

Latin symbols

$\begin{bmatrix} A & B_i \\ C_i & D_{ij} \end{bmatrix}$ $\qquad$ $(i,j) \in [1,2]$, state space matrices of a time domain system

$\begin{bmatrix} A & B \\ C & D \end{bmatrix}$ $\qquad$ state space matrices of time domain system J

$\begin{bmatrix} A_h & B_h \\ C_h \end{bmatrix}$ $\qquad$ elements of the time domain R-ILC controller

$A_{Ti}, \; i \in [1,2]$ $\qquad$ system matrix of (partially) decoupled R-ILC controller

C $\qquad$ time domain feedback controller

d $\qquad$ scaling factor

$d_k(t)$ $\qquad$ trial varying disturbance signal

d_γ $\qquad$ tuning parameter for R-ILC control

D $\qquad$ scaling matrix

D_M $\qquad$ block diagonal scaling matrix

D_P $\qquad$ scaling matrix

$\mathcal{D}_M$ $\qquad$ the set of scaling matrices D_M

e $\qquad$ error signal

f $\qquad$ command signal

f_{init} $\qquad$ initial value for command signal f

$F_{Ti}, \; i \in [1,2]$ $\qquad$ system matrix of (partially) decoupled R-ILC controller

g $\qquad$ learning gain

$g(t)$ $\qquad$ state of the (partially) decoupled R-ILC controller

G $\qquad$ generalized plant

$\begin{bmatrix} H_{ij} & F_i \\ G_i & H_y \end{bmatrix}$ $\qquad$ $(i,j) \in [1,2]$, state space matrices of R-ILC controller

H $\qquad$ general system

H_c $\qquad$ element of general system H with full row rank

H_o $\qquad$ element of general system H with full column rank

H_Δ $\qquad$ uncertain general system H

I_j $\qquad$ $j \times j$ dimensional identity matrix

$j(t)$ $\qquad$ impulse response of system J

J	system
J_c	element of system J with full row rank
J_H	Hankel system
J_o	element of system J with full column rank
J_Δ	uncertain system J
$\mathcal{J}$	objective function
k	trial index
ℓ	trial periodicity
L	ILC control element
L_c	ILC control element
L_c^{im}	ILC control element L_c, including basis function matrix T_f
L_o	ILC control element
m	number of samples in 1) actuation time interval 2) basis functions in T_f
m_1	first sample of actuation time interval
m_2	final sample of actuation time interval
M	closed loop system
M_c	element of ILC control element L_c
n	number of samples in 1) observation time interval 2) basis functions in T_y
n_1	first sample of observation time interval
n_2	final sample of observation time interval
N	number of samples in a trial
p	rank of system matrix J
p_k	output signal of norm-bounded uncertainty Δ
P	plant
P_o	element of ILC control element L_o
$\mathcal{P}_\xi$	performance measure for variable ξ_k
$\mathcal{P}_{\xi,opt}$	optimal performance measure for variable ξ_k
q	number of inputs and outputs of uncertainty Δ
q_i	number of system inputs
q_k	input signal of norm-bounded uncertainty Δ
q_o	number of system outputs
Q	weighting matrix
Q_h	matrix element of the time domain R-ILC controller
$\mathcal{Q}$	ILC control element
r	weighting scalar
R	weighting matrix
R_h	matrix element of the time domain R-ILC controller
R_{jj}	covariance matrix of signal j
s	weighting scalar
S	weighting matrix
S_c	element of ILC control element L_c
S_h	matrix element of the time domain R-ILC controller
S_o	element of ILC control element L_o

t	time index
T	similarity transformation matrix
T_c	element of ILC control element L_c
T_f	matrix with input basis functions
T_s	sample time
T_y	matrix with output basis functions
U	left singular matrix
$u(t)$	controller output at time index t
u_k	trial domain state vector
V	right singular matrix
V_i	system description of additive uncertainty in system H_Δ
V_o	system description of additive uncertainty in system H_Δ
$w(t)$	exogenous input signal at time index t
W	system description of additive uncertainty in system J_Δ
W_i	system description of additive uncertainty in system J_Δ
W_o	system description of additive uncertainty in system J_Δ
W_β	weighting matrix
$x_k(t)$	time domain state vector
X	variable in Sylvester equation
y_d	reference signal
y	system output signal
y_{ref}	reference signal
Y	Riccati variable
$z(t)$	performance objective at time index t
z_k	trial domain state vector

Greek symbols

α_d	reference vector filtered by output basis function matrix T_y
α_k	output signal filtered by output basis function matrix T_y
β_{init}	initial value for input signal of input basis function matrix T_f
β_k	input signal of input basis function matrix T_f
γ	tuning parameter for R-ILC control
γ_{min}	approximate for γ_{opt}
γ_{opt}	optimal value for the tuning parameter γ
Δ	norm-bounded uncertainty
$\boldsymbol{\Delta}$	the set of norm-bounded uncertainty Δ
Δ_f	maximum rate change of time domain command signal
Δ_G	norm-bounded uncertainty of generalized plant G
Δ_M	structured norm-bounded uncertainty of system M
$\boldsymbol{\Delta}_M$	the set of structured norm-bounded uncertainty Δ_M
Δ_P	unstructured norm-bounded uncertainty
$\boldsymbol{\Delta}_P$	the set of unstructured norm-bounded uncertainty Δ_P

ϵ_k	error signal filtered by output basis function matrix T_y
ε	infinitely small positive scalar
$\zeta(t)$	costate of fully decoupled R-ILC controller
θ	frequency [rad/s]
$\lambda(t)$	costate of the R-ILC controller
ξ_k	performance variable
Π	the set of uncertain systems J_Δ over a finite time interval
Π_z	the set of z-domain uncertain systems $J_\Delta(z)$
Σ	singular value matrix
Ψ	the set of uncertain systems H_Δ over a finite time interval

Subscripts, superscripts, and indices

$a(t)$	signal a at time index t
$a(z)$	z-domain representation of signal a
a_k	vector a at trial k
a_k^{as}	asymptotic value of a after convergence (trial varying)
a_0	initial condition of state a at trial $k = 0$
a_∞	asymptotic value of a after convergence (trial invariant)
a^i	i^{th} input of output signal of multi input multi output system
$A(s)$	Laplace domain representation of system A
$A(z)$	z-domain representation of system A
A_{ij}	element (i, j) of matrix A

Special symbols and operations

a^T	transpose of vector a
$\dot{a}$	time derivative of signal a
$|a|$	amplitude of scalar a
$\|a\|_2$	2-norm of vector a
$E\{a\}$	expected value of signal a
A^T	transpose of matrix A
A^{-1}	inverse of matrix A
$A^\dagger$	Moore-Penrose inverse of matrix A
$A^{(1)}$	{1}-inverse of matrix A
$\|A\|_{i2}$	induced 2-norm of (system) matrix A
$\text{im}(A)$	image space of matrix A
$\text{im}(A)^\perp$	space perpendicular to the image space of matrix A
$\text{ker}(A)$	kernel space of matrix A

$\text{rank}(A)$	rank of matrix A
$\lambda(A)$	eigenvalue of matrix A
$\rho(A)$	spectral radius of matrix A
$\overline{\sigma}(A)$	largest singular value of matrix A
$\mu_B(A)$	structured singular value of matrix A with respect to B
$\frac{\partial a}{\partial b}$	partial derivative of a with respect to b
w	one trial shift operator
$\mathbb{R}$	the set of real numbers
$\mathbb{R}^n$	the set of all $n \times 1$ vectors with elements in $\mathbb{R}$
$\mathbb{R}^{n \times m}$	the set of all $n \times m$ matrices with elements in $\mathbb{R}$
$\mathbb{C}$	the set of complex numbers
$\mathbb{C}^{n \times m}$	the set of all $n \times m$ matrices with elements in $\mathbb{C}$
L^∞	the set of ∞-norm bounded signals
$\emptyset$	empty set
$\in$	is an element of
$\forall$	for all
$\mapsto$	maps to
$\approx$	is approximately equal to
$:=$	is defined as
$\neq$	is not equal to
$\sum_i^j$	summation from element i to j
Π_i^j	multiplication from element i to j

Acronyms and Abbreviations

det	determinant
diag	diagonal
inf	infimum
lim	limit
max	maximum
min	minimum
2D	2-dimensional
CITE	current iteration tracking error
DARE	discrete algebraic Riccati equation
DOF	degrees of freedom
HO	higher order
i/o	input/output
IMP	internal model principle
iff	if and only if
ILC	Iterative Learning Control
LP	linear programming
LQ	linear quadratic

LTI	linear time invariant
LTV	linear time varying
MC	monotonic convergence
MIMO	multi-input multi-output
P/PI/PD	proportional/proportional plus intergral/proportional plus derivative
R-ILC	robust Iterative Learning Control
RC	robust convergence
RMC	robust monotonic convergence
SISO	Single-input single-output
SVD	singular value decomposition

Chapter 1

Introduction

In this chapter, we define our research objectives. For that, the idea behind Iterative Learning Control (ILC) is introduced and its relation to other control techniques briefly discussed. Moreover, the use of time-windows in ILC is highlighted, and the consequences of model uncertainty on ILC control design addressed.

1.1   Background

In numerous applications, a system has to perform a repeated batch task, e.g., a pick and place machine or batch chemical process which has to follow a given reference trajectory. Characteristic features of a batch task are that 1) each repetition (trial) spans a finite time interval which is known on beforehand, and 2) each trial starts from the same initial conditions due to resetting of the system before each trial. Since the reference signal is, in general, the dominant disturbance in the system, this batch repetitiveness yields a servo error that is (approximately) equal for each trial. If this servo error does not meet the performance specifications, Iterative Learning Control (ILC) can be introduced into the system to increase performance.

ILC iteratively improves the performance of repeated batch processes, by updating the feedforward signal (command signal) from one trial to the next using measured data from previous trials, i.e., by learning from previous experience. The concept behind ILC is illustrated in Figure 1.1 and Figure 1.2. In Figure 1.1, a reference signal and measured output are shown. In this example, ILC significantly reduces the error between the reference signal and measured output within three trials.
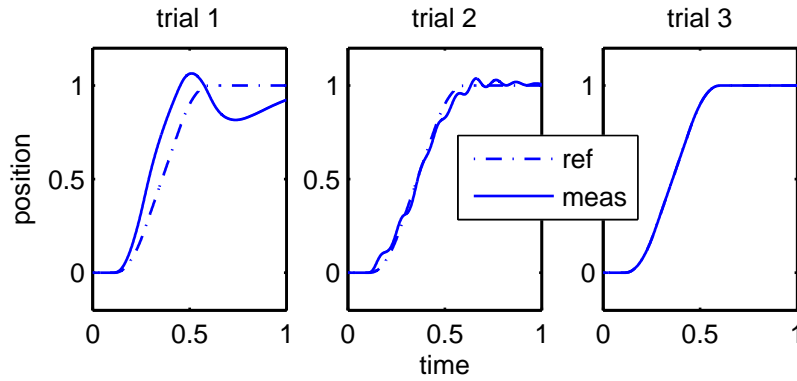
Figure 1.1: Reference signal and measured output of the system for trials 1 to 3. Note that in trial 3, the measured output and reference signal coincide.
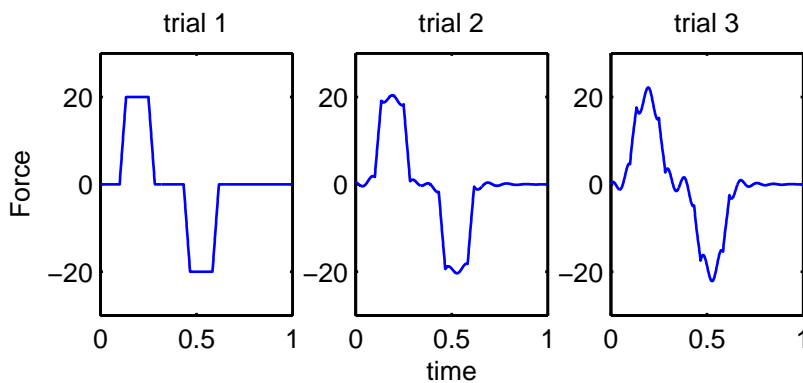
Figure 1.2: Command signal generated by ILC for trials 1 to 3.

This is accomplished by iteratively updating the command signal, until the desired command signal is obtained, see Figure 1.2.

The idea of using an iterative strategy to deal with repetitive disturbances is first described in a US patent from 1971, [53]. What seems to be the first academic publication on ILC stems from 1978, [126]. But since it was in Japanese, the results did not become widely spread. In 1984, [10, 25, 31] independently published results on iterative improvement of performance. The term "*Iterative Learning Control* " was introduced in Arimoto *et al.* in the same year, [11]. A first monograph on ILC stems from Moore 1993, [87]. Since then, treatment of different topics in ILC can be found in, e.g., [17, 22, 56]. Extensive surveys of different (industrial) applications of ILC is presented in [2, 88].

When properly designed, the ILC controller iteratively finds that command signal that results in high performance, despite possible model uncertainty and unknown

trial invariant disturbances. With the update of the command signal based on previously measured data, the trial-to-trial behavior of ILC can be considered a feedback process. On the other hand, during the time interval of a trial, this command signal is applied to the system as a fixed feedforward signal. Consequently, it depends on the domain, trial domain or time domain, whether ILC can be considered as feedback or feedforward control.

Based on the feedforward characteristics of ILC in time domain, its iterative search for the optimal command signal in trial domain, and the fact that ILC is designed to compensate for (trial) repetitive disturbances, we briefly discuss similarities and differences between ILC for linear systems and ILC related control strategies.

Model-based feedforward control
The basic idea of feedforward control is to find a feedforward signal f such that the system's output y follows the reference signal y_{ref}, i.e., $y = Pf$ with f such that $y_{ref} - y = 0$. Under the assumption that a model P of the system dynamics is known and P^{-1} is stable, inverse model feedforward control can be applied to obtain the optimal feedforward signal: $f = P^{-1}y_{ref}$, see e.g., [18]. Note that causality of the inverse is of no importance, since the input of the feedforward controller (the reference signal) is assumed known for all time, both past and future.

A benefit of model-based feedforward over ILC is that a feedforward signal can be obtained for arbitrary reference signals without the need for iterative learning. A drawback of these controllers is, however, that the amount of performance improvement strongly depends on the accuracy of the model, see e.g., [36].

Adaptive feedforward control
If the system structure is known but its parameters are uncertain, then the feedforward signal can be obtained using an adaptive feedforward controller, i.e., a feedforward controller which recursively estimates system (related) parameters, see e.g., [9, 74]. To obtain the optimal command signal such that $y_{ref} - y = 0$, we require the inverse of the true system structure to be contained in the model structure of the controller. However, even if the inverse system structure is not contained in the controller, this approach will result in optimized performance in the space in which parameter estimation can occur. Estimation of the parameters can subsequently be performed on-line in time domain, leading to the condition of persistency of excitation of the reference signal, or off-line in trial domain, between two trials. In this thesis, we consider trial domain adaptive feedforward control in a restricted input/output (i/o) space to be a specific case of ILC, see Chapter 4.

Repetitive control

ILC is comparable to repetitive control, [35, 63, 118, 124], in the sense that they both strive after performance improvement by reducing the effects of periodic disturbances on the error. An essential difference between repetitive control and ILC, however, is that an ILC controlled system is reset between two trials, while a system controlled with a repetitive controller is not. A first consequence is, that ILC can handle batch repetitive disturbances in time domain, e.g., a reference disturbance which is equal from trial to trial, and repetitive control can handle disturbances which are repetitive (periodic) in time domain, e.g., a continuously rotating disc with a disturbance that occurs each revolution. A second consequence is, that repetitive control can be considered a feedback control strategy in time domain, instead of a feedforward control strategy in time domain.

1.2   Research objectives

In this section, we formulate the research objectives which form the basis for this thesis. These objectives can be divided into two subjects: The first subject addresses the use of time windows in ILC. The second subject raises the issue of robustness of ILC against model uncertainty.

1.2.1   Motivation

Our interest for ILC for time-windowed systems is founded in industrial applications. One application in which time-windowed ILC is used (implicitly), is the semiconductor industry. In [85], for example, the ILC control problem is modified such that performance is only improved during the time intervals in a trial where the repetitive disturbances dominate the non-repetitive disturbances. In [13], a batch iterative approach is used to improve the performance during the scanning time interval of a trial. Another application is given by the Ultra High Pressure (UHP) lamp for projection systems, [122]. Due to computation and memory demands, in [122] the lamp is actuated over a time interval which is shorter than the time interval in which the lamp's output is measured. Although the implementations have been shown to be successful, the implications of time-windowed systems on ILC control design are not yet known.

In ILC literature, many successful implementations of ILC have been presented. These results are, however, most often based on the implementation of ILC on a single sample system (of a mass produced system). Furthermore, the experiments are often conducted over a limited time span, e.g., days, weeks. What will happen, if a designed ILC controller is applied to a different sample system, or to a system whose dynamics have changed due to wear? To our opinion, ILC literature does not provide fully satisfying answers to these for industry essential questions.

1.2.2   ILC for time-windowed systems

Before any proper ILC design can take place, it has to be apparent which task ILC is expected to carry out, i.e., the ILC problem formulation has to be clear. As we discuss below, in many situations a correct formulation of the problem requires the use of time windows. These windows can be used to select specific time samples at the input and output of the system, as illustrated in Figure 1.3.
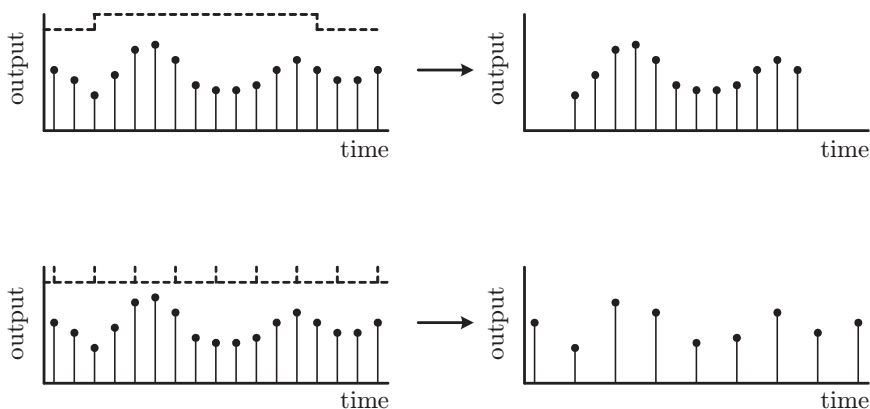
Figure 1.3: Top: A time window is used to select a specific time interval of the time signal. Bottom: Downsampling of the time signal.

One of the most well known problem formulations in ILC deals with the servo task. In this task, ILC control has to iteratively generate a command signal which actuates the system during the complete time span of a trial, such that the observed output of the system follows a certain predefined reference trajectory during the complete time span of a trial.

In another ILC task, one is only interested in the output of the system at the end of the trial, see e.g., [29, 54, 137]. Actuation in this so-called terminal ILC takes place during the complete time span of the trial, while observation of the error occurs only at the final time sample of the trial. An example of terminal ILC is rapid thermal processing, [137]. The goal is to control the chemical vapor deposition thickness on a wafer at the end of the process by controlling the wafer temperature. Any thickness errors during the process are of no interest.

A third ILC task is found in residual vibration suppression in point-to-point motion problems, see [40, 78, 79, 133]. This problem formulation covers the case in which residual vibrations are to be suppressed, after the system has been moved from an initial position to a desired position. This requires actuation of the system *during* the motion from initial to final position, and observation of residual vibrations *after* arrival at the desired point.

The previous three ILC problem formulations resulted in the definition of specific time intervals in which actuation and observation of the system is allowed. Other uses for time windows are, however, also possible, e.g., to study the time domain and trial domain behavior of the servo error signal. In [7, 66, 76], performance and convergence properties of systems with nonzero relative degrees and delays are studied. To properly analyze the convergence properties of the system under study, [7, 66, 76] implicitly make use of time windows. Namely, the actuation interval of the system is reduced by removal of the final samples of the trial interval, and the observation time interval is reduced by removal of the first samples of the trial interval. In [68, 142], the error convergence from trial to trial has to satisfy specific monotonicity conditions. By downsampling of the original system, these conditions are met. Downsampling for reduction of inter-sample behavior in ILC is discussed in [77]. In [72], reduction of inter-sample behavior is achieved by removing the first number of actuation samples in a trial. Finally, in [98, 99], inter-sample behavior in ILC is studied using a multirate system representation which is constructed with time windows.

From the previous discussion, we conclude that time windows in ILC are widely, though often implicitly, used to properly formulate ILC problems. This observation leads to the first research objective:

Objective 1. Explore the design issues, i.e., problem formulation, convergence analysis, and ILC control design, in ILC for time-windowed systems.

Time-windowed systems can be considered a specific subset of systems with i/o basis functions. This observation leads to the second research objective:

Objective 2. Formulate a unifying ILC design framework which encompasses the different ILC problem formulations for linear systems with basis functions, and determine the for ILC relevant properties of this framework.

In Section 2.1, we elaborate on different ILC control suggestions and formulations in ILC literature, and discuss which ones we will consider in this thesis. In objective 2, we aim at formulating a unifying framework which is valid for these considered systems and ILC control suggestions.

1.2.3 ILC for uncertain systems

Although the command signal generated by the ILC control strategies is based on measured data, most often the ILC controller is designed using a model of the system. The majority of the ILC control strategies discussed in ILC literature can be divided into three categories, [96].

Arimoto gains
Arimoto gains (or P/PD/PI-type), [26, 48, 76, 140], are ILC controllers in which the command signal is updated with a scaled, positive time shifted error signal. These controllers have as great benefit that they can iteratively find optimal command signal using very little information about the system. This, however, goes at the expense of the ease with which specific convergence properties can be achieved.

Inverse model based ILC
In inverse model based ILC, [12, 83, 106, 119, 132, 139], the ILC controller is based on the inverse of a model of the system. With an accurate model, convergence of the ILC algorithm occurs in just a few iterations. On the other hand, with a poor model, the ILC algorithm can result in unstable behavior.

Linear quadratic (LQ) norm optimal ILC
Finally, LQ norm optimal ILC, [7, 38, 58, 107], focusses on ILC control design which results from a quadratic optimization problem. Depending on the formulated objective, different parameters in the ILC controller can be used to influence different properties of the ILC algorithm. In its most simple form, LQ norm optimal ILC equals inverse model based ILC. Although this control strategy does require a model of the system, and tuning of the controller can be more extensive than the other two control strategies, it can be designed to be less sensitive against model uncertainty than inverse model based ILC.

Since no model can truly reflect the real system behavior, the controller is required to have some robustness against model uncertainty. Depending on the amount of uncertainty present and on the properties of the controller itself, the ILC controlled system can become unstable in trial direction, rendering ILC useless.

Robustness analysis of ILC controllers
It is known that, to a certain extent, each ILC controller incorporates robustness against model uncertainty. In [64], it is shown that there exists inverse model based ILC controllers for which the ILC controlled system is robustly monotonically convergent, provided that the multiplicative uncertainty description is positive real. In [6, 52, 55, 56, 70], the robustness properties of LQ norm optimal ILC controllers are discussed. Although in [6, 52], the finite time interval aspect

of ILC is explicitly included in the robust convergence analysis, the approach does not leave room to include uncertainty models. As a result, the robustness properties of the solution can not be quantified. In contrast, in [55], uncertainty models can be included in the analysis. With the analysis based on a frequency domain representation of the ILC controller, however, the results are only approximate when applied to a finite time interval. Namely, the Fourier transform on the infinite time interval which is used in this approach, leads to a linear time invariant (LTI) control law. The application of this LTI controller on a finite time interval of a trial may result in errors in the initial part of the transient behavior. In [56], the finite time interval presentation of the system and controllers is approximated in a Fourier basis, leading to a not fully clear definition of the uncertainty model and a number of approximate robustness results. Robustness of LQ norm optimal ILC over a finite time interval for multiplicative model uncertainty represented by a gain is studied in [70]. Finally, in [4], a robust convergence analysis approach is presented which is applicable to any linear trial invariant ILC controller. However, the specific problem formulation used in [4] may restrict the utility of the results.

Robustness by design of robust ILC controllers
Next to analysis of given ILC controllers with respect to robustness, robustness can be enforced by design of robust ILC controllers. Robust ILC controllers incorporate an uncertainty model in the design of a controller, so as to improve robustness and performance of the ILC controlled system. Most of these control strategies pose the ILC control design problem as an $\mathcal{H}_\infty$ optimization problem. In [51, 114], the robust control problem is represented by a 2D system representation. Subsequently, a combined state feedback controller in time domain and Arimoto gain ILC controller in trial domain is designed. Hence, full knowledge of the time domain system states is required. In [8, 34, 41, 120, 135], the design problem is posed in frequency domain, and therefore only approximates the true finite time interval problem. Moreover, the resulting $\mathcal{H}_\infty$ optimal controllers are causal, i.e., the command signal in trial $k + 1$ at time index t^* only depends on information of trial k at time indices $t \in [0, 1, \ldots, t^*]$ (see Section 2.2 for a formal introduction of the terms "causal" and "noncausal" in ILC). It is shown, see e.g., [97], that specific (often desirable) convergence properties of the ILC controlled system can be achieved with noncausal ILC controllers only. In [89], the robust ILC control problem is formulated as an $\mathcal{H}_\infty$ problem in the trial domain, with model uncertainty which is assumed to be trial varying, i.e., model uncertainty which can change from one trial to the next.

To solve a constrained robust ILC control problem for systems under worst case trial varying uncertainty, in [70], a min-max optimization problem is formulated. Due to the problem formulation, no analytical solution for the ILC controller can be given. Moreover, the solution is computationally demanding. Finally, robust ILC control design for systems with interval uncertainty is studied in [1]. The uncertainty model used puts an individual error bound on each element of the impulse response, which leads to a large computational load for a realistic problem.

Summarizing this discussion, the following aspects should ideally be covered in ILC control design approaches for uncertain systems:

- the finite time interval aspect of a trial (for an accurate representation of the ILC problem),

- the freedom to include uncertainty models in the design process (to improve achievable performance, and to be able to quantify robustness properties),

- and the possibility to analyze the robustness properties of various ILC control strategies (generality of the analysis).

The current approaches in literature all neglect one or more of these aspects. This observation leads to the following final two objectives:

Objective 3. Develop a robust convergence analysis approach which covers the finite time interval aspect of ILC, is applicable to linear trial invariant ILC strategies, and can incorporate uncertainty models in its analysis.

Objective 4. Develop a robust ILC control strategy which exploits knowledge about model uncertainty in its design, is not restricted to be causal, and incorporates the finite time interval aspect of ILC.

1.3 Outline of the thesis

This thesis is organized as follows. In Chapter 2, we introduce the ILC representation used throughout this thesis. Based on this representation, the system notations and ILC control structure are introduced, together with preliminary results on ILC control objectives such as convergence and performance.

Chapters 3 to 6 follow the order of the objectives as given in Section 1.2. As a result, in Chapter 3, we focus on Objective 1. With ILC for residual vibration suppression in point-to-point motion systems largely unexplored, we use this ILC task as an exemplary case to analyze ILC for time-windowed systems. This analysis not only leads to a better understanding of ILC for point-to-point motion problems, it also reveals new design freedom in ILC. We illustrate this new freedom by presenting experimental results on flexible systems.

In Chapter 4, we formalize and extend the results of Chapter 3 to systems with basis functions by formulating an ILC framework which encompasses the discussed time-windowed systems as a special case. An ILC analysis and design theory for systems with basis functions reveals how multiple ILC control objectives can be reached without the need to compromise between them, including the compensation for the effects of trial varying disturbances on performance.

In Chapter 5, we derive a robust convergence analysis approach for ILC controlled systems. The proposed approach is based on well developed μ analysis [103, 117, 143], in a form which respects the finite time interval aspect of ILC. Moreover, the analysis can handle additive and multiplicative uncertainty models in its problem formulation, and can be applied to MIMO linear time invariant systems controlled with any possibly noncausal linear trial invariant ILC controller. To exemplify the results, we analyze the robust convergence properties of LQ norm optimal ILC.

In Chapter 6, we develop a robust ILC control strategy which incorporates an additive uncertainty representation in its design. For the derivation of the controller, we use an approach similar to $\mathcal{H}_\infty$ optimization, however, formulated such that the solution is not restricted to be causal and explicitly acts on a finite time interval. By means of experiments, we show that the proposed R-ILC controller can outperform LQ norm optimal ILC and robust ILC based on a frequency domain μ procedure.

Finally, conclusions and recommendations are presented in Chapter 7.

Chapter 2

Iterative Learning Control

In this chapter, we discuss different formulations in ILC and extract the ILC representation which we will use throughout this thesis. Based on this representation, the system notations and ILC control structure are presented. Moreover, ILC control objectives are introduced and preliminary results with respect to these objectives are given.

Introduction

The general idea of ILC is illustrated in Figure 2.1, [87]. In Figure 2.1, J represents the system under study, ILC is the ILC algorithm, and the subscript k denotes the trial index with $k = 0, 1, 2, \ldots$. The idea behind ILC is as follows. During trial k, a command signal f_k is applied to system J. This command signal is stored in a memory, together with the error e_k which equals the difference between the reference signal y_d and system output y_k. After the trial has ended, the command and error signal are fed to the ILC algorithm, resulting in a command signal for trial $k + 1$, i.e., $f_{k+1} = ILC(f_k, e_k)$. Ideally, the ILC controller will iteratively generate a command signal, from trial to trial, such that the error e_k converges to zero.

Throughout this thesis, we assume the following to hold, [17, chap. 1].

1. Every trial has a fixed finite time span.

2. The system under study is reset to the same initial conditions at the beginning of each trial, i.e., $x_k(0) = x_0$ for $k = 0, 1, 2, \ldots$. Without loss of generality, we can take $x_0 = 0$.
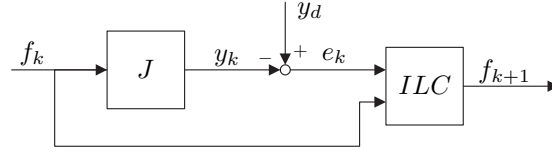
Figure 2.1: General ILC framework.

3. The system dynamics are trial invariant.

4. The output signal used for ILC is available from measurements.

2.1 A brief overview of ILC

From the ILC literature, multiple suggestions for the formulation of the ILC problem are available. In this section, we briefly discuss some of the more well known suggestions and discuss which we will use in this thesis. For a more elaborate overview of the different issues in ILC, see e.g., [2, 88].

2.1.1 Problem description

The ILC problem is a 2-dimensional (2D) control problem, i.e., information propagation occurs in two independent directions, e.g., [87]. On the one hand, we have the finite time domain behavior of the system during a trial. On the other hand, we have the trial behavior from trial to trial. To capture the 2D system behavior, different problem descriptions are possible.

It is possible to formulate the ILC problem as 2D control problem, e.g., using a Roesser or Fornasini-Marchesini state-space model, [51, 73, 102, 114]. Within this formulation, the finite time domain behavior and discrete trial domain behavior are easily captured. Furthermore, control design can incorporate both time and trial domain objectives. ILC analysis and control design is, however, more involved.

To simplify ILC analysis and design, the ILC problem can be approximated by considering the time domain to be infinite in length. As a result, the time domain behavior of systems can be represented by transfer functions and analysis can be done in frequency domain, e.g., [8, 23, 139]. The use of the frequency domain representation over a finite time interval does, however, lead to approximation errors (see Chapters 5 and 6).

Finally, the ILC problem can be described using a lifted notation, see e.g., [12, 60, 86, 100, 105, 119]. The idea behind the lifted notation is, that the finite time

domain behavior of a system is enclosed in a 1D notation in trial domain. As a result, ILC analysis can be executed using standard linear control theory, and time domain behavior is defined in a finite time interval. In contrast to 2D ILC, where stability can be considered in both time and trial domain, stability analysis in lifted ILC is restricted to trial domain convergence. Furthermore, "lifting" of the time domain behavior can result in large system representations, e.g., system matrices J of dimensions of 1000×1000 (which in ILC literature is sometimes abusively referred to as "curse-of-dimensionality").

Due to the simplicity of the ILC problem description, available analysis theory from linear control theory and linear algebra, the explicit inclusion of the finite time aspect in its description, and the ease with which basis functions can be included in this representation, in this thesis, we use the lifted ILC notation to describe our ILC problems.

2.1.2   (Non)linear systems

In many applications, the system behaves nonlinearly. In general, ILC control design for nonlinear systems is more complex than that for linear systems, see e.g., [28, 136]. One approach to obtain a linear system behavior of a nonlinear system, is to linearize the system using feedback linearization, e.g., [83]. This results in a linear time invariant (LTI) system description. Another approach is to apply time domain feedback control to the nonlinear system to get the system's output in the vicinity of desired trajectory. Subsequently, the feedback controlled system can be linearized around the trajectory to give a linear time varying (LTV) system representation, e.g., [107].

In this thesis, we limit ourselves to applications which can be described by, or well enough approximated by, LTI or LTV models. These models can be properly captured by the lifted system representation.

2.1.3   Continuous versus discrete time

In ILC, information propagation occurs in two independent directions: the time and trial direction. While the behavior in trial domain is discrete, the behavior of the physical time domain system is most often continuous. This can be taken into account in ILC control design by describing the time domain behavior by a continuous time model, see e.g., [10, 17, 104, 136]. Implementation of the ILC controller, however, must be digital, due to storage of the command and error signal in a digital memory. Using the reasoning: "*With the implementation of ILC control digital, the design of the controller might as well acknowledge this from the start*", [17, chap. 7], in this thesis we represent the time domain system behavior in discrete domain.

2.1.4 First order, higher order, and current iteration tracking error ILC

The basic idea behind ILC is to use the command signal f and error signal e from trial k to determine the command signal for trial $k + 1$, i.e., $f_{k+1} = ILC(f_k, e_k)$. In case calculation of f_{k+1} is based on these signals only, the ILC controller is referred to as first order ILC.

If signals from earlier trials are also included in the ILC algorithm, i.e., if $f_{k+1} = ILC(f_k, f_{k-1}, \ldots, e_k, e_{k-1}, \ldots)$, the algorithm is referred to as higher order (HO) ILC, [5, 17]. Depending on the proposed ILC control strategy, performance of HO ILC in presence of trial varying disturbances can be increased, [59], or not [91, 111]. Similarly, depending on the used ILC control strategy, robustness and/or convergence properties can be improved, [66, 89], or not, [91].

Next to inclusion of multiple past trial signals, it is also possible to use current iteration error signals in the ILC algorithm, i.e., $f_{k+1} = ILC(f_k, e_k, e_{k+1})$. This ILC controller is referred to as current iteration tracking error (CITE) ILC, [27, 30, 97]. A closer look at the structure of CITE ILC reveals that this ILC algorithm combines first order ILC with time domain feedback control. As a result, CITE ILC can improve performance of the ILC controlled system in presence of trial varying disturbances and improve robustness, similar to time domain feedback control.

In this thesis, the emphasis is on trial invariant phenomena. Furthermore, we assume that the system under study is already stable, or stabilized by a time domain feedback controller. Consequently, we consider first order ILC only.

2.1.5 Trial (in)variance

Up to now, the discussed ILC strategies have been trial invariant, i.e., the ILC controllers do not vary from one trial to the next. In presence of trial varying phenomena, the ILC control algorithms can be made trial varying, i.e., $f_{k+1} = ILC_k(f_k, e_k)$, e.g., [49, 50, 65, 67, 84, 92]. Using the argument that the emphasis in this thesis is on trial invariant phenomena, we restrict ourselves to trial invariant ILC.

2.1.6 Model uncertainty

Since no model can fully capture the dynamic behavior of the real system, model uncertainty will always be present. This uncertainty can be ignored in ILC control design, i.e., ILC control design is based on the assumption that the model and system behavior coincide. Conversely, model uncertainty can be explicitly taken into account in ILC control design, see e.g., [1, 34, 56, 92, 121].

In this thesis, we dedicate a significant part to ILC for uncertain systems (see Chapter 5 and Chapter 6).

2.1.7 Disturbance aspects

Finally, we address the issue of disturbances in ILC, [7]. Next to the trial invariant reference signal y_d, external trial varying disturbances, e.g., originating from measurement noise, neighboring systems, etc., can be present in the ILC problem, see [30, 70, 94, 111, 112, 123]. Another source of disturbances originates from errors in the resetting of the system at the beginning of a trial, denoted as initial condition disturbances, [27, 46, 82, 101].

We briefly discuss performance in presence of trial varying disturbances (see Section 4.5). In contrast, as discussed in the introduction of this chapter, we assume that the initial conditions remain unchanged from one trial to the next. In other words, we do not consider initial condition disturbances.

2.2 Notations

Based on the choices made in Section 2.1, in this section, we introduce the system representation and a commonly used ILC control framework. The control objectives related to this framework are defined in Section 2.3.

2.2.1 Lifted system representation

Consider the LTV system J as given in (2.1), with $f(T_s t) \in \mathbb{R}^{q_i}$ the command signal, and $y(T_s t) \in \mathbb{R}^{q_o}$ the output signal.

$$J : \begin{cases} x(T_s(t+1)) &=& A(T_s t)x(T_s t) + B(T_s t)f(T_s t) \\ y(T_s t) &=& C(T_s t)x(T_s t) + D(T_s t)f(T_s t). \end{cases} \tag{2.1}$$

Time index t denotes the sample number, and T_s represents the sample time. Note that in ILC, the time span of a trial is finite, and hence that $T_s t \in [0, T_s(N-1)]$ with $N \in \mathbb{N}$ the number of samples in a trial. The sample time T_s is omitted for brevity.

In time domain, system J represents an open or closed loop system, see Figure 2.2 (possibly with $C = 0$). Input $y_{ref}(t) \in \mathbb{R}^{q_o}$ in Figure 2.2 denotes the reference signal, $f(t) \in \mathbb{R}^{q_i}$ the command signal generated by the ILC algorithm, $f_{init}(t)$ a user defined initial feedforward signal (possibly zero), and $e(t) \in \mathbb{R}^{q_o}$ the measured error signal.
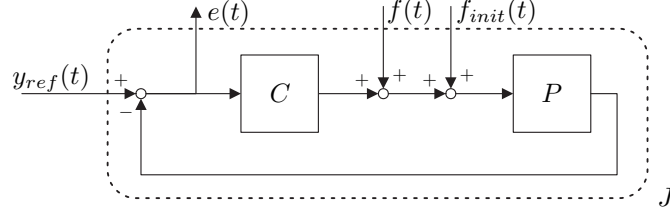
Figure 2.2: General time domain closed loop system.

The i/o mapping $(y_{ref}(t), f(t), f_{init}(t)) \mapsto e(t)$ is given by

$$e(t) = (I_{q_o} + PC)^{-1} y_{ref}(t) - (I_{q_o} + PC)^{-1} P(f(t) + f_{init}(t)).$$

To fit this mapping to the ILC framework of Figure 2.1, we define $y_d(t) \in \mathbb{R}^{q_o}$ and $J : f(t) \mapsto -e(t)$ by

$$y_d(t) := (I_{q_o} + PC)^{-1}(y_{ref}(t) - Pf_{init}(t))$$
$$J := (I_{q_o} + PC)^{-1} P,$$

resulting in

$$e(t) = y_d(t) - Jf(t). \tag{2.2}$$

An initial command signal $f_{init}(t)$ is hence enclosed in the definition of signal $y_d(t)$. For $f_{init}(t) = 0$ and $C = 0$, clearly $y_d(t) = y_{ref}(t)$. For $f_{init}(t) \neq 0$ and/or $C \neq 0$, signal $y_d(t)$ represents the servo error signal in absence of ILC. Nevertheless, independent of the specific choice for C, the goal of ILC is to find a command signal $f(t)$ such that $e(t) = 0$.

Using the definitions of y_d and J, Figure 2.2 is equivalent to Figure 2.3. In the remainder of this thesis, we refer to $y_d(t)$ as the reference signal and J as the system (under study).
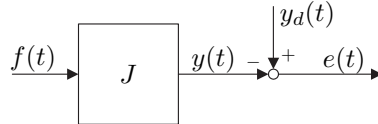
Figure 2.3: General time domain closed loop system with definitions y_d and J.

For the time span of a trial $t = 0, 1, \ldots, N - 1$, the i/o behavior of J can be

represented in lifted notation given by

$$
\underbrace{\begin{bmatrix} y(0) \\ \vdots \\ y(N-1) \end{bmatrix}}_{y} = J \underbrace{\begin{bmatrix} f(0) \\ \vdots \\ f(N-1) \end{bmatrix}}_{f} \tag{2.3}
$$

$$
\text{with} \quad J = \begin{bmatrix} D(0) & & 0 \\ \vdots & & \ddots & \\ C(N-1)\prod_{t=1}^{N-2} A(N-1-t)B(0) & \dots & D(N-1) \end{bmatrix},
$$

and $J \in \mathbb{R}^{Nq_o \times Nq_i}$. As a result, the lifted notation of the mapping $J : f_k \mapsto y_k$ for $t \in [0, N-1]$ during trial k equals $y_k = Jf_k$. Due to causality of J, system J is a lower triangular block matrix.

It is straightforward to see that the lifted system representation for LTI systems J equals

$$
\begin{bmatrix} y(0) \\ \vdots \\ y(N-1) \end{bmatrix} = \begin{bmatrix} D & & 0 \\ \vdots & \ddots & \\ CA^{N-2}B & \dots & D \end{bmatrix} \begin{bmatrix} f(0) \\ \vdots \\ f(N-1) \end{bmatrix} \tag{2.4}
$$

In this LTI case, system J has a lower triangular block Toeplitz matrix structure.

Note that matrices $(D, BC, BAC, \dots, CA^{N-2}B)$ in J correspond to the Markov parameters $j(t)$ (impulse response data) of system J. If this impulse response is available from measurements, system matrix J can directly be constructed using these measurements, without the need to first model the system dynamics (see Section 3.5).

2.2.2 ILC control algorithm

A commonly used first order, trial invariant ILC algorithm is given by

$$
f_{k+1} = ILC(f_k, e_k) \rightarrow f_{k+1} = f_k + Le_k, \tag{2.5}
$$

with $L \in \mathbb{R}^{Nq_i \times Nq_o}$ being the ILC controller. The structure of this ILC controller is founded on the Internal Model Principle (IMP) (see Section 3.2 for a derivation of this structure). Related to the structure of L, (2.6), we introduce the following definitions.

$$
L = \begin{bmatrix} \ell_{11} & \cdots & \ell_{1N} \\ \vdots & \ddots & \vdots \\ \ell_{N1} & \cdots & \ell_{NN} \end{bmatrix}, \quad \ell_{i,j} \in \mathbb{R}^{q_o \times q_i}. \tag{2.6}
$$

Definition 2.1 (Causal ILC control)**.** Given ILC controller L, (2.6). Then L is called causal if $\ell_{ij} = 0$ for $j > i$.

For L causal, the command signal $f_{k+1}(t^*)$ is a function of $e_k(t)$ with $t \in [0, t^*]$, i.e., the update of the command signal $f_{k+1} - f_k$ at time $t^* \in [0, N-1]$ depends only on error samples e_k in the past (time interval $0 \le t \le t^*$).

Definition 2.2 (Noncausal ILC control)**.** Given ILC controller L, (2.6). Then L is called noncausal if $\ell_{ij} \neq 0$ for (some) $j > i$.

For L noncausal, the command signal $f_{k+1}(t^*)$ is a function of $e_k(t)$ with $t \in [0, N-1]$, i.e., the update of the command signal $f_{k+1} - f_k$ at time $t^* \in [0, N-1]$ depends on error samples in the future ($t^* < t \le N-1$).

Definition 2.3 (Linear time invariant ILC control)**.** Given ILC controller L, (2.6). Then ILC controller L is called LTI if $\ell_{i,j} = \ell_{i,i-k}$ for $k \in [-N+1, N-1]$, i.e, if L has a block Toeplitz structure.

Definition 2.4 (Linear time varying ILC control)**.** Given ILC controller L, (2.6). Then ILC controller L is called LTV if it is not LTI, i.e, if L does not have a block Toeplitz structure.

2.2.3 ILC controlled system

By combining the lifted representation of (2.2) with (2.5), we find the ILC framework presented in Figure 2.4, with w corresponding to the one trial shift operator: $f_{k+1} = wf_k$. We refer to the feedback system in Figure 2.4 as the ILC controlled system. Throughout this thesis, the dimensions of the system blocks in the diagrams represent the dimensions of the corresponding system matrices.
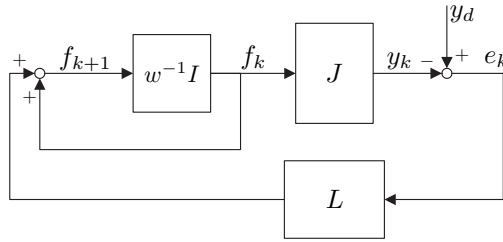
Figure 2.4: First order, trial invariant ILC framework.

With the ILC controlled system a feedback system in trial domain, we can express its trial domain open loop dynamics by

$$f_{k+1} = f_k + Le_k, \quad f_0 = 0 \tag{2.7}$$
$$y_k = Jf_k, \quad e_k = y_d - y_k,$$

and trial domain closed loop dynamics by

$$f_{k+1} = (I - LJ)f_k + Ly_d, \tag{2.8}$$

with $f_0 = 0$. Recall that any nonzero initial command signal f_{init} is enclosed in the definition of y_d, and hence that we can consider $f_0 = 0$ without loss of generality.

In Section 2.3, we use these dynamics to study properties of the ILC controlled system.

2.3 ILC control objectives

The ILC control objectives that we discuss in this section are shown in Figure 2.5. In the discussions, we make use of the following definitions: The 2-norm of a vector p is given by $\|p\|_2 = \sqrt{p^T p} \geq 0$. The induced 2-norm of a finite dimensional system matrix P is given by $\|P\|_{i2} = \overline{\sigma}(P)$, with $\overline{\sigma}(P)$ the largest singular value of P.
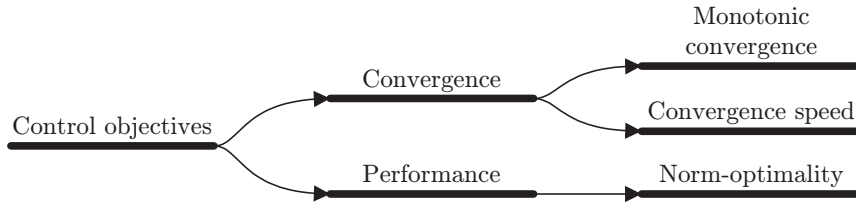
Figure 2.5: ILC control objectives.

2.3.1 Convergence

Convergence of the ILC controlled system in trial domain is essential, see e.g., [95, 109]. With (2.8) describing the evolution of the system in trial domain and f_k representing the state in trial domain, convergence of the ILC controlled system can be defined as follows.

Definition 2.5 (Convergence). Given ILC controlled system (2.8) with $y_d = 0$ and $f_0 \in \mathbb{R}^{Nq_i}$. Then (2.8) is convergent iff $f_\infty = 0 \ \forall f_0 \in \mathbb{R}^{Nq_i}$, with $f_\infty = \lim_{k\to\infty} f_k$.

Note that convergence can also be defined as function of the output y_k or the error e_k. We, however, choose to focus on convergence of the command signal f_k.

A standard result in stability theory now states that convergence is achieved if and only if the coefficient matrix of (2.8) has spectral radius smaller than one, i.e. $\rho(I_{Nq_i} - LJ) < 1$ with $\rho(\cdot) = \max_i |\lambda_i(\cdot)|$ and $|\lambda_i|$ the absolute value of the ith eigenvalue.

Convergence states that for any initial state f_0, the command signal f_k will be zero after an infinite number of trials. It does, however, not provide any information about transient behavior of f_k between $k = 0$ and $k \to \infty$. In Definition 2.6, this trial domain transient behavior of f_k is taken into account.

Definition 2.6 (Monotonic Convergence (MC)). Given ILC controlled system (2.8) with $y_d = 0$ and $f_0 \in \mathbb{R}^{Nq_i}$. Then (2.8) is monotonically convergent (MC) in the variable f_k if there exists $0 \leq \kappa < 1$ such that

$$\|f_{k+1}\|_2 \leq \kappa \|f_k\|_2, \ \forall f_0 \in \mathbb{R}^{Nq_i}, \tag{2.9}$$

and $\|f_{k+1}\|_2 = \|f_k\|_2$ only for $f_k = f_{k+1} = 0$.

Based on Definition 2.6, the following sufficient MC condition can be formulated.

Lemma 2.1. *Given ILC controlled system* (2.8). *Then* (2.8) *is MC in* f_k *if* $\|I_{Nq_i} - LJ\|_{i2} < 1$.

Proof. See Appendix A.2.1.   □

Lemma 2.1 states that a sufficient condition for monotonic convergence of (2.8) in f_k is given by $\|I_{Nq_i} - LJ\|_{i2} < 1$. Or, in other words, monotonic convergence requires that the largest gain in $I_{Nq_i} - LJ$ is smaller than one, i.e., that $\overline{\sigma}(I_{Nq_i} - LJ) < 1$. Consequently, demands on monotonic convergence of (2.8) can be represented by demands on the gain $\overline{\sigma}(I_{Nq_i} - LJ)$.

Remark 2.1. With $\rho(\cdot) \leq \|\cdot\|_{i2}$, monotonic convergence of the ILC controlled system in f_k implies convergence of the ILC controlled system.

Remark 2.2. We derived the MC condition based on Definition 2.6. Alternatively, the same MC condition can be found by considering $y_d \neq 0$ and $f_0 = 0$. The only difference between the two approaches is found in the definition of MC. For $y_d \neq 0$ and $f_0 = 0$, monotonic convergence requires $\|f_{k+1} - f_\infty\|_2 < \kappa \|f_k - f_\infty\|_2$.

Remark 2.3. In general, monotonic convergence of the command signal f_k does not imply monotonic convergence of the output signal e_k, [3, 22]. In certain cases, however, monotonic convergence of the command signal with ILC controllers based on the model inverse or LQ norm optimal objectives with diagonal weightings can ensure monotonic convergence of the error, see e.g., [6].

2.3.2 Convergence speed

Convergence speed deals with the speed with which $\|f_k\|_2$ converges to zero for given $f_0 \neq 0$, i.e., with the factor $\kappa = \frac{\|f_{k+1}\|_2}{\|f_k\|_2}$. From Lemma 2.1, we can conclude that if $\|I_{Nq_i} - LJ\|_{i2} = \kappa$, then $\|f_{k+1}\|_2 \leq \kappa \|f_k\|_2$. As a result, the gain $\overline{\sigma}(I_{Nq_i} - LJ)$ does not only reveal monotonicity of convergence, it is also specifies the upper bound on the convergence speed of (2.8).

For $\|I_{Nq_i} - LJ\|_{i2} = 0$, we obtain deadbeat control, i.e., the ILC controlled system converges in one trial for all f_0. For $\|I_{Nq_i} - LJ\|_{i2} = 1 - \varepsilon$ with $0 < \varepsilon \ll 1$, there exist f_0 for which convergence of the ILC controlled system is arbitrarily slow.

2.3.3 Performance

Performance $\mathcal{P}_\xi$ is used as a measure of how well a convergent ILC controlled system is capable of reducing a performance variable ξ_k for $k \to \infty$, i.e., of reducing the asymptotic value ξ_∞. Most often, ξ_k equals the error e_k.

Definition 2.7 (Performance). Consider the ILC controlled system (2.8) with performance variable ξ_k, and assume that (2.8) is convergent. Then performance $\mathcal{P}_\xi$ and optimal performance $\mathcal{P}_{\xi,opt}$ are defined by (2.10) and (2.11), respectively.

$$\mathcal{P}_\xi(L) = \lim_{k \to \infty} \|\xi_k\|_2 \tag{2.10}$$

$$\mathcal{P}_{\xi,opt}(L) = \min_L \mathcal{P}_\xi(L). \tag{2.11}$$

In Lemma 2.2, we show that for arbitrary reference signal y_d, optimal performance with $\xi_\infty = e_\infty = 0$ can only be achieved under stringent system conditions.

Lemma 2.2. *Given a convergent system* (2.8) *with asymptotic error* e_∞. *Then* $e_\infty = 0$ *for any* y_d *iff* $q_o = q_i$, *i.e., iff the number of system outputs equals the number of system inputs.*

Proof. See Appendix A.2.2. $\qquad\qquad\square$

Lemma 2.2 extends the results of [7].

Chapter 3

Time-windowed ILC

To exemplify ILC design issues for time-windowed systems, in this chapter we present an approach for suppression of residual vibrations in point-to-point motions, based on ILC. The approach is to add a signal to the command input during the point-to-point motion in order to compensate for residual vibrations after arrival at the desired position. A special form of ILC with separate actuation and observation time windows, referred to as Hankel ILC, is shown to converge to the required signal. Designed Hankel ILC control strategies are implemented on a SISO and MIMO flexible system and shown to be successful in suppression of residual vibrations.

Introduction

In many applications, a flexible structure has to be repositioned to perform a task. The corresponding point-to-point motion can, however, introduce vibrations into the structure, thereby increasing settling time or degrading the reachable performance of the operation, Figure 3.1.

In existing literature on input shaping, see [33, 115, 116] for overviews, the problem of suppressing residual vibrations is, in general, dealt with by convolving a designed command signal with a pulse sequence. This approach requires an accurate model of the system capturing all modes if all vibration modes are to be suppressed. To somewhat relax this condition, adaptive techniques have been proposed, [32, 108, 125].

We suggest an alternative approach for residual vibration suppression, based on ILC. Instead of computing the command signal using a model (model-based feed-
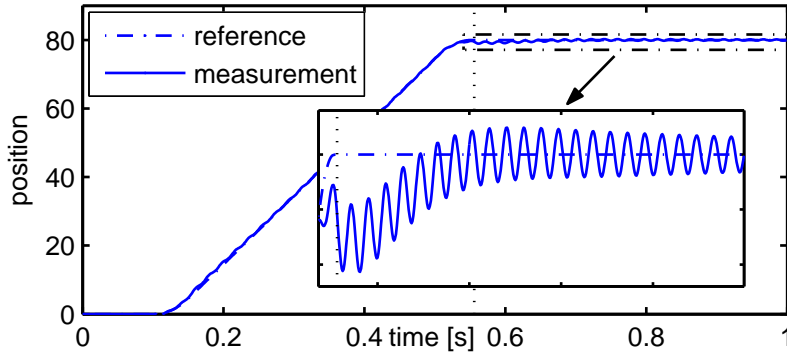
Figure 3.1: Residual vibrations after a point-to-point motion.

forward control), ILC converges to the sought command signal iteratively by executing a number of experiments. Since the converged ILC command signal follows from experiments, it will in general outperform command signals which are explicitly based on a model.

Preliminary results of ILC for residual vibration suppression in point-to-point motion problems are presented in [37, 40, 133]. To properly formulate the ILC control problem, [37, 40, 133] introduce time windows in the system description. Subsequently, the obtained time-windowed system is plugged into an existing LQ norm optimal control strategy, and shown to suppress residual vibrations on experimental setup. What is lacking in [37, 40, 133], is any analysis of the ILC controlled system with time windows.

In this chapter, we discuss the several steps taken from formulation of the residual vibration suppression problem in Section 3.1, via system representation (Section 3.2) and ILC control design (Section 3.3), to implementation of this problem on experimental setups in Section 3.4 and Section 3.5. This chapter ends with concluding remarks in Section 3.6.

The contents of this chapter is published in [127–130].

3.1 Point-to-point motion problem

3.1.1 Point-to-point control problem

The problem of moving a flexible structure to a desired position and leaving it without residual vibration can be handled by a properly designed command signal. With the desire to be at rest after completion of the motion, i.e., a command signal which is constant (usually zero) after arrival at the desired position, the command

signal should accomplish suppression of this vibration during the point-to-point motion.

Definition 3.1. *Point-to-point control problem:*
The design of a command signal actuating the system *during* the point-to-point motion, resulting the system to be positioned at the desired position without residual vibrations *after* completion of the motion.

A benefit of the point-to-point motion approach over the servo approach is that the command signal can be guaranteed to be at rest after arrival at the desired position. Moreover, as long as the system arrives at the desired position without any residual vibrations, errors between a reference signal and the actual system's output during the motion are irrelevant in the point-to-point motion approach.

In Figure 3.2, the point-to-point control structure is illustrated: for $t \in [m_1, m_2]$ the system is subjected to a command signal so that for $t \in [n_1, n_2]$ the system is at rest. In this chapter, we assume that the actuation and observation intervals are adjacent and non-overlapping, i.e., that $n_1 = m_2 + 1$, in correspondence with input shaping techniques. Other choices for the time windows are left for Chapter 4.
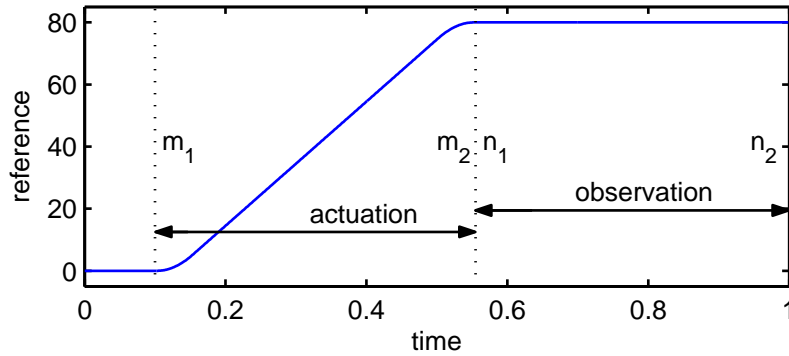
Figure 3.2: Reference signal with separate actuation and observation interval. m_1, m_2, n_1, and n_2 are sample instants and $n_1 = m_2 + 1$.

Suppression of residual vibrations during the observation time interval can be seen as the compensation of disturbed initial conditions $x(n_1)$ at the beginning of the observation interval. To see this, realize that actuation and observation take place in separate but adjacent time intervals. With actuation of the flexible structure limited to the actuation interval, the system behaves autonomously during the observation interval. Consequently, any nonzero response of this autonomous system (the residual vibration) originates from the disturbed initial conditions $x(n_1)$ at the initial time instant of the observation interval. Compensation for these disturbed initial conditions results in compensation for the residual vibration.

3.1.2 Point-to-point problem formulation

In this section, we formulate the problem of residual vibration suppression as compensation of a disturbed initial condition.

Given the discrete-time LTI system J, $t = 0, 1, 2, \ldots$ of minimal order

$$J : \begin{cases} x(t+1) = Ax(t) + Bf(t) \\ \quad\;\; y(t) = Cx(t) + Df(t), \end{cases} \tag{3.1}$$

with $x \in \mathbb{R}^p$, $f(t) \in \mathbb{R}^{q_i}$ the command signal, and $y(t) \in \mathbb{R}^{q_o}$ the measured position. Then the convolutive mapping from $f(t)$ to $y(t)$ for $t \in [0, N-1]$ is given by

$$\begin{bmatrix} y(0) \\ \vdots \\ y(N-1) \end{bmatrix} = \underbrace{\begin{bmatrix} D & 0 & \ldots & 0 \\ CB & D & \ddots & \vdots \\ \vdots & \ddots & \ddots & 0 \\ CA^{N-2}B & \ldots & CB & D \end{bmatrix}}_{J} \begin{bmatrix} f(0) \\ \vdots \\ f(N-1) \end{bmatrix}. \tag{2.4*}$$

Next, with the actuation interval defined by $t \in [m_1, m_2]$, observation interval by $t \in [n_1, n_2]$, and $n_1 = m_2 + 1$ (all in accordance with Figure 3.2), the convolutive mapping from $f(t)$ during the actuation interval to $y(t)$ during the observation interval equals

$$\begin{bmatrix} y(n_1) \\ \vdots \\ y(n_2) \end{bmatrix} = \underbrace{\begin{bmatrix} CA^{m-1}B & \ldots & CB \\ \vdots & \ddots & \vdots \\ CA^{n+m-2}B & \ldots & CA^{n-1}B \end{bmatrix}}_{J_H} \begin{bmatrix} f(m_1) \\ \vdots \\ f(m_2) \end{bmatrix}, \tag{3.2}$$

$$m = m_2 - m_1 + 1, \quad n = n_2 - n_1 + 1, \quad n_1 = m_2 + 1,$$

with $J_H \in \mathbb{R}^{nq_o \times mq_i}$.

After reversing the command sequence in time, the system J_H corresponds to the Hankel operator which is known to have a rank equal to the order of the observable and controllable part of the underlying system, e.g., [110]. With this order equal to p, for $\min(mq_i, nq_o) > p$, the matrix J_H is rank deficient. In case $\mathrm{rank}(J_H) = p < \min(mq_i, nq_o)$, we can represent J_H as the product of two full rank matrices using full rank decomposition,

$$J_H = J_o J_c, \quad \text{with} \;\; J_o \in \mathbb{R}^{nq_o \times p}, \; J_c \in \mathbb{R}^{p \times mq_i}, \tag{3.3}$$

representing the following two mappings

$$
\begin{bmatrix} y(n_1) \\ \vdots \\ y(n_2) \end{bmatrix} = J_o x(n_1), \quad x(n_1) = J_c \begin{bmatrix} f(m_1) \\ \vdots \\ f(m_2) \end{bmatrix} \tag{3.4}
$$

with, e.g., $J_o = \begin{bmatrix} C^T & (CA)^T & \ldots & (CA^{n-1})^T \end{bmatrix}^T$
and $J_c = \begin{bmatrix} A^{m-1}B & A^{m-2}B & \ldots & B \end{bmatrix}$.

Rewriting (3.4) yields

$$
y = J_o x(n_1) \rightarrow x(n_1) = J_o^\dagger y = (J_o^T J_o)^{-1} J_o^T y, \tag{3.5}
$$

with $J_o^\dagger$ the Moore-Penrose inverse of J_o. Taking, without loss of generality, the desired position during the observation interval equal to $y_d = 0$, the system has zero residual vibrations if $y(t) = y_d$ for $t \in [n_1, n_2]$. With $y = 0$, we have $x(n_1) = 0$.

Previous reasoning shows that residual vibrations are the result of disturbed initial condition $x(n_1)$. As we will discuss next, this result is essential for the formulation of a convergent ILC control algorithm.

3.2 ILC for residual vibration suppression: Hankel ILC

To comply with the ILC problem formulation of residual vibration suppression in point-to-point motions, in this section, we modify the original system J using time windows. After showing that the ILC controlled system of Figure 2.4 can not be made convergent for this modified system, we derive a new ILC framework and prove that this framework can be made convergent.

3.2.1 Hankel ILC

To make ILC capable of handling residual vibrations, system J is first transformed to J_H of (3.2). This is accomplished by defining T_f, T_y, and J_H as

$$
\begin{aligned}
T_f &= \begin{bmatrix} 0_{mq_i \times m_1 q_i} & I_{mq_i} & 0_{mq_i \times (N-m_2-1)q_i} \end{bmatrix}^T, \quad T_f \in \mathbb{R}^{N \times mq_i} \\
T_y &= \begin{bmatrix} 0_{nq_o \times n_1 q_o} & I_{nq_o} & 0_{nq_o \times (N-n_2-1)q_o} \end{bmatrix}, \quad T_y \in \mathbb{R}^{nq_o \times N} \\
J_H &= T_y J T_f.
\end{aligned} \tag{3.6}
$$

Due to the rank properties of system J_H, we will denote ILC applied to point-to-point motion problems as *Hankel* ILC.

Consequences of time windows in ILC

To analyze the consequences of time windows in the ILC controlled system, recall
the framework of Figure 2.4 with trial domain dynamics

$$f_{k+1} = f_k + Le_k, \quad f_0 = 0 \tag{2.7*}$$
$$y_k = Jf_k.$$

By combining (3.6) and (2.7), we obtain the ILC control framework of Figure 3.3.
In Figure 3.3, vector u_k is the trial state with $u_0 = 0$, α_k represents the system
output during the observation time interval, $\alpha_d = T_y y_d$ contains the residual
vibrations during the observation interval before ILC is applied, and $\epsilon_k = T_y(y_d -
y_k) = \alpha_d - \alpha_k$ is the residual vibration during the observation time interval in trial
k. From Figure 3.3, we find the trial domain dynamics for the time-windowed
system J_H

$$u_{k+1} = u_k + L\epsilon_k, \quad f_k = T_f u_k, \quad u_0 = 0$$
$$u_{k+1} = (I_{mq_i} - LJ_H)u_k + L\alpha_d, \tag{3.7}$$

with $u_k \in \mathbb{R}^{mq_i}$.
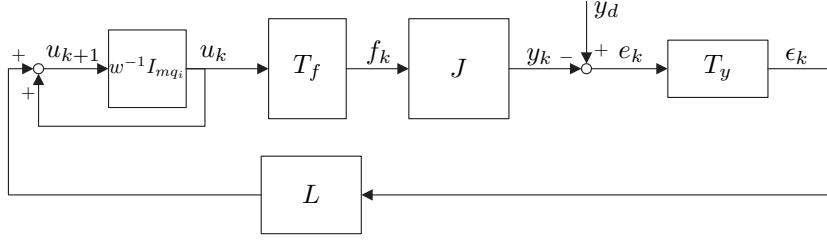
Figure 3.3: ILC framework including actuation window matrix T_f and observation
window matrix T_y.

From Chapter 2, we know that (3.7) is convergent iff $\rho(I_{mq_i} - LJ_H) < 1$. For the
(common) case $p = \text{rank}(J_H) < mq_i$, however, we find

$$\rho(I_{mq_i} - LJ_H) = \max_j |\lambda_j(I_{mq_i} - LJ_H)|$$
$$= \max_j |1 - \lambda_j(LJ_H)|$$
$$\geq 1, \tag{3.8}$$

where the last step in (3.8) follows from the fact that for singular J_H, there exists
$j \in [1, mq_i]$ such that $\lambda_j(LJ_H) = 0$. As a result, it depends on the rank properties
of J_H whether or not there exist an L for which the ILC framework of Figure 3.3
can be made convergent.

A convergent ILC control framework

To find an ILC control framework for system J_H with which convergence can be achieved for all values $\text{rank}(J_H) = p \leq mq_i$, we apply the internal model principle (IMP), [47]. Based on the IMP, a disturbance can be asymptotically rejected provided that 1) the dynamic disturbance model is added to a feedback controller, 2) this feedback controller stabilizes the feedback controlled system, and 3) the correcting input signal is not canceled by transmission zeros in the system. For ILC, the disturbance corresponds to the trial invariant reference signal $\alpha_d \in \mathbb{R}^{nq_o}$, whose trial domain dynamics are represented by nq_o trial domain integrators. For systems with $\text{rank}(J_H) = p < \min(mq_i, nq_o)$, however, maximally p trial domain integrators can be stabilized. Stabilization of the ILC controlled system with p trial domain integrators can subsequently be accomplished by design of controllers $L_o \in \mathbb{R}^{p \times nq_o}$ and $L_c \in \mathbb{R}^{mq_i \times p}$.

Based on the IMP results, a convergent ILC framework is shown in Figure 3.4, with corresponding ILC algorithm (3.9) and trial domain dynamics (3.10).

$$u_{k+1} = u_k + L_o \epsilon_k, \quad \beta_k = L_c u_k, \quad u_0 = 0 \tag{3.9}$$

$$u_{k+1} = (I_p - L_o J_H L_c) u_k + L_o \alpha_d, \tag{3.10}$$

with $u_k \in \mathbb{R}^p$, and β_k the command signal during the actuation time interval, i.e., $\beta_k = T_f^T f_k$.
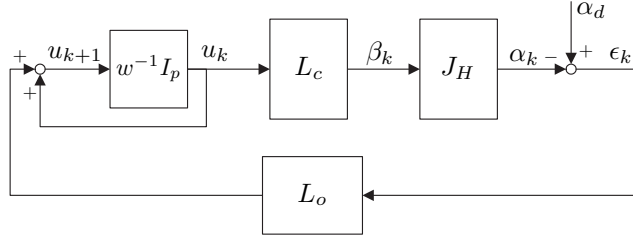
Figure 3.4: Hankel ILC framework in trial domain, with ILC controllers (L_o, L_c).

To prove that the ILC controlled system of Figure 3.4 can be made convergent, we present Lemma 3.1.

Lemma 3.1. *Given ILC controlled system* (3.10), *Figure 3.4, with p the state dimension, i.e., $u_k \in \mathbb{R}^p$. Then there exist trial invariant L_o and L_c such that* (3.10) *is convergent iff $p \leq \text{rank}(J_H)$. In that case, $\text{rank}(L_o) = \text{rank}(L_c) = p$.*

Proof. See Appendix A.3.1. ☐

In the remainder of this chapter, we consider $p = \text{rank}(J_H)$.

Additional conditions for convergence with L_o and L_c are presented in Lemma 3.2.

Lemma 3.2. *Consider the ILC controlled system* (3.10), *with* $p = \text{rank}(J_H)$. *Then given* L_o, *arbitrary pole placement in* (3.10) *by choice of* L_c *is possible, iff* $\text{rank}(L_o J_o) = p$. *Conversely, given* L_c, *then arbitrary pole placement in* (3.10) *by choice of* L_o *is possible, iff* $\text{rank}(J_c L_c) = p$.

Proof. See Appendix A.3.2. □

To illustrate the results of Lemma 3.2, say we want $I_p - L_o J_H L_c = I - K$, with $I_p - K$ representing the desired pole locations. Then pole placement with L_c gives $L_c = J_c^\dagger (L_o J_o)^{-1} K$, with $J_c^\dagger = J_c^T (J_c J_c^T)^{-1}$ the Moore-Penrose inverse of J_c. Similarly, pole placement with L_o gives $L_o = K(J_c L_c)^{-1} J_o^\dagger$.

Remark 3.1. The result of Lemma 3.1 is not restricted to J_H. Rather, it is applicable to any system $T_y J T_f$, regardless of size and rank.

Remark 3.2. The interpretation of Lemma 3.1 is to never place more trial domain shift operators w^{-1} (or trial domain integrators) in the trial loop than can be stabilized. With the inner loop of Figure 3.4 a unit feedback loop (the integrator), stabilization must be accomplished by the outer loop by design of L_o and L_c.

3.2.2 Interpretation of reduced learning space

Intuitively, the equivalence and difference between the frameworks of Figure 3.3 and Figure 3.4 can be explained as follows. From Section 3.1, we know that the two frameworks are equivalent in the sense that they both consider residual vibration suppression. However, in (3.7), this goal is strived after by directly finding a command signal during the actuation time interval, while in (3.9) this goal is achieved by compensating for a disturbed time domain state $x(n_1)$.

A more formal explanation is found by realizing that frameworks Figure 3.3 and Figure 3.4 are equivalent in the sense that the loop gains obtained by opening the loop in between J_o and J_c inside $J_H = J_o J_c$ can be made identical. These loop gains are

$$J_c(I_{mq_i} - wI_{mq_i})^{-1} L J_o = (1 - w)^{-1} J_c L J_o, \quad \text{and}$$

$$J_c L_c (I_p - wI_p)^{-1} L_o J_o = (1 - w)^{-1} J_c L_c L_o J_o,$$

respectively, and are equal if

$$J_c L J_o = J_c L_c L_o J_o. \tag{3.11}$$

Now, given L, the choice $L_c = J_c^\dagger$ and $L_o = J_c L$ verifies (3.11). Conversely, given L_o and L_c, the choice $L = L_c L_o$ verifies (3.11). The difference between the frameworks lies in the presence (or absence) of uncontrollable/unobservable trial domain states. As a result, convergence of the ILC controlled system of Figure 3.3 can not be achieved, while convergence of the ILC controlled system of Figure 3.4 can be achieved. For this reason, in the remainder of this chapter, we focus on Hankel ILC control design with the ILC framework of Figure 3.4 .

3.3 Hankel ILC control design

With the Hankel ILC control framework discussed, in this section we propose multiple control strategies for (L_o, L_c).

Initially, we choose to design L_c such that $J_c L_c = I_p$. As a result, we leave pole placement to L_o.

Proposition 3.1. *Consider controller L_c with $J_c L_c = I_p$. Then the general solution for L_c is given by*

$$L_c = J_c^\dagger + T_c^\dagger M_c, \tag{3.12}$$

with matrix $T_c^\dagger$ following from the full rank decomposition $T_c^\dagger T_c := I_{mq_i} - J_c^\dagger J_c$, $J_c^\dagger = J_c^T (J_c J_c^T)^{-1}$ the Moore-Penrose inverse of J_c, and $M_c \in \mathbb{R}^{(mq_i - p) \times p}$ arbitrary.

Proof. The general solution for $J_c L_c = I_p$ is given by $L_c = J_c^{(1)} + (I_{mq_i} - J_c^{(1)} J_c) M_c^*$, [16], with $M_c^* \in \mathbb{R}^{mq_i \times p}$ arbitrary, and $J_c^{(1)}$ any {1}-inverse of J_c, i.e., satisfying $J_c J_c^{(1)} J_c = J_c$. With $J_c^{(1)} = J_c^\dagger$ a valid {1}-inverse of J_c, and with full rank decomposition $T_c^\dagger T_c := I_{mq_i} - J_c^\dagger J_c$ yielding $T_c = \mathbb{R}^{(mq_i - p) \times mq_i}$, we find $M_c = T_c M_c^*$. $\qquad \square$

The design freedom M_c in Hankel ILC corresponds to the freedom to alter the command signal during the actuation time interval, β_k, without influencing the corresponding output signal during the observation time interval, α_k. A possible use of this design freedom is to minimize the command signal amplitude of β_k to avoid input saturation. Design of M_c will be discussed in Section 3.3.2. Examples of the use of M_c are presented in Sections 3.4 and 3.5.

As a result of Proposition 3.1, Hankel ILC control design consists of specifying L_o and M_c. In Lemma 3.3, we show that design of L_o and M_c can be done in two separate steps.

Lemma 3.3. *Consider the ILC algorithm (3.9), Hankel ILC controlled system (3.10), $\epsilon_k = \alpha_d - J_H \beta_k$, and ILC controller (L_o, L_c) with L_c from Proposition 3.1. Then for arbitrary $M_c \in \mathbb{R}^{(mq_i - p) \times p}$, convergence and performance objectives of (3.10) can be reached by design of L_o. Furthermore, every command signal β_k which results from (3.9) with arbitrarily designed L_o, can be reached by design of M_c.*

Proof. See Appendix A.3.3. $\qquad \square$

Based on Lemma 3.3, we first design L_o to cover the convergence and performance aspects, and second, design M_c to minimize the amplitude of the command signal β_k.

3.3.1 Step L_o: Convergence and performance

Convergence

For $J_c L_c = I_p$, convergence of the ILC controlled system requires $\rho(I_p - L_o J_o) < 1$. Now, a straightforward solution for L_o can be given by inverse model based control

$$I_p - L_o J_o = (1 - g)I_p \rightarrow L_o = g J_o^\dagger, \quad g \in (0, 2), \tag{3.13}$$

resulting in $\lambda_i(I_p - L_o J_o) = 1 - g$. Note that for $g = 1$, the inverse model ILC controller is deadbeat, i.e., that the Hankel ILC controlled system converges in only one trial.

An alternative expression for L_o can be obtained by solving an LQ norm optimization problem, see Proposition 3.2.

Proposition 3.2. *Given system* (3.3) *with* L_c *from Proposition 3.1, the ILC controlled system depicted in Figure 3.4, and the optimization problem defined by*

$$\min_{u_{k+1}} \mathcal{J}, \quad \text{with}$$
$$\mathcal{J} = \epsilon_{k+1}^T \epsilon_{k+1} + (\beta_{k+1} - \beta_k)^T R(\beta_{k+1} - \beta_k),$$

with $R = R^T \geq 0$. *Then solving this optimization problem yields the ILC algorithm*

$$u_{k+1} = u_k + \underbrace{(J_o^T J_o + L_c^T R L_c)^{-1} J_o^T}_{L_o} \epsilon_k, \tag{3.14}$$

with L_o *referred to as the LQ norm optimal ILC controller.*

Proof. See Appendix A.3.4. $\qquad\square$

By taking $R := r L_c (L_c^T L_c)^{-2} L_c^T$ with $r > 0$ and adding a learning gain $0 < g < 2$ to L_o, the LQ norm optimal Hankel ILC controller can be simplified to $L_o = g(J_o^T J_o + r I_p)^{-1} J_o^T$. The consequence of this choice for R is, however, that we penalize trial state u_k instead of command signal β_k.

As we will show in Chapter 4, parameters g and r can be used to adjust the convergence speed of the ILC controlled system, and to reduce the influence of trial varying disturbances on performance. Additionally, in Appendix B, we briefly illustrate that g can also be used to achieve convergence in presence of model uncertainty.

Performance

Performance of the ILC controlled system with L_o depends on $\epsilon_\infty = (I_{nq_o} - J_o(L_o J_o)^{-1} L_o)\alpha_d$, (A.4). By substituting the inverse model based ILC controller or LQ norm optimal ILC controller in ϵ_∞, we find

$$\|\epsilon_\infty\|_2 = \|(I_{nq_o} - J_o J_o^\dagger)\alpha_d\|_2.$$

Although in general we have $\epsilon_\infty \neq 0$, in Chapter 4 we will show that with this ϵ_∞ we achieved optimal performance $\mathcal{P}_{\epsilon,opt}$, i.e. we achieved a minimized $\|\epsilon_\infty\|_2$ over all possible (L_o, L_c).

3.3.2 Step M_c: Command signal manipulation

Our goal of command signal manipulation is to reduce the larger amplitudes in the command signal. By reducing the amplitude, we reduce the possibility of saturating the command signal.

We propose two approaches to reach this goal: The first one is based on minimization of the maximum amplitude of the command signal, referred to as ℓ_∞ control, [134]. The second approach is based on minimization of the weighted converged command signal $\|\beta_\infty\|_{W_\beta}^2$, denoted as ℓ_2 control.

ℓ_∞ control
With the initial command signal during the actuation interval given by $\beta_{init} = T_f^T f_{init}$, the total command signal applied to the system during the actuation interval equals

$$\beta_{k,tot} = \beta_k + \beta_{init} = J_c^\dagger u_k + T_c^\dagger M_c u_k + \beta_{init}, \tag{3.15}$$

with elements β_{init} and $J_c^\dagger u_k$ in (3.15) known, and $T_c^\dagger M_c u_k$ yet undefined. Since there are no restrictions imposed on M_c, we can alter $T_c^\dagger M_c u_k$ to $T_c^\dagger \theta_k$ with $\theta_k \in \mathbb{R}^{mq_i - p}$ to make it independent of u_k. The goal of minimizing the maximum command amplitude can now be expressed as

$$\min_{\theta_k} \max |\beta_{k,tot}| = \min_{\theta_k} \max |J_c^\dagger u_k + \beta_{init} + T_c^\dagger \theta_k|. \tag{3.16}$$

This min-max optimization problem can subsequently be rewritten as the linear programming (LP) problem

$$\min_{\theta_k} \beta_{max}, \text{ subject to } -\mathbf{1}\beta_{max} \leq F_k + T_c^\dagger \theta_k \leq \mathbf{1}\beta_{max}, \tag{3.17}$$

with $F_k := J_c^\dagger u_k + \beta_{init}$, and $\mathbf{1} = [1 \ \dots \ 1]^T \in \mathbb{R}^{mq_i}$. Finally, a general notation for (3.17) is given by

$$\min c^T \varphi_k, \text{ subject to } A\varphi_k \leq b \tag{3.18}$$

with $c = \begin{bmatrix} 0 \\ 1 \end{bmatrix}$, $A = \begin{bmatrix} T_c^\dagger & -\mathbf{1} \\ -T_c^\dagger & -\mathbf{1} \end{bmatrix}$, $b = \begin{bmatrix} -F_k \\ F_k \end{bmatrix}$, and $\varphi_k = \begin{bmatrix} \theta_k^T & \beta_{max} \end{bmatrix}^T$.

Note that inclusion of additional constraints in the optimization problem is straightforward, e.g., to limit the maximum rate change $\Delta_f > 0$ of the command signal in time domain: $-\Delta_f < \beta_k(t+1) - \beta_k(t) < \Delta_f$.

After the optimization problem is solved, command signal β_{k+1} is obtained by applying the optimal $\theta_{k+1,opt}$ in $\beta_{k+1} = J_c^\dagger u_{k+1} + T_c^\dagger \theta_{k+1,opt}$, with u_{k+1} from (3.9).

ℓ_2 control
In ℓ_2 control, L_c is obtained by solving a quadratic optimization problem based on the converged command signal $\beta_\infty = \lim_{k\to\infty} \beta_k$. With $\beta_\infty = L_c u_\infty$ and u_∞ given by $u_\infty = (L_o J_o)^{-1} L_o \alpha_d$, (A.3), the converged command signal is given by

$$\beta_\infty = L_c (L_o J_o)^{-1} L_o \alpha_d. \tag{3.19}$$

The focus of the optimization problem is to minimize $\|\beta_\infty\|_{W_\beta}^2$, with $W_\beta \in \mathbb{R}^{mq_i \times mq_i}$ a user defined positive definite weighting matrix. This W_β can be used to penalize those parts of β_∞ where reduction of the command amplitude is desired. Note that any amplitudes of an initial β_{init} have to be taken into account in the design of W_β.

Proposition 3.3. *Given L_c from Proposition 3.1, the ILC controlled system depicted in Figure 3.4, and the optimization problem*

$$\min_{M_c} \mathcal{J}_M = \min_{M_c} \beta_\infty^T W_\beta \beta_\infty,$$

with β_∞ from (3.19) and $W_\beta \in \mathbb{R}^{mq_i \times mq_i}$ a user defined positive definite weighting matrix. Then the minimizing M_c yields

$$L_c = (I_{mq_i} - T_c^T (T_c W_\beta T_c^T)^{-1} T_c W_\beta) J_c^\dagger. \tag{3.20}$$

Proof. See Appendix A.3.5. $\square$

We illustrate the use of the discussed Hankel ILC controllers by implementing them on a SISO and MIMO flexible system in Sections 3.4 and 3.5, respectively.

3.4 Example: two-inertia setup

In this section, we apply the ℓ_2 and ℓ_∞ Hankel ILC control strategies of Section 3.3 to the SISO two-inertia setup discussed in Appendix C, see also Figure 3.5. The impulse response of a model of the system is shown in Figure 3.6.

To be able to compare the ℓ_2 and ℓ_∞ Hankel ILC controllers with $M_c \neq 0$ with the case $M_c = 0$, we additionally introduce an LQ norm optimal ILC controller given by an ℓ_2 Hankel ILC controller with $W_\beta = I_{mq_i}$ (giving $M_c = 0$).

The initial situation
The reference signal y_{ref} and initial command signal f_{init} are presented in Figure 3.7. Since we are dealing with a closed loop system in time domain, the
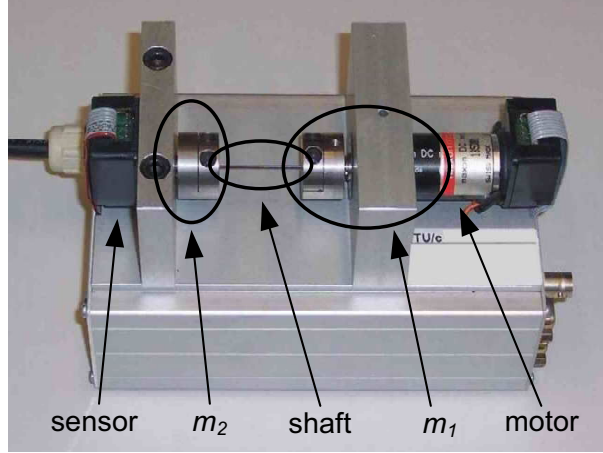
Figure 3.5: Two-inertia setup used for the experiments.
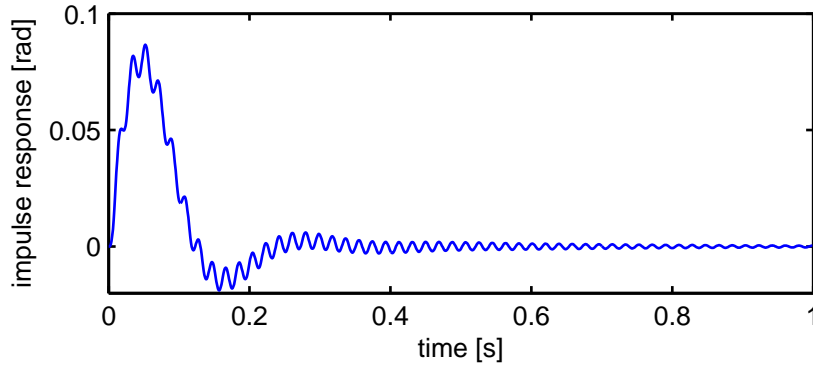
Figure 3.6: Impulse response of system $J(z)$.

reference signal y_d equals the initial error signal $(1 + PC)^{-1}(y_{ref} - Pf_{init})$. Furthermore, from Figure 3.7, we can state that only 58 samples are used to actuate the system, while 443 samples are used for observation. Consequently, we have $J_H \in \mathbb{R}^{443 \times 58}$. With the order of our model J equal to 7, we find rank$(J_H) = p = 7$, $J_c \in \mathbb{R}^{7 \times 58}$, and $J_o \in \mathbb{R}^{443 \times 7}$.

Hankel ILC control design

Controller L_c is based on Proposition 3.1, and L_o is designed according to LQ norm optimal ILC, (3.14), with $R = rL_c(L_c^T L_c)^{-2}L_c^T$ for simplicity (Note that the inverse term in L_o corresponds to a 7×7 matrix). Subsequently, for ℓ_2 control, the weighting matrix W_β is chosen diagonal, with

$$\text{diag}(W_\beta) = 500|\beta_\infty + \beta_{init}|, \tag{3.21}$$

and β_∞ the converged command signal (3.19) for $M_c = 0$. By defining W_β as in
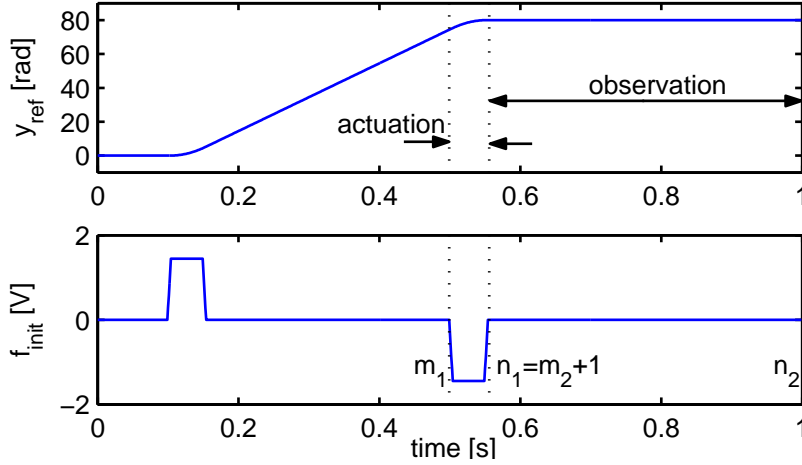
Figure 3.7: Reference signal y_{ref} and initial command signal f_{init}.

(3.21), the command signal is penalized most at those time instants where theoretically β_∞ has the largest amplitude. Note that this is just one possible choice for W_β.

Experimental results

The experimental results for LQ norm optimal, ℓ_2, and ℓ_∞ control strategies are shown in Figure 3.8 to Figure 3.11. The values $r = 0.1$ and $g = 0.5$ used for the experiments are obtained experimentally.

The initial residual vibration α_d during $k = 0$ is shown in Figure 3.8, and the error norms $\|\epsilon_k\|_2$ as function of trial number k are presented in Figure 3.9. Although the Hankel ILC controllers are merely designed to be convergent, it can be seen that the norms actually converge monotonically up to approximately -20dB. For $\|\epsilon_k\|_2 < -25$dB, the signals are dominated by sensor noise (the finite resolution of the encoder).

The error signals during the observation time interval are presented in Figure 3.10. After convergence, the measured errors are in-between the optimal errors presented in the left three plots of Figure 3.10, and the "worst case" converged errors in the right three plots. The oscillations in Figure 3.10 (right) are caused by the finiteness of the encoder resolution, and the fact that the desired reference angle of 80 rad is not an integer times the resolution. Note, however, that with the resolution of the encoder equal to $\pi \cdot 10^{-3}$ rad, even the worst case errors are within one encoder count.

Though the error signals for all three control strategies look similar, the command signals clearly differ. In the top plot of Figure 3.11, the converged command sig-
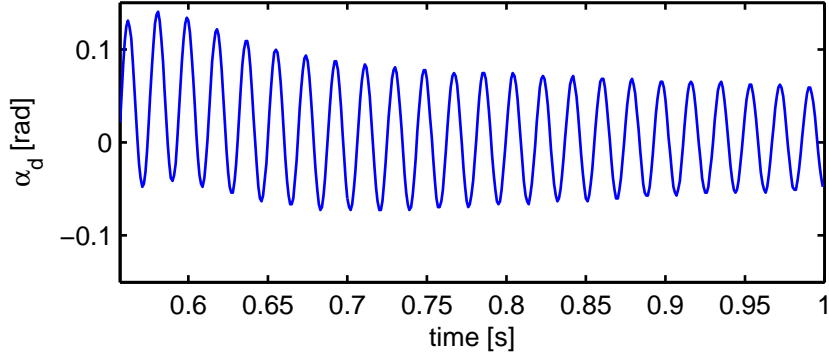
Figure 3.8: Residual vibration during observation interval, α_d, without Hankel ILC ($k = 0$).
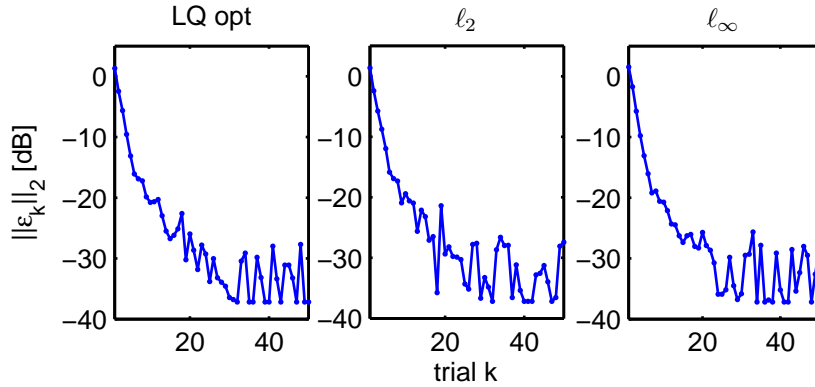
Figure 3.9: 2-norm of the error ϵ_k as function of trial k. Left: LQ norm optimal Hankel ILC. Center: ℓ_2 Hankel ILC. Right: ℓ_∞ Hankel ILC.

nals for LQ norm optimal control and ℓ_2 control are shown. Due to the chosen W_β, the ℓ_2 command signal has a maximum amplitude which is 5 percent smaller than the LQ norm optimal command signal. In the bottom plot, LQ norm optimal control is compared to ℓ_∞ control. In this case, the reduction in maximum amplitude is 18 percent.
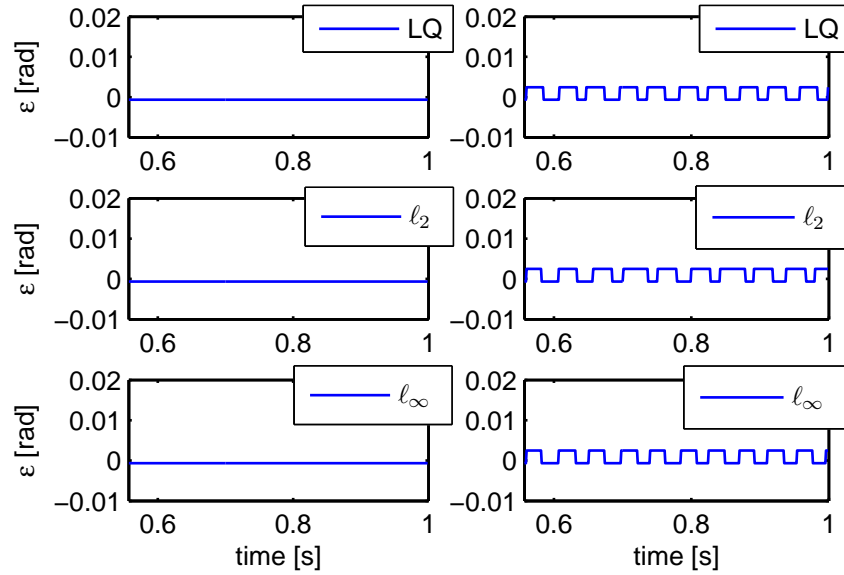
Figure 3.10: Error signals ϵ_k during observation interval. Top: LQ norm optimal Hankel ILC, Center: ℓ_2 Hankel ILC, Bottom: ℓ_∞ Hankel ILC. Left, top to bottom: optimal error signals after convergence (trials $k = 50$, $k = 47$, and $k = 48$, respectively), Right, top to bottom: worst case error signals after convergence (trials $k = 48$, $k = 50$, and $k = 50$, respectively).
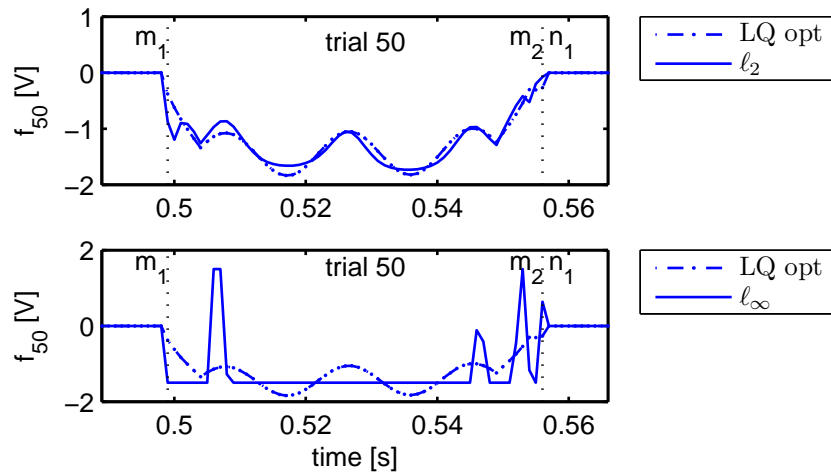
Figure 3.11: Converged command signals for LQ norm optimal, ℓ_2, and ℓ_∞ Hankel ILC.
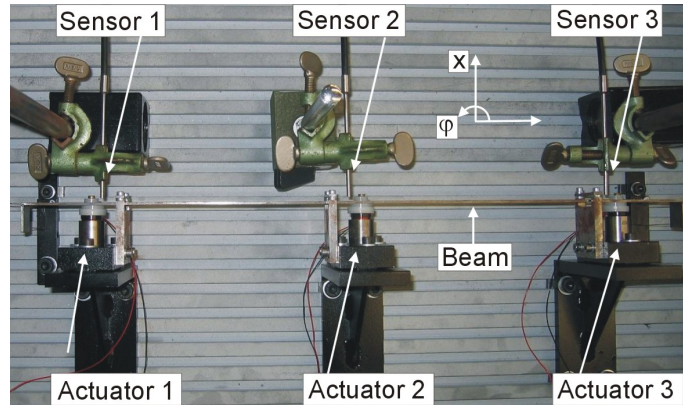
Figure 3.12: The flexible beam setup used for the experiments.
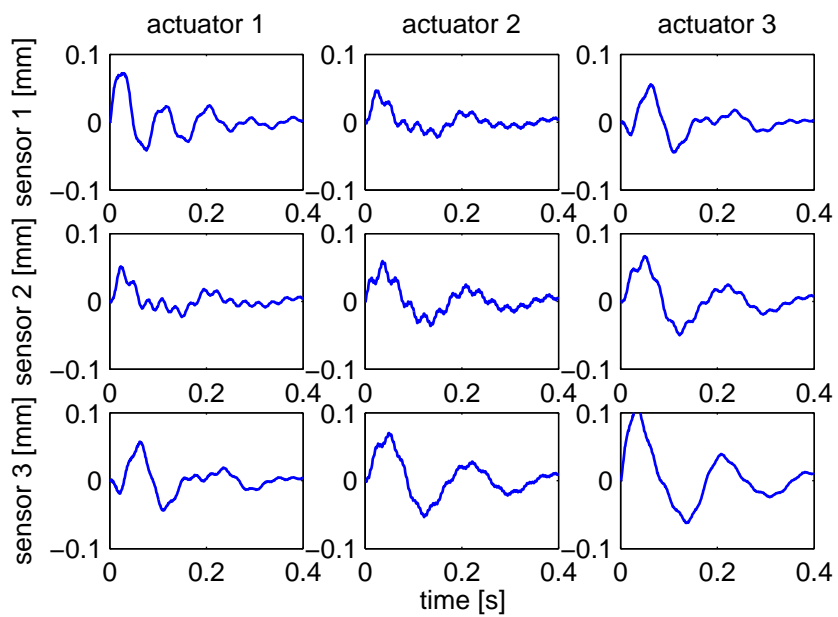
Figure 3.13: Impulse response of the MIMO flexible beam.

3.5 Example: flexible beam setup

In this section, we apply standard ILC (ILC for servo tasks), ℓ_2, and ℓ_∞ Hankel ILC to the MIMO flexible beam setup discussed in Appendix D, see also Figure 3.12. The measured impulse response of the time domain feedback controlled system is presented in Figure 3.13.

3.5.1   ILC for servo tasks

Initial situation

The reference signal used for the servo task is presented in Figure 3.14. The total number of samples in a trial is given by $N = 400$, and the sample time equals $T_s = 1 \cdot 10^{-3}$s.
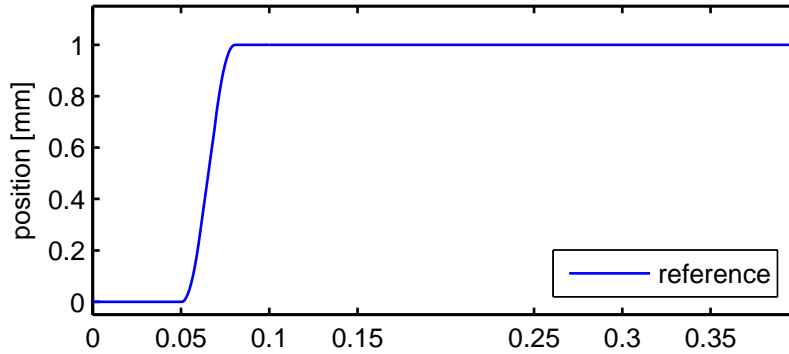
Figure 3.14: Reference signal for ILC for servo tasks.

To apply standard ILC on the setup, we first construct the convolution matrix J using the impulse response data of Figure 3.13. Although we could directly use the measured impulse response to define the model $J \in \mathbb{R}^{1200 \times 1200}$, due to uncertainty in the response (non repetitive elements such as noise), we consider only the first 300 singular values and directions of J for ILC control design ($p = 300$). Using the SVD of J, see Appendix A.3.6, we find $J_c = V_1^T \in \mathbb{R}^{300 \times 1200}$ and $J_o = U_1 \Sigma_1 \in \mathbb{R}^{1200 \times 300}$.

ILC control design and experimental results

Controller L_c is based on Proposition 3.1 with $M_c = 0$, and L_o is designed according to (3.14), with $R = rL_c(L_c^T L_c)^{-2} L_c^T = rL_c L_c^T$ since $L_c^T L_c = I_{300}$. The values $g = 0.5$ and $r = 0.01$ are determined experimentally.

The error e_k and command signal f_k during trial $k = 15$ are presented in Figure 3.15. Although the error norm $||e_k||_2$ decreases as function of k, the command signal has an undesired signal form for $T_s t \to 0.4$s. Clearly, the ILC controller has problems of generating a nonzero command signal near the end of the trial. Increasing p and/or decreasing r does improve the effect near $T_s t = 0.4$ s, but results in less smoother command signals during the trial, or even in trial domain instability. The fact that an increase in p reduces this effect, suggests that the signal forms in J which can generate the nonzero output for $T_s t \to 0.4s$ are present in the 900 singular directions which have been removed for ILC control design.

A (pragmatic) solution for this problem is found by adding time domain integrators to the system, and subsequently designing a convergent trial domain ILC
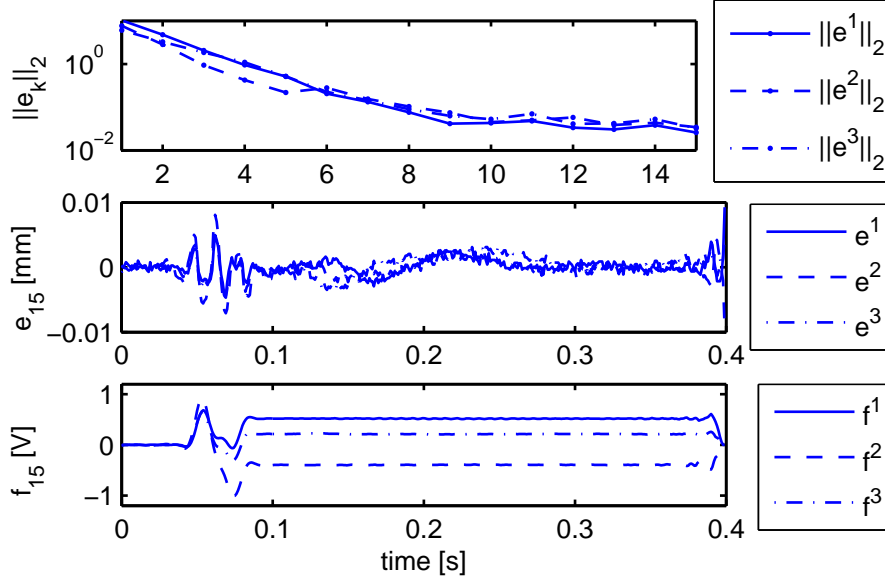
Figure 3.15: Standard ILC. Top: 2-norm of the error as function of trial number. Center: Error signal during trial $k = 15$. Bottom: Command signal during trial $k = 15$.

controller for this modified time domain system. As a consequence, ILC control design of L_o is now based on $J \rightarrow JT_{f_{int}}$, with

$$T_{f_{int}} = \begin{bmatrix} I_{q_i} & & 0 \\ \vdots & \ddots & \\ I_{q_i} & \cdots & I_{q_i} \end{bmatrix}$$

the lifted domain representation of the time domain integrator $\beta_k(t+1) = \beta_k(t) + \Delta\beta_k(t)$. Furthermore, controller L_c is now given by $L_c = T_{f_{int}}J_c^\dagger$. In this modified case, the trial state $u_k \neq \beta_k$. Rather, u_k corresponds to the rate change of the command signal β_k, i.e., $u_k(t) = \beta_k(t) - \beta_k(t-1)$.

In Figure 3.16, the error and command signal during trial 30 are shown. As can be seen, with the time domain integrators included in the ILC controller, the command signal now is capable of generating the nonzero output near $T_s t = 0.4$s.

Note that, although the reference signal is constant for $T_s t \in [0.081, 0.4]$s, the command signal during that time interval is not constant. This can be the result of trial varying disturbances for $T_s t > 0.081$ s. However, due to its periodic behavior, it is more likely that controller L_c is not capable of generating a constant command signal, i.e., there does not exist a linear combination of the vectors in L_c such that the output is constant. This phenomenon is explained by the fact that we designed L_c using only the first 300 singular vectors of $JT_{f_{int}}$. A less

oscillatory behavior of the command signals for $T_s t > 0.081$ s is obtained by increasing the number of singular vectors in L_c.
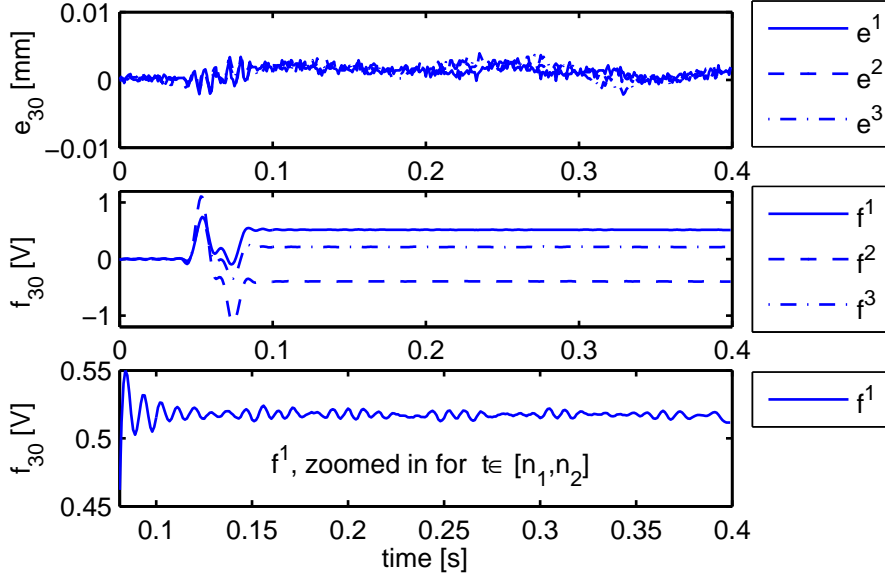
Figure 3.16: Standard ILC with additional integrators. Top: Error signal e_k during trial $k = 30$. Center: Command signal f_k during trial $k = 30$. Bottom: Command signal f_k during trial $k = 30$, zoomed in.

3.5.2 Hankel ILC design

Initial situation

For Hankel ILC, we use the reference signal shown in Figure 3.17, with actuation time interval: $m_1 = 50$ and $m_2 = 81$, giving $m = 32$, and observation time interval: $n_1 = 82$ and $n_2 = 400$, giving $n = 319$. Moreover, the residual vibrations α_d for trial $k = 0$ are presented in Figure 3.18. Although these vibrations are dominated by a resonance of 5.5Hz (translation mode), errors e^1 and e^2 also show higher frequency resonances.

The time-windowed system J_H for Hankel ILC equals $J_H = T_y J T_f$, with T_y given in (3.6) and T_f defined by

$$
T_f = T_{f_{int}} \begin{bmatrix} 0_{m_1 q_i \times m q_i} \\ I_{m q_i} \\ 0_{(N-m_2-1)q_i \times m q_i} \end{bmatrix}. \tag{3.22}
$$

Since the model for J is based on measurement data, we can only estimate the order of J_H. Using the singular values of J_H, see Figure 3.19, we choose $p = 12$.
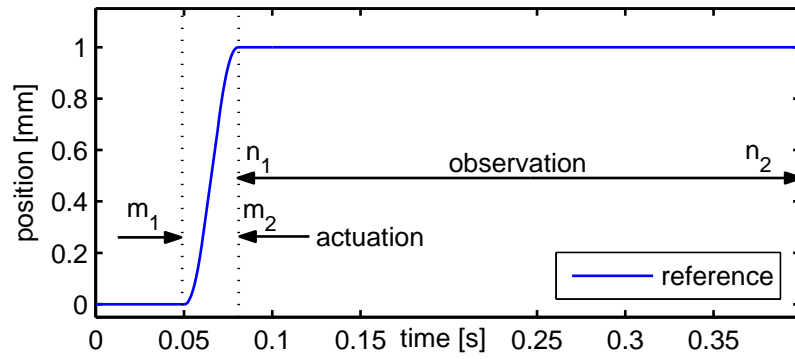
Figure 3.17: Reference signal with separated actuation and observation time interval.
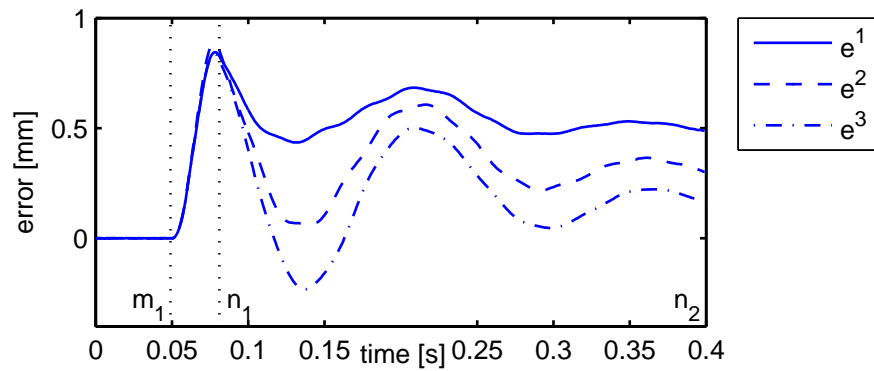
Figure 3.18: Residual vibration α_d for the three outputs corresponds to the error signals during $t \in [n_1, n_2]$.
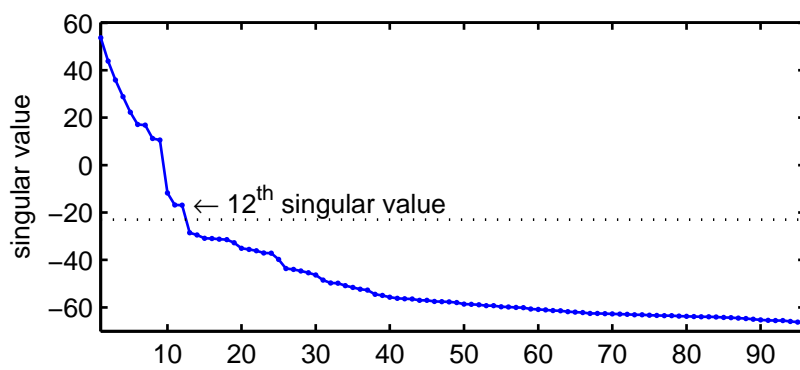
Figure 3.19: Singular values of J_H.

Hankel ILC control design

Based on J_H and $p = 12$, we design three Hankel ILC controllers. The three controllers have the same control element L_o, (3.14), with experimentally obtained values $g = 0.5$ and $R = rL_c(L_c^T L_c)^{-2}L_c^T$ with $r = 1$ (note that $L_c^T L_c \in \mathbb{R}^{12 \times 12}$). Moreover, the structure of the three L_c is also chosen equal: $L_c = T_{f_{int}}J_c^\dagger + T_{f_{int}}T_c^\dagger M_c$. The Hankel ILC controllers differ in the choice for M_c.

Experimental results

The first controller L_c equals (3.12) with $W_\beta = I_{mq_i}$. The resulting error signals as function of trial and time are presented in Figure 3.20. In accordance with Hankel ILC control design, the residual vibrations during the observation time interval are suppressed, while the error outside the interval is not compensated for.
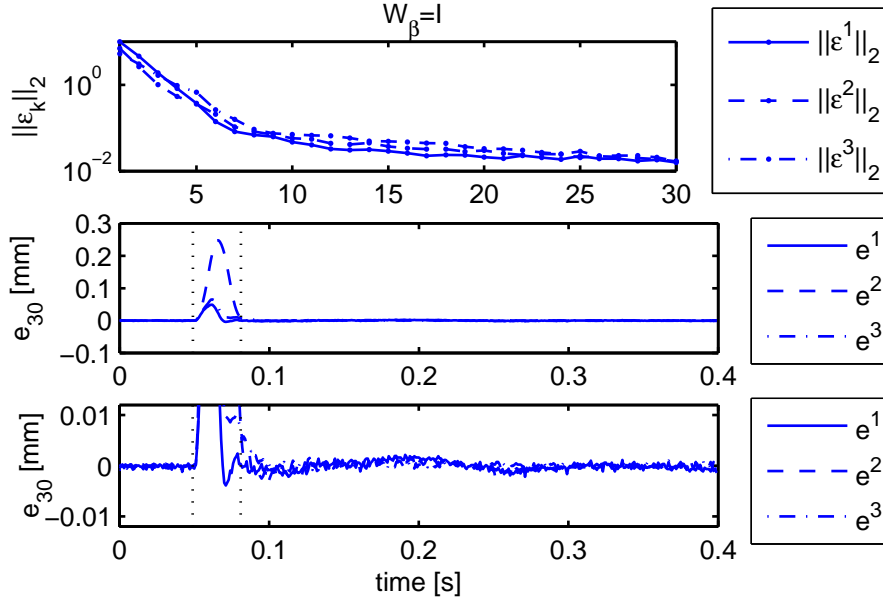
Figure 3.20: Hankel ILC with $W_\beta = I_{mq_i}$. Top: 2-norm of error ϵ_k as function of the trial. Center: Error signal e_k during trial $k = 30$. Bottom: Error signal e_k during trial $k = 30$, zoomed in.

The second controller L_c is similar to the first controller, but with a W_β given by

$$W_\beta = \mathrm{diag}(I_{q_i}, \ldots, 1.5I_{q_i}). \tag{3.23}$$

The diagonal matrix in (3.23) is used to penalize the command signal amplitudes, with gain 1 for $\beta_\infty(1)$ up to gain 1.5 for $\beta_\infty(m)$.

The results obtained with this second controller are presented in Figure 3.21. Although the error ϵ_{30} is slightly larger than ϵ_{30} of Figure 3.20, this Hankel ILC
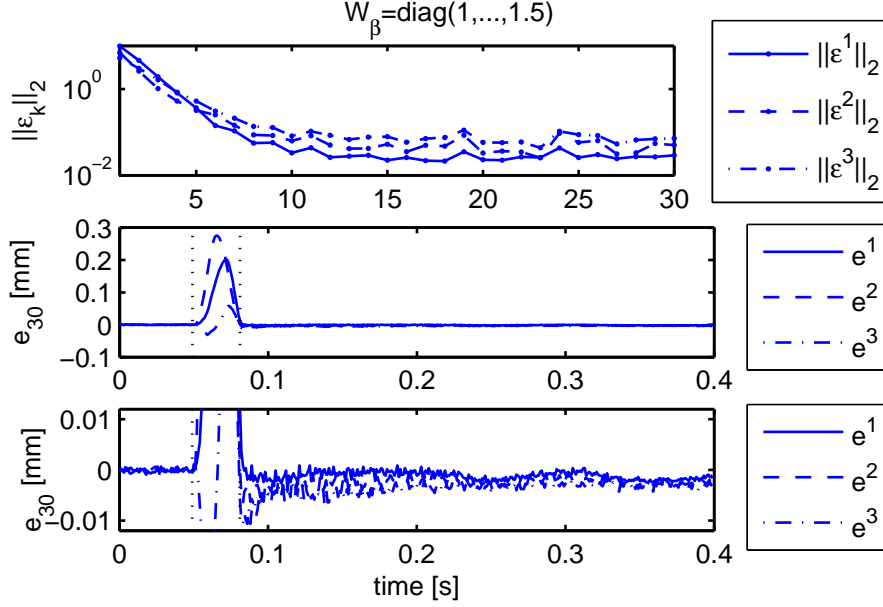
Figure 3.21: Hankel ILC with W_β of (3.23). Top: 2-norm of error ϵ_k as function of the trial. Center: Error signal e_k during trial $k = 30$. Bottom: Error signal e_k during trial $k = 30$, zoomed in.

controlled system is still very capable of suppressing the residual vibrations.

Finally, the third controller is based on ℓ_∞ Hankel ILC with an additional constraint on the rate change of the command signal: $\Delta_f = 1$ volt. The error signals obtained with this controller are given in Figure 3.22. The error is again slightly larger than ϵ_{30} of Figure 3.20, but still most of the residual vibrations are removed.

The differences in the size of the error signals can be explained as follows. During the design of the ℓ_2 and ℓ_∞ controllers, we assumed that $J_H T_{f_{int}} T_c^\dagger = 0$. Hence, we assumed that any signal $J_H T_{f_{int}} T_c^\dagger M_c u_k$ would give an output equal to zero. In this application, however, $J_H T_{f_{int}} T_c^\dagger > 0$ resulted in nonzero outputs. Consequently, for the cases $M_c \neq 0$, additional signal forms were present in the error signals which could not be compensated for by the Hankel ILC controller.

Based on the error results, it looks like all three controllers behave approximately equal. This is to be expected, since all three controllers have similar L_o and $T_{f_{int}} J_c^\dagger$. The difference between the controllers is found in M_c, and hence in the command signal forms applied to the system to obtain the above error signals, see Figure 3.23. Clearly, the signal forms of the different command signals differ during the actuation time interval. After $t = m_2$ though, all three command signals are constant and approximately equal (in contrast to standard ILC, Figure 3.16). Furthermore, when comparing the maximum amplitude of the command signals
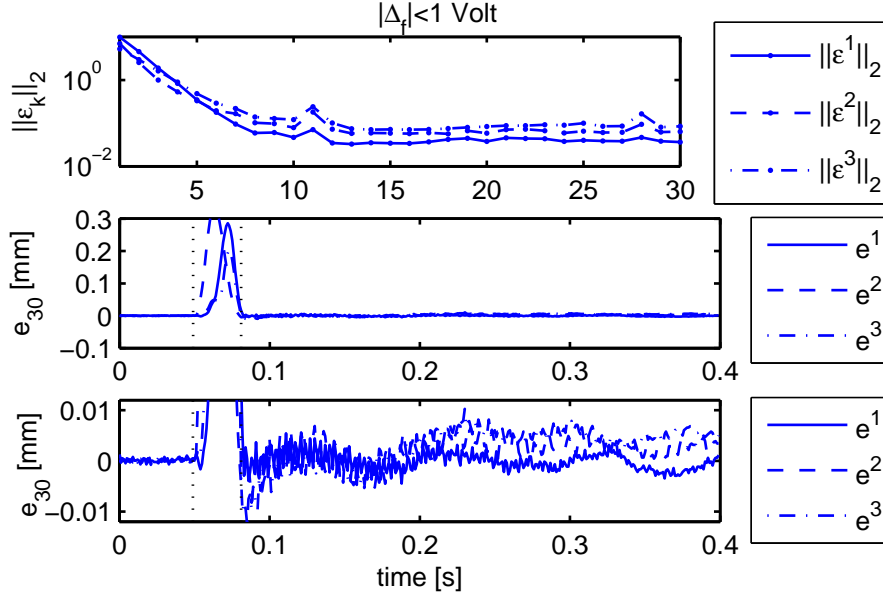
Figure 3.22: Hankel ILC with minimized maximum command signal amplitude. Top: 2-norm of error ϵ_k as function of the trial. Center: Error signal e_k during trial $k = 30$. Bottom: Error signal e_k during trial $k = 30$, zoomed in.

from the first controller with the second controller, a reduction in maximum signal amplitude of 25% is achieved. The maximum amplitude of the command signals of the third controller is even 48% smaller than that of the first controller.

3.6   Concluding remarks

We have derived a special form of ILC, denoted by Hankel ILC, which is capable of suppressing residual vibrations in flexible systems performing point-to-point motions. This special form has been obtained by introducing an actuation and observation time window in the ILC control framework. As a result, the time interval during a trial in which the system is actuated is separated from the time interval in which the measured output values used for ILC are collected.

Within a newly proposed ILC framework, we have shown that convergence of the ILC controlled system can be achieved. Furthermore, we have proven that there is the additional freedom in Hankel ILC control design to manipulate the amplitude of the command signal, and illustrated this with experiments on flexible motion systems.

From an input shaping point of view, Hankel ILC can be considered a new input
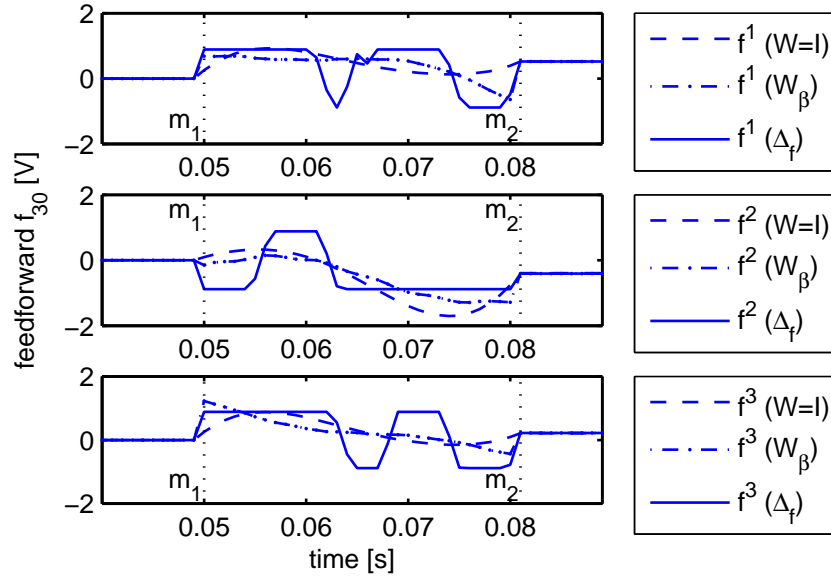
Figure 3.23: Command signal f^i, $i = 1, 2, 3$, for the three Hankel ILC controllers.

shaping technique capable of iteratively suppressing residual vibrations originating from multiple modes in presence of model uncertainty. From an ILC point-of-view, Hankel ILC has resulted in a better understanding of ILC for point-to-point motion problems. Moreover, it has revealed the different modeling and design issues in ILC for time-windowed systems.

Chapter 4

ILC for systems with basis functions

In this chapter, we extend and formalize the results of ILC for time-windowed systems from Chapter 3 to a larger class of systems consisting of linear systems with input/output (i/o) basis functions. First, we show that various different ILC formulations in the literature can be captured by a common system representation involving i/o basis functions. Second, analysis of this framework reveals how different ILC objectives (monotonic convergence, performance, minimization of input amplitudes) can be reached by design of separate parts of the ILC controller. The analysis is subsequently expanded by studying the effects of trial varying disturbances on performance. This results in suggestions for compensation of these effects. Finally, we use these results to systematically design ILC controllers for the representation under study, and we show that the obtained results are applicable to existing ILC problem formulations with i/o basis functions, and problem formulations which can be interpreted as such.

4.1   Basis functions in ILC

In this section, we show that time windows can be considered a specific class of basis functions. Based on this observation, in this chapter, we will extend and formalize the Hankel ILC results of Chapter 3 to the class of linear systems with basis functions.

Originally, in Chapter 2 we introduced an ILC framework which can be used to servo problems, Figure 4.1 (top). Subsequently, in Chapter 3 we discussed ILC for time-windowed systems using the example of Hankel ILC. For that purpose, we included time windows (T_f, T_y) in the ILC framework, resulting in Figure 4.1 (bottom).

In Figure 4.1, T_f is the matrix with input basis functions which maps the coefficient vector β_k to the command signal f_k, y_k equals the output signal, and α_k denotes the projected output onto a space spanned by the output basis functions contained in matrix T_y. Furthermore, α_d is the reference signal in the space spanned by the basis functions in T_y.
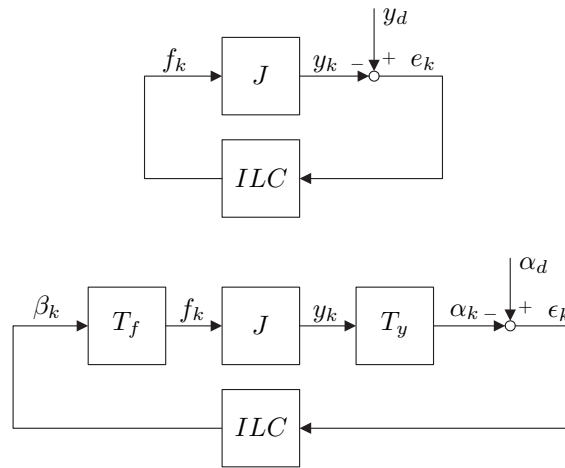
Figure 4.1: Top: Original ILC framework for servo problems. Bottom: ILC framework with additional input filter T_f and output filter T_y representing, e.g., time window filters.

As mentioned, in Hankel ILC the filters (T_f, T_y) correspond to time windows. This is, however, only one possible choice for basis functions. To analyze the use of basis functions in ILC (both implicitly and explicitly), and to give examples of interpretations of β_k, α_k, and (T_f, T_y), we investigate the following systems and applications.

Basis functions for restricted time windows
References [7, 66] and [76] study performance and convergence properties of systems with nonzero relative degrees and delays. With the original system not suitable for analysis, the i/o mapping of the system is reduced by removal of the final samples and first samples from i/o mapping, Figure 4.2, and by defining the reference signal to comply with this projected output time interval.

Basis functions for restricted command-output space
The authors of [50, 61, 62, 69, 132] and [138] overcome the high-dimensional problem of describing linear systems for ILC by capturing the i/o behavior of the system in a restricted i/o space. This is accomplished by describing the command

Figure 4.2: Top: The command signal (time signal) is constructed from a coefficient vector of length $m + 1$ and $m + 1$ unit pulse basis functions (bf) which represent the time window. The final $N - m - 1$ samples of the command signal equal zero. Bottom: The output (time signal) is filtered by unit pulse basis functions to obtain a projected output of length $N - n$. This projected output equals the output signal for time interval $t \in [n, N - 1]$.

as a linear combination of a relatively small set of basis functions (in comparison with the number of samples N in a trial), and by mapping the output onto a reduced output space, Figure 4.3. These basis functions are a function of the original reference signal and system dynamics, or are user defined. Moreover, the original reference signal is mapped onto the lower dimensional projected output space.
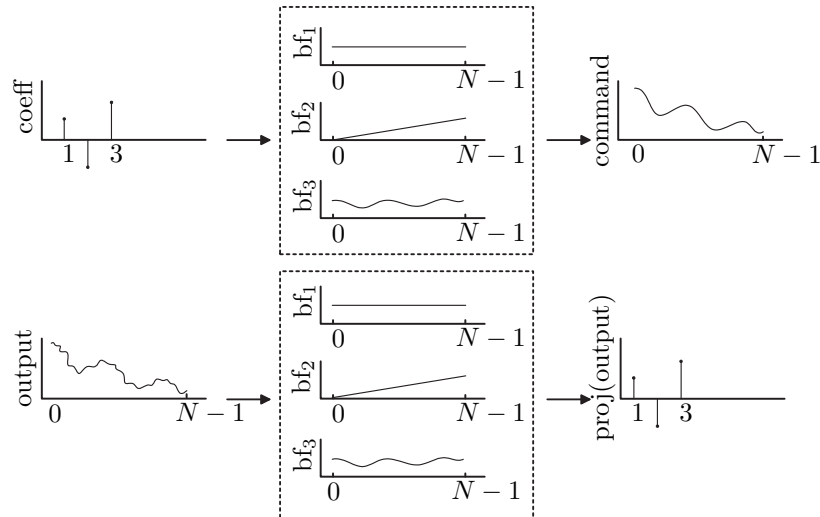
Figure 4.3: Top: The command signal (time signal) is the scaled sum of three basis functions (bf), with the scaling factors captured in the coefficient vector. Bottom: The output signal is projected onto an output space with three components.

Basis functions for specialized tasks

References [29, 54, 137] demand the suppression of the terminal error sample at the end of a trial by actuating the system with a single command signal (terminal ILC). This solution can be seen as the result of applying a single basis function to construct the command signal and a time window to the output of the system, Figure 4.4. Note that in terminal ILC, the reference signal consists of only one sample.
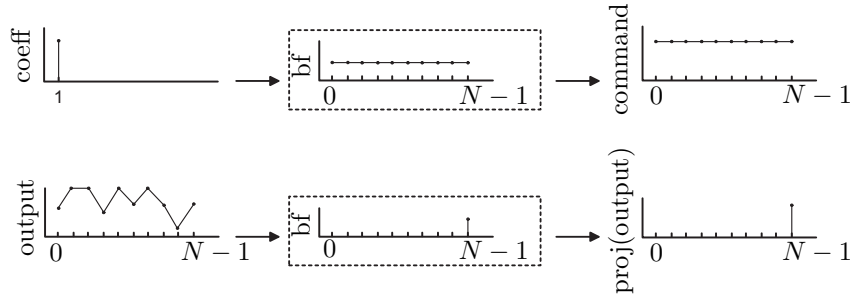
Figure 4.4: Terminal ILC. Top: The command signal is the result of one scaled basis function, with the scaling factor captured in the coefficient vector. Bottom: The projected output signal equals the final time sample the output signal.

The authors [68, 142] downsample the i/o signals of the system using time windows to achieve specific convergence properties of the ILC controlled system, see Figure 1.3 (bottom). In this case, the reference signal is defined using the lower sample rate.

In Chapter 3, we used ILC for residual vibration suppression in point-to-point motion problems. Since these problems require a system that is being actuated during the point-to-point motion while the residual vibrations are being measured after arrival at the desired position, we introduced time window based basis functions corresponding to actuation and observation time windows in the control problem, Figure 4.5. In this case, the reference signal corresponds to the desired position during the observation time interval.

The discussed systems and applications all have in common that the i/o behavior of the original system J is modified to comply with the desired ILC problem statements. Moreover, the reference signals α_d are problem dependent. Based on these observations, in this chapter we formulate a system description which encompasses the discussed systems and applications as special cases, and introduce an ILC framework suitable for this system description. Moreover, we derive an ILC analysis and design theory for systems with basis functions, based on the proposed ILC framework.

Note that the ILC framework is similar to Figure 3.4. In contrast, the derivation of the analysis and design theory is based on existing ILC control theory, however, modified such that it is applicable to the proposed ILC framework. Consequently,
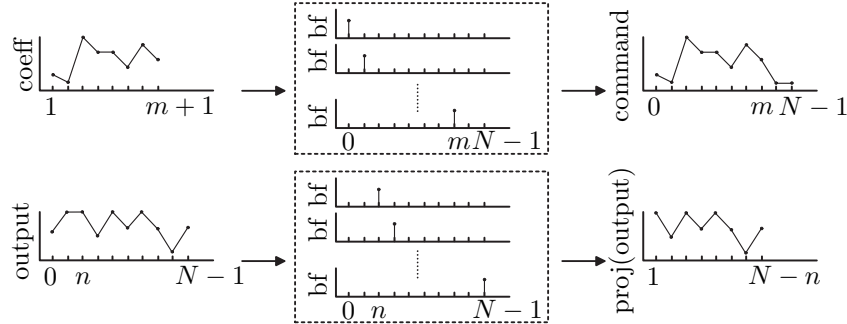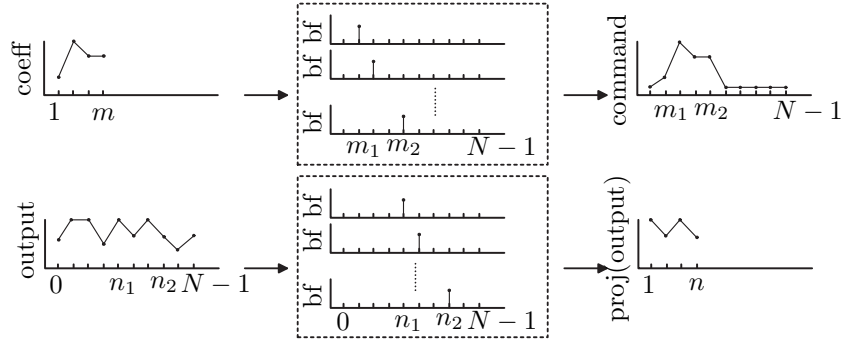
Figure 4.5: Hankel ILC: Top: The command signal (time signal) is constructed from a coefficient vector of length $m = m_2 - m_1 + 1$ and m unit pulse basis functions (bf) which represent the time window. The first m_1 and final $N - m_2 - 1$ samples of the command signal equal zero. Bottom: The output (time signal) is filtered by unit pulse basis functions to obtain a projected output of length $n = n_2 - n_1 + 1$. This projected output equals the output signal for time interval $t \in [n_1, n_2]$.

the analysis and design theory is the extension of existing ILC control theory to linear systems with basis functions.

In the discussion on the analysis and design theory for the proposed ILC framework, we focus on the ILC control objectives presented in Figure 4.6. As a result, in this chapter we do not focus on, e.g., robustness aspects of ILC in presence of model uncertainty [43, 89], or initial condition disturbances due to errors in the resetting of the system between two trials [71, 142].

The outline of this chapter is as follows. In Section 4.2, a system description
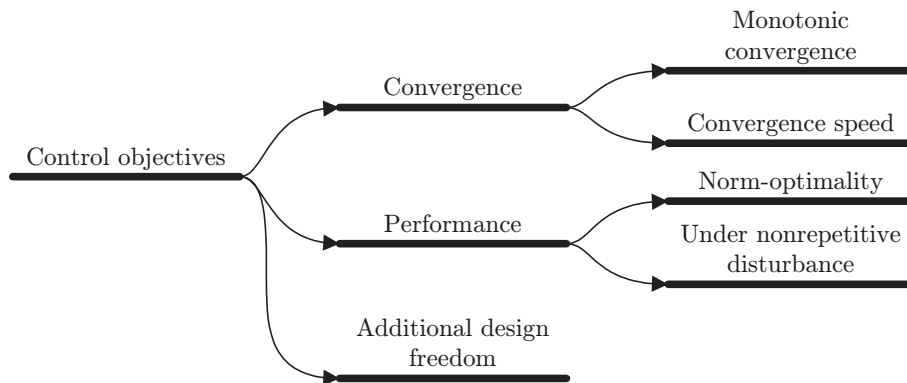
Figure 4.6: ILC control objectives.

is presented which encompasses the discussed systems and applications as special cases. Moreover, we introduce an ILC framework which is suitable for this generalized system. ILC control objectives in this ILC framework are analyzed from a system perspective in Section 4.3, yielding ILC controller conditions which are required for convergence and optimal performance. In Section 4.4, the ILC framework is analyzed from an ILC control design perspective. This reveals how different ILC objectives can be reached by design of separate parts of the ILC controller. Performance under trial varying disturbances is subsequently analyzed in Section 4.5, resulting in guidelines on how to reduce the effects of the trial varying disturbances on performance. In Section 4.6, the obtained analysis results are used in the design of ILC controllers for systems with basis functions. In addition, practical suggestions and choices are given to facilitate straightforward design. To briefly exemplify the generality of the obtained results, in Section 4.7 three examples from ILC literature are discussed. And finally, concluding remarks are given in Section 4.8.

Part of the contents of this chapter is published in [128].

4.2 General ILC system description

In this section, we consider LTV systems J as given in (2.1), with $f(t) \in \mathbb{R}^{q_i}$ the command signal, and $y(t) \in \mathbb{R}^{q_o}$ the output signal. For the time span of a trial $t \in [0, N-1]$, the i/o behavior of J is represented by J of (2.3).

The discussed systems and applications in Section 4.1 all have in common that they modify the original system to meet the ILC problem statements. Starting with the original system $y = Jf$, the manipulation of the command signal f corresponds to f becoming a function of a new command signal β, and a matrix T_f containing basis functions, i.e., $f = T_f \beta$. Similarly, the new manipulated output α is the result of the mapping of the output y onto a limited output space spanned by the basis functions contained in the matrix T_y, i.e., $\alpha = T_y y$. Depending on the problem formulation, the basis functions correspond to time windows, or to reference signals and user defined signals.

Let $\phi_j \in \mathbb{R}^{N q_i}$, $j = 1, 2, \ldots, m$, be the basis functions used to build the command signal, and $\theta_i \in \mathbb{R}^{N q_o}$, $i = 1, 2, \ldots, n$, the basis functions used to define a lower dimensional output space. These basis functions form the matrices T_f and T_y defined by (4.1).

$$
\begin{aligned}
T_f &= \begin{bmatrix} \phi_1 & \phi_2 & \ldots & \phi_m \end{bmatrix}, & T_f &\in \mathbb{R}^{N q_i \times m}, \\
T_y &= \begin{bmatrix} \theta_1 & \theta_2 & \ldots & \theta_n \end{bmatrix}^T, & T_y &\in \mathbb{R}^{n \times N q_o}.
\end{aligned}
\tag{4.1}
$$

The result of modifying the i/o behavior of the original system J using the basis functions is presented in Figure 4.7. The mapping $H : \ \beta_k \mapsto \alpha_k$ is obtained by

considering T_f and T_y as part of the new system $H = T_y J T_f$. Consequently, ILC control design shifts from design for system J with time signals (f_k, y_k) to design for system H with coefficient signals (β_k, α_k).
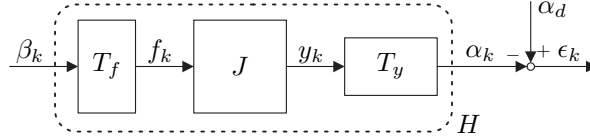
Figure 4.7: General system $H \in \mathbb{R}^{n \times m}$ consisting of system J and matrices T_f and T_y, with T_f and T_y containing the input and output basis functions, respectively.

The error signal $\epsilon_k \in \mathbb{R}^n$ in Figure 4.7 corresponds to the difference between the reference signal $\alpha_d \in \mathbb{R}^n$ and $\alpha_k \in \mathbb{R}^n$. As illustrated in Section 4.1, this reference signal is problem dependent, and defined in the space spanned by T_y.

As is already demonstrated in Chapter 3, the rank of $H \in \mathbb{R}^{n \times m}$ can be smaller than the smallest dimension of H, i.e., $p = \text{rank}(H) < \min(m, n)$. This can be caused by the properties of J, e.g., time delays and non-minimum phase zeros, [123], or by the number and the characteristics of basis functions present in the T_f and T_y, e.g., time windows. To properly handle these situations, decomposition of H using a full rank decomposition is essential, (4.2).

$$H_o H_c := H, \quad \alpha_k = H_o x_k, \quad x_k = H_c \beta_k, \tag{4.2}$$

with $x_k \in \mathbb{R}^p$, $H_o \in \mathbb{R}^{n \times p}$, $H_c \in \mathbb{R}^{p \times m}$, and $\text{rank}(H_o) = \text{rank}(H_c) = \text{rank}(H) = p$ by definition.

Following the IMP reasoning of Section 3.2, we use the ILC algorithm given by

$$u_{k+1} = u_k + L_o \epsilon_k, \quad \beta_k = L_c u_k, \quad u_0 = 0, \tag{4.3}$$

with $u_k \in \mathbb{R}^p$ the trial domain state. By combining (4.2) and (4.3), we find the control framework presented in Figure 4.8. Although we focus on this system representation for our ILC analysis and control design, for implementation of the framework we use Figure 4.9. Note that choosing $L_c^{im} = T_f L_c$ makes the structure of Figure 4.9 equivalent to that of Figure 4.8.

Remark 4.1. As we have seen in Chapter 3, in the case that the basis functions are defined by time windows, the coefficient signals β_k and α_k are time signals.

Remark 4.2. With $H = T_y J T_f$ capturing the various ILC control problems discussed in Section 4.1, we refer to H as the general system description. The explicit formulation of H as the product of two full rank matrices can be considered a minimal representation of H.

Remark 4.3. The ILC control structure of (4.3) encompasses, among others, trial invariant ILC controllers with Arimoto gains, inverse model based ILC, and LQ norm optimal ILC.
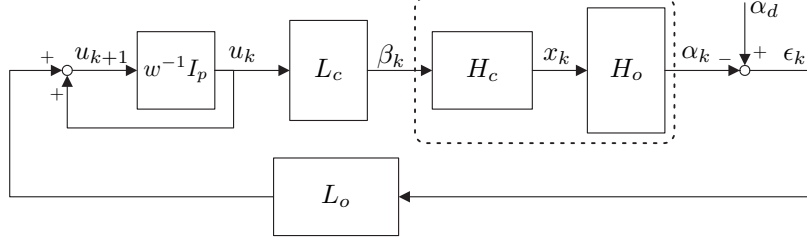
Figure 4.8: ILC framework in trial domain, with ILC controllers (L_o, L_c).
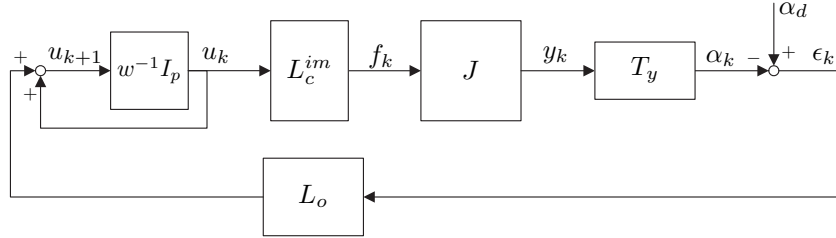
Figure 4.9: Implementable form of the ILC framework of Figure 4.8.

4.3 ILC analysis for systems with basis functions, a system perspective

Analysis of the ILC framework of Figure 4.8 consists of studying the different ILC control objectives presented in Figure 4.6. In this section, the control objectives are discussed from a system perspective. In Section 4.4, we discuss the objectives from an ILC control design perspective. The discussion of performance under trial varying disturbances is left for Section 4.5.

4.3.1 Convergence

Using (4.2) and (4.3), the trial domain dynamics are given by

$$u_{k+1} = (I_p - L_o H L_c)u_k + L_o \alpha_d, \quad u_0 = 0 \tag{4.4a}$$
$$f_k = L_c^{im} u_k. \tag{4.4b}$$

By combining the definition of monotonic convergence, Definition 2.6, and the formulation of the trial domain dynamics, (4.4), we can formulate a sufficient condition for monotonic convergence for the proposed ILC controlled system.

Lemma 4.1. *Consider the ILC controlled system* (4.4). *Then* (4.4) *is* convergent *iff the spectral radius* $\rho(I_p - L_o H L_c) < 1$, *and* monotonically convergent *in* f_k *if* $\|T^{-1}(I_p - L_o H L_c)T\|_{i2} < 1$, *with* T *satisfying* $T^T L_c^{im^T} L_c^{im} T = I_p$.

Proof. See Appendix A.4.1. □

The matrix T can be obtained by factorizing $L_c^{im^T} L_c^{im}$ using, e.g., a Cholesky decomposition. Lemma 4.1 states that MC of the trial state $z_k = T^{-1} u_k$ implies MC of the command signal f_k. For $L_c^{im} = L_c = I_{Nq_i}$ and $L = L_o T_y$, the monotonic convergence condition from Lemma 4.1 equals that of Lemma 2.1.

Finally, we refer to Section 2.3 for an interpretation of convergence speed of command signal f_k. Note that, as a result of the introduction of framework of Figure 4.8, $\|I_{Nq_i} - LJ\|_{i2} = \kappa$ in Section 2.3 should be replaced by $\|T^{-1}(I_p - L_o H L_c)T\|_{i2} = \kappa$ for a proper interpretation.

4.3.2 Performance

Definition 2.7 states that performance is a function of the performance variable ξ_k for $k \to \infty$. Furthermore, optimal performance corresponds to the minimized ξ_∞ over all stabilizing ILC controllers L, (2.11). Based on these definitions, we propose the following measures for (optimal) performance based on the ILC framework of Figure 4.8.

Proposition 4.1. *Consider ILC controlled system* (4.4a), *and assume that* (4.4a) *is convergent. Furthermore, consider performance variable* $\xi_k = \epsilon_k$. *Then performance* $\mathcal{P}_\epsilon$ *and optimal performance* $\mathcal{P}_{\epsilon,opt}$ *are given by* (4.5) *and* (4.6), *respectively.*

$$\mathcal{P}_\epsilon(L_o, L_c) = \lim_{k \to \infty} \|\epsilon_k\|_2 \tag{4.5}$$

$$\mathcal{P}_{\epsilon,opt}(L_o, L_c) = \min_{L_o, L_c} \mathcal{P}_\epsilon(L_o, L_c). \tag{4.6}$$

Based on Proposition 4.1, we can state the following:

Lemma 4.2. *Consider ILC controlled system* (4.4a), *and assume that* (4.4a) *is convergent. Then there exist a lower bound for* $\mathcal{P}_{\epsilon,opt}$ *equal to* $\|(I_n - H_o H_o^\dagger)\alpha_d\|_2$.

Proof. Given $\epsilon_\infty = \alpha_d - H_o x_\infty$, with $\epsilon_\infty = \lim_{k \to \infty} \epsilon_k$ the asymptotic error. Then optimal performance is achieved for $x_\infty^* = \arg\min_{x_\infty} \|\epsilon_\infty\|_2 \to x_\infty^* = H_o^\dagger \alpha_d$. As a result, the lower bound for $\mathcal{P}_{\epsilon,opt}$ equals $\|\epsilon_\infty^*\|_2$, with $\epsilon_\infty^* = (I_n - H_o H_o^\dagger)\alpha_d$. □

From Lemma 4.2, we can conclude that optimal performance is reached if $\epsilon_\infty \in \text{im}(H)^\perp \ \forall \alpha_d \in \mathbb{R}^n$. In Corollary 4.1, we study the set of ILC controllers for which $\mathcal{P}_{opt}$ is reached.

Corollary 4.1. *Consider ILC controlled system* (4.4a), *and assume that* (4.4a) *is convergent. Then optimal performance* $\mathcal{P}_{\epsilon,opt}$ *is reached iff* $(L_o, L_c) \in \{(L_o, L_c) : H_c L_c (L_o H L_c)^{-1} L_o = H_o^\dagger\}$.

Proof. Given $u_\infty = (L_o H L_c)^{-1} L_o \alpha_d$ and $x_\infty = H_c L_c u_\infty$. Then the asymptotic error equals $\epsilon_\infty = \alpha_d - H_o x_\infty$, with $x_\infty = H_c L_c (L_o H L_c)^{-1} L_o \alpha_d$. From Lemma 4.2, we know that $\mathcal{P}_{\epsilon,opt}$ requires $x_\infty^* = H_o^\dagger \alpha_d$. Consequently, $\mathcal{P}_{\epsilon,opt}$ is reached iff $(L_o, L_c) \in \{(L_o, L_c) \in (\mathbb{R}^{p \times n}, \mathbb{R}^{m \times p}) : H_c L_c (L_o H L_c)^{-1} L_o = H_o^\dagger\}$. $\qquad\square$

Note that optimal performance is a function of $\operatorname{im}(H) = \operatorname{im}(H_o)$. With H_o a function of (T_f, T_y), the number of basis functions and their characteristics both influence the reachable performance.

4.4 ILC analysis for systems with basis functions, a design perspective

In this section, we show that the different control objectives discussed in Section 4.3 can be linked to different parts of the ILC controllers (L_o, L_c). To accomplish this, $L_o \in \mathbb{R}^{p \times n}$ and $L_c \in \mathbb{R}^{m \times p}$ are parameterized by (4.7) and (4.8), respectively, see Figure 4.10.

$$L_o = S_o P_o, \quad \text{with } S_o \in \mathbb{R}^{p \times p} \text{ and } P_o \in \mathbb{R}^{p \times n} \tag{4.7}$$

$$L_c = H_c^\dagger S_c + T_c^\dagger M_c, \quad \text{with } S_c \in \mathbb{R}^{p \times p}, \ T_c^\dagger = \mathbb{R}^{m \times (m-p)}, \tag{4.8}$$

and $M_c \in \mathbb{R}^{(m-p) \times p}$ arbitrary. Matrix $T_c^\dagger$ follows from the full rank decomposition $T_c^\dagger T_c := I_m - H_c^\dagger H_c$. Note that, due to the definition of $T_c^\dagger$, matrices S_c and M_c operate in two independent subspaces.

Intuitively, the parametrization can be explained as follows. By parameterizing L_o as done in (4.7), we explicitly reveal the design choices in L_o. On the one hand, we have a performance filter P_o which can be chosen to pass through signals in a specific subspace, e.g., the signal forms $\epsilon_k \in \operatorname{im}(H_o)$, since these signal forms are the only signals that can be compensated for by ILC anyway. On the other hand, we obtain an additional gain matrix S_o which can be used for stabilization of the ILC controlled system. The parametrization of L_c is based on the fact that the coefficient vector $\beta_k = L_c u_k$ is divided into a part $T_c^\dagger M_c u_k$ operating in the kernel space of H_c, and a part $H_c^\dagger S_c u_k$ operating in the space perpendicular to $\ker(H_c)$. By design of M_c, the signal $T_c^\dagger M_c u_k$ can be used to modify the specific values in the vector β_k without influencing the stability properties of the ILC controlled system (since $H_c T_c^\dagger M_c = 0$). Conversely, the signal $H_c^\dagger S_c u_k$ does influence stability, and hence S_c is to be designed such that the ILC controlled system is convergent.
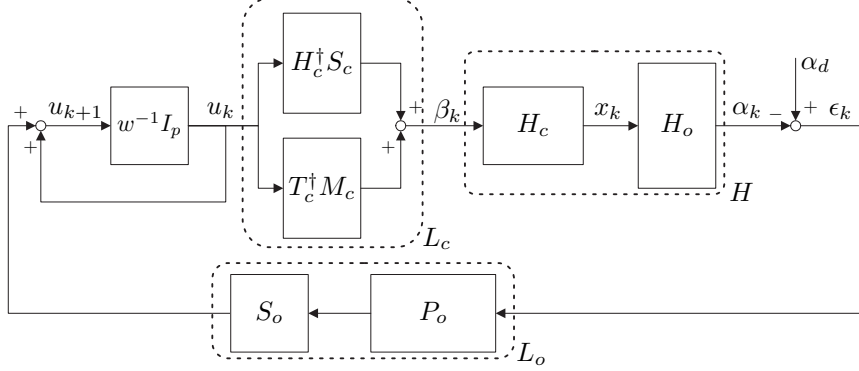
Figure 4.10: ILC framework in trial domain, with parameterized ILC controllers (4.7) and (4.8).

Lemma 4.3. *Given ILC controller (L_o, L_c), then there exists parameters (S_o, S_c, P_o, M_c) such that (4.7) and (4.8) hold. Conversely, given the parameters (S_o, S_c, P_o, M_c), then there exists (L_o, L_c) such that (4.7) and (4.8) hold.*

Lemma 4.3 shows that the parametrization of (4.7) and (4.8) does not restrict design freedom in (L_o, L_c).

In the following sections, we discuss the relation between the parametrization of L_o and L_c and the control objectives presented in Figure 4.6.

4.4.1 Convergence

The following Lemma refines the results of Lemma 3.1.

Lemma 4.4. *Consider (4.7) and (4.8) which explain how (L_o, L_c) are formed by the choice of (S_o, S_c, P_o, M_c). Then 1) for any given M_c, any S_c with $\mathrm{rank}(S_c) = p$, and any P_o with $\mathrm{rank}(P_o H_o) = p$, there exist S_o such that (4.4) is monotonically convergent in f_k with any desired convergence speed, and 2) for any given M_c, any S_o with $\mathrm{rank}(S_o) = p$, any P_o with $\mathrm{rank}(P_o H_o) = p$, there exist S_c such that (4.4) is monotonically convergent in f_k with any desired convergence speed.*

Proof. Follows from Lemma 3.1. $\qquad\square$

Note that the gains in P_o do not restrict the gain $\overline{\sigma}(T^{-1}(I_p - L_o H L_c)T)$. On the contrary, Lemma 4.4 states that after design of P_o, S_o and S_c can be chosen such that $\overline{\sigma}(T^{-1}(I_p - L_o H L_c)T)$ has any desired gain.

Note furthermore, that the rank condition $\mathrm{rank}(P_o H_o) = p$ in the monotonic convergence condition imposes only a minor constraint on P_o. The actual mechanism

behind P_o is that it maps the signal $\epsilon_k \in \text{im}(H_o)$ to a lower dimensional space. In Section 4.4.2 and Section 4.5, choices for P_o will be given based on performance demands.

In Lemma 4.5, we focus on conditions for (S_o, S_c) which are required for assignment of the gain $\overline{\sigma}(T^{-1}(I_p - L_o H L_c)T)$.

Lemma 4.5. *Let $K \in \mathbb{R}^{p \times p}$ be chosen such that $I_p - K$ has the desired gains, i.e., such that $I_p - K$ is monotonically convergent with any desired convergence speed. Furthermore, consider (4.7) and (4.8) which explain how (L_o, L_c) are formed by the choice of (S_o, S_c, P_o, M_c). Then for any given M_c and any P_o with $\text{rank}(P_o H_o) = p$, the set of (S_o, S_c) for which (4.4) has gains equal to those of $I_p - K$ is given by*

$$\{(S_o, S_c) \in (\mathbb{R}^{p \times p}, \mathbb{R}^{p \times p}) : S_o P_o H_o S_c = TKT^{-1},$$
$$T^T(S_c + T_c^\dagger M_c)^T T_f^T T_f(S_c + T_c^\dagger M_c)T = I_p\}. \tag{4.9}$$

Proof. Follows from substitution of (4.7) and (4.8) in Lemma 4.1. □

Note that in Lemma 4.5, matrix T is a function of (S_c, M_c). Substitution of T in $S_o P_o H_o S_c = TKT^{-1}$ subsequently reveals that for given (S_o, P_o, M_c), finding S_c such that (4.4) has the desired gains requires solving a nonlinear relation in S_c. On the other hand, for given (S_c, M_c), matrix T follows directly. Subsequent assignment of the desired gains by S_o requires solving $S_o P_o H_o S_c = TKT^{-1}$, which is linear in S_o. Hence, gain assignment by S_o is more transparant and more straightforward then gain assignment by S_c.

Corollary 4.2. *Let $K \in \mathbb{R}^{p \times p}$ be chosen such that $I_p - K$ is monotonically convergent with any desired convergence speed. Furthermore, let (S_c, P_o, M_c) be given and let T follow from $T^T L_c^T T_f^T T_f L_c T = I_p$. Then $S_o = TKT^{-1} S_c^{-1}(P_o H_o)^{-1}$ results in (4.4) which is monotonically convergent in f_k and has the desired convergence speed.*

An extreme case of convergence is deadbeat convergence, as defined in Section 4.3 by $\|T^{-1}(I_p - L_o H L_c)T\|_{i2} = 0$. This case is worked out in detail in the following Corollary.

Corollary 4.3. *Consider the set of (S_o, S_c) of Lemma 4.5. Then the subset of (S_o, S_c) for which (4.4) is deadbeat, is given by*

$$\{(S_o, S_c) \in (\mathbb{R}^{p \times p}, \mathbb{R}^{p \times p}) : S_o P_o H_o S_c = I_p\}.$$

Note that for deadbeat ILC control, the expression TKT^{-1} of Lemma 4.5 equals I_p (since $K = I_p$). Since I_p is not a function of T, in Corollary 4.3 we do not need to determine T.

4.4.2 Performance

In Lemma 4.6, we reveal the relation between performance, as specified in Proposition 4.1, and the parametrization presented in (4.7) and (4.8). Consequently, Lemma 4.6 makes precise what we stated intuitively about P_o in the beginning of this section.

Lemma 4.6. *Consider (4.7) and (4.8) which explain how (L_o, L_c) are formed by the choice of (S_o, S_c, P_o, M_c). Then for any (S_o, S_c) for which (4.4) is convergent, and for any M_c, 1) performance is a function of P_o only, i.e., does not depend on the specific choice of (S_o, S_c, M_c), and 2) optimal performance is achieved with $P_o = H_o^T$.*

Proof. See Appendix A.4.2.   □

The choice $P_o = H_o^T$ in Lemma 4.6 is not unique. Indeed, optimal performance is achieved for any P_o satisfying $\{P_o : (P_o H_o)^{-1} P_o = H_o^\dagger\}$.

We have discussed monotonic convergence and performance as ILC control objectives. These objectives turn out to be separately attainable by the choice of matrices (S_o, S_c) to obtain monotonic convergence, and P_o to obtain performance. As a result, there is considerable design freedom left, to be appointed to a yet undefined control objective. As we will show next, for the parametrization (4.7) and (4.8), this freedom is found in the choice for M_c.

4.4.3 Additional design freedom:
exploiting command non-uniqueness

Lemma 4.7. *Consider (4.7) and (4.8) which explain how (L_o, L_c) are formed by the choice of (S_o, S_c, P_o, M_c). Then the choice for $M_c \in \mathbb{R}^{(m-p) \times p}$ neither influences the monotonic convergence objective, nor the performance objective.*

Proof. Follows from Lemma 4.4 and Lemma 4.6.   □

The additional design freedom in the ILC control framework in Figure 4.8 is due to the fact that the map between β_k and α_k has a low rank. That M_c does not influence α_k is due to the fact that $H T_c^\dagger M_c = 0$ for all M_c. An example of when $M_c \neq 0$ is useful can be found in Section 3.3.

In Proposition 4.2, we extend the results of Proposition 3.3.

Proposition 4.2. *Given L_c from (4.8), the ILC controlled system (4.4), and optimization problem $\min_{M_c} \beta_\infty^T W_\beta \beta_\infty$, with $\beta_\infty = \lim_{k \to \infty} \beta_k$ and $W_\beta \in \mathbb{R}^{m \times m}$ a user defined positive definite weighting matrix. Then the minimizing value M_c yields*

$$L_c = (I_m - T_c^T (T_c W_\beta T_c^T)^{-1} T_c W_\beta) H_c^\dagger S_c.$$

4.4.4 ILC for systems with basis functions

The complete ILC control design procedure for systems with basis functions is captured in Result 4.1.

Result 4.1. *Design of an ILC controller for systems with basis functions is realized by separate design of (S_o, S_c), P_o, and M_c, in which the ILC control objectives monotonic convergence, performance, and coefficient vector amplitude reduction can be achieved, respectively. Design freedom in (S_o, S_c) is discussed in Lemma 4.5 and Corollary 4.2, freedom in P_o in Lemma 4.6, and freedom in M_c in Proposition 4.2.*

Note that the original problem formulation in Figure 4.8, which deals with convergence only, shows a symmetry in its structure in the sense that the dual system resulting from $H \to H^T$, $L_c \to L_o^T$, and $L_o \to L_c^T$ shows identical convergence properties. This symmetry is actually lost in later steps by introducing additional objectives like monotonic convergence, performance, and minimization of input amplitudes. This motivates to use a non-symmetrical parametrization (4.7) and (4.8).

4.5 Analysis of trial varying disturbances

To extend the previously obtained results, in this section we assume that trial varying output disturbances d_k are present in the ILC controlled system. The source of the disturbance is assumed to be either stochastic, e.g., measurement noise, or deterministic, e.g., vibrations from neighboring rotating systems.

Including trial varying output disturbance d_k into the ILC control framework of Figure 4.8 results in Figure 4.11. The trial dynamics of Figure 4.11 are subsequently given by

$$u_{k+1} = (I_p - L_o H L_c) u_k + L_o (\alpha_d - d_k), \quad u_0 = 0. \tag{4.10}$$

Since d_k is an external disturbance, it does not influence the convergence properties of the ILC controlled system. It does, however, influence performance. In the following, we discuss the influence of both stochastic and deterministic disturbances on performance.
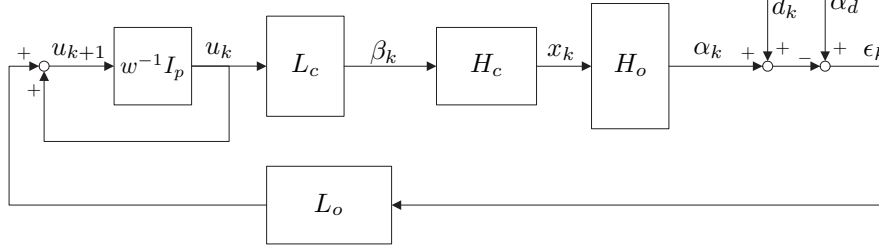
Figure 4.11: ILC framework in trial domain, including trial varying disturbances d_k.

4.5.1 Stochastic disturbances d_k

The stochastic disturbance that we consider is trial domain white noise d with $E\{d\} = 0$ and covariance matrix $E\{dd^T\} = R_{dd}$. Furthermore, we assume α_d and d_k to be independent. The trial domain dynamics and error equal

$$u_{k+1} = (I_p - L_o H L_c)u_k + L_o(\alpha_d - d_k) \tag{4.11a}$$

$$\epsilon_{k+1} = \alpha_d - d_{k+1} - H L_c u_{k+1}. \tag{4.11b}$$

To study the influence of stochastic d_k on the performance, we focus on the asymptotic value for $E\{\epsilon_\infty\}$ and the covariance $R_{\epsilon\epsilon} = \lim_{k\to\infty} R_{\epsilon\epsilon,k}$ with $R_{\epsilon\epsilon,k} = E\{(\epsilon_k - E\{\epsilon_k\})(\epsilon_k - E\{\epsilon_k\})^T\}$. Consequently, we assume that (4.11) is convergent.

Due to linearity and $E\{d\} = 0$, $E\{\epsilon_\infty\}$ is not affected by d_k. Moreover, the covariance matrix $R_{\epsilon\epsilon}$ is given by

$$R_{\epsilon\epsilon} = R_{dd} + H L_c R_{uu} L_c^T H^T \tag{4.12}$$

$$0 = R_{uu} - (I_p - L_o H L_c)R_{uu}(I_p - L_o H L_c)^T - L_o R_{dd} L_o^T, \tag{4.13}$$

where (4.13) is a discrete Lyapunov equation.

In Lemma 4.8, we study the influence of convergence speed on the value of $R_{\epsilon\epsilon}$.

Lemma 4.8. *Given ILC controlled system* (4.11)*, ILC controller* (4.7) *and* (4.8) *which explain how* (L_o, L_c) *are formed by the choice of* (S_o, S_c, P_o, M_c)*, any* P_o *with* $\mathrm{rank}(P_o H_o) = p$*, and any* M_c*. Furthermore, let* (S_o, S_c) *be given by* $S_o = g(P_o H_o)^{-1}$ *with* $g \in (0, 2)$ *and* $S_c = I_p$*, i.e., let the singular values of the ILC controlled system equal* $|1 - g|I_p$*. Then for*

$$g \downarrow 0 : \ \|R_{\epsilon\epsilon}\|_{i2} \downarrow \|R_{dd}\|_{i2}$$

$$g = 1 : \ R_{\epsilon\epsilon} = H_o(H_o P_o)^{-1} P_o R_{dd} P_o^T (H_o P_o)^{-1^T} H_o^T + R_{dd}$$

$$g \uparrow 2 : \ \|R_{\epsilon\epsilon}\|_{i2} \uparrow \infty.$$

Proof. See Appendix A.4.3. □

From Lemma 4.8, we can conclude that near zero convergence speed ($g \downarrow 0$) results in $R_{\epsilon\epsilon}$ in which R_{dd} appears unfiltered. Furthermore, with deadbeat ILC ($g = 1$), we find $R_{\epsilon\epsilon} = 2R_{dd}$ for disturbances d_k which lie in the space $H_o(H_oP_o)^{-1}P_o$. Finally, for $g \uparrow 2$, the effects of d_k on $R_{\epsilon\epsilon}$ are clearly disastrous. Note that these results confirm the frequency domain performance results in [21], but contradict the results given in [93].

Remark 4.4. P_o can be chosen to deviate from the optimal solution $P_o = H_o^T$, Lemma 4.6, if the contribution of d_k in a specific direction is larger than that of α_d. For example, consider the vector α_d whose elements along the vector are dominated by relatively low frequencies, and the vector d_k whose elements along the vector are dominated by relatively higher frequencies. Then we can choose $P_o = H_o^T Q$, with Q a Toeplitz matrix in the coefficient space describing the behavior of a zero phase low pass filter, to filter out d_k from the error signal ϵ_k. Although optimal performance, as given in Lemma 4.6, is not achieved, performance reduction in α_d is compensated for by less performance loss due to d_k.

4.5.2 Deterministic trial periodic disturbances d_k

The considered deterministic trial periodic disturbances are defined by $d_k(\ell) \in \mathbb{R}^n$:

$$d_k(\ell) \ : \ d_{k+\ell} = d_k, \text{ with } \ell \geq 2,$$

with ℓ representing the trial periodicity of the disturbance. Using the trial shift operator w, this equals $d_{k+\ell} = w^\ell d_k = d_k$. As an example of such a disturbance, consider a sinusoidal disturbance signal with a period time of 0.2 seconds, and an ILC controlled system with a trial length of 0.45 seconds (including the resetting of the system between two trials). Then the ILC controlled system will encounter the same sinusoidal disturbance every four trials ($\ell = 4$), see Figure 4.12.
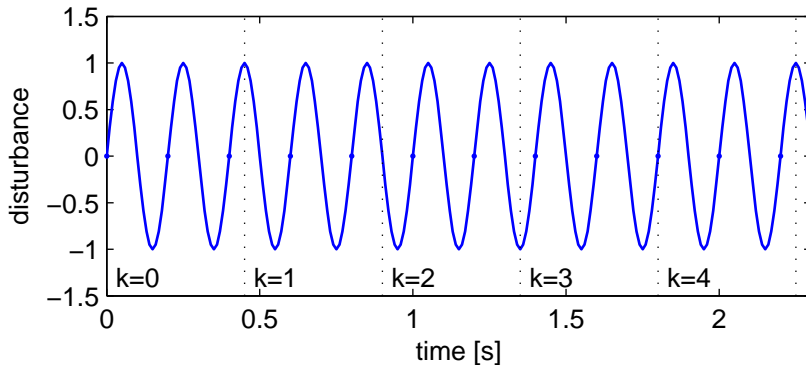
Figure 4.12: Sinusoidal disturbance with period time of 0.2s, and time interval of a trial of 0.45s. During trial $k = 4$, the disturbance is equal to that during trial $k = 0$.

Note that for d_k with known period ℓ, the internal model principle, [47], can be used in the ILC controller design to asymptotically reject the periodic disturbance. In this section, however, we assume ℓ to be unknown, and use the ILC controller given in (4.3).

The trial domain behavior of the asymptotic error of an ILC controlled system with deterministic disturbance $d_k(\ell)$ can be given by

$$\epsilon_k^{as} = \epsilon_\infty - (I - HL_c(wI - I_p + L_oHL_c)^{-1}L_o)d_k(\ell), \tag{4.14}$$

with $\epsilon_\infty = (I - HL_c(L_oHL_c)^{-1}L_o)\alpha_d$, and $w = e^{j2\pi/\ell}$. In (4.14), we substituted $w^{-1} = 1$ for trial invariant α_d ($\ell = 1$).

In Lemma 4.9, we study the effects of convergence speed and trial periodicity ℓ on ϵ_k^{as}.

Lemma 4.9. *Given (4.14) with deterministic trial periodic disturbance $d_k(\ell)$ with $\ell \geq 2$, ILC controller (4.7) and (4.8) which explain how (L_o, L_c) are formed by the choice of (S_o, S_c, P_o, M_c), any P_o with* $\mathrm{rank}(P_oH_o) = p$, *and any M_c. Let (S_o, S_c) be given by $S_o = g(P_oH_o)^{-1}$ with $g \in (0,2)$ and $S_c = I_p$, i.e., let the singular values of the ILC controlled system equal $|1 - g|I_p$. Then for*

$$
\begin{aligned}
g \downarrow 0 : \ & \epsilon_k^{as} \approx \epsilon_\infty - d_k(\ell \geq 2) \\
g = 1 : \ & \epsilon_k^{as} \approx \epsilon_\infty - (I_p - H_o(H_oP_o)^{-1}P_o)d_k(\ell \to \infty) \\
& \epsilon_k^{as} = \epsilon_\infty - (I_p + H_o(H_oP_o)^{-1}P_o)d_k(2) \\
g \uparrow 2 : \ & \epsilon_k^{as} \approx \epsilon_\infty - (I_p - H_o(H_oP_o)^{-1}P_o)d_k(\ell \to \infty) \\
& \|\epsilon_k^{as}\|_2 \to \infty \ \text{ for } d_k(2).
\end{aligned}
$$

Proof. See Appendix A.4.4. $\qquad\qquad\square$

From Lemma 4.9, we can conclude that, independent of the trial periodicity ℓ of $d_k(\ell)$, ϵ_k^{as} is approximately equal to $\epsilon_\infty - d_k$ for ILC controllers with near zero convergence speed. On the other hand, with, e.g., deadbeat control, the attenuation or amplification of the disturbance does depend on the value of ℓ.

To illustrate these results, consider $H = 1$, $L_c = 1$, and $L_o = g$, with $g \in (0,1]$ the tuning parameter used to influence convergence speed. For $g \downarrow 0$, we have arbitrarily slow convergence, for $g = 1$ we have deadbeat control. In Figure 4.13, we show the amplitude $|\epsilon_k^{as}(\ell)| = |(1 - (e^{j2\pi/\ell} - 1 + g)^{-1}g)|$ as function of ℓ (trial). Clearly, independent of the value for g, trial invariant disturbances ($\ell \to \infty$) are fully rejected. On the other hand, it depends on the trial periodicity of the disturbance (ℓ), whether slow convergence or deadbeat control provides the best disturbance rejection.
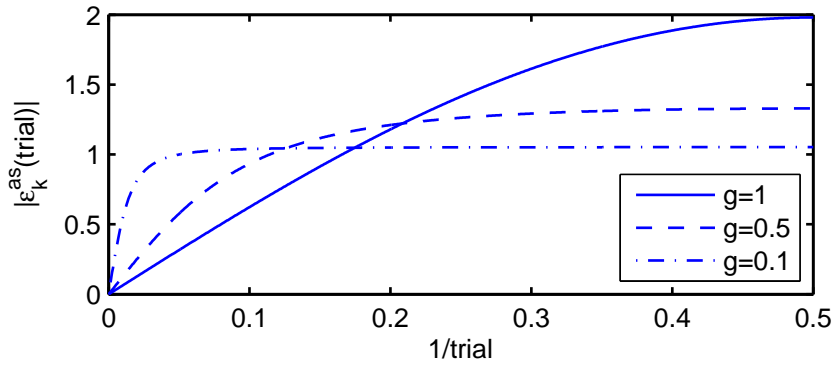
Figure 4.13: Effect of tuning gain g on asymptotic amplitude rejection of trial periodic disturbance.

4.6 ILC controller design for systems with basis functions

In this section, we discuss the design of ILC controllers for systems with basis functions by choosing a specific full rank decomposition for H and defining (S_o, S_c, P_o, M_c). Thereto, we apply the results of the previous sections as summarized in Figure 4.14. Note that the only (possibly) conflicting control objectives correspond to convergence speed and performance under trial varying disturbances.
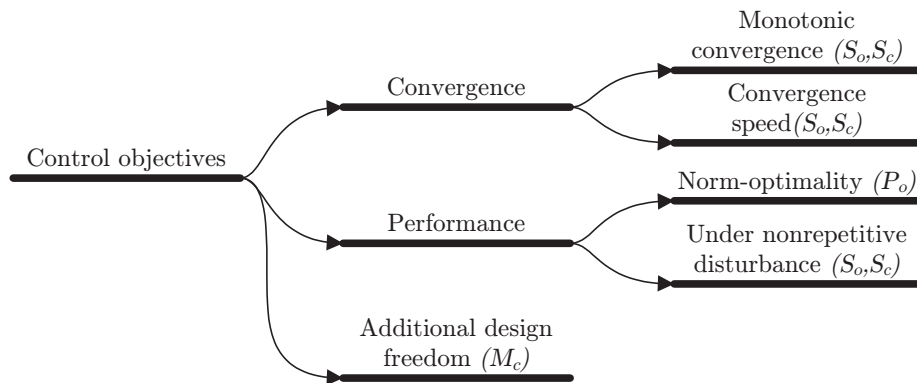
Figure 4.14: ILC control objectives as function of (S_o, S_c, P_o, M_c).

Before an ILC controller can actually be designed, we first need a full rank decomposition of H. Due to the properties of a SVD, see Appendix A.3.6, we suggest

to use SVD of H to find H_o and H_c.

With H_o and H_c given, ILC control design of (L_o, L_c) can be accomplished by design of (S_o, S_c, P_o, M_c). Using Proposition 4.2, the general structure of the ILC controller is given by

$$L_o = S_o P_o, \quad L_c = (I_m - T_c^T (T_c W_\beta T_c^T)^{-1} T_c W_\beta) H_c^\dagger S_c.$$

As a result, the design freedom in M_c is represented by design freedom in W_β.

S_c: As a result of Lemma 4.5, we leave the assignment of $\overline{\sigma}(T^{-1}(I_p - L_o H L_c)T)$ to S_o, and choose $S_c = I_p$.

P_o: If trial varying disturbances are not taken into account in the ILC controller design, or are fully unknown, Lemma 4.6 states to design $P_o = H_o^T$ for optimal performance. In case trial varying disturbances are considered, we can alter P_o to $P_o = H_o^T Q$, with Q a matrix which filters out the unwanted disturbances, e.g., a filter with low pass characteristics, see Section 4.5.

W_β: Reduction of the amplitudes of the values in the coefficient vector β_∞ corresponds to the design of W_β, see Proposition 4.2. An initial estimate of the amplitudes in β_∞ can be obtained by using the analytical expression for β_∞ with $W_\beta = I_m$: $\beta_\infty(W_\beta = I_m) = H_c^\dagger (P_o H_o)^{-1} P_o \alpha_d$. Now, one possible suggestion for W_β is to choose $W_\beta = g_\beta \text{diag}(|\beta_\infty(W_\beta = I_m)|)$ with $g_\beta \in \mathbb{R} > 0$ a tuning gain. For this choice of W_β, the larger amplitudes in β_∞ are penalized more than the smaller amplitudes. Note that in general, however, design and tuning of W_β remains an iterative process.

S_o: Finally, we design S_o. A first design choice for S_o is given by deadbeat ILC, Corollary 4.3: $S_o = (P_o H_o)^{-1}$. To be able to modify the convergence speed of this inverse model ILC controller, we can additionally introduce a tuning gain $g \in (0, 2)$ in S_o, yielding $S_o = g(P_o H_o)^{-1}$. The effects of g on convergence speed and trial varying disturbances is discussed in Section 4.5.

In case the smaller singular values in H_o are uncertain, we can apply a Tikhonov inverse of $P_o H_o T$, which for a different case was suggested by [12], with tuning parameters $g \in (0, 2)$ and $r \geq 0$

$$S_o := g T (T^T H_o^T P_o^T P_o H_o T + rI)^{-1} T^T H_o^T P_o^T \rightarrow$$
$$I - T^{-1} S_o P_o H_o T = (1 - g)I + rg(T^T H_o^T P_o^T P_o H_o T + rI)^{-1}.$$

With the singular values $\sigma_i(rg(T^T H_o^T P_o^T P_o H_o T + rI)^{-1}) < g$ (since $\sigma_i(P_o H_o T) > 0 \; \forall i \in [1, p]$), we find that monotonic convergence of (4.4) is guaranteed with this S_o. While parameter g can be used to alter the overall convergence speed, parameter r can be used to alter the convergence speed of the smaller gains in the $P_o H_o T$. For $\sigma_i(P_o H_o T) \ll r$ we find $rg(T^T H_o^T P_o^T P_o H_o T + rI)^{-1} \uparrow g$. This can subsequently result in arbitrarily slow convergence, see Section 4.3. For $\sigma_i(P_o H_o T) \gg r$, we find $rg(T^T H_o^T P_o^T P_o H_o T + rI)^{-1} \approx 0$ and a convergence speed of $|1 - g|$.

4.7 Reconsideration of basis function based ILC approaches in ILC literature

To illustrate that the results of this chapter are directly applicable to various ILC problems, we present three distinct ILC problem formulations with basis functions. Thereby, we focus on reformulating the ILC control problems to comply with the framework discussed in this chapter.

4.7.1 Arimoto gains for systems with nonzero relative degrees

In [86], Arimoto gains are applied to control an LTI system with a relative degree equal to one. For that purpose, the original system is modified using time window based basis functions, (4.15).

$$
T_f = \begin{bmatrix} I_{N-1} \\ 0 \end{bmatrix}, \quad T_y = \begin{bmatrix} 0 & I_{N-1} \end{bmatrix} \rightarrow H = \begin{bmatrix} CB & & 0 \\ \vdots & \ddots & \\ CA^{N-2}B & \dots & CB \end{bmatrix}, \quad (4.15)
$$

with $H^{N-1 \times N-1}$. Since [86] assumes full rank of H, the minimal realization of H can correspond to $(H_o, H_c) = (H, I_{N-1})$. Furthermore, the input β_k and output α_k of H correspond to $\beta_k(t) = f_k(t)$ and $\alpha_k(t) = y_k(t+1)$ with $t \in [0, N-2]$, respectively.

The applied ILC control strategy corresponds to $f_{k+1}(t) = f_k(t) + ge_k(t+1) \rightarrow \beta_{k+1} = \beta_k + g\epsilon_k$, with $0 < g \le 2(CB)^{-1}$ the Arimoto gain. Formulation of this ILC control strategy in terms of (L_o, L_c) gives (gI_{N-1}, I_{N-1}). With $L_o = S_o P_o$, we can find $S_o = g(H^T)^{-1}$ and $P_o = H^T$.

4.7.2 Inverse model based ILC for systems with a reduced input-output space

In [132], ILC is used for a system with a reduced input space. Given an original reference signal $r \in \mathbb{R}^N$, the matrix with input basis functions equals

$$
T_f = \begin{bmatrix} \dot{r} & \ddot{r} & r^{(3)} & r^{(4)} \end{bmatrix}, \quad (4.16)
$$

resulting in the modified system $H = JT_f \in \mathbb{R}^{N \times 4} \rightarrow (H_o, H_c) = (H, I_4)$. While $\alpha_k = y_k$, the input is modified from f_k to coefficient vector $\beta_k \in \mathbb{R}^4$.

System H is controlled using an inverse model based ILC controller with $(L_o, L_c) = (g(H^T H)^{-1} H^T, I_4)$ and $g \in (0, 2)$. Using (4.7), we obtain $S_o = g(H^T H)^{-1}$ and $P_o = H^T$.

4.7.3   ILC for residual vibration suppression

In Chapter 3, we applied ILC to suppress residual vibrations in systems performing point-to-point motions. With the generalized system $H = J_H$ discussed extensively in Chapter 3, here we focus on the properties of the ILC controller.

To control H, we designed an ILC controller L_o with

$$(P_o, S_o) = (H_o^T, g(H_o^T H_o + rI_p)^{-1}), \ g \in (0, 2), \ r \geq 0,$$

and an L_c with $S_c = I_p$. With $\ker(H) \neq \emptyset$, we used the additional design freedom M_c to reduce the amplitude of the command signal.

4.8   Concluding remarks

Basis functions appear in ILC in various ways. In this chapter, we brought together these appearances in one system description and ILC framework. In addition, we have presented a general system solution for this framework, and provided results on monotonic convergence, performance, minimization of input amplitudes, and disturbance rejection.

The derivation of the analysis and design theory for this ILC framework has extended existing ILC control theory such that it is applicable to the proposed ILC framework. From a system perspective, analysis of ILC control objectives in this framework has yielded ILC controller properties which are required for monotonic convergence and optimality of performance. Since these conditions have been defined as function of the system properties, they apply to any ILC controller fitting the proposed framework. From an ILC control design perspective, analysis has revealed how the ILC objectives given by monotonic convergence, optimality of performance, and minimization of input amplitudes, can be reached by design of separate parts of the ILC controller. Analysis has furthermore shown that convergence speed and performance under trial varying disturbances are the only two possibly conflicting control objectives.

The obtained analysis results have been used in the design of ILC controllers for systems with basis functions. In addition, practical suggestions and choices have been given to facilitate straightforward ILC control design. Finally, we have shown that the obtained results are applicable to ILC problems formulations with basis functions, and problem formulations which can be interpreted as such.

Chapter 5

ILC for uncertain systems: Robust convergence analysis

In this chapter, we discuss a Robust Monotonic Convergence (RMC) analysis approach for ILC for uncertain systems over a finite time interval. For this purpose, a finite time interval representation of an uncertain system description is introduced. This model is subsequently used in an RMC analysis based on μ analysis. As a result, we are capable of handling additive and multiplicative uncertainty models in the RMC problem formulation, analyze RMC of linear time invariant MIMO systems controlled by any linear trial invariant ILC controller, and formulate additional straightforward RMC conditions for ILC controlled systems. To illustrate the derived results, we analyze the RMC properties of LQ norm optimal ILC.

Introduction

The expression "uncertain system" can be interpreted in multiple ways. One interpretation is to consider model uncertainty as the difference between a model and a specific system, resulting in one specific, fixed, model error. If we assume that measurement data of the impulse response of the system is available, then this model uncertainty corresponds to the difference between the true impulse response and that of the model. While ILC control design can be based on a model of the system, convergence analysis can be based on the true system, i.e., on measurement data.

In this chapter and in Chapter 6, however, we consider the uncertain system to correspond to a nominal model together with an uncertainty set. The true system is assumed to lie somewhere in this set. In contrast to the previous model uncertainty interpretation, in this case no explicit system response is available. As a result, we can not use it to analyze the ILC controlled system. What we can do (and will do), is to analyze the convergence properties of the complete uncertain model set. With the true system assumed to be captured in this set, convergence of each system in the set results in convergence of the true ILC controlled system.

The outline of this chapter is as follows. We introduce the uncertain system description over a finite time interval in Section 5.1. Subsequently, the robust monotonic convergence objective is defined in Section 5.2, and tackled in Section 5.3. In Section 5.4, we work out the obtained robust monotonic convergence conditions for three specific uncertainty models. We introduce basis functions into the analysis in Section 5.5. To illustrate our findings, in Sections 5.6 and 5.7 we analyze the robustness properties of LQ norm optimal ILC. This chapter ends with concluding remarks in Section 5.8.

Part of the contents of this chapter is published in [43].

Definition. The induced 2-norm of a discrete time transfer function $P(z)$ is given by $\|P(z)\|_{i2} = \max_{\theta \in [-\pi, \pi]} \overline{\sigma}(P(e^{j\theta}))$ with θ real valued.

5.1 Uncertain system description

The focus of this chapter is on analysis of the robust convergence properties of ILC controlled systems over a finite time interval with systems that are uncertain. The finite time interval system representations follow from infinite time system descriptions. The infinite time systems under study are assumed to be defined by a real rational discrete time transfer function $P(z)$, which can be causal or noncausal in the shift operator z. Given a time signal $y(t)$, z is defined as $y(t+1) = zy(t)$. Consequently, $P(z)$ has discrete time domain inputs and outputs defined over the time axis $t \in (\ldots, -2, -1, 0, 1, 2, \ldots)$.

Restriction of an infinite time mapping $P(z)$ to a finite time interval $t \in [0, N-1]$ is achieved in two steps. First, observe that the mapping $P(z)$ is equivalent to the mapping given by the infinite dimensional convolution matrix P_∞, with P_∞ a block Toeplitz matrix filled with the impulse response (Markov parameters) $p(t)$ of $P(z)$. Second, truncate the infinite matrix P_∞ such that it describes the i/o mapping for time interval $t \in [0, N-1]$, see, e.g., [20].

The finite time interval model J_Δ for our uncertain system is obtained by following the uncertain system modeling steps as used in infinite time robust control theory, e.g., Section 7.2 of [117], Section 9.1 of [143], see Figure 5.1. In Figure 5.1, the infinite time uncertain system $J_\Delta(z) : \ f(z) \in \mathbb{C}^{q_i} \mapsto y(z) \in \mathbb{C}^{q_o}$ consists of a

nominal model $J(z)$ which is assumed to be causal, and the filters $(W_i(z), W_o(z))$ which are user defined. $(W_i(z), W_o(z))$ describe the specific uncertainty of the system under study, and are designed such that they are stable causal filters whose inverses are again stable and causal. The $\Delta(z)$ (with $\Delta(e^{j\theta}) \in \mathbb{C}^{q \times q}$) is a causal system with known structure, see Sections 7.3 and 7.4 of [117]. Moreover, $\Delta(z)$ is assumed to satisfy $\|\Delta(z)\|_{i2} \leq 1$, i.e., $\Delta(z)$ is assumed to be normalized. As a result, the set of uncertain systems Π_z is given by

$$\Pi_z = \{ J_\Delta(z) : J_\Delta(z) = J(z) + W_i(z)\Delta(z)W_o(z), \|\Delta(z)\|_{i2} \leq 1,$$
$$\Delta \text{ structured}\}, \tag{5.1}$$
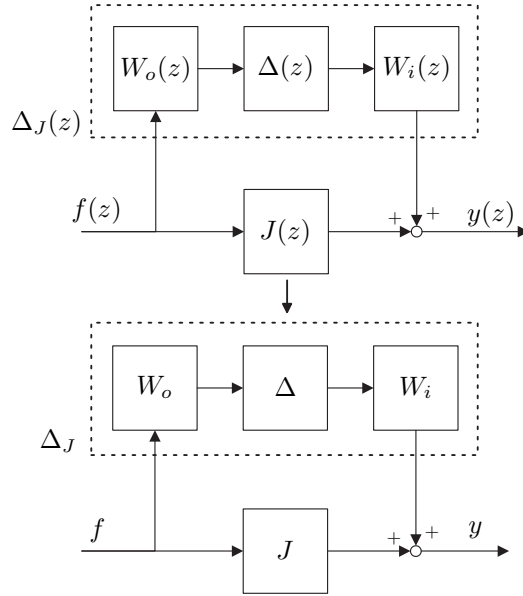
Figure 5.1: Top: infinite time uncertain system $J_\Delta(z)$, consisting of a nominal model $J(z)$ and additive model uncertainty $\Delta_J(z)$. Bottom: uncertain system J_Δ over a finite time interval.

For given infinite time system $J_\Delta(z)$, the finite interval mapping $J_\Delta \in \mathbb{R}^{Nq_o \times Nq_i}$ maps the input signal $f \in \mathbb{R}^{Nq_i}$ to the output signal $y \in \mathbb{R}^{Nq_o}$. Furthermore, with $J(z)$ causal and LTI, the system matrix $J \in \mathbb{R}^{Nq_o \times Nq_i}$ is a lower triangular block Toeplitz matrix. Equally, the finite interval representations of $(W_i(z), W_o(z))$ are given by the lower triangular block Toeplitz matrices $W_i \in \mathbb{R}^{Nq_o \times Nq}$ and $W_o \in \mathbb{R}^{Nq \times Nq_i}$.

With $\Delta(z)$ causal and LTI, its i/o behavior for a finite time interval can be expressed by a lower triangular block Toeplitz matrix $\Delta \in \mathbb{R}^{Nq \times Nq}$. Moreover, for finite dimensional lower triangular (block) Toeplitz matrices we find that $\|\Delta\|_{i2} \leq \|\Delta(z)\|_{i2}$, see Section 6.4 of [20], i.e., the induced 2-norm of a finite interval lower triangular (block) Toeplitz matrix can never exceed the 2-norm of the underlying

transfer function. Consequently, the set of uncertain systems over a finite time interval, Π, can be given by

$$\Pi = \{J_\Delta : J_\Delta = J + W_i \Delta W_o, \Delta \in \boldsymbol{\Delta}\}, \tag{5.2}$$

where $\boldsymbol{\Delta} = \{\Delta \in \mathbb{R}^{Nq \times Nq} : \|\Delta\|_{i2} \leq 1, \Delta \text{ structured}\}$.

Remark 5.1. Although the set of uncertain systems Π is derived by assuming Δ to be LTI, in Section 5.4 we show that for given LTI mappings (J, W_i, W_o), Δ can also be chosen to be linear time varying (LTV). In that case, we do have to assume that the LTV mapping $W_i \Delta W_o$ properly captures the finite interval model uncertainty of the system.

Remark 5.2. To fit multiplicative uncertainty models into the additive uncertainty description of (5.2), define $W_i = W_i^o$ and $W_o = W_o^o J$ for output multiplicative uncertainty $(I + W_i^o \Delta W_o^o)J$, and $W_i = JW_i^i$ and $W_o = W_o^i$ for input multiplicative uncertainty $J(I + W_i^i \Delta W_o^i)$. For singular J, the modification from multiplicative uncertainty to additive uncertainty results in rank deficient W_i or W_o.

As we will show in Section 5.3, the norm-bounded uncertainty Δ is the key element in the uncertain system description, since it allows the use of well developed robust control theory for the robust convergence analysis.

5.2 Robust Monotonic Convergence objective

In this section, the concept of robust monotonic convergence of ILC for uncertain systems is introduced, based on the ILC control framework consisting of an uncertain system J_Δ and ILC controller $(\mathcal{Q}, L_o, L_c)$, as depicted in Figure 5.2. In Figure 5.2, $p = \text{rank}(J)$ and $e_k = y_d - J_\Delta f_k$. Introduction of basis functions in the ILC framework is left for Section 5.5.

Note the additional ILC filter $\mathcal{Q}$ in Figure 5.2. This filter is referred to as robustness filter, since it can be used to increase the robustness properties of the ILC controlled system. In this chapter, we show that, depending on the amount of model uncertainty, $\mathcal{Q} \neq I_p$ is indeed required to obtain robustness against model uncertainty. In frequency domain ILC control strategies, $\mathcal{Q}$ is often defined as a zero phase low pass filter. In Arimoto gain ILC, it is common to take $\mathcal{Q} = gI_p$ with $g \leq 1$. $\mathcal{Q}$ design in LQ norm optimal ILC is discussed in 5.6.

As shown in Figure 5.2, we will consider the ILC control strategy $(\mathcal{Q}, L_o, L_c)$ given by

$$u_{k+1} = \mathcal{Q}u_k + L_o e_k, \quad f_k = L_c u_k, \quad u_0 = 0, \tag{5.3}$$

with $(\mathcal{Q}, L_o, L_c) \in (\mathbb{R}^{p \times p}, \mathbb{R}^{p \times Nq_o}, \mathbb{R}^{Nq_i \times p})$.
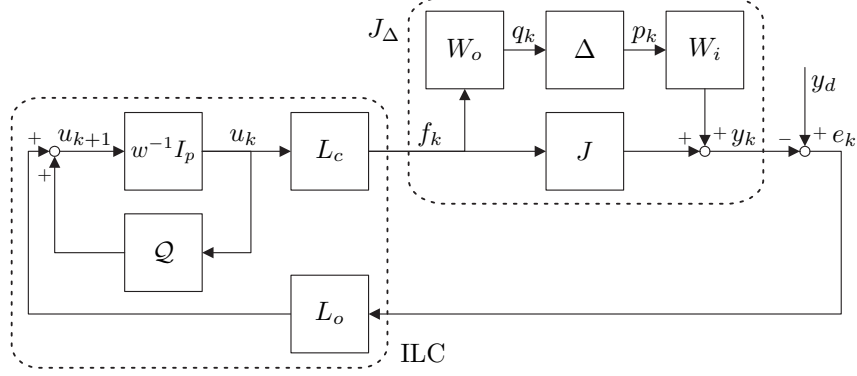
Figure 5.2: ILC control framework in trial domain, with ILC controller $(\mathcal{Q}, L_o, L_c)$.

Substitution of $e_k = y_d - J_\Delta f_k$ in (5.3) subsequently results in the trial domain behavior

$$u_{k+1} = (\mathcal{Q} - L_o J_\Delta L_c)u_k + L_o y_d \qquad (5.4)$$
$$f_k = L_c u_k,$$

with $u_0 = 0$.

The ILC controlled system represented by (5.4) is called robustly convergent (RC) in trial domain iff $\rho(\mathcal{Q} - L_o J_\Delta L_c) < 1 \ \forall J_\Delta \in \Pi$. Although this condition is necessary and sufficient for convergence of (5.4), mere convergence of (5.4) can lead to undesirable transient behavior of the input and error signal norms in trial domain, [76], e.g., the 2-norm or the maximum amplitude of the time signals during a trial can become unacceptably high (they can become harmful to the system). To avoid this undesirable behavior, (5.4) is required to be monotonically convergent.

We consider two definitions for monotonic convergence: Monotonic convergence of (5.4) with J_Δ replaced by J, i.e., $\Delta = 0$, as defined by Definition 2.6, and robust monotonic convergence of (5.4) for $J_\Delta \in \Pi$.

Definition 5.1 (Robust Monotonic Convergence (RMC))**.** Given the ILC controlled system (5.4) and ILC controller (5.3), with $y_d = 0$ and $u_0 \in \mathbb{R}^p$. Then (5.4) is robustly monotonically convergent (RMC) in f_k if there exists $0 \leq \kappa < 1$ such that

$$\|f_{k+1}\|_2 < \kappa \|f_k\|_2, \ \forall u_0 \in \mathbb{R}^p \text{ and } \forall J_\Delta \in \Pi,$$

and $\|f_{k+1}\|_2 = \|f_k\|_2$ only for $f_k = f_{k+1} = 0$.

Remark 5.3. We derive the RMC condition based on Definition 5.1. Alternatively, the same RMC condition can be found by considering $y_d \neq 0$ and $u_0 = 0$. The only difference between the two approaches is found in the definition of RMC.

For $y_d \neq 0$ and $u_0 = 0$, robust monotonic convergence requires $\|f_{k+1} - f_\infty\|_2 < \|f_k - f_\infty\|_2 \ \forall J_\Delta \in \Pi$ with $f_\infty = \lim_{k \to \infty} f_k$.

Finally, we extend the optimal performance result of Lemma 2.2 to the ILC framework presented in Figure 5.2.

Lemma 5.1. *Given a robustly convergent system* (5.4) *with asymptotic error e_∞. Then $e_\infty = 0$ for any y_d iff* $\text{rank}(J_\Delta) = Nq_o \ \forall J_\Delta \in \Pi$ *and $\mathcal{Q} = I_p$.*

Proof. Follows the proof of Lemma 2.2, with $e_\infty = (I_{Nq_o} - J_\Delta L_c(I_p - \mathcal{Q} + L_o J_\Delta L_c)^{-1} L_o) y_d$. $\qquad\square$

5.3 Robust Monotonic Convergence conditions

Now that the RMC problem is defined, we tackle it for given uncertain systems (J, W_i, W_o) and ILC controller $(\mathcal{Q}, L_o, L_c)$. For comparison with frequency domain RMC results from ILC literature, we include an RMC condition based on transfer function notations.

5.3.1 RMC condition

Using Definition 5.1 and Lemma 4.1 with $H \to J_\Delta$, we can formulate the following sufficient RMC condition.

Corollary 5.1. *Consider the ILC controlled system* (5.4) *with $y_d = 0$. Furthermore, let T satisfy $T^T L_c^T L_c T = I_p$. Then* (5.4) *is RMC in f_k if $\|T^{-1}(\mathcal{Q} - L_o J_\Delta L_c) T\|_{i2} < 1 \ \forall J_\Delta \in \Pi$.*

Proof. Follows the proof of Lemma 4.1. $\qquad\square$

At this point, it is useful to bring the one trial shift operator $w^{-1} I_p$ into a format which is compatible with our uncertainty description. This is done in the following Proposition.

Proposition 5.1. *Let $T = I_p$ and $\Delta_P \in \{\Delta_P = \delta_P I_p : \delta_p \in \mathbb{C}, |\delta_P| < 1\}$. Then RC of system* (5.4) *of Figure 5.2 is equivalent to RC of the system in Figure 5.3. Furthermore, let T satisfy $T^T L_c^T L_c T = I_p$ and $\Delta_P \in \mathbf{\Delta}_P$ with $\mathbf{\Delta}_P = \{\Delta_P \in \mathbb{C}^{p \times p}, \|\Delta_P\|_{i2} < 1\}$, i.e., Δ_P normalized and unstructured. Then RMC of system* (5.4) *of Figure 5.2 in f_k is equivalent to RMC of the system in Figure 5.3 in z_k.*

Proof. See Appendix A.5.1. $\qquad\square$
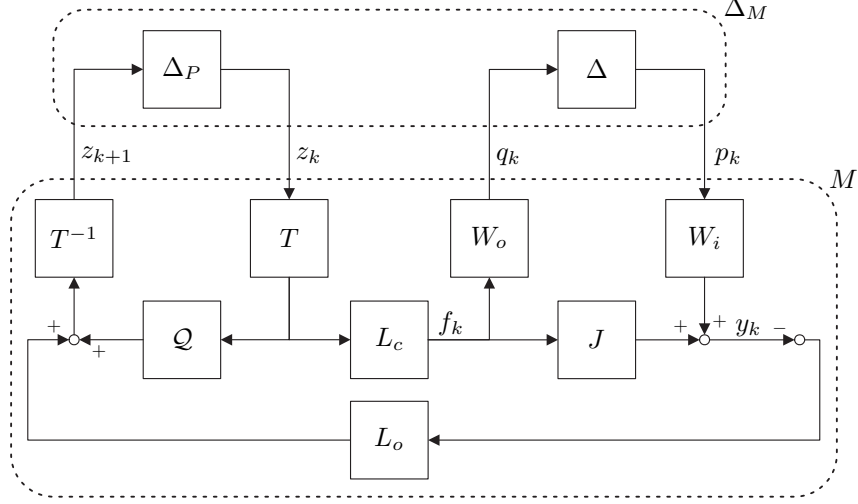
Figure 5.3: $M\Delta_M$ structure.

Proposition 5.1 makes it possible to study the convergence properties of (5.4) by analyzing the properties of M in Figure 5.3. System M is given by

$$\begin{bmatrix} q_k \\ z_{k+1} \end{bmatrix} = \underbrace{\begin{bmatrix} 0 & W_o L_c T \\ -T^{-1} L_o W_i & T^{-1}(\mathcal{Q} - L_o J L_c)T \end{bmatrix}}_{M} \begin{bmatrix} p_k \\ z_k \end{bmatrix}, \tag{5.5}$$

and the corresponding norm bounded uncertainty set $\boldsymbol{\Delta}_M$ by

$$\boldsymbol{\Delta}_M = \{\Delta_M = \mathrm{diag}(\Delta, \Delta_P) : \Delta \in \boldsymbol{\Delta}, \Delta_P \in \boldsymbol{\Delta}_P\}. \tag{5.6}$$

Based on the $M\Delta_M$ structure of Figure 5.3, a sufficient condition for monotonic convergence of $M\Delta_M$ is given by $\|M\Delta_M\|_{i2} < 1$. While an unstructured Δ_M would result in the arbitrarily conservative RMC condition $\|M\|_{i2} < 1$, exploitation of the structure in Δ_M using μ analysis can result in less conservative RMC results. More specifically, based on the results of μ analysis in [103], it can be stated that (5.5) is RMC if $\mu_{\Delta_M}(M) < 1$, with $\mu_{\Delta_M}(M)$ defined by

$$\mu_{\Delta_M}(M) = \min_{\Delta_M \in \boldsymbol{\Delta}_M} \{\bar{\sigma}(\Delta_M) : \det(I - M\Delta_M) = 0\}^{-1}. \tag{5.7}$$

If there exists no $\Delta_M \in \boldsymbol{\Delta_M}$ such that $\det(I - M\Delta_M) = 0$, then $\mu_{\Delta_M}(M) := 0$.

Remark 5.4. Because the formulations in [103] are defined for matrices, i.e., are not related to any application, the results are directly applicable to our system, without any restrictions.

With $\mu_{\Delta_M}(M)$ in general difficult to determine directly, we use an upper bound for $\mu_{\Delta_M}(M)$ to derive the RMC condition for M, Proposition 5.2.

Proposition 5.2. *Given system M of (5.5) with M real valued. Then an upper bound for $\mu_{\Delta_M}(M)$ is given by*

$$\mu_{\Delta_M}(M) \leq \inf_{D_M \in \mathcal{D}_M} \|D_M^{1/2} M D_M^{-1/2}\|_{i2}, \tag{5.8}$$

with $\mathcal{D}_M = \{D_M = \mathrm{diag}(D, D_P) : \mathrm{rank}(D_M) = Nq + p, D_M \in \mathbb{R}^{(Nq+p)\times(Nq+p)}, D_M^{1/2}\Delta_M = \Delta_M D_M^{1/2}\}$.

Proof. The upper bound is suggested in Section 4 of [45]. The properties of $\mathcal{D}_M$ follow from Section 3 and Theorem 9.10 of [103]. $\qquad\square$

From Proposition 5.2, it can be concluded that for a given uncertain system (J, W_i, W_o) and ILC controller $(\mathcal{Q}, L_o, L_c)$, checking RMC is equivalent to first calculating M and specifying the structure in $\boldsymbol{\Delta}_M$, and subsequently checking the existence of $D_M \in \mathcal{D}_M$ such that (5.8) is smaller than one.

Remark 5.5. Since no assumptions have been made about $(\mathcal{Q}, L_o, L_c)$ in M, Proposition 5.2 is applicable to any linear trial invariant ILC controller: causal and noncausal in time domain, time invariant and time varying, square and non-square.

Remark 5.6. To illustrate the difference in allowable Δ between RC and RMC, in Appendix B, we have worked out an example for an uncertain system with $(W_i^i, W_o^i) = (I, I)$, and $(\mathcal{Q}, L_o, L_c) = (I, gJ^{-1}, I)$.

5.3.2   RMC condition in frequency domain

In ILC literature, the frequency domain is often used to analyze the convergence properties of ILC controlled system, [8, 23, 139]. To compare our RMC results with RMC results from frequency domain ILC, in this section we derive an RMC condition using the transfer function notations from Section 5.1. This formulation implies that trials have an infinite time interval. As a result, frequency domain RMC can be interpreted as RMC over an infinite time interval. For simplicity of the results, we consider the case $L_c(z) = I$, which is common in ILC literature.

The following Lemma reveals that frequency domain RMC implies RMC over a finite timer interval, if $L_o(z)$ is causal.

Lemma 5.2. *Consider $L_c(z) = I$, and $(\mathcal{Q}(z), L_o(z), J_\Delta(z)) \in L^\infty(z)$ for $z = e^{j\theta}$, $\theta \in [-\pi, \pi]$. Moreover, let $(\mathcal{Q}, L_o, J_\Delta)$ be the finite dimensional (block) Toeplitz matrix structures of the corresponding infinite dimensional (block) Toeplitz matrices representing $(\mathcal{Q}(z), L_o(z), J_\Delta(z))$. Then $\|\mathcal{Q}(z) - L_o(z)J_\Delta(z)\|_{i2} < 1$ implies $\|\mathcal{Q} - L_o J_\Delta\|_{i2} < 1$, if $L_o(z)$ is causal.*

Proof. See Appendix A.5.2. $\qquad\square$

Note that, in contrast to $L_o(z)$, $\mathcal{Q}(z)$ is not restricted to be causal. Furthermore, note that if $L_o(z)$ is noncausal, then the condition $\|\mathcal{Q}(z) - L_o(z)J_\Delta(z)\|_{i2} < 1$ does not necessarily imply $\|\mathcal{Q} - L_oJ_\Delta\|_{i2} < 1$. As an example, consider $J(z) = z^{-1}$, $\mathcal{Q}(z) = 1$, and $L_o(z) = gz$ with $g \in \mathbb{R}$. Furthermore, consider the finite dimensional Toeplitz matrices (with $N = 2$)

$$J = \begin{bmatrix} 0 & 0 \\ 1 & 0 \end{bmatrix}, \ \mathcal{Q} = \begin{bmatrix} 1 & 0 \\ 0 & 1 \end{bmatrix}, \ L_o = \begin{bmatrix} 0 & 1 \\ 0 & 0 \end{bmatrix}.$$

Then $\|\mathcal{Q}(z) - L_o(z)J(z)\|_{i2} = |1 - g|$, which is smaller than 1 for $g \in (0, 2)$. In contrast, $\|\mathcal{Q} - L_oJ\|_{i2} = \max(|1 - g|, 1)$, which is equal to or larger than 1 $\forall g$.

For $L_o(z)$ causal and $L_c(z) = I$, $M(z)$ and $\Delta_M(z)$ are given by

$$M(z) = \begin{bmatrix} 0 & W_o(z) \\ -L_o(z)W_i(z) & \mathcal{Q}(z) - L_o(z)J(z) \end{bmatrix}$$
$$\Delta_M(z) = \mathrm{diag}(\Delta(z), \Delta_P(z)).$$

The uncertainty $\Delta_M(z)$ for $z = e^{j\theta}$, with given $\theta \in [-\pi, \pi]$, has the structure of a two-block diagonal matrix, with each block assumed to be unstructured. As a result, $\mu_{\Delta_M}(M(e^{j\theta}))$ equals its upper bound (5.8), as shown in Lemma 2.1 of [113] and Section 9 of [103]. Standard μ tools can be used to determine $\mu_{\Delta_M}(M(e^{j\theta}))$, e.g., the function `mussv` from Matlab®.

Remark 5.7. Note that there is a basic difference between Lemma 5.2 and the commonly used frequency domain convergence result $\|\mathcal{Q}(z)\|_{i2}\|I - L_o^*(z)J(z)\|_{i2} < 1$, with $L_o^*(z) = Q^{-1}(z)L_o(z)$, e.g., [95]. In Lemma 5.2, the monotonic convergence problem is explicitly formulated as a finite time interval problem, for which an upper bound by an infinite time interval system representation exists under the condition of causality of $L_o(z)$. In contrast, this causality condition has not been mentioned before in frequency domain convergence analysis, e.g., [95, 139].

Remark 5.8. Because exploitation of non-causality is an essential part of the success of ILC, [97], we wil not use the frequency domain representation as a tool to analyze the convergence properties of the ILC controlled system.

5.4 RMC conditions for structured Δ_M

In this section, Proposition 5.2 is elaborated on for different Δ in $\boldsymbol{\Delta}_M$. Thereby, the focus is on the tightness of the upper bound (5.8), the design freedom in D_M, and formulation of easy-to-calculate RMC conditions. The uncertainty models Δ discussed in this section are presented in Table 5.1.

In Proposition 5.2, it is stated that $D_M \in \mathcal{D}_M$ must commute with $\Delta_M \in \boldsymbol{\Delta}_M$, i.e.,

$$D_M^{1/2}\Delta_M = \Delta_M D_M^{1/2} \Leftrightarrow \left(D^{1/2}\Delta = \Delta D^{1/2}, \ D_P^{1/2}\Delta_P = \Delta_P D_P^{1/2} \right).$$

Table 5.1: Different uncertainty models Δ.

$\Delta \in \mathbb{R}^{Nq \times Nq}$ Linear Time Varying (LTV), [113]:
$\Delta = \begin{bmatrix} \Delta_0 & 0 & & 0 \\ \vdots & \Delta_N & & \\ \vdots & \vdots & \ddots & \\ \Delta_{N-1} & \Delta_{2N-2} & \cdots & \Delta_{N(N+1)/2} \end{bmatrix}$, $\Delta_{t \in [0, N(N+1)/2]} \in \mathbb{R}^{q \times q}$
$\Delta \in \mathbb{R}^{Nq \times Nq}$ Linear Time Invariant (LTI):
$\Delta = \begin{bmatrix} \Delta_0 & 0 & & 0 \\ \vdots & \Delta_0 & & \\ \vdots & \vdots & \ddots & \\ \Delta_{N-1} & \Delta_{N-2} & \cdots & \Delta_0 \end{bmatrix}$, $\Delta_{t \in [0, N-1]} \in \mathbb{R}^{q \times q}$
$\Delta \in \mathbb{R}^{Nq \times Nq}$ Interval uncertainty:
$\Delta = \begin{bmatrix} \Delta_0 & 0 & & 0 \\ \vdots & \Delta_0 & & \\ \vdots & \vdots & \ddots & \\ \Delta_{N-1} & \Delta_{N-2} & \cdots & \Delta_0 \end{bmatrix}$, $\Delta_{t \in [0, N-1]} = \delta_t I_q, \ \delta_t \in [-1, 1]$

With Δ_P fully unstructured, see Proposition 5.1, D_P which commutes with Δ_P is given by $D_P = d_P I$, $d_P \in \mathbb{R} > 0$. As a result, we find $D_M = \text{diag}(D, d_P I)$. Moreover, application of Section 3 of [103] to our situation reveals that one element in D_M can be set equal to 1. Hence, by defining $d_P = 1$, in our case we find that the condition $D_M^{1/2} \Delta_M = \Delta_M D_M^{1/2}$ can be simplified to $D^{1/2} \Delta = \Delta D^{1/2}$.

5.4.1   Case 1: Δ LTV

For LTV Δ, the RMC condition in Proposition 5.2 is only sufficient, see Table 1 of [103]. Furthermore, a matrix D commuting with LTV Δ is given by $D = d^2 I$. A sufficient condition for $\mu_{\Delta_M}(M) < 1$ with Δ LTV can consequently obtained by inserting (5.5) and $D_M = \text{diag}(d^2 I, I)$ in (5.8):

$$\inf_d \| \begin{bmatrix} 0 & dW_o L_c T \\ -d^{-1} T^{-1} L_o W_i & T^{-1}(\mathcal{Q} - L_o J L_c) T \end{bmatrix} \|_{i2} < 1. \tag{5.9}$$

Remark 5.9. For $M \in \mathbb{R}^{Nq+p \times Nq+p}$ with $Nq + p$ relatively large, a line search can be used to find an optimal value for d. For relatively small dimensional M, d can be obtained using the linear matrix inequality (LMI), see Theorem 3.9 of [103],

$$M^T D_M M - D_M \prec 0, \quad D_M \in \mathcal{D}_M.$$

It depends on the available computational power, what "relatively large $Nq + p$" is. Our experience has revealed that with a Pentium 4 2.6 GHz with 1Gb RAM, the computational load restricted the use of LMI's to $Nq + p < 100$.

For ILC controllers $(\mathcal{Q}, L_o, L_c)$ with $\mathcal{Q} = L_o J L_c$ (deadbeat ILC control), condition (5.9) can be simplified to a single RMC condition:

Corollary 5.2. *Consider* (5.5), *Δ LTV, and $\mathcal{Q} = L_o J L_c$. Then a sufficient condition for $\mu_{\Delta_M}(M) < 1$ is given by*

$$\|T^{-1} L_o W_i\|_{i2} \cdot \|W_o L_c T\|_{i2} < 1.$$

Proof. See Appendix A.5.3. $\qquad\qquad\qquad\qquad\qquad\qquad\qquad\qquad\qquad\square$

In Section 5.6, we will show that the results of Corollary 5.2 are equally applicable to a class of LQ norm optimal ILC controllers for which $\mathcal{Q} \neq L_o J L_c$.

5.4.2 Case 2: Δ LTI

For LTI Δ, the RMC condition in Proposition 5.2 is only sufficient, see Table 1 of [103]. Furthermore, a matrix D commuting with LTI Δ is given by

$$D^{1/2} = \begin{bmatrix} d_0 I_q & & 0 \\ \vdots & \ddots & \\ d_{N-1} I_q & \dots & d_0 I_q \end{bmatrix}, \quad \text{with } d_{t \in [0, N-1]} \in \mathbb{R}, \ d_0 \neq 0. \tag{5.10}$$

By inserting (5.5) and D from (5.10) in (5.8), a sufficient condition for $\mu_{\Delta_M}(M) < 1$ with Δ LTI is given by

$$\inf_D \left\| \begin{bmatrix} 0 & D^{1/2} W_o L_c T \\ -T^{-1} L_o W_i D^{-1/2} & T^{-1}(\mathcal{Q} - L_o J L_c) T \end{bmatrix} \right\|_{i2} < 1. \tag{5.11}$$

In general, the RMC analysis for LTI Δ requires solving a nonlinear optimization problem with N variables. For specific W_o and $(\mathcal{Q}, L_o, L_c)$, however, the following straightforward result can be obtained.

Corollary 5.3. *Consider* (5.5) *with W_o given by*

$$W_o = \begin{bmatrix} w_0 I_q & & 0 \\ \vdots & \ddots & \\ w_{N-1} I_q & \dots & w_0 I_q \end{bmatrix}, \quad \text{with } w_{t \in [0, N-1]} \in \mathbb{R}, \ w_0 \neq 0. \tag{5.12}$$

Furthermore, assume Δ LTI, and $\mathcal{Q} = L_o J L_c$. Then a sufficient condition for $\mu_{\Delta_M}(M) < 1$ is given by

$$\|T^{-1} L_o W\|_{i2} < 1,$$

with $W := W_i W_o$.

Proof. See Appendix A.5.4. □

Corollary 5.3 can be applied to all SISO LTI systems with LTI Δ, since W_o can always be described by (5.12). Moreover, in Section 8.2 of [117] LTI uncertainty descriptions for MIMO systems are presented which fit the structure of (5.12). Consequently, the results of Corollary 5.3 can also be applied to uncertain MIMO systems.

In Section 5.6, we will show that the results of Corollary 5.3 are also valid for a class of LQ norm optimal ILC controllers for which $\mathcal{Q} \neq L_o J L_c$.

5.4.3   Case 3: Interval uncertainty

For completeness of the RMC analysis, we study model uncertainty represented by interval uncertainty in the impulse response of J_Δ. This problem formulation is equal to that in [4]. Note that interval uncertainty puts a norm bound on each individual Markov parameter, instead of on the Toeplitz matrix as a whole.

A sufficient RMC condition for Δ corresponding to interval uncertainty is presented in the following Lemma.

Lemma 5.3. *Consider* (5.5), *and interval uncertainty* Δ *from Table 5.1. Let the Toeplitz structure of* Δ *define the interconnection matrices* T_1 *and* T_2, *such that* $\Delta = T_1 \Delta^* T_2$, *with* Δ^* *defined by*

$$\Delta^* = \mathrm{diag}(\underbrace{\Delta_0, \dots, \Delta_0}_{N}, \underbrace{\Delta_1, \dots, \Delta_1}_{N-1}, \dots, \Delta_{N-1}). \tag{5.13}$$

Furthermore, let M^* *be given by*

$$M^* = \begin{bmatrix} T_2 & 0 \\ 0 & I_p \end{bmatrix} M \begin{bmatrix} T_1 & 0 \\ 0 & I_p \end{bmatrix}. \tag{5.14}$$

Then a sufficient condition for $\mu_{\Delta_M}(M) < 1$ *is given by the LMI*

$${M^*}^T D_M^* M^* - D_M^* \prec 0, \quad D_M^* \in \mathcal{D}_M^*, \tag{5.15}$$

with $\mathcal{D}_M^* = \{D_M^* = \mathrm{diag}(d_0 I_{Nq}, d_1 I_{q(N-1)}, \dots, d_N I_q, I_p) : d_t > 0\}$.

Proof. See Appendix A.5.5. □

The fact that the individual $\Delta_{t \in [0, N-1]}$ in interval uncertainty Δ from Table 5.1 are repeated $N - t$ times, inherently leads to an LMI solution which is high dimensional. Note furthermore, that the LMI solution of Lemma 5.3 is completely different from the solution presented in [4].

Remark 5.10. The structure of $\Delta_M^* = \text{diag}(\Delta^*, \Delta_P)$ for interval uncertainty is of the form

$$\Delta_M^* = \text{block diag}(\delta_0^r I_{Nq}, \ldots, \delta_{N-1}^r I_q, \Delta_P),$$

with $\delta_i^r \in [-1, 1]$ real scalars, i.e., we are dealing with Δ_M^* which contains both real and complex valued uncertainties. Furthermore, the structure of this Δ_M^* coincides with the uncertainty structure used in mixed μ problems, see e.g., [141]. Consequently, it is possible to find an upper bound for $\mu_{\Delta_M}(M)$ using a mixed μ upper bound which can be less conservative than the complex μ upper bound of Proposition 5.2.

5.5 RMC for the uncertain systems with basis functions

To expand the RMC results to a larger class of systems, in this section, we discuss the RMC conditions for systems with basis functions, as defined in Chapter 4.

The general system description with original uncertain system J_Δ and matrices with basis functions (T_f, T_y) is depicted in Figure 5.4. By considering T_f and T_y part of the uncertain system, we obtain the uncertain general system description

$$H_\Delta = T_y J_\Delta T_f \rightarrow H_\Delta = H + V_i \Delta V_o, \quad \text{with } V_i = T_y W_i, \ V_o = W_o T_f, \quad (5.16)$$
$$\Psi = \{H_\Delta : H_\Delta = H + V_i \Delta V_o, \Delta \in \boldsymbol{\Delta}\}.$$
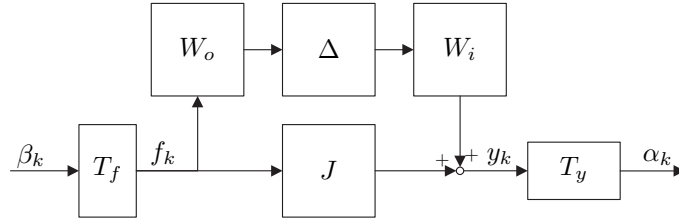
Figure 5.4: General system description with uncertainty $W_i \Delta W_o$.

As a consequence of the basis functions, the ILC control framework of Figure 5.2 changes to the framework presented in Figure 5.5, and the trial dynamics correspond to

$$u_{k+1} = \mathcal{Q} u_k + L_o \epsilon_k, \quad \beta_k = L_c u_k, \quad u_0 = 0 \quad (5.17)$$
$$u_{k+1} = (\mathcal{Q} - L_o H_\Delta L_c) u_k + L_o \alpha_d, \quad f_k = \underbrace{T_f L_c}_{L_c^{im}} u_k, \quad u_0 = 0. \quad (5.18)$$

Using Lemma 4.1 and Corollary 5.1, we can find a sufficient RMC condition for systems with basis functions.
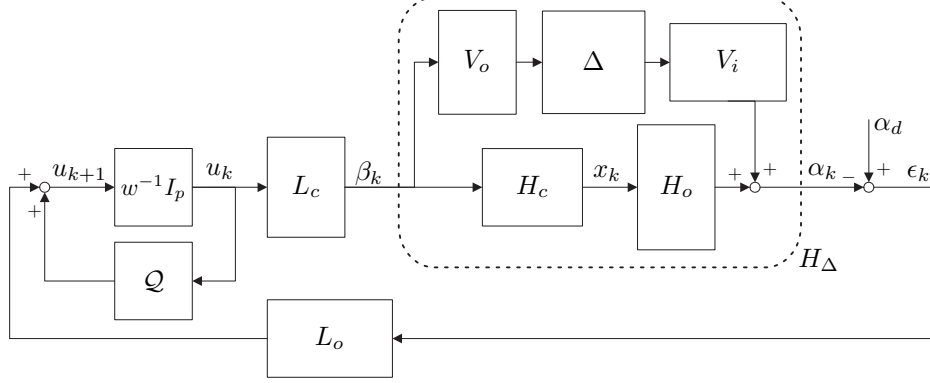
Figure 5.5: ILC framework in trial domain including model uncertainty $V_i \Delta V_o$.

Corollary 5.4. *Consider the ILC controlled system* (5.18), *and let T satisfy $T^T L_c^{im^T} L_c^{im} T = I_p$. Then* (5.18) *is RMC in f_k if $\|T^{-1}(\mathcal{Q} - L_o H_\Delta L_c)T\|_{i2} < 1$ $\forall H_\Delta \in \Psi$.*

Additionally, using (4.7), (4.8), and $\mathcal{Q}$, we can formulate convergence conditions as function of $(\mathcal{Q}, S_o, S_c)$, similar to Lemma 4.4.

Lemma 5.4. *Consider* (4.7), (4.8), *and the ILC controlled system* (5.18) *for given (V_i, V_o). Then for any M_c and any P_o with $\mathrm{rank}(P_o H_o) = p$, there exists $(\mathcal{Q}, S_o, S_c)$ such that* (5.18) *is robustly monotonically convergent in f_k.*

Proof. Given the robust monotonic convergence condition
$\|T^{-1}(\mathcal{Q} - S_o P_o H_\Delta (H_c^\dagger S_c + T_c^\dagger M_c))T\|_{i2} < 1$ $\forall \Delta \in \mathbf{\Delta}$. Then for any M_c and any P_o with $\mathrm{rank}(P_o Ho) = p$, there exists $\mathcal{Q}$ with $\overline{\sigma}(\mathcal{Q}) \leq c$ and (S_o, S_c) with $\overline{\sigma}(S_o P_o H_\Delta (H_c^\dagger S_c + T_c^\dagger M_c)) \leq r$ $\forall H_\Delta \in \Psi$, such that $c + r < 1$. One such solution is given by $(\mathcal{Q}, S_o) = (gI_p, gI_p)$ with $g \downarrow 0$ and $S_c = I_p$. $\qquad \square$

Based on Lemma 5.4, we state that RMC can be obtained for any uncertain system: Any trial domain shift operator w^{-1} that is not stabilized by $L_o H_\Delta L_c$ (the outer loop) can now be stabilized by proper design of $\mathcal{Q}$ (the inner loop). Furthermore, we can see that RMC approaches MC if $P_o V_i \to 0$, or if $V_o H_c^\dagger \to 0$ with $M_c = 0$, i.e., if the output signal generated by V_i is canceled by P_o, or if the command signal resulting from L_c does not excite V_o, respectively.

To obtain easy-to-calculate RMC conditions for systems with basis functions, we define a $M\Delta_M$ structure similar to that of Section 5.3. While Δ_M for systems

with basis function is equal to (5.6), matrix M is expressed by

$$\begin{bmatrix} q_k \\ z_{k+1} \end{bmatrix} = \underbrace{\begin{bmatrix} 0 & W_o T_f L_c T \\ -T^{-1} L_o T_y W_i & T^{-1}(\mathcal{Q} - L_o H L_c)T \end{bmatrix}}_{M} \begin{bmatrix} p_k \\ z_k \end{bmatrix}. \tag{5.19}$$

With M and Δ_M known, the results from Section 5.4 are directly applicable.

Corollary 5.5. *Consider M from (5.19), Δ LTV, and $\mathcal{Q} = L_o H L_c$. Moreover, let T satisfy $T^T L_c^{im^T} L_c^{im} T = I_p$. Then a sufficient condition for $\mu_{\Delta_M}(M) < 1$ is given by*

$$\|T^{-1} L_o T_y W_i\|_{i2} \cdot \|W_o T_f L_c T\|_{i2} < 1.$$

Corollary 5.6. *Consider M from (5.19) with W_o given by (5.12). Furthermore, assume Δ LTI, $\mathcal{Q} = L_o H L_c$, and let T satisfy $T^T L_c^{im^T} L_c^{im} T = I_p$. Then a sufficient condition for $\mu_{\Delta_M}(M) < 1$ is given by*

$$\|T^{-1} L_o T_y W\|_{i2} < 1,$$

with $W = W_i W_o$.

5.6 Example: RMC of LQ norm optimal ILC control

In this section, we first introduce LQ norm optimal ILC control, and briefly discuss its convergence and performance properties. Subsequently, we analyze the RMC conditions of LQ norm optimal ILC. To simplify the analysis, we choose $T_f = T_y = I$, i.e., we focus on LQ norm optimal ILC for servo tasks (Section 5.4). Moreover, we consider $L_c = I$, and hence the situation $f_k = u_k$ and $T^T L_c^T L_c T = I_p \rightarrow T = I_p$.

5.6.1 LQ norm optimal ILC control design

The LQ norm optimal ILC control problem solves the optimization problem ([50, 56, 58]):

$$\min_{f_{k+1}} \mathcal{J}, \text{ with } \mathcal{J} = e_{k+1}^T Q e_{k+1} + f_{k+1}^T S f_{k+1} + (f_{k+1} - f_k)^T R(f_{k+1} - f_k), \tag{5.20}$$

with (Q, R, S) symmetric, positive (semi-)definite matrices, often chosen to be diagonal: $(Q, R, S) = (qI, rI, sI)$. Since only the ratio between q, r, and s is of importance in the optimization problem, r and s are usually defined relative to $q = 1$. Note however, that for specific ILC problem formulations, a non-diagonal

(Q, R, S) can be preferred, see e.g., the contour tracking problem in [14], and Chapter 6.

With the derivation of the LQ norm optimal controller similar to that of Proposition 3.2, we directly present the resulting controller

$$
\begin{aligned}
f_{k+1} &= \mathcal{Q} f_k + L_o e_k, \quad f_0 = 0 \\
\mathcal{Q} &= (J^T Q J + S + R)^{-1} (J^T Q J + R) \\
L_o &= (J^T Q J + S + R)^{-1} J^T Q
\end{aligned}
\tag{5.21}
$$

Note the difference between the weight Q and the ILC control element $\mathcal{Q}$.

Monotonic convergence

For LQ norm optimal ILC controlled systems, monotonic convergence in f_k requires $\|T^{-1}(\mathcal{Q} - L_o J L_c) T\|_{i2} = \|(J^T Q J + S + R)^{-1} R\|_{i2} < 1$. From this, we can conclude that for $S > 0$, MC for LQ norm optimal ILC is always achieved. On the other hand, for $S = 0$ ($\mathcal{Q} = I_p$), the LQ norm optimal controlled system is MC, if and only if J has full column rank, see Lemma 3.1. If we want to consider $S = 0$ a valid solution for our LQ norm optimal problem, we need to define the LQ norm optimal ILC controller L_o using J_o instead of J, and introduce $L_c = J_c^\dagger$ (as is done in Section 3.3).

In this example, however, we simply solve the convergence problem by explicitly taking $S > 0$. With $S > 0$, the trial domain shift operators w^{-1} which are not stabilized by $L_o J$ (the outer loop), are stabilized by $\mathcal{Q}$ (the inner loop).

Convergence speed

The weighting R strongly influences the convergence speed: For $R = 0$, we find $\|(J^T Q J + S + R)^{-1} R\|_{i2} = 0$. As a result, the ILC controlled system converges in one trial, i.e., we have deadbeat ILC control. If $R \gg J^T Q J + S$ for some gains in R, we find that $\|(J^T Q J + S + R)^{-1} R\|_{i2} = 1 - \varepsilon$ with $0 < \varepsilon \ll 1$. Consequently, the convergence speed can be arbitrarily slow.

Performance

In ILC for servo tasks, the performance measure $\mathcal{P}_\xi$ equals $\mathcal{P}_e$, i.e., the performance measure focusses on the asymptotic error e_∞. With $\mathcal{P}_e = \|e_\infty\|_2$ and e_∞ given by

$$
\begin{aligned}
f_\infty &= (\mathcal{Q} - L_o J L_c) f_\infty + L_o y_d \\
&= (I_{Nq_i} - \mathcal{Q} + L_o J L_c)^{-1} L_o y_d \\
e_\infty &= y_d - J f_\infty \\
&= (I_{Nq_o} - J(I_{Nq_i} - \mathcal{Q} + L_o J L_c)^{-1} L_o) y_d \\
&= (I_{Nq_o} - J(J^T Q J + S)^{-1} J^T Q) y_d,
\end{aligned}
\tag{5.22}
$$

we can state that $\|e_\infty\| = 0$ for arbitrary y_d iff $\text{rank}(J) = Nq_o$ (and hence $q_i \geq q_o$) and $\mathcal{Q} = I_p$ ($S = 0$), see Lemma 5.1. Furthermore, weighting R does not influence the value for e_∞ in (5.22).

Moreover, from Section 4.5, we can conclude that the effects of trial varying disturbances on the error signal can be reduced by reducing the convergence speed. With R the dominant factor in the convergence condition $\|(J^T Q J + S + R)^{-1} R\|_{i2}$, R can be used to suppress the effects of trial varying disturbances on the asymptotic error.

5.6.2 RMC for LQ norm optimal ILC

Based on the LQ norm optimal controller (5.21) and Corollary 5.1, RMC of the ILC controlled system (5.4) requires

$$\|T^{-1}(\mathcal{Q} - L_o J_\Delta L_c)T\|_{i2} < 1, \ \forall \Delta \in \mathbf{\Delta} \Rightarrow \tag{5.23}$$
$$\|(J^T Q J + S + R)^{-1}(R - J^T Q W_i \Delta W_o)\|_{i2} < 1, \ \forall \Delta \in \mathbf{\Delta}.$$

Formulation of the RMC problem in $M\Delta_M$ structure results in

$$M = \begin{bmatrix} 0 & W_o \\ -(J^T Q J + S + R)^{-1} J^T Q W_i & (J^T Q J + S + R)^{-1} R \end{bmatrix} \tag{5.24}$$
$$\Delta_M = \text{diag}(\Delta, \Delta_P).$$

With these M and Δ_M, the RMC properties of LQ norm optimal ILC are derived. This is done for two cases: a) the case $R = 0$, and b) $R = rI$ with $r \geq 0$.

Case a: $R = 0$
From (5.24), it can be seen that $R = 0$ implies $\mathcal{Q} = L_o J L_c$. As a result, the RMC results from Section 5.4 can directly be applied to LQ norm optimal ILC as a corollary to Corollary 5.2 and Corollary 5.3, respectively.

Corollary 5.7. *Consider* (5.24), $R = 0$, *and* Δ *LTV. Then a sufficient condition for RMC of* (5.24) *in* f_k *is given by*

$$\|(J^T Q J + S)^{-1} J^T Q W_i\|_{i2} \cdot \|W_o\|_{i2} < 1.$$

Corollary 5.8. *Consider* (5.24) *with* W_o *given by* (5.12), $R = 0$, *and* Δ *LTI. Then a sufficient condition for RMC of* (5.24) *is given by*

$$\|(J^T Q J + S)^{-1} J^T Q W\|_{i2} < 1,$$

with $W = W_i W_o$.

Remark 5.11. From Corollaries 5.7 and 5.8, it can be concluded that RMC of (5.24) can be achieved by increasing S, independent of the structure of Δ_M. On the other hand, with $\overline{\sigma}(S) \downarrow 0$ leading to smaller $\|e_\infty\|_2$, tuning of S provides a compromise between robust monotonic convergence and performance.

Based on Corollaries 5.7 and 5.8, in Corollary 5.9 we show that for specific model uncertainty, RMC can be achieved with inverse model based ILC.

Corollary 5.9. *Consider the ILC controlled system* (5.24) *with J of full rank and $q_i \leq q_o$, Δ LTI, and W_o given by* (5.12). *Then a sufficient condition for RMC of* (5.24) *in f_k with inverse model based ILC controller $L_o = J^\dagger$ and $L_c = I$ is given by $\|J^\dagger W_i W_o\|_{i2} < 1$.*

From Corollary 5.9, we can conclude that RMC is guaranteed with inverse model based ILC, if the gains in W in the principal directions (singular vectors) of J are smaller than the gains of J. In many applications, though, the condition of Corollary 5.9 can not be satisfied. As a result, in practice we often need to include the additional $\mathcal{Q}$ filter in the ILC controller.

Case b: $R = rI$
For $R = 0$, Corollaries 5.7 and 5.8 provide easy-to-calculate RMC conditions for LQ norm optimal ILC. For $R = rI > 0$, however, these RMC conditions are also directly applicable, see Lemma 5.5.

Lemma 5.5. *Consider the ILC controlled system* (5.24) *with $R = rI \geq 0$, and Δ having any of the structures in Table 5.1. Furthermore, assume* (5.24) *to be RMC in f_k for the case $R = 0$. Then* (5.24) *is RMC in f_k for any $r \geq 0$.*

Proof. See Appendix A.5.6. □

From Lemma 5.5, it can be concluded that if (5.24) is RMC in f_k for $R = 0$, then $R = rI \geq 0$ does not influence the RMC properties of LQ norm optimal ILC. (this confirms results in [52, 55, 56]).

5.7 Example: RMC simulations for LQ norm optimal ILC

We illustrate the RMC results of Section 5.6 by means of simulation examples. After introducing the uncertain system, we compare the finite time and frequency domain RMC results of Section 5.6. Subsequently, we show the influence of the tuning parameters R and S on the ILC controlled system behavior.

The uncertain system used in this section represents a mass produced mechanical SISO system showing production tolerances. The frequency response measurements of different sample systems $J_\Delta(z)$ of this system are presented in Figure 5.6. Variations in experimental data are caused by the production tolerances.
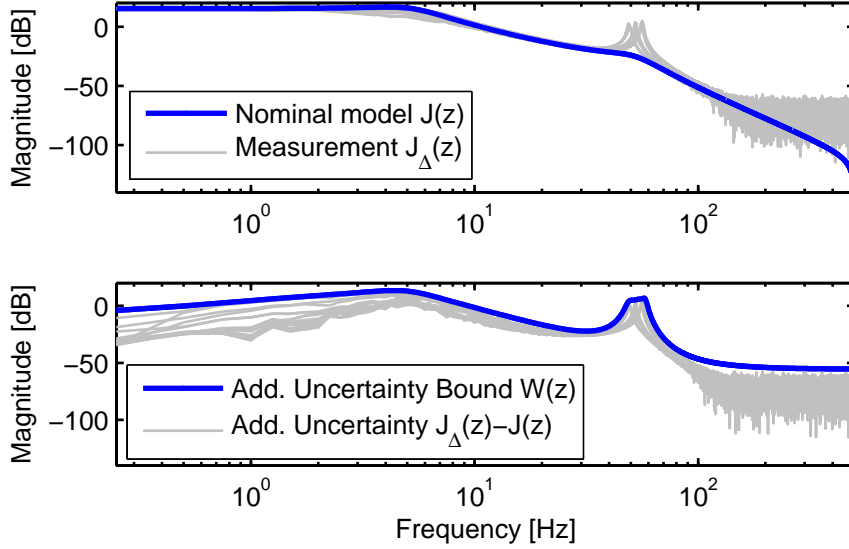
Figure 5.6: Top: Magnitude plot of the uncertain system $J_\Delta(z)$ and nominal model $J(z)$. Bottom: Additive uncertainty $J_\Delta(z) - J(z)$ and user defined upper bound for the additive upper bound $W(z)$.

Since in this example we are dealing with a SISO system, $W(z)$ can be appointed to either $W_i(z)$ or $W_o(z)$. We select $W_i(z) = 1$ and $W_o(z) = W(z)$ to illustrate the differences between the RMC conditions of Corollary 5.2 and Corollary 5.3.

With $J(z)$, $W_i(z)$, and $W_o(z)$ known, the lifted domain system descriptions can be calculated. Thereto, we consider $N = 500$ samples in one trial. The obtained $J \in \mathbb{R}^{500 \times 500}$ is square and rank deficient due to a nonzero relative degree (see [123] for reasons of rank loss in J), and W_i and W_o are square and of full rank. Furthermore, the LQ norm optimal controller used in the simulations is given by

$$\mathcal{Q} = (J^T J + (r+s)I)^{-1}(J^T J + rI)$$
$$L_o = (J^T J + (r+s)I)^{-1}J^T, \quad L_c = I,$$

with $r \geq 0$, and $s > 0$ due to the rank deficiency of J.

In this example, we compare the finite time interval RMC results from Section 5.6 with the frequency domain condition $\mu_{\Delta_M}(M(e^{j\theta})) < 1$. For this purpose, the matrix $M(e^{j\theta})$ for $r = 0$ given by

$$M(e^{j\theta}) = \begin{bmatrix} 0 & W_o(e^{j\theta}) \\ -(J(e^{-j\theta})J(e^{j\theta}) + s)^{-1}J(e^{-j\theta}) & 0 \end{bmatrix}.$$

To determine $\mu_{\Delta_M}(M(e^{j\theta}))$, $D_M(e^{j\theta_i})$ is defined as $\text{diag}(d(e^{j\theta_i}), 1)$ for $\theta_i \in \theta^*$, with θ^* a frequency grid. Subsequently, for each $\theta_i \in \theta^*$ $\mu_{\Delta_M}(M(e^{j\theta_i}))$ is calculated using the function `mussv` from Matlab®. $\mu_{\Delta_M}(M(e^{j\theta}))$ then approximately equals $\max_{\theta_i} \mu_{\Delta_M}(M(e^{j\theta_i}))$. Note that this procedure closely resembles to that of, e.g., [34, 42].

With the various systems defined, the finite time interval RMC conditions from Section 5.6 are compared with $\mu_{\Delta_M}(M(e^{j\theta}))$ for the uncertainty models presented in Table 5.2.

Table 5.2: Uncertainty models used in the simulations.

Case	Δ	RMC condition
1	LTV	$\|W_o\|_{i2} \cdot \|L_o\|_{i2}$
2	LTI	$\|L_o W_o\|_{i2}$

To study conservatism of the RMC conditions of Table 5.2 and $\mu_{\Delta_M}(M(e^{j\theta}))$, the minimal value for s for which RMC is achieved is plotted as function of the total number of samples N in a trial, Figure 5.7. Recall that for arbitrary y_d, a smaller s leads to better performance. From Figure 5.7, it can be concluded that for this example case 1 is more conservative than case 2 for all N, but less conservative than $\mu_{\Delta_M}(M(e^{j\theta}))$ for $N < 35$. Moreover, it can be stated that case 2 is less conservative than the frequency domain $\mu_{\Delta_M}(M(e^{j\theta}))$ for all N. For example, for $N = 50$ the value for s in case 2 is 318% smaller than the value for $\mu_{\Delta_M}(M(e^{j\theta}))$, and for $N = 500$, they differ 6%.
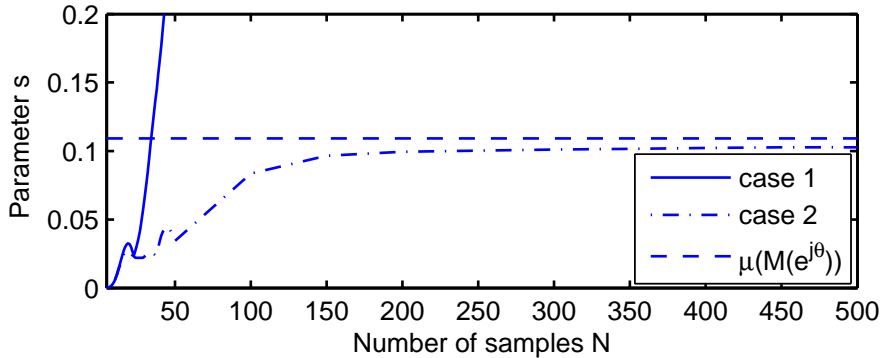
Figure 5.7: Minimal value for s for cases 1 and 2 of Table 5.2 and $\mu_{\Delta_M}(M(e^{j\theta}))$ for which RMC is achieved.

Next, the influence of s and r on the RMC properties and the asymptotic error e_∞ of the ILC controlled system are studied. With $z_0 = 0$ and $y_d \neq 0$ in this example, RMC requires $\|z_{k+1} - z_\infty\|_2 < \|z_k - z_\infty\|_2$, with z_∞ the asymptotic value of z_k for $k \to \infty$. The shown results are based on $J_\Delta = J + W_i \Delta W_o$ for 10 different samples Δ.

In Figure 5.8, convergence of the trial state $\|z_k - z_\infty\|_2$ with $z_k \in \mathbb{R}^{500}$ is presented as function of different s, and $r = 0$. Thereby, it is verified that each sample system J_Δ is robustly convergent, and hence that for each J_Δ the z_∞ exists and is bounded. Using $\mu_{\Delta_M}(M) \leq \|L_o W\|_{i2}$, we find $\mu_{\Delta_M}(M) \leq 0.99$ for $s = 0.103$, $\mu_{\Delta_M}(M) \leq 1.34$ for $s = 0.075$, and $\mu_{\Delta_M}(M) \leq 1.95$ for $s = 0.05$. Conform the results from Section 5.6, from Figure 5.8 it can be concluded that convergence is not guaranteed to be monotonic for $\mu_{\Delta_M}(M) > 1$.
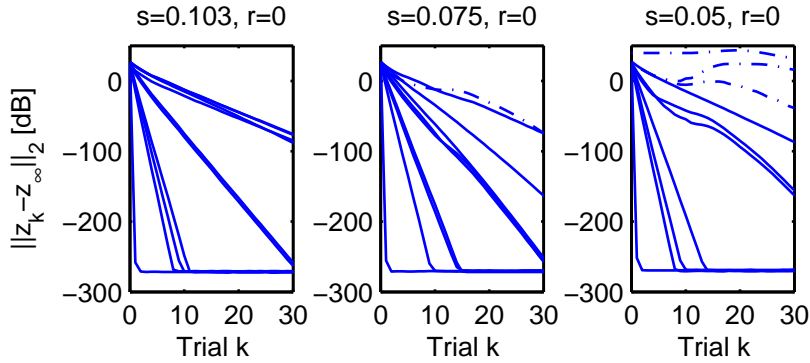
Figure 5.8: Propagation of $\|z_k - z_\infty\|_2$ for different values of s, and $r = 0$. Dashed-dotted lines correspond to sample systems which are not RMC. The asymptotic value for $\|z_k - z_\infty\|_2$ of approximately -270 dB is due to numerical issues.

While ILC control design often focusses on monotonic convergence of the command signal, in numerous ILC publications nominal monotonic convergence of the ILC controlled system is illustrated by showing $\|e_k\|_2$. Although for LQ norm optimal ILC with $\Delta = 0$, MC of the command signal can give MC of the error, RMC of the command signal does not directly imply RMC of the error, see Figure 5.9. Note that this issue seems not to be given much attention in ILC literature. Furthermore, since in this example the different J_Δ *are* convergent, the errors will eventually converge to their asymptotic value e_∞. Consequently, the behavior in the right plot of Figure 5.9 does not present unstable behavior, but trial domain transient behavior as discussed in [76]. Finally, note that the asymptotic error e_∞ increases for increasing s, as expected from (5.22).

In Figure 5.10, we illustrate that r does not influence the RMC properties of the ILC controlled system. Although a larger r does lead to slower convergence and can provide RC, as illustrated in Appendix B, it does not alter the RMC properties of the ILC controlled system (see Lemma 5.5).
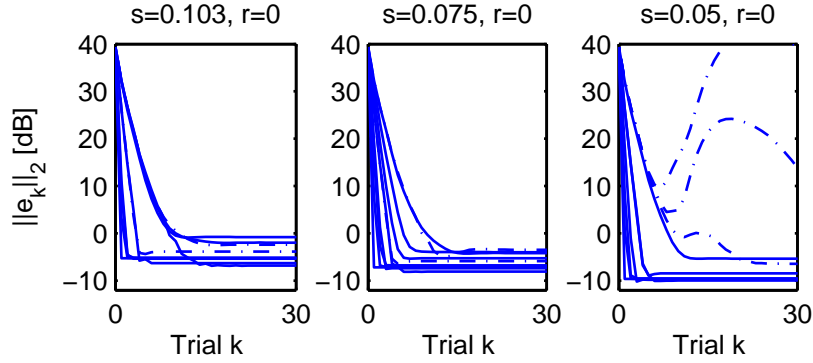
Figure 5.9: Propagation of $\|e_k\|_2$ for different values of s, and $r = 0$. Dashed-dotted lines correspond to sample systems for which the error does not convergence monotonically.
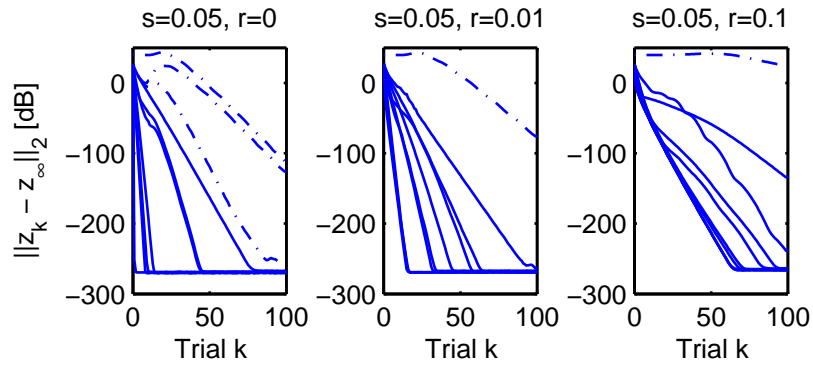
Figure 5.10: Propagation of $\|z_k - z_\infty\|_2$ for different values of r, and $s = 0.05$. Dashed-dotted lines correspond to sample systems which are not RMC.

5.8 Concluding remarks

In this chapter, an RMC analysis approach for ILC for uncertain systems has been presented. Initially, a model for uncertain systems has been derived by following the uncertain system modeling steps in infinite time robust control theory, while taking into account the finite time interval aspect of ILC. Subsequently, this model has been used in an RMC analysis based on μ analysis. Within this RMC analysis framework, it is possible to 1) include additive and multiplicative uncertainty models in the RMC problem formulation, 2) analyse RMC of linear time invariant MIMO systems controlled by any linear trial invariant ILC controller (causal and noncausal in time domain, time invariant and time varying, square and nonsquare), and 3) formulate additional straightforward RMC conditions for ILC controlled systems.

To illustrate the obtained results, the RMC properties of LQ norm optimal ILC have been analyzed. In the presented examples, it is shown that the RMC analysis approach proposed in this chapter can lead to less conservative RMC conditions than provided by a frequency domain RMC analysis. Moreover, the presented RMC results have resulted in straightforward tuning guidelines for LQ norm optimal ILC.

Conservatism

Until now, we have not focussed on possible conservatism in the finite time interval representation of the uncertainty model J_Δ, with respect to the original uncertainty model $J_\Delta(z)$. In other words, how large is the gap between $\|J_\Delta(z)\|_{i2}$ (infinite time) and $\|J_\Delta\|_{i2}$ for a given trial interval of N samples (finite time interval)?

To illustrate possible conservatism in the uncertainty representation over a finite time interval, we consider an uncertain model represented by a low pass filter $J_\Delta(z)$ (an 8th order Butterworth filter), with uncertain cut-off frequency ω, $\|J_\Delta(z)\|_{i2} = 1$, and sample time $T_s = 1 \cdot 10^{-3}$s. Moreover, given this $J_\Delta(z)$, we construct lower triangular Toeplitz matrices $J_\Delta \in \mathbb{R}^{N \times N}$ for different values for N.

The resulting $\|J_\Delta\|_{i2}$ as function of N and ω are shown in Figure 5.11. Based on his example, we state that for systems with relatively high frequent behavior, i.e., systems with time constants which are (roughly) more than 3 times smaller than the time interval of a trial, conservatism in induced 2-norm $\|J_\Delta\|_{i2}$ with respect to $\|J_\Delta(z)\|_{i2} = 1$ is less than a few percent.

With a nominal model $J(z)$ in ILC often dominated by low frequent dynamics, e.g., due to the implementation of a time domain feedback controller, and with model uncertainty $\Delta_J(z)$ often dominant at higher frequencies, the discussed example suggests that, in general, there can be little conservatism in the finite time interval uncertainty model representation. Note, however, that more research has to be conducted to formalize this statement.
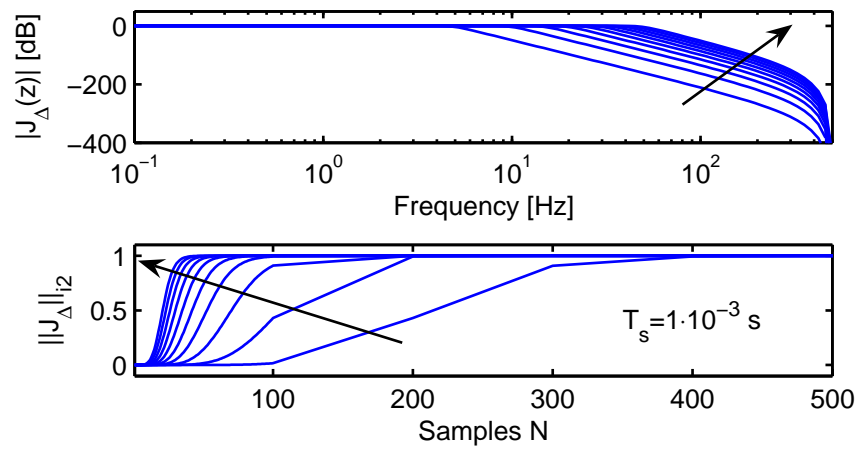
Figure 5.11: Top: Magnitude plot $|J_\Delta(z)|$. Bottom: Induced 2-norm $\|J_\Delta\|_{i2}$ as function of the number of samples N in a trial, using sample time $T_s = 1 \cdot 10^{-3}$s. The arrows point in the direction of increasing cut-off frequency ω.

Chapter 6

Noncausal finite time interval robust ILC control design

In this chapter, we present an ILC control strategy that is robust against model uncertainty as given by an additive uncertainty model. The design methodology hinges on $\mathcal{H}_\infty$ optimization, however, modified such that the obtained ILC controller is not restricted to be causal and inherently operates on a finite time interval. We subsequently analyze the convergence and performance properties of the resulting ILC controlled system, and provide guidelines to achieve optimized performance while remaining robustly monotonically convergent. Finally, in an example, we compare the presented robust ILC control strategy with LQ norm optimal ILC and a robust ILC approach based on a frequency domain μ procedure.

Introduction

The finite time interval robust ILC (R-ILC) controller that we derive in this chapter is based on the uncertain system description and ILC framework of Chapter 5. A practical reason for choosing additive uncertainty is that penalizing the input and output of the additive uncertainty model directly results in penalizing the (weighted) command signal and output of system J, similar to LQ norm optimal ILC. As a result, we can interpret the obtained robust controller as if it were a regular LQ norm optimal controller.

Under the assumption that $L_c = I_{Nq_i}$, in Section 6.1 to Section 6.3 we derive, analyze, and optimize the robust ILC controller in lifted domain, respectively.

Subsequently, we present a finite time interval state space representation of this controller in Section 6.4. And finally, we remove the assumption on L_c, resulting in R-ILC control design for systems with basis functions in Section 6.5. In Section 6.6, we compare the robust controller with other ILC control strategies on an experimental setup.

Part of the contents of this chapter is published in [44, 131].

6.1 Noncausal finite time interval robust ILC control design

We derive our R-ILC controller using a theory similar to $\mathcal{H}_\infty$ control theory for discrete time systems, [15, 75], but formulated to result in a finite time interval controller which is not restricted to be causal. Since the Hardy space refers to a class of stable, causal transfer functions, the name $\mathcal{H}_\infty$ is not appropriate for the presented solution.

6.1.1 General robust control formulation

In robust control theory, it is common to formulate the problem using the generalized plant paradigm, see Figure 6.1. In Figure 6.1, the signal $w_o(t)$ is referred to as exogenous input, and can include reference signals, noise signals, disturbance signals, etc. The signal $z_o(t)$ contains the performance variables, e.g., command signals and error signals. The signal $y(t)$ corresponds to the controller input, and $u(t)$ is the controller output. Finally, $q(t)$ and $p(t)$ are the input and output signal of uncertainty block Δ_G, respectively.
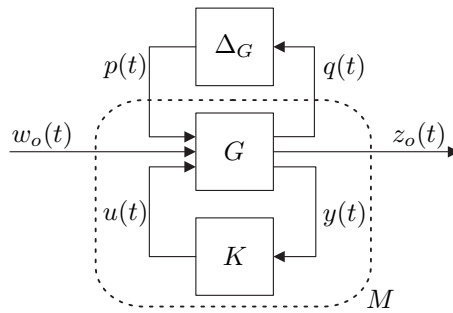
Figure 6.1: Generalized plant formulation with generalized plant G, controller K, and norm bounded uncertainty Δ_G.

For a generalized plant G with

$$ w(t) := \begin{bmatrix} p^T(t) & w_o^T(t) \end{bmatrix}^T, \quad z(t) := \begin{bmatrix} q^T(t) & z_o^T(t) \end{bmatrix}^T, $$

the finite time interval robust control problem consists of finding a robust controller K which minimizes the induced 2-norm of the mapping $M : w(t) \mapsto z(t)$, subject to a worst case disturbance $w(t)$, [15, 75]:

$$\gamma_{opt} = \min_{u(t)} \max_{w(t)} \|M\|_{i2}, \quad t \in [0, N-1]. \tag{6.1}$$

Since the solution of (6.1) is in general difficult to obtain, see, e.g., [143], we focus on finding a solution to a sub-optimal robust control problem for $\gamma > \gamma_{opt}$. For that purpose, we require the following result.

Lemma 6.1. *Given the optimization problem*

$$\max_{x} 1/2 x^T Q x + c^T x, \quad \text{subject to } Ax = b.$$

This optimization problem has a unique solution if A is of full rank and $Q \prec 0$ on the subspace $\ker(A)$, i.e., on the subspace $\{x : Ax = 0\}$.

Proof. See Section 10.3 and Section 14.1 in [80]. $\qquad\square$

Based on Lemma 6.1, we can pose the finite interval sub-optimal robust control problem.

Proposition 6.1. *Let (z, w, u, y) be the lifted representation of the finite time interval signals $(z(t), w(t), u(t), y(t))$ for $t = 0, \ldots, N-1$. Furthermore, consider the generalized plant*

$$\begin{bmatrix} z \\ y \end{bmatrix} = \begin{bmatrix} G_{11} & G_{12} \\ G_{21} & 0 \end{bmatrix} \begin{bmatrix} w \\ u \end{bmatrix}, \tag{6.2}$$

and the finite interval sub-optimal robust control problem

$$\min_{u} \max_{w} \mathcal{J}, \quad \text{with} \tag{6.3}$$
$$\mathcal{J} = 1/2 (G_{11}w + G_{12}u)^T (G_{11}w + G_{12}u) - 1/2\gamma^2 w^T w$$
$$+ \lambda^T (y - G_{21}w),$$

where λ is a Lagrange multiplier.

Given γ, then there exists a solution for (6.3), i.e., a saddle point, if G_{12} has full column rank, G_{21} has full row rank, and $G_{11}^T G_{11} - \gamma^2 I \prec 0$ on the subspace $\ker(G_{21})$, i.e., on the subspace $\{w : G_{21}w = 0\}$.

Proof. See Appendix A.6.1 for a sketch of the proof. $\qquad\square$

Note that existence of a unique solution for (6.3), i.e., the saddle point, does not necessarily imply that $\|M\|_{i2} < \gamma$. Optimization of γ such that $\|M\|_{i2}$ *is* smaller than γ is left for Section 6.3.

Under the conditions of Proposition 6.1, the solution for (6.3) is obtained by differentiating $\mathcal{J}$ with respect to u, w, and λ, and setting the expressions equal to zero. The controller K then corresponds to the mapping $K : y \mapsto u$.

Due to the definition of our robust control problem (6.1), the controller K clearly operates on a finite time span $t \in [0, N-1]$. That this K is not restricted to be causal will become clear in the following section.

6.1.2 Noncausal finite time interval robust ILC control design

In the previous section, we have formulated the finite time interval robust control problem for an arbitrary generalized plant G. Here, we formulate a specific generalized plant and solve (6.3) to find the finite time interval R-ILC controller.

To find the expression for the generalized plant, we define the variables (z, y, w, u) based on the following considerations:

- The desired control structure is given by (5.3).

- The main objective of our R-ILC control problem is to minimize the error at trial $k + 1$, i.e., e_{k+1}. With e_k given by $e_k = y_d - J f_k - W_i p_k$, the error e_{k+1} can be given by

$$e_{k+1} = e_k + J(f_k - f_{k+1}) + W_i(p_k - p_{k+1}). \tag{6.4}$$

- e_{k+1} is a function of both p_k and p_{k+1}. As a result, in Figure 6.1 we consider $\Delta_G = \text{diag}(\Delta, \Delta)$ with inputs q_k and q_{k+1}.

- We want to include an additional objective to penalize the change of the command signal between two trials, i.e., $f_\Delta = f_{k+1} - f_k$, using a weighting $R^{1/2}$ with $R = (R^{1/2})^T R^{1/2}$.

Based on these considerations, (z, y, w, u) can be given by (6.5), and the generalized plant G by (6.6). The resulting generalized plant formulation is presented in Figure 6.2.

$$z = \begin{bmatrix} q_k^T & q_{k+1}^T & e_{k+1}^T & f_\Delta^T \end{bmatrix}^T \tag{6.5a}$$

$$y = \begin{bmatrix} e_k^T & f_k^T \end{bmatrix}^T \tag{6.5b}$$

$$w = \begin{bmatrix} p_k^T & p_{k+1}^T & e_k^T & f_k^T \end{bmatrix}^T \tag{6.5c}$$

$$u = f_{k+1}. \tag{6.5d}$$

$$
\begin{bmatrix} q_k \\ q_{k+1} \\ e_{k+1} \\ \dfrac{f_\Delta}{e_k} \\ f_k \end{bmatrix} = \underbrace{\left[\begin{array}{cccc|c} 0 & 0 & 0 & W_o & 0 \\ 0 & 0 & 0 & 0 & W_o \\ W_i & -W_i & I & J & -J \\ 0 & 0 & 0 & -R^{1/2} & R^{1/2} \\ \hline 0 & 0 & I & 0 & 0 \\ 0 & 0 & 0 & I & 0 \end{array} \right]}_{G} \begin{bmatrix} p_k \\ p_{k+1} \\ e_k \\ \dfrac{f_k}{f_{k+1}} \end{bmatrix}.
\tag{6.6}
$$
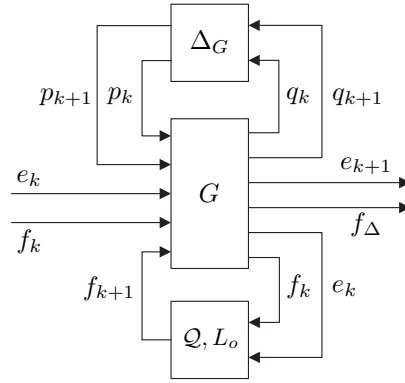
Figure 6.2: Generalized plant formulation for the R-ILC problem.

Using Lemma 6.1, in Corollary 6.1 we present existence conditions of a robust controller for the generalized plant (6.6).

Corollary 6.1. *Given the robust control problem* (6.3) *for generalized plant* (6.6). *There exists a unique solution for* (6.3), *if* $R > 0$ *and* $\gamma > \sqrt{2}\overline{\sigma}(W_i)$.

Proof. See Appendix A.6.2. $\qquad\qquad\square$

Given the generalized plant and existence conditions, we solve (6.3) to find the finite time interval R-ILC controller, see Proposition 6.2.

Proposition 6.2. *Given* (6.6) *with its inputs and outputs defined by* (6.5), $R > 0$ *and* $\gamma > \sqrt{2}\overline{\sigma}(W_i)$. *Then the controller that solves* (6.3) *is given by*

$$
\mathcal{Q} = (J^T Q J + S + R)^{-1}(J^T Q J + R)
\tag{6.7a}
$$

$$
L_o = (J^T Q J + S + R)^{-1} J^T Q,
\tag{6.7b}
$$

with

$$
Q = (I - 2\gamma^{-2} W_i W_i^T)^{-1} \text{ and } S = W_o^T W_o.
\tag{6.8}
$$

Proof. See Appendix A.6.3. $\qquad\qquad\square$

Note that the existence condition $\gamma > \sqrt{2}\overline{\sigma}(W_i)$ is also visible in the condition $Q \succ 0$.

Remark 6.1. Since $\mathcal{Q}$ and L_o both are a function of the upper triangular block Toeplitz matrix J^T, for this case the obtained ILC controller is noncausal.

Remark 6.2. In the derivation of the R-ILC controller, we find that the worst case disturbance satisfies $p_{k+1} = -p_k$. With the trial periodicity of this disturbance equal to $\ell = 2$, it corresponds to the worst case trial varying disturbance found in Section 4.5.

6.2 R-ILC analysis

In this section, the convergence and performance properties of R-ILC controlled system are studied. The obtained insight will subsequently be used in Section 6.3 to optimize the R-ILC controller parameters.

Since the R-ILC controller of Proposition 6.2 fits the LQ norm optimal ILC control solution, the results from LQ norm optimal ILC (Section 5.6) are exploited in the analysis. The difference between LQ norm optimal ILC and R-ILC lies in the fact that in LQ norm optimal ILC the weightings Q and S are user defined, while in R-ILC these weightings are the result of the specific robust problem formulation.

6.2.1 Convergence

As we already discussed in Section 5.6, monotonic convergence of R-ILC requires $J^TQJ + S$ to be positive definite. With W_o a full rank matrix and $Q > 0$ for all permissable γ, MC with R-ILC is always achieved.

Based on Corollaries 5.7 and 5.8, we know that RMC of the R-ILC controller is achieved for sufficiently large S. We leave it for Section 6.3, to show how to optimize the R-ILC controller such that RMC can be guaranteed for given model uncertainty (W_i, W_o).

Finally, equal to LQ norm optimal ILC, the weighting R is the dominant factor for convergence speed.

6.2.2 Performance

For performance, we focus on the asymptotic error e_∞. With $e_\infty = y_d - J_\Delta f_\infty$, and asymptotic command signal f_∞ given by

$$f_\infty = (\mathcal{Q} - L_o J_\Delta) f_\infty + L_o y_d$$
$$= (I - \mathcal{Q} + L_o J_\Delta)^{-1} L_o y_d,$$

the asymptotic error equals

$$e_\infty = \left(I - J_\Delta \left(I - \mathcal{Q} + L_o J_\Delta \right)^{-1} L_o \right) y_d. \tag{6.9}$$

Substitution of (6.7) in (6.9) subsequently yields

$$e_\infty = (I - J_\Delta (J^T Q J_\Delta + S)^{-1} J^T Q) y_d. \tag{6.10}$$

From (6.10), we can see that R (still) does not influence e_∞ of (6.10). In contrast, in Section 4.5, we showed that the influence of trial varying disturbances on performance can be reduced by increasing R.

From Lemma 5.1, we know that the asymptotic error can be made smaller by reducing the gains in S relative to Q, i.e., reducing the penalty on f_{k+1} relative to e_{k+1}. For Q and S defined by (6.8), $e_\infty = 0$ can not be achieved for all y_d. As we will show in Section 6.3, though, freedom in the definition of (W_i, W_o) can be used to reduce $\|e_\infty\|_2$.

6.3 R-ILC parameter optimization

6.3.1 Optimizing over γ

The R-ILC controller from Proposition 6.2 has only one parameter γ. Optimizing this R-ILC controller consists of finding an approximate for γ_{opt}, denoted by γ_{min}, within a user defined bound $\varepsilon > 0$: $\gamma_{min} < \gamma_{opt} + \varepsilon$, such that $\|M\|_{i2} < \gamma_{min}$.

To find γ_{min}, we first need the expression for the mapping $M : w \mapsto z$. This mapping M is obtained by closing the loop between G and $(L_o, \mathcal{Q})$, and equals

$$\begin{bmatrix} q_k \\ q_{k+1} \\ e_{k+1} \\ f_\Delta \end{bmatrix} = \underbrace{\begin{bmatrix} 0 & 0 & 0 & W_o \\ 0 & 0 & W_o L_o & W_o \mathcal{Q} \\ W_i & -W_i & I - J L_o & J(I - \mathcal{Q}) \\ 0 & 0 & R^{1/2} L_o & R^{1/2}(\mathcal{Q} - I) \end{bmatrix}}_{M} \begin{bmatrix} p_k \\ p_{k+1} \\ e_k \\ f_k \end{bmatrix}. \tag{6.11}$$

Using (6.11), γ_{min} can be obtained using a bisection algorithm, see Algorithm 1, [117, Section 9.3] and [131]. Initiation of this bisection algorithm requires the definition of an upper and lower bound on the possible values for γ ($\overline{\gamma}$ and $\underline{\gamma}$, respectively). The upper bound $\overline{\gamma}$ must be chosen sufficiently large to ensure an initial solution to the algorithm, i.e., to ensure that initially $\|M\|_{i2} < \overline{\gamma}$. The lower bound is defined by $\underline{\gamma} > \sqrt{2}\overline{\sigma}(W_i)$. Furthermore, $\varepsilon > 0$ is used as a tolerance for the distance between $\underline{\gamma}$ and $\overline{\gamma}$.

Note that, similar to $\mathcal{H}_\infty$ feedback control, the minimum value for γ_{min} does not have to result in robust monotonic convergence of the ILC controlled system.

This issue of RMC of the R-ILC controlled system can, however, be resolved, as we show now.

6.3.2 Optimizing over γ and d

In this section, we introduce a second parameter in the controller: d. Optimizing the R-ILC controller now consists of finding desired values for both γ and d.

Gain d in R-ILC is based on the equivalence of uncertainty models $W_i \Delta W_o$ and $(d^{-1} W_i)\Delta(d W_o)$, and originates from D-scaling, see Proposition 5.2. Consequently, optimization of the R-ILC controller through γ and d is comparable to the DK-iteration in μ-synthesis.

As a result of the introduction of d, the weighting matrices Q and S, (6.8), change to

$$Q = (I - 2\gamma^{-2}d^{-2}W_i W_i^T)^{-1}, \quad S = d^2 W_o^T W_o.$$

This, in turn, can be rewritten to

$$Q = (d^2 I - 2\gamma^{-2}W_i W_i^T)^{-1}, \quad S = W_o^T W_o, \tag{6.12}$$

with $\gamma > \sqrt{2}d^{-1}\overline{\sigma}(W_i)$.

Optimizing the R-ILC control parameters deals with optimizing performance, i.e., minimizing the asymptotic error e_∞, while satisfying RMC conditions. While from Lemma 5.1 and (6.10), it can be concluded that performance improvement requires an increase of Q relative to S, from Corollary 5.7 and Corollary 5.8, it can be concluded that RMC demands Q to be sufficiently small compared to

---

Algorithm 1 Bisection algorithm.

Initiation: $\gamma := \overline{\gamma}$, $\Omega := 1$.
while $\Omega = 1$, **do**
  Determine $\|M\|_{i2}$ for given γ, with M from (6.11).
  if $\|M\|_{i2} < \gamma$ holds, **then**
    $\overline{\gamma} \leftarrow \gamma$
  else
    $\underline{\gamma} \leftarrow \gamma$
  end if
  if $\overline{\gamma} - \underline{\gamma} \leq \varepsilon$, **then**
    $\gamma_{min} \leftarrow \overline{\gamma}$
    $\Omega \leftarrow 0$
  else
    $\gamma \leftarrow 0.5(\overline{\gamma} + \underline{\gamma})$
  end if
end while

S. The goal of optimizing the R-ILC controller hence consists of manipulating γ and d such that Q is maximized relative to S, while RMC of the ILC controlled system is guaranteed. This goal can be translated to: minimize d using, e.g., a line search, subject to the constraint that the ILC controlled system is RMC. For each value of d, find γ_{min} using Algorithm 1, with $\underline{\gamma} > \sqrt{2}d^{-1}\overline{\sigma}(W_i)$. The resulting d and γ_{min} for which the ILC controlled system is just RMC, i.e., for which $\|D_M^{1/2}MD_M^{-1/2}\|_{i2} = 1-\varepsilon$, with $0 < \varepsilon \ll 1$, constitutes the optimized R-ILC controller.

The idea behind this optimization approach is to minimize the difference between d^2 and $2\gamma^{-2}\overline{\sigma}(W_i)^2$ to increase Q relative to S, while remaining RMC. Thereby, realize that the induced 2-norm of M is lower bounded by the induced 2-norm of its elements, and hence that the difference between d^2 and $2\gamma^{-2}\overline{\sigma}(W_i)^2$ is lower bounded by the minimal value for γ_{min}:

$$\gamma_{min} > \|M\|_{i2} \geq \max(\sqrt{2}d^{-1}\overline{\sigma}(W_i), d\overline{\sigma}(W_o)).$$

While the suggested optimization approach can be applied to all (W_i, W_o), for the special case $(W_i, W_o) = (I, W)$, optimization of γ and d can actually be simplified considerably, see Proposition 6.3.

Proposition 6.3. *Consider the optimal R-ILC controller of Proposition 6.2 given by (6.7), uncertainty $(W_i, W_o) = (I, W)$, and resulting control weightings $Q = I$ and $S = d_\gamma W^T W$ with $d_\gamma = d^2 - 2\gamma^{-2} > 0$. Then optimizing the R-ILC controller with respect to performance while remaining RMC is equivalent to minimizing d_γ while satisfying the RMC conditions.*

The idea behind Proposition 6.3 is to minimize S relative to Q while remaining RMC, i.e., to optimize for performance under the constraint of RMC.

Once d_γ is minimized, using, e.g., a bisection algorithm, there always exists γ_{min} and d for which $\|M\|_{i2} < \gamma_{min}$ and $d_\gamma = d^2 - 2\gamma_{min}^{-2}$, namely

$$\gamma_{min} = \|M\|_{i2} + \varepsilon, \quad d = \sqrt{d_\gamma + 2\gamma_{min}^{-2}}.$$

Note, however, that design of L_o and $\mathcal{Q}$ is a function of d_γ only, and hence that there is no need to determine d and γ_{min} explicitly.

6.3.3 Achievable performance as function of W_i and W_o

In general, there is a difference in achievable performance between the cases $(W_i, W_o) = (W, I)$ and $(W_i, W_o) = (I, W)$. This can be explained by studying the influence of W_i and W_o on Q and S, respectively.

The case $(W_i, W_o) = (I, W)$ gives $Q = I$ and $S = d_\gamma W^T W$. For larger values for $\sigma(W)$ and d_γ, we can find $d_\gamma \sigma(W)^2 > 1$ (less error suppression in case of larger

model uncertainty), and for smaller values for $\sigma(W)$, we have gains in $S \downarrow 0$ (near full error suppression in case of no model uncertainty).

The case $(W_i, W_o) = (W, I)$ gives $Q = (d^2 I - 2\gamma^{-2} W W^T)^{-1}$ and $S = I$. While for larger values for $\sigma(W)$ and smaller values for d, we can find $Q \to \infty$ (near full error suppression in the presence of large model uncertainty), for smaller values for $\sigma(W)$, we approach the lower bound $Q \approx d^{-2} I$ (less error suppression in case of no model uncertainty). Based on this reasoning, we can conclude that this case considers the situation where the main disturbance in the ILC controlled system is generated by W_i, instead of by y_d.

Since ILC focusses on suppression of y_d instead of error suppression due to model uncertainty, the best performance is obtained with $(W_i, W_o) = (I, W)$. In Section 6.6, this case will be discussed.

6.4 R-ILC design: State space solutions

The R-ILC solution of Proposition 6.2 can also be expressed in state space notation. A huge benefit of this state space solution over the matrix solution, is the reduction in required buffer size to store the controller. Furthermore, the state space solution does not have to be redesigned if the trial length changes, and this formulation might simplify the inclusion of different uncertainty structures in the R-ILC control problem. Note, however, that inclusion of basis functions in the state space solution is, in general, not straightforward, and that determination of γ_{min} can be difficult.

To find the state space solution for the R-ILC controller, we use the generalized plant presented in Figure 6.1. The underlying structure of the generalized plant G is given by

$$
G \ : \ \left\{ \begin{bmatrix} x(t+1) \\ \hline z(t) \\ y(t) \end{bmatrix} = \left[\begin{array}{c|cc} A & B_1 & B_2 \\ \hline C_1 & D_{11} & D_{12} \\ C_2 & D_{21} & D_{22} \end{array} \right] \begin{bmatrix} x(t) \\ w(t) \\ u(t) \end{bmatrix} \right. . \tag{6.13}
$$

Without loss of generality, D_{22} can be set equal to zero, [81, 143]. Moreover, to guarantee the existence of a converging ILC controller, the generalized plant (6.13) is assumed to satisfy the following conditions, [117].

1. (C_2, A) is detectable.

2. (A, B_2) is stabilizable.

3. D_{12} has full column rank.

4. D_{21} has full row rank.

5. $\begin{bmatrix} A - e^{j\theta} & B_1 \end{bmatrix}$ has full row rank $\forall \theta \in [0, 2\pi]$.

6. $\begin{bmatrix} A - e^{j\theta} \\ C_1 \end{bmatrix}$ has full column rank $\forall \theta \in [0, 2\pi]$.

Note that conditions 5) and 6) are actually not required for finite time intervals. Nonetheless, throughout this section, we assume that the conditions 1) to 6) are satisfied, and that a solution for the robust control problem exists.

6.4.1 General finite time interval robust solution

Although the following results are known from literature, e.g., [15, 24], we present a summary of the results in a way suitable for ILC.

Based on Proposition 6.1, the robust optimization problem with G of (6.13) can be given by

$$\max_{w(t)} \min_{u(t)} \sum_{t=0}^{N-1} \left[1/2 z^T(t) z(t) - \frac{\gamma^2}{2} w^T(t) w(t) \right],\tag{6.14}$$

$$\text{subject to } \begin{cases} x(t+1) = Ax(t) + B_1 w(t) + B_2 u(t) \\ \quad\quad y(t) = C_2 x(t) + D_{21} w(t). \end{cases}$$

By introducing the Lagrange multipliers $\lambda(t)$ and $\lambda_2(t)$, the constraints in (6.14) can be incorporated in the cost function. Consequently, the constrained optimization problem (6.14) can be replaced by the unconstrained optimization problem

$$\max_{w(t)} \min_{u(t)} \mathcal{J},\tag{6.15}$$

$$\text{with } \mathcal{J} = \sum_{t=0}^{N-1} \Big[1/2 z^T(t) z(t) - \frac{\gamma^2}{2} w^T(t) w(t)$$
$$+ \lambda^T(t+1)(-x(t+1) + Ax(t) + B_1 w(t) + B_2 u(t))$$
$$+ \lambda_2^T(t+1)(-y(t) + C_2 x(t) + D_{21} w(t)) \Big].$$

The solution for (6.15), i.e., the saddle point, is obtained by differentiating $\mathcal{J}$ with respect to $x(t)$, $u(t)$, $w(t)$, $\lambda(t+1)$, and $\lambda_2(t+1)$, and setting the expressions equal to zero. To simplify the result, we assume that $C_2 = 0$. As we will show, this assumption holds for the generalized plant used in the design of the state space R-ILC controller.

After some algebraic manipulations, see Appendix A.6.4, the solution is given by

$$\begin{bmatrix} x(t+1) \\ \lambda(t) \end{bmatrix} = \begin{bmatrix} H_{11} & H_{12} \\ H_{21} & H_{11}^T \end{bmatrix} \begin{bmatrix} x(t) \\ \lambda(t+1) \end{bmatrix} + \begin{bmatrix} F_1 \\ F_2 \end{bmatrix} y(t)$$

$$u(t) = \begin{bmatrix} G_1 & G_2 \end{bmatrix} \begin{bmatrix} x(t) \\ \lambda(t+1) \end{bmatrix} + H_y y(t),$$

$$\begin{bmatrix} x(0) \\ \lambda(N) \end{bmatrix} = \begin{bmatrix} x_0 \\ 0 \end{bmatrix}, \tag{6.16}$$

with the elements in (6.16) equal to

$$\begin{aligned}
H_{11} &= A + B_1 E_2 D_{11}^T C_1 \\
&\quad - (B_1 E_2 D_{11}^T D_{12} + B_2) E_3^{-1} (D_{12}^T C_1 + D_{12}^T D_{11} E_2 D_{11}^T C_1) \\
H_{12} &= B_1 E_2 B_1^T - (B_1 E_2 D_{11}^T D_{12} + B_2) E_3^{-1} (D_{12}^T D_{11} E_2 B_1^T + B_2^T) \\
H_{21} &= C_1^T C_1 + C_1^T D_{11} E_2 D_{11}^T C_1 \\
&\quad - (C_1^T D_{12} + C_1^T D_{11} E_2 D_{11}^T D_{12}) E_3^{-1} (D_{12}^T C_1 + D_{12}^T D_{11} E_2 D_{11}^T C_1) \\
F_1 &= \left(B_1 - (B_1 E_2 D_{11}^T D_{12} + B_2) E_3^{-1} D_{12}^T D_{11} \right) E_1^{-1} D_{21}^T (D_{21} E_1^{-1} D_{21}^T)^{-1} \\
F_2 &= \left(C_1^T D_{11} - (C_1^T D_{12} + C_1^T D_{11} E_2 D_{11}^T D_{12}) E_3^{-1} D_{12}^T D_{11} \right) \\
&\quad E_1^{-1} D_{21}^T (D_{21} E_1^{-1} D_{21}^T)^{-1} \\
G_1 &= -E_3^{-1} (D_{12}^T C_1 + D_{12}^T D_{11} E_2 D_{11}^T C_1) \\
G_2 &= -E_3^{-1} (D_{12}^T D_{11} E_2 B_1^T + B_2^T) \\
H_y &= -E_3^{-1} D_{12}^T D_{11} E_1^{-1} D_{21}^T (D_{21} E_1^{-1} D_{21}^T)^{-1}, \tag{6.17}
\end{aligned}$$

and matrices E_1, E_2, and E_3 defined as

$$\begin{aligned}
E_1 &:= (\gamma^2 I - D_{11}^T D_{11})^{-1} \\
E_2 &:= E_1^{-1} - E_1^{-1} D_{21}^T (D_{21} E_1^{-1} D_{12}^T)^{-1} D_{21} E_1^{-1} \\
E_3 &:= D_{12}^T D_{12} - D_{12}^T D_{11} E_2 D_{11}^T D_{12}.
\end{aligned}$$

6.4.2 Finite time interval robust ILC

With the desire to express the R-ILC controller in state space notation, we use state space models J and $W_o = dW$ to construct the ILC controller. To simplify the solution, we consider filter $W_i = d^{-1} I$, $d > 0$. The gain d is a tuning gain, equal to the gain discussed in Section 6.3.

$$J: \begin{cases} x_j(t+1) &= A_j x_j(t) + B_j f(t) \\ y(t) &= C_j x_j(t) \end{cases} \tag{6.18a}$$

$$W_o: \begin{cases} x_w(t+1) &= A_w x_w(t) + B_w f(t) \\ q(t) &= \underbrace{dC_w^*}_{C_w} x_w(t) + \underbrace{dD_w^*}_{D_w} f(t) \end{cases} \tag{6.18b}$$

$$W_i: \quad y_w(t) \quad = \quad W_i p(t). \tag{6.18c}$$

Given (6.5), (6.13), and (6.18), we can formulate the generalized plant representing our robust control problem with state $x(t)$ given by

$$x(t) = \begin{bmatrix} x_{k_j}(t) \\ x_{k+1_j}(t) \\ x_{k_w}(t) \\ x_{k+1_w}(t) \end{bmatrix}.$$

A closer look at the generalized plant, however, reveals that we can reduce its order. This follows from the fact that 1) the states $x_{k_j}(t)$ and $x_{k+1_j}(t)$ are independently driven by command signals $f_k(t)$ and $f_{k+1}(t)$, respectively,

$$\begin{bmatrix} x_{k_j}(t+1) \\ x_{k+1_j}(t+1) \end{bmatrix} = \begin{bmatrix} A_j & 0 \\ 0 & A_j \end{bmatrix} \begin{bmatrix} x_{k_j}(t) \\ x_{k+1_j}(t) \end{bmatrix} + \begin{bmatrix} B_j & 0 \\ 0 & B_j \end{bmatrix} \begin{bmatrix} f_k(t) \\ f_{k+1}(t) \end{bmatrix},$$

and that 2) these states only appear in the performance output $e_{k+1}(t)$ as $x_{k+1_j}(t) - x_{k_j}(t)$

$$e_{k+1}(t) = e_k(t) - C_j(x_{k+1_j}(t) - x_{k_j}(t)) - W_i(p_{k+1}(t) - p_k(t)).$$

Hence, only the change of the states $x_j(t)$ from one trial to the next is of importance for ILC.

By defining $x(t)$ using state $\tilde{x}_{k_j}(t) = x_{k+1_j}(t) - x_{k_j}(t)$ instead of $x_{k_j}(t)$ and $x_{k+1_j}(t)$, we find the reduced order generalized plant with variables

$$x(t) = \begin{bmatrix} \tilde{x}_{k_j}(t) \\ x_{k_w}(t) \\ x_{k+1_w}(t) \end{bmatrix}, \qquad w(t) = \begin{bmatrix} p_k(t) \\ p_{k+1}(t) \\ e_k(t) \\ f_k(t) \end{bmatrix}, \quad u(t) = \begin{bmatrix} f_{k+1}(t) \end{bmatrix}$$

$$\tag{6.19}$$

$$z(t) = \begin{bmatrix} q_k(t) \\ q_{k+1}(t) \\ e_{k+1}(t) \\ f_{k+1}(t) - f_k(t) \end{bmatrix}, \quad y(t) = \begin{bmatrix} e_k(t) \\ f_k(t) \end{bmatrix},$$

with the different elements in the generalized plant of (6.16) given by

$$
A = \begin{bmatrix} A_j & 0 & 0 \\ 0 & A_w & 0 \\ 0 & 0 & A_w \end{bmatrix}, \quad
B_1 = \begin{bmatrix} 0 & 0 & 0 & -B_j \\ 0 & 0 & 0 & B_w \\ 0 & 0 & 0 & 0 \end{bmatrix}, \quad
B_2 = \begin{bmatrix} B_j \\ 0 \\ B_w \end{bmatrix}
$$

$$
C_1 = \begin{bmatrix} 0 & C_w & 0 \\ 0 & 0 & C_w \\ -C_j & 0 & 0 \\ 0 & 0 & 0 \end{bmatrix}, \quad
D_{11} = \begin{bmatrix} 0 & 0 & 0 & D_w \\ 0 & 0 & 0 & 0 \\ W_i & -W_i & I & 0 \\ 0 & 0 & 0 & -R^{1/2} \end{bmatrix}
$$

$$
C_2 = 0, \quad D_{11} = \begin{bmatrix} 0 & 0 & I & 0 \\ 0 & 0 & 0 & I \end{bmatrix}, \quad
D_{12} = \begin{bmatrix} 0 \\ D_w \\ 0 \\ R^{1/2} \end{bmatrix}, \quad D_{22} = 0. \tag{6.20}
$$

Substitution of (6.20) in (6.17), see Appendix A.6.5, yields the desired finite time interval R-ILC controller (6.16), with elements

$$
\begin{bmatrix} H_{11} & H_{12} \\ H_{21} & H_{11}^T \end{bmatrix} = \begin{bmatrix} A_h & -B_h R_h^{-1} B_h^T \\ C_h^T Q_h C_h & A_h^T \end{bmatrix} \tag{6.21}
$$

$$
B_h = \begin{bmatrix} B_j \\ 0 \\ B_w \end{bmatrix}, \qquad\qquad
S_h = \begin{bmatrix} 0 & 0 & (D_w^T D_w + R)^{-1} D_w^T \end{bmatrix}
$$

$$
C_h = \begin{bmatrix} C_j & 0 & 0 \\ 0 & C_w & 0 \\ 0 & 0 & C_w \end{bmatrix}, \quad
A_h = \begin{bmatrix} A_j & 0 & 0 \\ 0 & A_w & 0 \\ 0 & 0 & A_w \end{bmatrix} - B_h S_h C_h
$$

$$
R_h^{-1} = (D_w^T D_w + R)^{-1}, \quad
Q_h = \begin{bmatrix} \frac{\gamma^2}{\gamma^2 - 2W_i^2} I & 0 & 0 \\ 0 & I & 0 \\ 0 & 0 & (I + D_w R^{-1} D_w^T)^{-1} \end{bmatrix},
$$

and

$$
F_1 = B_h R_h^{-1} \begin{bmatrix} 0 & R \end{bmatrix} + \begin{bmatrix} -I & 0 & 0 \\ 0 & 0 & I \\ 0 & 0 & 0 \end{bmatrix} B_h \begin{bmatrix} 0 & I \end{bmatrix}, \quad G_1 = -S_h C_h
$$

$$
F_2 = C_h^T Q_h \begin{bmatrix} -I & 0 \\ 0 & D_w \\ 0 & D_w R_h^{-1} R \end{bmatrix}, \qquad\qquad G_2 = -R_h^{-1} B_h^T \tag{6.22}
$$

$$
H_y = \begin{bmatrix} 0 & R_h^{-1} R \end{bmatrix}.
$$

Finally, note that determination of a value for γ_{min} of noncausal state space models over a finite time interval is not always straightforward, due to the finiteness

of the state space representation of M. For relatively short trial spans, e.g., in our experience $N < 500$, we can find γ_{min} by constructing M of (6.11), and using the bisection algorithm presented in Algorithm 1. For larger trial spans, however, the computational load of the lifted notation becomes too large. Although a frequency domain expression of M makes it possible to handle longer trial spans, expressing the controller in frequency domain and subsequently analyzing $M(e^{j\theta})$ only results in approximate results, see Lemma 5.2. How to find a value for γ_{min} for larger trial spans remains unanswered in this thesis.

6.4.3 Implementation of the finite time interval robust controller

Solution (6.16) is not implementable in its current form, since the causal and anti-causal dynamics are not separated. This implementation issue can, however, be resolved by performing a similarity transformation which separates the causal part of the system from the anti-causal part, see [15, 90].

In this section, we discuss a time varying and time invariant similarity transformation. Both transformed R-ILC controllers show the time domain behavior which is hidden in the lifted R-ILC controller $(\mathcal{Q}, L_o)$. The benefit of the time varying transformation over the time invariant one is, that boundary conditions do not play a role in the solution. A drawback is, that a larger buffer size is required to store the time varying system matrices.

Conform the findings in Lemma 5.2, the time invariant transformation reveals that an LTI representation of the finite time interval ILC controller includes nonzero boundary conditions. Moreover, due to its LTI structure, the LTI solution can be used for a frequency domain interpretation of the obtained R-ILC controller.

Time varying similarity transformation
Although different time varying similarity transformations are possible, we use the time varying transformation discussed in [90]:

$$\begin{bmatrix} g(t) \\ \lambda(t) \end{bmatrix} = \begin{bmatrix} I & Y(t) \\ 0 & I \end{bmatrix} \begin{bmatrix} x(t) \\ \lambda(t) \end{bmatrix}. \tag{6.23}$$

Substitution of (6.23) in (6.16), see Appendix A.6.6, subsequently results in

$$\begin{bmatrix} g(t+1) \\ \lambda(t) \end{bmatrix} = \begin{bmatrix} A_{T1}(t) & 0 \\ A_{T2}(t) & (A_{T1}(t))^T \end{bmatrix} \begin{bmatrix} g(t) \\ \lambda(t+1) \end{bmatrix} + \begin{bmatrix} F_{T1}(t) \\ F_{T2}(t) \end{bmatrix} y(t),$$

$$u(t) = \begin{bmatrix} G_1 & G_2 \end{bmatrix} \begin{bmatrix} g(t) \\ \lambda(t+1) \end{bmatrix} - G_1 Y(t) \lambda(t) + H_y y(t),$$

$$\begin{bmatrix} g(0) \\ \lambda(N) \end{bmatrix} = \begin{bmatrix} x_0 + Y(0)\lambda(0) \\ 0 \end{bmatrix} = \begin{bmatrix} x_0 \\ 0 \end{bmatrix}, \tag{6.24}$$

with the different matrices described by

$$
\begin{aligned}
A_{T1}(t) &= A_h(I + Y(t)C_h^T Q_h C_h)^{-1} \\
A_{T2}(t) &= (I + C_h^T Q_h C_h Y(t))^{-1} C_h^T Q_h C_h \\
F_{T1}(t) &= F_1 - A_h Y(t)\left(I + C_h^T Q_h C_h Y(t)\right)^{-1} F_2 \\
F_{T2}(t) &= \left(I + C_h^T Q_h C_h Y(t)\right)^{-1} F_2.
\end{aligned}
\tag{6.25}
$$

The expression for $Y(t)$ is obtained by setting the mapping $\lambda(t+1) \mapsto g(t)$ equal to zero. As a result of this, we find the time varying Riccati equation

$$
\begin{aligned}
Y(t+1) &= A_h Y(t)(I + C_h^T Q_h C_h Y(t))^{-1} A_h^T + B_h R_h^{-1} B_h^T \\
&= A_h Y(t) A_h^T + B_h R_h^{-1} B_h^T \\
&\quad - A_h Y(t) C_h^T \left(Q_h^{-1} + C_h Y(t) C_h^T\right)^{-1} C_h Y(t) A_h^T,
\end{aligned}
\tag{6.26}
$$

with $Y(0) = 0$.

For implementation of (6.24), first determine $Y(t)$ for $t = 0, 1, \ldots, N-1$ and use $Y(t)$ to determine (6.25). Next, calculate $g(t+1)$, followed by $\lambda(t)$. Finally, determine $u(t)$. Note that calculation of $Y(t)$ and (6.25) has to be done only once, before the first trial. The computational burden between trials is limited to calculating $g(t+1)$, $\lambda(t)$, and $u(t)$.

Time invariant similarity transformation
The results presented here are based on the LQ norm optimal solutions presented in [37, 39, 57]. An important difference between the results from [37, 39] and the ones presented here, is that we obtain a (minimal order) state space solution for the ILC controller as a whole, while in [37, 39] the state space solution consists of the Hamiltonian system (6.16) together with an adjoint system.

The first step in finding an LTI implementable counterpart for (6.16) is similar to (6.23), but then with constant matrix Y

$$
\begin{bmatrix} g(t) \\ \lambda(t) \end{bmatrix} = \begin{bmatrix} I & Y \\ 0 & I \end{bmatrix} \begin{bmatrix} x(t) \\ \lambda(t) \end{bmatrix}.
\tag{6.27}
$$

Unsurprisingly, this transformation results in time invariant (6.24) and (6.25) in which $Y(t)$ is replaced by Y. The expression for Y is obtained by solving the discrete algebraic Riccati equation (DARE)

$$
Y = A_h Y A_h^T + B_h R_h^{-1} B_h^T - A_h Y C_h^T \left(Q_h^{-1} + C_h Y C_h^T\right)^{-1} C_h Y A_h^T,
\tag{6.28}
$$

Note that solving this DARE requires Q_h to be of full rank.

The second step is based on the similarity transformation

$$
\begin{bmatrix} g(t) \\ \zeta(t) \end{bmatrix} = \begin{bmatrix} I & 0 \\ X & I \end{bmatrix} \begin{bmatrix} g(t) \\ \lambda(t) \end{bmatrix}.
\tag{6.29}
$$

After algebraic computations, see Appendix A.6.7, we find the decoupled LTI R-ILC controller

$$\begin{bmatrix} g(t+1) \\ \zeta(t) \end{bmatrix} = \begin{bmatrix} A_{T1} & 0 \\ 0 & A_{T1}^T \end{bmatrix} \begin{bmatrix} g(t) \\ \zeta(t+1) \end{bmatrix} + \begin{bmatrix} F_{T1} \\ F_{T2} - (A_{T1})^T X F_{T1} \end{bmatrix} y(t)$$

$$u(t) = \begin{bmatrix} G_1(I+YX) & -G_2 X \end{bmatrix} \begin{bmatrix} g(t) \\ g(t+1) \end{bmatrix}$$

$$+ \begin{bmatrix} -G_1 Y & G_2 \end{bmatrix} \begin{bmatrix} \zeta(t) \\ \zeta(t+1) \end{bmatrix} + H_y y(t), \tag{6.30}$$

with X the solution to the Sylvester equation

$$A_{T1}^{-T} X - X A_{T1} = -A_{T1}^{-T} A_{T2}.$$

Although these LTI dynamics of (6.30) capture the time domain behavior of the R-ILC controller, we do not yet know the value of the boundary conditions for $g(0)$ and $\zeta(N)$. We do, however, know that

$$g(N) = A_{T1}^N g(0) + \underbrace{\sum_{j=0}^{N-1} A_{T1}^{N-1-j} F_{T1} y(j)}_{\phi_g}$$

$$\zeta(0) = (A_{T1}^T)^N \zeta(N) + \underbrace{\sum_{j=0}^{N-1} (A_{T1}^T)^{N-1-j} (F_{T2} - A_{T1}^T X F_{T1}) y(N-1-j)}_{\phi_\zeta}.$$

Together with the overall similarity transformation

$$\begin{bmatrix} g(t) \\ \zeta(t) \end{bmatrix} = \begin{bmatrix} I & Y \\ X & I+XY \end{bmatrix} \begin{bmatrix} x(t) \\ \lambda(t) \end{bmatrix} \rightarrow \begin{bmatrix} x(t) \\ \lambda(t) \end{bmatrix} = \begin{bmatrix} I+YX & -Y \\ -X & I \end{bmatrix} \begin{bmatrix} g(t) \\ \zeta(t) \end{bmatrix}, \tag{6.31}$$

we can find the relation

$$\begin{bmatrix} x(0) \\ \lambda(N) \\ \phi_g \\ \phi_\zeta \end{bmatrix} = \underbrace{\begin{bmatrix} I+YX & -Y & 0 & 0 \\ 0 & 0 & -X & I \\ -A_{T1}^N & 0 & I & 0 \\ 0 & I & 0 & -(A_{T1}^T)^N \end{bmatrix}}_{T_{bound}} \begin{bmatrix} g(0) \\ \zeta(0) \\ g(N) \\ \zeta(N) \end{bmatrix}$$

$$\begin{bmatrix} g(0) \\ \zeta(0) \\ g(N) \\ \zeta(N) \end{bmatrix} = T_{bound}^{-1} \begin{bmatrix} x(0) \\ \lambda(N) \\ \phi_g \\ \phi_\zeta \end{bmatrix}. \tag{6.32}$$

With the righthand side of (6.32) fully known, the boundary conditions $g(0)$ and $\zeta(N)$ can be calculated using (6.32).

Before implementing the LTI R-ILC controller, determine matrices Y and X, and the values of the elements in (6.30) and T_{bound}^{-1}. Between each trial, calculate the boundary values $g(0)$ and $\zeta(N)$, see (6.32), and solve (6.30).

Remark 6.3. Instead of using a Riccati and Sylvester equation to decouple the controller dynamics, we can also use

$$\begin{bmatrix} x(t) \\ \lambda(t) \end{bmatrix} = \begin{bmatrix} I & -Y \\ X & I \end{bmatrix} \begin{bmatrix} g(t) \\ \zeta(t) \end{bmatrix}$$

$$\begin{bmatrix} g(t) \\ \zeta(t) \end{bmatrix} = \begin{bmatrix} (I+YX)^{-1} & (I+YX)^{-1}Y \\ -(I+XY)^{-1}X & (I+XY)^{-1} \end{bmatrix} \begin{bmatrix} x(t) \\ \lambda(t) \end{bmatrix}.$$

In this case, Y results from (6.28), and X from the DARE

$$X = A_h^T X A_h - A_h^T X B_h (R_h + B_h^T X B_h)^{-1} B_h^T X A_h + C_h^T Q_h C_h.$$

Finally, to make a frequency domain representation of the LTI controller possible, (6.30) is rewritten to

$$\begin{bmatrix} g(t+1) \\ \zeta(t+1) \end{bmatrix} = \begin{bmatrix} A_{T1} & 0 \\ 0 & (A_{T1}^{-1})^T \end{bmatrix} \begin{bmatrix} g(t) \\ \zeta(t) \end{bmatrix} + \begin{bmatrix} F_{T1} \\ -(A_{T1}^{-1})^T F_{T2} - X F_{T1} \end{bmatrix} y(t)$$

$$u(t) = \begin{bmatrix} G_1(I+YX) - G_2 X A_{T1} & G_2(A_{T1}^{-1})^T - G_1 Y \end{bmatrix} \begin{bmatrix} g(t) \\ \zeta(t) \end{bmatrix}$$

$$+ \left(-G_2(A_{T1}^{-1})^T F_{T2} + H_y \right) y(t).$$

Although the boundary conditions are an essential part of the R-ILC controller, in a frequency domain representation, they are not taken into account. Consequently, the frequency domain R-ILC controller description can only be used for a frequency interpretation of the controller, not for implementation.

6.5　R-ILC design for uncertain systems with basis functions

Until now, we focussed on R-ILC for systems performing servo tasks. In this section, we consider lifted R-ILC design for systems with basis functions. For this purpose, we explicitly take into account the rank conditions of the system, resulting in $L_c \neq I_p$. Design of L_c is, however, not considered here. For suggestions for L_c, see Section 3.3.

The R-ILC design problem in this section is based on the uncertain system given by H_Δ and ILC framework presented in Figure 5.5. Due to the introduction of basis functions, the error objective in (6.5) changes from e_{k+1} to ϵ_{k+1}. Furthermore, the input of the R-ILC controller is chosen as u_k and ϵ_k, and the output as u_{k+1}. Finally, the command signal f_{k+1} is given by $f_{k+1} = L_c^{im} u_{k+1}$.

The generalized plant G used to derive the R-ILC controller now equals

$$
\begin{bmatrix} q_k \\ q_{k+1} \\ \epsilon_{k+1} \\ \hline f_{k+1} - f_k \\ \hline \epsilon_k \\ u_k \end{bmatrix} = \left[\begin{array}{cccc|c} 0 & 0 & 0 & V_o L_c & 0 \\ 0 & 0 & 0 & 0 & V_o L_c \\ V_i & -V_i & I_n & H L_c & -H L_c \\ 0 & 0 & 0 & -R^{1/2} L_c^{im} & R^{1/2} L_c^{im} \\ \hline 0 & 0 & I_n & 0 & 0 \\ 0 & 0 & 0 & I_p & 0 \end{array} \right] \begin{bmatrix} p_k \\ p_{k+1} \\ \epsilon_k \\ \hline u_k \\ \hline u_{k+1} \end{bmatrix}. \qquad (6.33)
$$

With the generalized plant defined, we use Proposition 6.2 to find the R-ILC controller:

$$
\mathcal{Q} = (L_c^T H^T Q H L_c + S + L_c^{im^T} R L_c^{im})^{-1} (L_c^T H^T Q H L_c + L_c^{im^T} R L_c^{im}) \qquad (6.34)
$$

$$
L_o = (L_c^T H^T Q H L_c + S + L_c^{im^T} R L_c^{im})^{-1} L_c^T H^T Q, \qquad (6.35)
$$

with

$$
Q = (I - 2\gamma^{-2} V_i V_i^T)^{-1} \text{ and } S = L_c^T V_o^T V_o L_c, \qquad (6.36)
$$

and $\gamma > \sqrt{2}\bar{\sigma}(V_i)$.

From Q and S in (6.36), we can see that for R-ILC design for systems with basis functions only model uncertainty $V_i = T_y W_i$ and $V_o = W_o T_f$ are relevant for R-ILC control design.

6.6 Example

In this section, the designed R-ILC controller is compared to LQ norm optimal ILC and robust ILC control based on a frequency domain μ procedure, [34]. First, experimental result are presented. Second, the frequency domain interpretation of the LTI R-ILC controller of Section 6.4 is compared to that of μ ILC.

6.6.1 System description

The uncertain system used in this section represents a mass produced mechanical SISO system showing production tolerances, see Figure 6.3 and Appendix C.

The frequency response of the nominal model $J(z)$, upper bound for the uncertainty of this system $W(z)$, and additive uncertainty data from measurements are presented in Figure 6.4. Variations in experimental data are caused by the production tolerances. Since even the inverse model based ILC is RMC for relatively
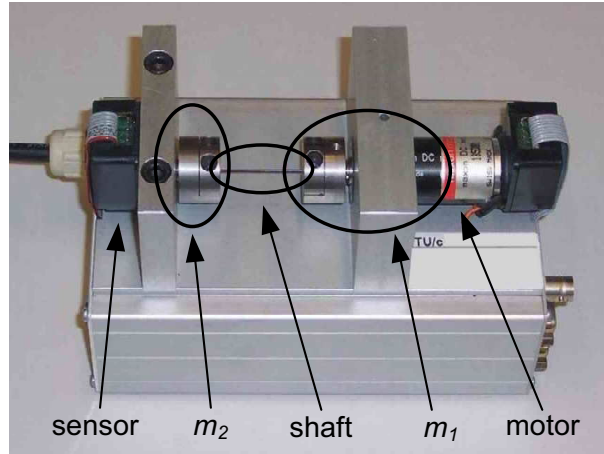
Figure 6.3: Two-inertia setup used for the experiments.

small model uncertainty, see Corollary 5.9, no attempts have been made to accurately upper bound the model uncertainty corresponding to low frequent dynamics. Using the impulse responses of $J(z)$ and $W(z)$, $N = 500$ and $T_s = 1 \cdot 10^{-3}$s, we find the finite time interval representation $J \in \mathbb{R}^{500 \times 500}$ (square and rank deficient due to a nonzero relative degree), and $W \in \mathbb{R}^{500 \times 500}$ (square and of full rank).
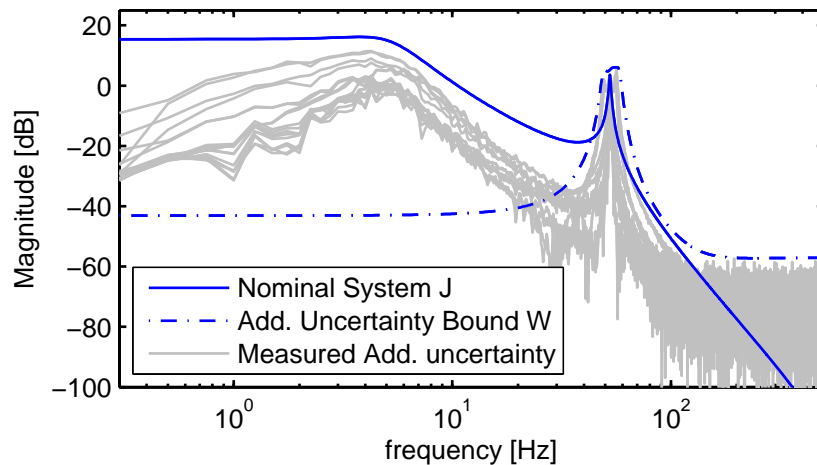
Figure 6.4: Frequency domain representation of nominal system $J(z)$, upper bound on the uncertainty $W(z)$, and additive uncertainty data from measurements.

6.6.2 Experimental results

The reference signal $y_d \in \mathbb{R}^{500}$ used for experimentation is presented in Figure 6.5. With this reference signal, the actuator in the feedback controlled system (without ILC) is pushed to its limits, i.e., approaches the saturation level of ± 2.5 volts.

Figure 6.5: Reference signal used for experimentation.

In the experiments, the R-ILC controller $(\mathcal{Q}^R, L_o^R)$ of (6.7) with weights $(Q, S, R) = (I, d_\gamma W^T W, 0)$ is compared to an LQ norm optimal ILC controller $(\mathcal{Q}^{LQ}, L_o^{LQ})$ with weights $(Q, S, R) = (I, sI, 0)$, and a robust ILC controller $(\mathcal{Q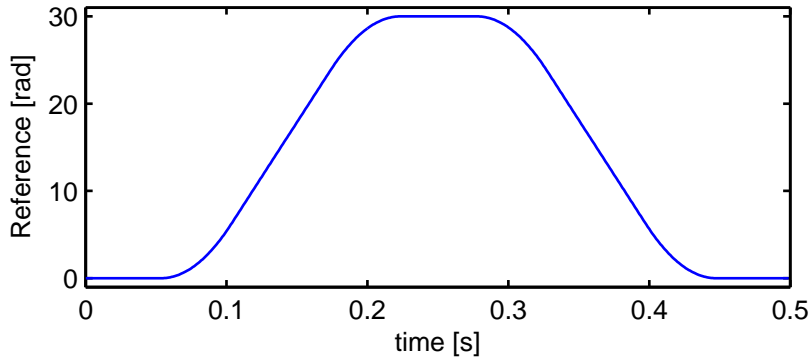}^\mu(z), L_o^\mu(z))$, with $L_o^\mu(z)$ designed using infinite-interval μ design and $\mathcal{Q}^\mu(z)$ a zero phase low pass filter, see [34]. Optimizing the R-ILC control parameters has resulted in $d_\gamma = 525$. For LQ norm optimal ILC, tuning has led to $s = 0.85$. In μ ILC, robustness is obtained by tuning the cut-off frequency of $\mathcal{Q}^\mu(z)$. The largest found cut-off frequency for which the system is RMC is 25 Hz.

Experiments are conducted on five different setups of the two-inertia system. In Figure 6.6, convergence of the different command signals is presented. Since in this case $u_0 = 0$ and $y_d \neq 0$, monotonic convergence of the ILC controlled systems equals $\|f_{k+1} - f_\infty\|_2 < \|f_k - f_\infty\|_2$. This is subsequently approximated by $\|f_{k+1} - f_{21}\|_2 < \|f_k - f_{21}\|_2$, since f_∞ is not available in practice. In Figure 6.6, we can see that the finite time interval ILC controllers converge to (near) zero, while the μ ILC controller remains to fluctuate. As we will show, this phenomenon is caused by oscillatory boundary effects in the command signal, due to the implementation of an infinite-interval solution over a finite interval.

The 2-norm of the initial errors and asymptotic errors are presented in Table 6.1. These values are obtained by first determining the 2-norm of the errors for each of the five setups, and subsequently averaging them. $\|e_0\|_2$ is approximately equal for R-ILC, LQ norm optimal ILC, and the μ ILC controller. Clearly, the 2-norm of the asymptotic error corresponding to R-ILC is significantly smaller than that of the other two control approaches.
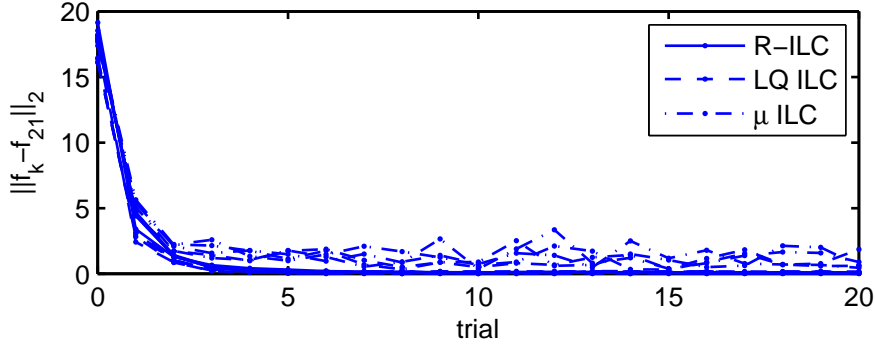
Figure 6.6: Convergence of the ILC controlled systems.

Table 6.1: 2-norms of the different asymptotic error signals.

2-norm	$\|e_0\|_2$	$\|e_{21}^R\|_2$	$\|e_{21}^{LQ}\|_2$	$\|e_{21}^\mu\|_2$
value	90.2	0.546	5.06	1.32

The time domain asymptotic command and error signals of the three ILC controlled system are presented in Figure 6.7 and Figure 6.8, respectively. From Figure 6.7, we can state that the command signals of the R-ILC and μ ILC controller contain higher frequencies than that of LQ norm optimal ILC. As a result, R-ILC and μ ILC can remove more high frequent error components which subsequently leads to smaller errors, see Table 6.1 and Figure 6.8. An explanation for this difference can be explained as follows. In LQ norm optimal ILC, the $\mathcal{Q}$ filter has a low pass characteristic that cuts off all singular values smaller than a certain threshold. Because the uncertainty of our example is associated with large singular values, the cut off value of the $\mathcal{Q}$ filter is relatively high. The $\mathcal{Q}$ filter of the R-ILC controller, however, cuts off singular values that are associated with singular vectors that are uncertain, independent of the magnitude of the singular value itself. As a result, R-ILC only gives robustness at the cost of performance where it is required.

From Figure 6.7 we can furthermore see that the command signals in R-ILC and μ ILC are comparable during $T_s t \in [0.05, 0.45]$s. Large transients (the boundary effects) in the command signals of μ ILC, however, result in errors which are larger than those of R-ILC. With these variations in the command signal of μ ILC per setup comparable to those between the different setups, the transients are the cause of the oscillatory convergence behavior of μ ILC in Figure 6.6. An explanation for this effect in μ ILC is found in the fact that the frequency domain μ ILC control solution is based on a time invariant behavior of the system which is valid for all time, i.e., a behavior in which transients do not play a role. Since

transients are in general not negligible for a finite time interval, the frequency domain μ ILC controller only generates a command signal (approximately) equal to that of the R-ILC controller during that part of the trial where transients are negligible. In this example, this time interval equals $T_s t \in [0.05, 0.45]$s.
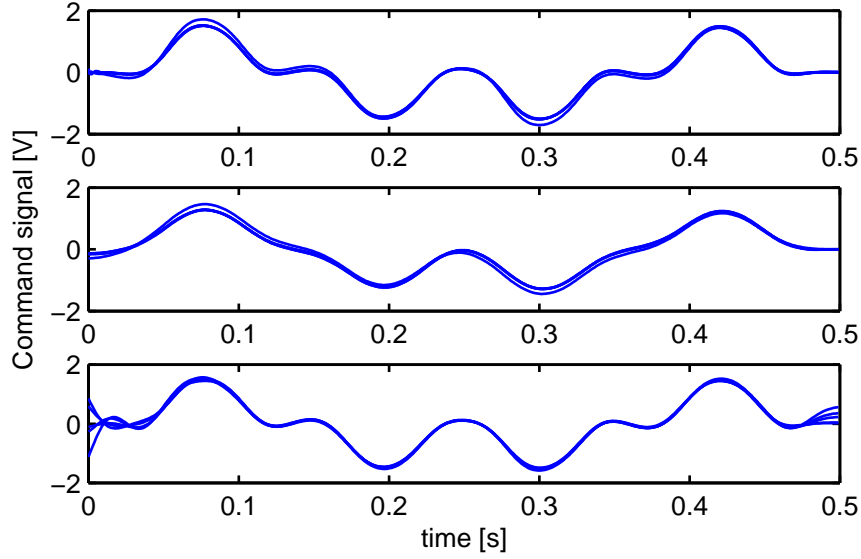
Figure 6.7: Asymptotic command signals for R-ILC (top), LQ norm optimal ILC (center), and μ ILC (bottom).

6.6.3 Frequency domain controller interpretation

In Section 6.4, we derived a causal state space representation of the R-ILC controller. Here, we compare the frequency domain representation of this state space model with the μ ILC controller to obtain insight in the frequency domain behavior of R-ILC.

$$f_{k+1}(z) = \mathcal{Q}^R(z)f_k(z) + L^R(z)e_k(z)$$
$$f_{k+1}(z) = \mathcal{Q}^\mu(z)f_k(z) + \mathcal{Q}^\mu(z)L^\mu(z)e_k(z),$$

The considered frequency domain convergence conditions are given by

$$|\mathcal{Q}^R(e^{j\theta}) - L^R(e^{j\theta})J(e^{j\theta})| < 1, \quad |\mathcal{Q}^\mu(e^{j\theta})(1 - L^\mu(e^{j\theta})J(e^{j\theta}))| < 1,$$

for $\theta \in [-\pi, \pi]$.

In Figure 6.9, the Bode plots of $L^R(z)$ and $\mathcal{Q}^\mu(z)L^\mu(z)$ are shown, together with the inverse of model $J(z)$. When focussing on the magnitude plot, we can see
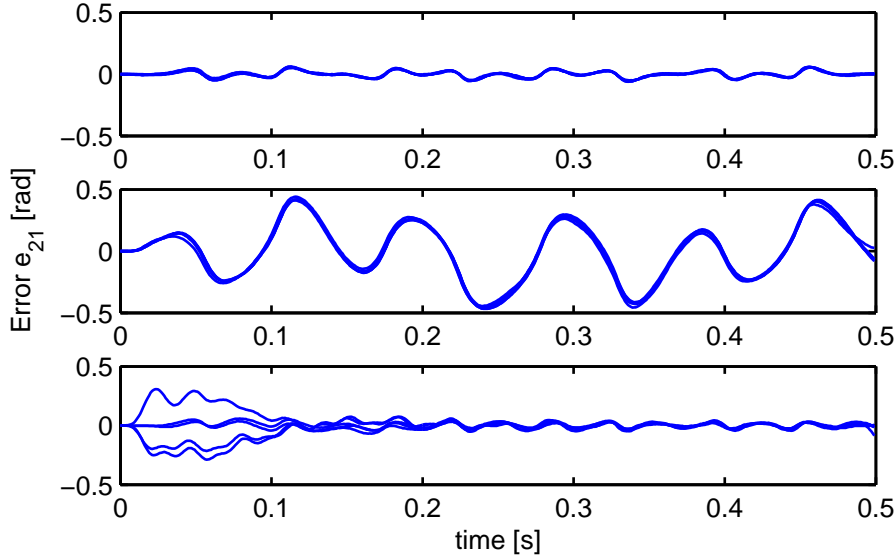
Figure 6.8: Asymptotic error signals for R-ILC (top), LQ norm optimal ILC (center), and μ ILC (bottom).

that the μ ILC controller approximates $J^{-1}(z)$ up to 23 Hz. Consequently, μ ILC equals an inverse model based ILC controller up to 23 Hz. Moreover, the significant high frequent roll-off of $\mathcal{Q}^\mu(z)L^\mu(z)$ can be explained by the high order of the user designed $\mathcal{Q}^\mu(z)$ low-pass filter. Contrary to $\mathcal{Q}^\mu(z)L^\mu(z)$, $L^R(z)$ already starts to deviate from $J^{-1}(z)$ above 13 Hz. This deviation, however, remains relatively small up to 60 Hz.

When focussing on the phase plot, we see that the phase of $L^R(z)$ matches the phase of $J^{-1}(z)$ exactly. With the μ ILC controller designed to match $J^{-1}(z)$ up to a cut-off frequency of 25 Hz, the phase of $\mathcal{Q}^\mu(z)L^\mu(z)$ only equals the phase of $J^{-1}(z)$ up to 25 Hz. The high frequent phase lag is subsequently explained by the fact that $L^\mu(z)$ is causal and $\mathcal{Q}^\mu(z)$ is designed to be zero phase.

Filters $\mathcal{Q}^R(z)$, $\mathcal{Q}^\mu(z)$, and $W(z)$ are depicted in Figure 6.10. The Bode plot of $\mathcal{Q}^\mu(z)$ can be fully explained by the fact that $\mathcal{Q}^\mu(z)$ is user designed zero phase low-pass filter. The explanation of $\mathcal{Q}^R(z)$ is more involved. The zero phase characteristic of $\mathcal{Q}^R(z)$ is most likely the result of the R-ILC objective regarding the minimization of the error: With $\mathcal{Q}^R(z) = I$ for optimal performance, Lemma 5.1, minimizing $\|I - \mathcal{Q}^R(z)\|_{i2}$ for each frequency results in $\mathcal{Q}^R(z)$ being zero phase. Furthermore, we can see that $\mathcal{Q}^R(z)$ has a magnitude of approximately 1 for frequencies smaller than 40 Hz and larger than 70 Hz. The low frequent gain can be explained by the relatively small amount of model uncertainty in comparison to $J(z)$, see Corollary 5.9. The explanation for the high frequent properties of $\mathcal{Q}^R(z)$ is found in the fact that the magnitude of the product $L^R(z)J_\Delta(z) \approx 0$.
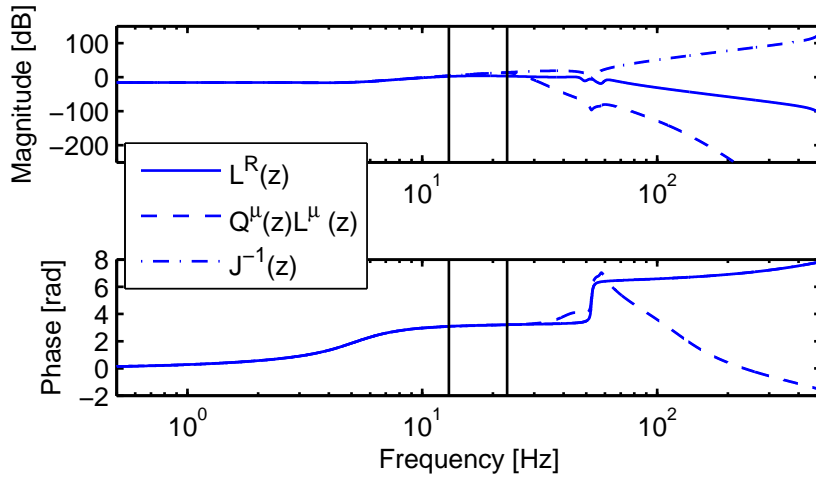
Figure 6.9: Bode plots of $L^R(z)$, $\mathcal{Q}^\mu(z)L^\mu(z)$, and $J^{-1}(z)$.

As a result, $\mathcal{Q}^R(z) = 1 - \varepsilon$ with $0 < \varepsilon \ll 1$ is sufficient to obtain convergence. The only frequencies with $|\mathcal{Q}^R(z)| < 1$ lie in the frequency band where both the control gain $L^R(z)$ and the uncertainty $W(z)$ is relatively large. Note that these results of $\mathcal{Q}^R(z)$ give a new perspective on the design considerations of the $\mathcal{Q}(z)$ filter.
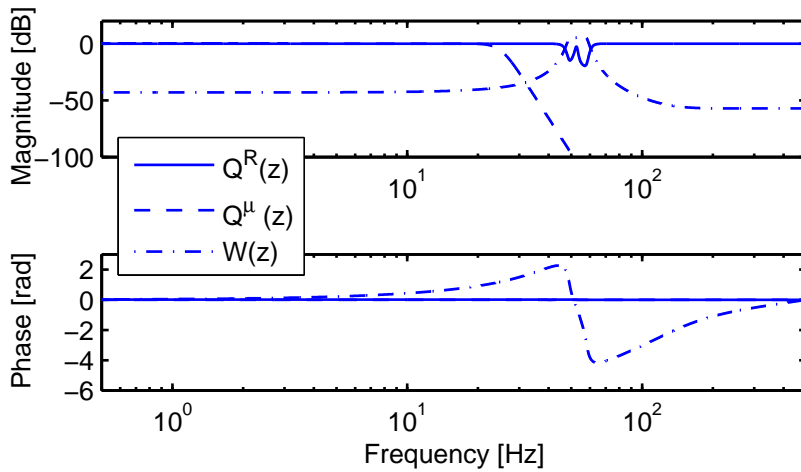
Figure 6.10: Bode plots of $\mathcal{Q}^R(z)$, $\mathcal{Q}^\mu(z)$, and $W(z)$.

The convergence conditions are presented in Figure 6.11. The nonzero magnitudes up to approximately 15 Hz can be explained by the small mismatches between the gains in $(L^R(z), L^\mu(z))$ and $J^{-1}(z)$. Moreover, the high frequent roll-off of the

μ condition can be explained by the characteristics of $\mathcal{Q}^\mu(z)$. The high frequent magnitude $1 - \varepsilon$ for R-ILC can be explained by the fact that for these frequencies $L^R(z)J_\Delta(z)$ is approximately zero, and hence that the convergence condition equals $\mathcal{Q}^R(z)$. Finally, the R-ILC convergence condition shows a dip between 40 Hz and 70 Hz to compensate for the relatively large uncertainty bound on $L^R(z)J_\Delta(z)$.
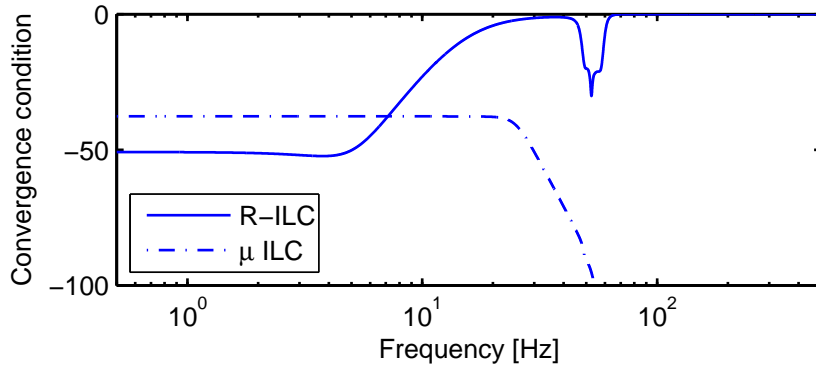
Figure 6.11: Convergence condition for R-ILC and μ ILC.

We conclude the comparison between R-ILC and μ ILC with a discussion on achievable performance with both controllers. For that, we study the mapping from reference signal y_d to asymptotic error e_∞, see (6.9) and Figure 6.12. From Figure 6.12, we can state that μ ILC can achieve a higher suppression of low frequent reference signals than R-ILC. On the other hand, above the cut-off frequency of 25 Hz, μ ILC does not improve performance at all (the gain equals 1). In contrast, the R-ILC controller can improve performance up to roughly 200 Hz, due to the specific characteristics of the $\mathcal{Q}^R(z)$ filter. Only in the frequency band of 40-70 Hz performance improvement by R-ILC is very limited, due to the relatively large uncertainty bound.

6.7 Concluding remarks

In this chapter, we have presented a robust ILC control strategy that is robust against model uncertainty as given by an additive uncertainty model. The design methodology has been based on $\mathcal{H}_\infty$ optimization, however, modified such that the obtained ILC controller is not restricted to be causal and inherently operates on a finite time interval. We have analyzed the convergence and performance properties of resulting ILC controlled system, and provided guidelines to achieve optimized performance while remaining robustly monotonically convergent. To circumvent the use of large dimensional system matrices in R-ILC, a state space representation for the R-ILC controller has been derived and implementation
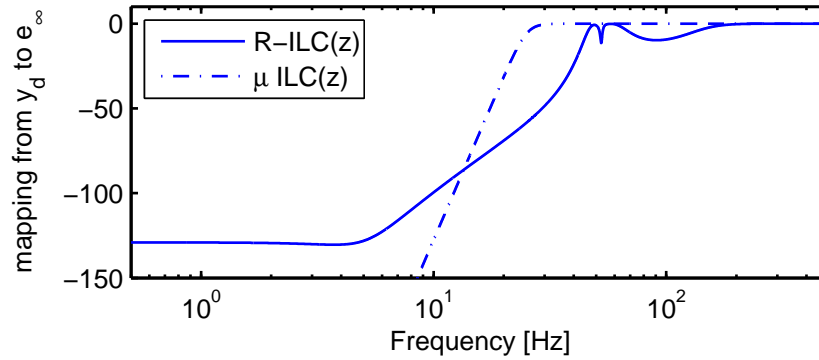
Figure 6.12: Amplitude mapping from reference signal y_d to asymptotic error e_∞ for R-ILC and μ ILC.

issues discussed. Finally, the R-ILC controller has been modified such that it is capable of handling systems with basis functions.

In an example, we have shown that the presented robust ILC control strategy has been able to outperform LQ norm optimal ILC control and robust ILC control based on a frequency domain μ procedure. Moreover, in a comparison between μ ILC and a frequency domain interpretation of the R-ILC controller, we have shown that the R-ILC clearly differs from μ ILC in phase characteristics of ILC control element $L(z)$, and magnitude characteristics in robustness filter $\mathcal{Q}(z)$.

Chapter 7

Conclusions and Recommendations

In this final chapter, the main results are recapitulated, and recommendations for further research presented.

7.1 Conclusions

We discuss the results of each research objective separately.

Objective 1
The first research objective dealt with exploration of the design issues in ILC for time-windowed systems (Chapter 3). With ILC for residual vibration suppression in point-to-point motion problems largely unexplored, we have used this ILC task as an exemplary case to analyze ILC for time-windowed systems. We have discussed the several steps taken from formulation of the residual vibration suppression problem, via system representation with time windows, and ILC control design, to implementation of this problem on a SISO and MIMO flexible motion system. Thereby, we have introduced a novel ILC control framework suitable for ILC for residual vibration suppression, and proven that there is the additional freedom in ILC control design for point-to-point motion problems related to manipulation of the amplitude of the command signal.

Objective 2
The second research objective focussed on the formulation of a unifying ILC framework, in which time-windowed systems and other ILC problem formulations are

enclosed (Chapter 4). Furthermore, the properties of this unified framework were to be studied. To meet the objective, first we have illustrated that various different ILC formulations in the literature can be captured by a common system representation involving i/o basis functions. Analysis of ILC for this system representation has revealed how different ILC objectives can be reached by design of separate parts of the ILC controller. Moreover, we have used these results to systematically design ILC controllers for the representation under study, and showed that the obtained results are applicable to existing ILC problem formulations with i/o basis functions, and problem formulations which can be interpreted as such.

Objective 3
The third objective was to develop an approach with which the robust convergence properties of existing finite time interval ILC controlled systems with model uncertainty can be analyzed (Chapter 5). For that purpose, a novel (MIMO) uncertain model representation over a finite time interval has been derived. This uncertainty representation, together with results from well developed μ analysis, has lead to the desired approach. Since the approach does not require the ILC controller to obey specific properties, it is applicable to any trial invariant LTI/LTV, (non)causal, non(square) ILC control strategy. As an example, the obtained result has been applied to LQ norm optimal ILC, yielding new insight in the tuning guidelines for LQ norm optimal ILC.

Objective 4
The fourth, and final, objective focussed on the design of a robust ILC control strategy which exploits knowledge about model uncertainty in its design, is not restricted to behave causal, and incorporates the finite time interval aspect of ILC (Chapter 6). The robust ILC design methodology which we have derived to meet this objective hinges on $\mathcal{H}_\infty$ optimization, but modified such that the obtained ILC controller is not restricted to be causal and explicitly operates on a finite time interval. Analysis of the ILC controlled system with robust ILC controller has revealed how to optimize the controller parameters so as to optimize performance while remaining robustly monotonically convergent. In experiments, we have illustrated that the designed robust ILC controller can outperform existing LQ norm optimal ILC controllers and causal μ based ILC controllers. Moreover, a comparison between the frequency domain interpretation of μ ILC (causal) and our proposed robust ILC (noncausal) has revealed differences in filter properties which, until now, have been unknown in ILC literature.

This thesis has extended existing ILC results on the following issues:

- Illustration of the use of time windows in ILC by analyzing ILC for residual vibration suppression in point-to-point motion problems (Chapter 3)

- ILC control design for time-windowed systems (Chapter 3, Section 3.3)

- Proof and demonstration of new design freedom in ILC concerning manipulation of the command signal form (Chapter 3 Section 3.3, and Chapter 4 Section 4.4)

- Introduction of a unifying ILC framework for linear systems with basis functions (Chapter 4, Section 4.2)

- Analysis and ILC control design for systems with basis functions in a unifying ILC framework (Chapter 4, Sections 4.3 to 4.5)

- Introduction of a novel uncertainty model representation over a finite time interval (Chapter 5, Section 5.1)

- Development of a robust monotonic convergence analysis approach for existing finite time interval ILC controllers (Chapter 5, Sections 5.3 and 5.4)

- Proof that a frequency domain monotonic convergence analysis provides a sufficient condition for finite time interval if the ILC controllers is causal. Illustration that for noncausal ILC controllers this does not necessarily hold (Chapter 5, Section 5.3)

- Analysis of the robustness properties of LQ norm optimal ILC controllers (Chapter 5, Section 5.5)

- Design and optimization of a noncausal finite time interval robust ILC controller (Chapter 6, Sections 6.1 to 6.5)

- The proof that finite time interval linear time invariant ILC control solutions require nonzero initial conditions (Chapter 6, Section 6.4)

7.2 Recommendations

The results of this thesis have given rise to suggestions for further research.

System identification for ILC
We showed that, even without additional robustness filters, ILC controllers are robustly monotonically convergent for relatively small amounts of model uncertainty. Consequently, we can achieve optimal performance in case of little uncertainty. Based on our findings, we expect that optimal performance can be reached if the true system can be captured by a nominal model with an uncertainty set with bounds which are smaller than 100% of the nominal model. The remaining questions are:

- Should system identification for ILC focus on reduction of the uncertainty set to maximally 100% of the nominal model?

- Do other issues play a role in system identification for ILC (or in system identification for feedforward control in general)?

Trial varying uncertainty
For a system that is subject to wear, the dynamics can change during its lifespan. As a result, an ILC controlled system which is convergent in the first part of operation, might become unstable later on. In our discussion on robust convergence conditions and robust ILC control design, we have not taken this issue into account. Inclusion of this type of model uncertainty in ILC analysis and design gives rise to the following questions:

- How do we capture trial varying model uncertainty, while respecting the finite time aspect of a trial?

- Can we modify the existing robust monotonic convergence conditions (Chapter 5) to accommodate for trial varying model uncertainty? A positive answer to this question might be found by first writing the trial varying uncertainty model as a trial domain state space model, and second, using the $M\Delta_M$ structure of Chapter 5 to find the robust convergence conditions. In this case, we expect Δ_M to be equal to $\Delta_M = \text{diag}(\Delta, \Delta_P, \delta I)$.

- Given a model of the trial varying disturbance, can we use the design approach of Chapter 6 to find the robustly monotonically converging ILC controller with optimized performance? Or can we combine the design approach of Chapter 6 with robust ILC control design of [89], to find the desired controller?

Robust monotonic convergence conditions
The robust monotonic convergence (RMC) conditions for LTI and LTV uncertainty models derived in this thesis (Chapter 5) are sufficient. Further research can focus deriving less conservative RMC results.

Optimization of state space robust ILC for relatively long trial spans
To avoid large dimensional system matrix representations and to be more flexible to changes in trial length, we introduced a state space representation of the robust controller (Chapter 6). Although we solved the design and implementation issues, it remains an open question how to properly optimize the controller parameters such that performance is optimized in presence of robust convergence.

Experimental validation
The main purpose of the experimental results in this thesis is to demonstrate feasibility of the proposed concepts. A next step is to implement Hankel ILC and robust ILC on industrial applications.

Appendix A

Proofs and Derivations

A.2 Chapter 2

A.2.1 Proof Lemma 2.1

With $f_{k+1} = (I_{Nq_i} - LJ)f_k$, MC requires

$$\|f_{k+1}\|_2 < \|f_k\|_2$$
$$\|(I_{Nq_i} - LJ)f_k\|_2 < \|f_k\|_2$$
$$f_k^T(I_{Nq_i} - LJ)^T(I_{Nq_i} - LJ)f_k < f_k^T f_k.$$

For this inequality to hold for all f_0, MC requires

$$\lambda_i((I_{Nq_i} - LJ)^T(I_{Nq_i} - LJ) - I_{Nq_i}) < 0 \ \forall i \in [1, Nq_i]$$
$$\Leftrightarrow \|I_{Nq_i} - LJ\|_{i2} < 1.$$

A.2.2 Proof Lemma 2.2

Given $J \in \mathbb{R}^{Nq_o \times Nq_i}$, (2.8), and rank$(LJ) = Nq_i$ due to convergence. Then for $k \to \infty$, the state $f_k = f_{k+1} = f_\infty$ equals $f_\infty = (LJ)^{-1}Ly_d$. As a result, $e_\infty = y_d - Jf_\infty$ is given by

$$e_\infty = \left(I_{Nq_o} - J(LJ)^{-1}L\right)y_d.$$

$e_\infty = 0 \; \forall y_d$ implies $I_{Nq_o} - J(LJ)^{-1}L = 0$. Using

$$\mathrm{rank}\left(\begin{bmatrix} A_{11} & 0 \\ 0 & A_{22} - A_{21}A_{11}^{-1}A_{12} \end{bmatrix}\right) = \mathrm{rank}\left(\begin{bmatrix} A_{11} & A_{12} \\ A_{21} & A_{22} \end{bmatrix}\right),$$

$e_\infty = 0 \; \forall y_d$ iff

$$\mathrm{rank}\left(\begin{bmatrix} LJ & L \\ J & I_{Nq_o} \end{bmatrix}\right) = Nq_i \Leftrightarrow \mathrm{rank}\left(\begin{bmatrix} 0 & 0 \\ J & I_{Nq_o} \end{bmatrix}\right) = Nq_i.$$

which holds iff $q_o = q_i$.

A.3 Chapter 3

A.3.1 Proof Lemma 3.1

Consider $L_o \in \mathbb{R}^{p \times nq_o}$, $L_c \in \mathbb{R}^{mq_i \times p}$, and $L_o J_H L_c \in \mathbb{R}^{p \times p}$. Then convergence requires $\rho(I_p - L_o J_H L_c) = \max_j |1 - \lambda_j(L_o J_H L_c)| < 1$ with $j \in [1, p]$.

Only if: Consider the case $p > \mathrm{rank}(J_H)$. Then $\mathrm{rank}(L_o J_H L_c) < p$ independent of the choice for (L_o, L_c). Consequently, there exists $j \in [1, p]$ for which $\lambda_j(L_o J_H L_c) = 0 \Rightarrow \rho(I_p - L_o J_H L_c) \geq 1$.

If: Consider $p \leq \mathrm{rank}(J_H)$. Then there exists (L_o, L_c) for which $\rho(I_p - L_o J_H L_c) < 1$. For example, $L_o = g J_o^\dagger$ with $g \in (0, 2)$ and $L_c = J_c^\dagger = J_c^T (J_c J_c^T)^{-1}$ yields $\rho(I_p - g I_p) = |1 - g| < 1$.

With $\rho(I_p - L_o J_H L_c) < 1$ implying $\mathrm{rank}(L_o J_H L_c) = p$, and with $\mathrm{rank}(L_o J_H L_c) \leq \min(\mathrm{rank}(L_o), \mathrm{rank}(J_H), \mathrm{rank}(L_c))$, convergence requires $\mathrm{rank}(L_o) = \mathrm{rank}(L_c) = p$.

A.3.2 Proof Lemma 3.2

Given L_o, then pole placement in system (3.10) is possible by L_c, iff $(I_p, \; L_o J_H)$ is controllable. $(I_p, \; L_o J_H)$ controllable $\Leftrightarrow \mathrm{rank}(L_o J_H) = p$. Using $\mathrm{rank}(L_o J_H) = \mathrm{rank}(L_o J_o J_c) \leq \min(\mathrm{rank}(L_o J_o), \mathrm{rank}(J_c)) = \min(\mathrm{rank}(L_o J_o), p)$, then $\mathrm{rank}(L_o J_H) = p$ implies $\mathrm{rank}(L_o J_o) = p$. Conversely, if $L_o J_o \in \mathbb{R}^{p \times p}$ is nonsingular, i.e., $\mathrm{rank}(L_o J_o) = p$, then $\mathrm{rank}(L_o J_o) = p$ and $\mathrm{rank}(J_c) = p$ together imply $\mathrm{rank}(L_o J_H) = p$.

Similarly, given L_c, then pole placement in system (3.10) is possible by L_o, iff $(J_H L_c, \; I_p)$ is observable. $(J_H L_c, \; I_p)$ observable $\Leftrightarrow \mathrm{rank}(J_H L_c) = p \Leftrightarrow \mathrm{rank}(J_c L_c) = p$.

A.3.3 Proof Lemma 3.3

With (3.12) from Proposition 3.1, the trial domain dynamics are given by

$$u_{k+1} = (I_p - L_o J_o)u_k + L_o \alpha_d \tag{A.1}$$

$$\beta_k = J_c^\dagger u_k + T_c^\dagger M_c u_k, \tag{A.2}$$

Furthermore, the asymptotic error ϵ_∞ follows from

$$u_\infty = (I_p - L_o J_H L_c)u_\infty + L_o \alpha_d$$
$$= (L_o J_o)^{-1} L_o \alpha_d. \tag{A.3}$$
$$\epsilon_\infty = \alpha_d - J_H L_c u_\infty$$
$$= (I_{nq_o} - J_o(L_o J_o)^{-1} L_o)\alpha_d, \tag{A.4}$$

since $J_c T_c^\dagger = 0$. Then for arbitrary $M_c \in \mathbb{R}^{(mq_i - p) \times p}$, convergence of Hankel ILC is defined by $\rho(I_p - L_o J_o) < 1$, (A.1), and performance by $\|\epsilon_\infty\|_2$, with ϵ_∞ from (A.4). Additionally, every command signal β_k which can be obtained from (A.1)-(A.4) by arbitrary L_o, can be reached by design of M_c.

A.3.4 Proof Proposition 3.2

Controller $L_o : (\epsilon_k, u_k) \mapsto u_{k+1}$ is obtained by minimizing

$$\min_{u_{k+1}} \mathcal{J}, \quad \text{with}$$
$$\mathcal{J} = \epsilon_{k+1}^T \epsilon_{k+1} + (\beta_{k+1} - \beta_k)^T R(\beta_{k+1} - \beta_k).$$

Using $\alpha_d = \epsilon_k + J_H L_c u_k = \epsilon_k + J_o u_k$, we find $\epsilon_{k+1} = \epsilon_k - J_o(u_{k+1} - u_k)$. Additionally, with $\beta_k = L_c u_k$, the optimization problem can be reformulated as

$$\min_{u_{k+1}} \mathcal{J}, \quad \text{with}$$
$$\mathcal{J} = (\epsilon_k - J_o(u_{k+1} - u_k))^T (\epsilon_k - J_o(u_{k+1} - u_k))$$
$$+ (u_{k+1} - u_k)^T L_c^T R L_c (u_{k+1} - u_k).$$

Solving this problem gives

$$\frac{\partial \mathcal{J}}{\partial u_{k+1}} = 0 \rightarrow u_{k+1} = u_k + \underbrace{(J_o^T J_o + L_c^T R L_c)^{-1} J_o^T}_{L_o} \epsilon_k. \tag{3.14*}$$

A.3.5 Proof Proposition 3.3

Using (3.19), the optimization problem is given by

$$\min_{M_c} \mathcal{J} = \min_{M_c} \beta_\infty^T W_\beta \beta_\infty$$
$$= \left((L_o J_o)^{-1} L_o \alpha_d\right)^T L_c^T W_\beta L_c \left((L_o J_o)^{-1} L_o \alpha_d\right).$$

Given L_c from (3.12) and $\gamma_m := (L_o J_o)^{-1} L_o \alpha_d$, $\mathcal{J}$ can be rewritten to

$$\mathcal{J} = \gamma_m^T (J_c^\dagger + T_c^\dagger M_c)^T W_\beta (J_c^\dagger + T_c^\dagger M_c) \gamma_m. \tag{A.5}$$

The minimum of $\mathcal{J}$ is obtained by differentiating $\mathcal{J}$ with respect to M_c and requiring it to be zero $\forall \gamma_m$. This results in $T_c^{\dagger^T} W_\beta T_c^\dagger M_c = -T_c^{\dagger^T} W_\beta J_c^\dagger$. With $T_c^\dagger = T_c^T (T_c T_c^T)^{-1}$, M_c equals $M_c = -T_c T_c^T (T_c W_\beta T_c^T)^{-1} T_c W_\beta J_c^\dagger$, which yields $L_c = (I_{mq_i} - T_c^T (T_c W_\beta T_c^T)^{-1} T_c W_\beta) J_c^\dagger$.

A.3.6   Singular value decomposition of J_H

$$J_H = U \Sigma V^T = \begin{bmatrix} U_1 & U_2 \end{bmatrix} \begin{bmatrix} \Sigma_1 & 0 \\ 0 & 0 \end{bmatrix} \begin{bmatrix} V_1^T \\ V_2^T \end{bmatrix} = U_1 \Sigma_1 V_1^T, \tag{A.6}$$

$$\text{with } J_H \in \mathbb{R}^{nq_o \times mq_i}, \quad U_1 \in \mathbb{R}^{nq_o \times p}, \quad \Sigma_1 \in \mathbb{R}^{p \times p}, \quad V_1 \in \mathbb{R}^{mq_i \times p},$$
$$\text{and } J_o := U_1 \Sigma_1, \quad J_c := V_1^T, \quad T_c^\dagger = V_2.$$

A.4   Chapter 4

A.4.1   Proof Lemma 4.1

Convergence: Follows from standard linear control theory.
MC: Consider transformation $z_k = T^{-1} u_k$ with T such that $T^T L_c^{im^T} L_c^{im} T = I_p$. Then with $z_{k+1} = T^{-1}(I_p - L_o H L_c) T z_k$ and $f_k = L_c^{im} T z_k$, $\|f_{k+1}\|_2 < \|f_k\|_2$ equals

$$\|L_c^{im}(I_p - L_o H L_c) T z_k\|_2 < \|L_c^{im} T z_k\|_2 \Leftrightarrow$$
$$z_k^T T^T (I_p - L_o H L_c)^T L_c^{im^T} L_c^{im}(I_p - L_o H L_c) T z_k < z_k^T T^T L_c^{im^T} L_c^{im} T z_k.$$

For this inequality to hold for all $z_0 \in \mathbb{R}^p$, MC requires

$$\lambda_i (T^T (I_p - L_o H L_c)^T L_c^{im^T} L_c^{im}(I_p - L_o H L_c) T - T^T L_c^{im^T} L_c^{im} T) < 0, \tag{A.7}$$

$\forall i \in [1, p]$. With $T^T L_c^{im^T} L_c^{im} T = I_p$, this equals

$$\lambda_i \left(T^T (I_p - L_o H L_c)^T (T^{-1})^T T^{-1}(I_p - L_o H L_c) T - I \right) < 0$$
$$\Leftrightarrow \|T^{-1}(I_p - L_o H L_c) T\|_{i2} < 1.$$

A.4.2 Proof Lemma 4.6

1) Using (4.7), (4.8), $u_\infty = (L_o H L_c)^{-1} L_o \alpha_d$, $\epsilon_\infty = \alpha_d - H L_c u_\infty$, and the rank condition from Lemma 3.2, we find

$$\begin{aligned}
\epsilon_\infty &= (I_p - H L_c (L_o H L_c)^{-1} L_o) \alpha_d \\
&= (I_p - H S_c (S_o P_o H S_c)^{-1} S_o P_o) \alpha_d \\
&= (I_p - H_o (P_o H_o)^{-1} P_o) \alpha_d.
\end{aligned}$$

2) From Corollary 4.1, we know that optimal performance is achieved for $\{(L_o, L_c) : H_c L_c (L_o H L_c)^{-1} L_o = H_o^\dagger\} \Rightarrow \{P_o : (P_o H_o)^{-1} P_o = H_o^\dagger\}$. One possible solution for P_o is given by $P_o = H_o^T$.

A.4.3 Proof Lemma 4.8

Given covariances (4.12) and (4.13), (4.7) with $S_o = g(P_o H_o)^{-1}$ and $g \in (0, 2)$, and (4.8) with $S_c = I_p$. Then R_{uu} equals

$$\begin{aligned}
R_{uu} &= (1 - g)^2 R_{uu} + g^2 (P_o H_o)^{-1} P_o R_{dd} P_o^T (P_o H_o)^{-1^T} \\
&= \frac{g}{2 - g} (P_o H_o)^{-1} P_o R_{dd} P_o^T (P_o H_o)^{-1^T},
\end{aligned}$$

and $R_{\epsilon\epsilon}$ is given by $R_{\epsilon\epsilon} = R_{dd} + \frac{g}{2-g} H_o (P_o H_o)^{-1} P_o R_{dd} P_o^T (P_o H_o)^{-1^T} H_o^T$. The results for $g = \{0^+, 1, 2^-\}$ follow directly from $R_{\epsilon\epsilon}$.

A.4.4 Proof Lemma 4.9

Given Given (4.7) with $S_o = g(P_o H_o)^{-1}$ and $g \in (0, 2)$, and (4.8) with $S_c = I_p$. Then (4.14) equals

$$\epsilon_k^{as} = \epsilon_\infty - (I_n - \frac{g}{w - 1 + g} H_o (P_o H_o)^{-1} P_o) d_k(\ell).$$

The results for $g = \{0^+, 1, 2^-\}$ are obtained by analyzing ϵ_k^{as} for trial periodic disturbance $d_k(\ell \to \infty)$ ($w = e^{j2\pi/\ell} \to 1$), i.e., almost trial invariant d_k, and $d_k(2)$ ($w = e^{j2\pi/\ell} = -1$), i.e., for disturbances $d_{k+1} = -d_k$.

A.5   Chapter 5

A.5.1   Proof Proposition 5.1

Given the system in Figure 5.3. Then the mapping of the trial state $z_k \mapsto z_{k+1}$ is given by

$$z_{k+1} = T^{-1}(\mathcal{Q} - L_o(J + W_i \Delta W_o)L_c)T z_k$$
$$= T^{-1}(\mathcal{Q} - L_o J_\Delta L_c)T z_k,$$

and $z_k = \Delta_P z_{k+1}$. RC of the system in Figure 5.3 requires $\rho(T^{-1}(\mathcal{Q} - L_o J_\Delta L_c)T)$ $< 1 \ \forall J_\Delta \in \Pi$, which is equivalent to RC of (5.4) for the choice $T = I_p$. The replacement $w^{-1} I_p$ in Figure 5.2 by $\Delta_P \in \{\Delta_P = \delta_P I_p : \delta_p \in \mathbb{C}, |\delta_P| < 1\}$ in Figure 5.3 is suggested and proven in Section 4.2 in [103].

RMC of the system in Figure 5.3 in z_k requires $\|T^{-1}(\mathcal{Q} - L_o J_\Delta L_c)T\|_{i2} < 1 \ \forall J_\Delta \in \Pi$. This RMC condition is equivalent to that of (5.4) for T satisfying $T^T L_c^T L_c T = I_p$. Furthermore, with the RMC condition in Lemma 5.1 equivalent to a robust performance condition in robust feedback control, as discussed in, e.g., Section 8.4 in [117], Δ_P in Figure 5.3 is defined as $\Delta_P \in \{\Delta_P \in \mathbb{C}^{p \times p}, \|\Delta_P\|_{i2} < 1\}$.

A.5.2   Proof Lemma 5.2

Consider J_Δ and $(\mathcal{Q}, L_o)$ the finite dimensional (block) Toeplitz matrices representing $J_\Delta(z)$ and (possibly noncausal) $(\mathcal{Q}(z), L_o(z))$ over a finite time interval of length N. Furthermore, consider $(LJ)_N$ the finite time interval representation of the product $(L_o(z)J_\Delta(z))$.

From Proposition 2.3 in [19], we find that

$$L_o J_\Delta = (LJ)_N - C,$$

with C containing truncation and Hankel operators. $C = 0$ iff both L_o and J_Δ are lower triangular (block) Toeplitz matrices. Moreover, for $A(z)$ with corresponding finite dimensional (block) Toeplitz matrix A_N, $\lim_{N \to \infty} \|A_N\|_{i2} = \|A(e^{j\theta})\|_{i2}$, and $\|A_N\|_{i2} \leq \|A(e^{j\theta})\|_{i2}$, see e.g., Section 1.3 and Section 6.4 of [20].

Now, Corollary 5.1 states that the ILC controlled system is RMC if $\|\mathcal{Q} - L_o J_\Delta\|_{i2} < 1$. Take $L_o(z)$ causal, then L_o is an lower triangular (block) Toeplitz matrix, $L_o J_\Delta = (LJ)_N$, $\mathcal{Q} - L_o J_\Delta$ is Toeplitz, and
$\|\mathcal{Q} - L_o J_\Delta\|_{i2} \leq \|\mathcal{Q}(e^{j\theta}) - L_o(e^{j\theta}) J_\Delta(e^{j\theta})\|_{i2}$.

A.5.3 Proof Corollary 5.2

Given (5.9) with $\mathcal{Q} = L_o J L_c$, and $\mu_{\Delta_M}(M) \leq \|D_M^{1/2} M D_M^{-1/2}\|_{i2}$. Then $\mu_{\Delta_M}(M) < 1$ if

$$\mu_{\Delta_M}(M) \leq \inf_d \| \begin{bmatrix} 0 & dW_o L_c T \\ -d^{-1} T^{-1} L_o W_i & 0 \end{bmatrix} \|_{i2} < 1$$

$$\Rightarrow \min_d \max(d\|W_o L_c T\|_{i2}, d^{-1}\|T^{-1} L_o W_i\|_{i2}) < 1.$$

Solving this for d gives

$$d = \|T^{-1} L_o W_i\|_{i2}^{1/2} \cdot \|W_o L_c T\|_{i2}^{-1/2}$$

$$\mu_{\Delta_M}(M) \leq \|T^{-1} L_o W_i\|_{i2}^{1/2} \cdot \|W_o L_c T\|_{i2}^{1/2}.$$

As a result, $\|T^{-1} L_o W_i\|_{i2} \cdot \|W_o L_c T\|_{i2} < 1 \Rightarrow \mu_{\Delta_M}(M) < 1$.

A.5.4 Proof Corollary 5.3

Consider (5.10), $\mathcal{Q} = L_o J L_c$, and the fact that the inequality in (5.8) holds for LTI Δ. Furthermore, let W_o be given by (5.12). Then
$\mu_{\Delta_M}(M) \leq \inf_{D^{1/2}} \max(\|D^{1/2} W_o L_c T\|_{i2}, \|T^{-1} L_o W_i D^{-1/2}\|_{i2})$, with $D^{1/2}$ having a structure equal to (5.10).

For $D^{1/2} := d W_o^{-1}$ we find $\mu_{\Delta_M}(M) \leq \min_d \max(d\|L_c T\|_{i2}, d^{-1}\|T^{-1} L_o W\|_{i2})$, with $W := W_i W_o$. Solving this for d gives $\mu_{\Delta_M}(M) \leq \|L_c T\|_{i2}^{1/2} \cdot \|T^{-1} L_o W\|_{i2}^{1/2}$. Since $\|L_c T\|_{i2} = 1$ by design of T, $\|T^{-1} L_o W\|_{i2} < 1 \Rightarrow \mu_{\Delta_M}(M) < 1$.

A.5.5 Proof Lemma 5.3

Given interval uncertainty as defined in Table 5.1 with $\|\Delta_t\|_{i2} \leq 1 \forall t \in [0, N-1]$. Then following Section 7 in [45], the interconnection matrices $T_1 \in \mathbb{R}^{Nq \times qN(N+1)/2}$ and $T_2 \in \mathbb{R}^{qN(N+1)/2 \times Nq}$ such that $\Delta = T_1 \Delta^* T_2$ are given by

$$T_1 = \begin{bmatrix} I_{Nq} & \begin{matrix} 0_{q \times q(N-1)} & \cdots & 0_{q(N-1) \times q} \\ I_{q(N-1)} & \cdots & I_q \end{matrix} \end{bmatrix}, \tag{A.8}$$

$$T_2 = \begin{bmatrix} I_{Nq} & \begin{matrix} I_{q(N-1)} & \cdots & I_q \\ 0_{q \times q(N-1)} & \cdots & 0_{q(N-1) \times q} \end{matrix} \end{bmatrix}^T. \tag{A.9}$$

Moreover, the block diagonal Δ^* is norm bounded by 1, i.e., $\|\Delta^*\|_{i2} \leq 1$. Knowing that $\det(I - M\Delta) = \det(I - M T_1 \Delta^* T_2) = \det(I - T_2 M T_1 \Delta^*) = \det(I - M^* \Delta^*)$, we find $\mu_{\Delta_M}(M)$ with Δ_M equal to $\mu_{\Delta_M}(M^*)$ with Δ_M^*. Consequently, we have $\mu_{\Delta_M}(M) \leq \|D_M^{*1/2} M^* D_M^{*-1/2}\|_{i2}$, with

$$\mathcal{D}_M^* = \{\mathrm{diag}(d_0 I_{Nq}, d_1 I_{q(N-1)}, \ldots, d_N I_q, I_p) : d_t > 0\}$$

commuting with $\Delta_M^* = \{\mathrm{diag}(\Delta^*, \Delta_P)\}$, see Section 7 of [45]. Finally, the upper bound can be formulated as the LMI of (5.15), see Theorem 3.9 of [103]. This condition is sufficient, since inequality in (5.8) holds for Δ LTI, see Table 1 in [103].

A.5.6 Proof Lemma 5.5

Assume (5.24) RMC for $r = 0$. Then Corollary 5.1 states that there exists α such that

$$\|(J^T QJ + S)^{-1} J^T QW_i \Delta W_o\|_{i2} \leq \alpha < 1 \; \forall \Delta \in \mathbf{\Delta}.$$

Due to the properties of (Q, S), $J^T QJ + S$ is symmetric positive definite. Consequently, its singular value decomposition equals $J^T QJ + S = U\Sigma U^T$, with U a unitary matrix and $\Sigma = \mathrm{diag}(\sigma_i)$, $i = 1, \ldots, Nq_i$, of full rank.

RMC for $R = rI > 0$ subsequently requires

$$\max_{\Delta \in \mathbf{\Delta}} \|(J^T QJ + S + rI)^{-1}(rI - J^T QW_i \Delta W_o)\|_{i2}$$
$$= \max_{\Delta \in \mathbf{\Delta}} \|(J^T QJ + S + rI)^{-1}(rI + J^T QW_i \Delta W_o)\|_{i2}$$
$$= \max_{\Delta \in \mathbf{\Delta}} \|(J^T QJ + S + rI)^{-1} \cdot$$
$$\quad (rI + (J^T QJ + S)(J^T QJ + S)^{-1} J^T QW_i \Delta W_o)\|_{i2}$$
$$\leq \|(J^T QJ + S + rI)^{-1}(rI + (J^T QJ + S)\alpha)\|_{i2}$$
$$= \|(U\Sigma U^T + rI)^{-1}(rI + \alpha U\Sigma U^T)\|_{i2}$$
$$= \|U(\Sigma + rI)^{-1}(rI + \alpha\Sigma)U^T\|_{i2}$$
$$= \|(\Sigma + rI)^{-1}(rI + \alpha\Sigma)\|_{i2}$$
$$= \max_i \left(\frac{\alpha\sigma_i + r}{\sigma_i + r} \right)$$
$$< 1 \; \forall r \geq 0.$$

A.6 Chapter 6

A.6.1 Sketch of Proof Proposition 6.1

For given $\gamma > \gamma_{opt}$ and $t = 0, \ldots, N - 1$, the sub-optimal finite interval robust control objective $\|M\|_{i2} < \gamma$ can be reformulated as

$$\|M\|_{i2} = \sup_{w,\|w\|>0} \frac{\|z(t)\|_2}{\|w(t)\|_2} < \gamma \rightarrow$$

$$\mathcal{J}^c = 1/2\|z(t)\|_2^2 - 1/2\gamma^2\|w(t)\|_2^2 < 0, \quad t \in [0, N-1].$$

The objective $\mathcal{J}_c$ can be used as an objective function for the robust control synthesis problem: Find a controller $K : y \mapsto u$ such that

$$\min_{u(t)} \max_{w(t)} \mathcal{J}^c = \min_{u(t)} \max_{w(t)} 1/2 \sum_{t=0}^{N-1} z^T(t)z(t) - \gamma^2 w^T(t)w(t),$$

is achieved, subject to the generalized plant relations.

Let $(z,\ w,\ u,\ y)$ be the lifted representation of the finite time interval signals $(z(t),\ w(t),\ u(t),\ y(t))$ for $t = 0, \ldots, N-1$. Then the sub-optimal robust control problem is given by: Find a controller $K : y \mapsto u$ such that

$$\min_{u} \max_{w} \mathcal{J}^c, \text{ subject to } \begin{bmatrix} z \\ y \end{bmatrix} = \begin{bmatrix} G_{11} & G_{12} \\ G_{21} & 0 \end{bmatrix} \begin{bmatrix} w \\ u \end{bmatrix}, \tag{A.10}$$

is achieved. An unconstrained robust control problem (6.3) follows by substituting $z = G_{11}w + G_{12}u$ in $\mathcal{J}^c$, and adding the constraint $y - G_{21}w = 0$ to $\mathcal{J}^c$ using a Lagrange multiplier λ.

The conditions that G_{21} has full row rank, and that $G_{11}^T G_{11} - \gamma^2 I \prec 0$ on the subspace $\ker(G_{21})$, follow from Lemma 6.1. The condition for G_{12} follows directly from the second-order condition $G_{12}^T G_{12} \succ 0$ which is required for the existence of a minimum of an unconstrained optimization problem, see Chapter 6 in [80].

A.6.2 Proof Corollary 6.1

Consider (6.6) with G_{11}, G_{21}, and G_{12} given by

$$G_{11} = \begin{bmatrix} 0 & 0 & 0 & W_o \\ 0 & 0 & 0 & 0 \\ W_i & -W_i & I & J \\ 0 & 0 & 0 & -R^{1/2} \end{bmatrix}, \quad G_{21} \begin{bmatrix} 0 & 0 & I & 0 \\ 0 & 0 & 0 & I \end{bmatrix},$$

$$G_{12} = \begin{bmatrix} 0 & W_o^T & -J^T & R^{1/2^T} \end{bmatrix}^T.$$

The robust control problem of (6.3) has a unique solution if 1) G_{12} has full column rank, 2) G_{21} has full row rank, and 3) $G_{11}^T G_{11} - \gamma^2 I \prec 0$ on $\ker(G_{21})$. A sufficient condition for condition 1) is given by $R > 0$. Condition 2) holds for given G.

The kernel space of G_{21} is spanned by

$$\left\{ \begin{bmatrix} I \\ 0 \\ 0 \\ 0 \end{bmatrix}, \begin{bmatrix} 0 \\ I \\ 0 \\ 0 \end{bmatrix} \right\}.$$

Now, $G_{11}^T G_{11} - \gamma^2 I \prec 0$ on $\ker(G_{21})$ is equivalent to

$$\begin{bmatrix} W_i^T W_i - \gamma^2 I & -W_i^T W_i \\ -W_i^T W_i & W_i^T W_i - \gamma^2 I \end{bmatrix} \prec 0 \Leftrightarrow$$

$$\begin{bmatrix} W_i^T W_i - \gamma^2 I & 0 \\ 0 & W_i^T W_i - \gamma^2 I - W_i^T W_i (W_i^T W_i - \gamma^2 I)^{-1} W_i^T W_i \end{bmatrix} \prec 0.$$

With $W_i^T W_i$ symmetric positive definite, there exists a unitary transformation $\mathrm{diag}(V, V)$, with $V^T W_i^T W_i V = \Sigma^2$ and Σ containing the singular values of W_i, such that the matrix inequality can be formulated as

$$\begin{bmatrix} \Sigma^2 - \gamma^2 I & 0 \\ 0 & \Sigma^2 - \gamma^2 I - \Sigma^2 (\Sigma^2 - \gamma^2 I)^{-1} \Sigma^2 \end{bmatrix} \prec 0.$$

This inequality is negative definite iff both $\sigma_i^2 - \gamma^2 < 0 \ \forall i \in [1, Nq] \to \gamma > \bar{\sigma}$, and

$$\sigma_i^2 - \gamma^2 - \frac{\sigma_i^4}{\sigma_i^2 - \gamma^2} < 0 \ \forall i \in [1, Nq] \Leftrightarrow \frac{(\sigma_i^2 - \gamma^2)^2 - \sigma_i^4}{\sigma_i^2 - \gamma^2} < 0 \ \forall i \in [1, Nq].$$

Since $\gamma > \bar{\sigma}$, we have $\sigma_i^2 - \gamma^2 < 0 \ \forall i \in [1, Nq]$. Consequently

$$(\sigma_i^2 - \gamma^2)^2 - \sigma_i^4 > 0 \ \forall i \in [1, Nq] \Leftrightarrow \gamma > \sqrt{2}\sigma_i \ \forall i \in [1, Nq] \Leftrightarrow \gamma > \sqrt{2}\bar{\sigma}(W_i).$$

A.6.3 Proof Proposition 6.2

Given (6.3) with G of (6.6) and inputs and outputs (6.5), $R > 0$, and $\gamma > \sqrt{2}\bar{\sigma}(W_i)$. Then, with e_k and f_k elements of both w and y, "substitution" of e_k and f_k from y in e_k and f_k of w takes care of the constraint $y - G_{21}w$ in (6.3). As a result, the unconstrained cost function can be given by

$$\begin{aligned} \mathcal{J} =\ & 1/2 p_k^T W_o^T W_o p_k + 1/2 p_{k+1}^T W_o^T W_o p_{k+1} \\ & + 1/2 (f_{k+1} - f_k)^T R (f_{k+1} - f_k) \\ & + 1/2 \left(e_k + J(f_k - f_{k+1}) + W_i(p_k - p_{k+1}) \right)^T \\ & \quad \left(e_k + J(f_k - f_{k+1}) + W_i(p_k - p_{k+1}) \right) \\ & - 1/2 \gamma^2 (p_k^T p_k + p_{k+1}^T p_{k+1} + e_k^T e_k + f_k^T f_k), \end{aligned}$$

The saddle point $\min_u \max_w \mathcal{J}$ is found where the partial derivatives of $\mathcal{J}$ with respect to p_k, p_{k+1}, and f_{k+1} equal zero:

$$\frac{\partial \mathcal{J}}{\partial p_k} = (W_i^T W_i - \gamma^2 I)p_k - W_i^T W_i p_{k+1}$$
$$+ W_i^T e_k + W_i^T J f_k - W_i^T J f_{k+1} = 0 \tag{A.11a}$$

$$\frac{\partial \mathcal{J}}{\partial p_{k+1}} = (W_i^T W_i - \gamma^2 I)p_{k+1} - W_i^T W_i p_k$$
$$- W_i^T e_k - W_i^T J f_k + W_i^T J f_{k+1} = 0 \tag{A.11b}$$

$$\frac{\partial \mathcal{J}}{\partial f_{k+1}} = -J^T W_i p_k + J^T W_i p_{k+1} - (J^T J + R)f_k$$
$$- J^T e_k + (J^T J + R + W_o^T W_o)f_{k+1} = 0. \tag{A.11c}$$

Adding (A.11a) to (A.11b) yields $p_{k+1} = -p_k$. Substitution of this into (A.11a) gives

$$p_k = (\gamma^2 I - 2W_i^T W_i)^{-1}(W_i^T e_k + W_i^T J f_k - W_i^T J f_{k+1}). \tag{A.12}$$

Finally, substitution of $p_{k+1} = -p_k$ and (A.12) in (A.11c) yields

$$(J^T(I - 2\gamma^{-2}W_i W_i^T)^{-1}J + W_o^T W_o + R)f_{k+1} =$$
$$J^T(I - 2\gamma^{-2}W_i W_i^T)^{-1}(e_k + J f_k) + R f_k,$$

from which (6.7) and (6.8) are obtained.

A.6.4 Derivation of (6.16)

Given the unconstrained objective function (6.15) with $C_2 = 0$

$$\mathcal{J} = \sum_{t=0}^{N-1} \left[1/2 z^T(t)z(t) - \frac{\gamma^2}{2} w^T(t)w(t) \right.$$
$$+ \lambda^T(t+1)(-x(t+1) + Ax(t) + B_1 w(t) + B_2 u(t))$$
$$\left. + \lambda_2^T(t+1)(-y(t) + D_{21}w(t)) \right]. \tag{A.13}$$

Then the partial derivatives of $\mathcal{J}$ are

$$\frac{\partial \mathcal{J}}{\partial x(t)} = C_1^T C_1 x(t) + C_1^T D_{11} w(t) + C_1^T D_{12} u(t)$$
$$- \lambda(t) + A^T \lambda(t+1) = 0 \tag{A.14}$$

$$\frac{\partial \mathcal{J}}{\partial w(t)} = D_{11}^T C_1 x(t) + (D_{11}^T D_{11} - \gamma^2 I)w(t) + D_{11}^T D_{12} u(t)$$
$$+ B_1^T \lambda(t+1) + D_{21}^T \lambda_2(t+1) = 0 \tag{A.15}$$

$$\frac{\partial \mathcal{J}}{\partial u(t)} = D_{12}^T C_1 x(t) + D_{12}^T D_{11} w(t) + D_{12}^T D_{12} u(t) + B_2^T \lambda(t+1) = 0 \tag{A.16}$$

$$\frac{\partial \mathcal{J}}{\partial \lambda(t+1)} = -x(t+1) + Ax(t) + B_1 w(t) + B_2 u(t) \tag{A.17}$$

$$\frac{\partial \mathcal{J}}{\partial \lambda_2(t+1)} = -y(t) + D_{21} w(t) = 0. \tag{A.18}$$

From (A.15), we find

$$w(t) = E_1^{-1} \left(D_{11}^T C_1 x(t) + D_{11}^T D_{12} u(t) + B_1^T \lambda(t+1) + D_{21}^T \lambda_2(t+1) \right), \tag{A.19}$$

with $E_1 := \gamma^2 I - D_{11}^T D_{11}$. Substitution of (A.19) in (A.18) yields

$$y(t) = D_{21} E_1^{-1} \left(D_{11}^T C_1 x(t) + D_{11}^T D_{12} u(t) + B_1^T \lambda(t+1) + D_{21}^T \lambda_2(t+1) \right). \tag{A.20}$$

Reorganizing (A.20) gives

$$\lambda_2(t+1) = (D_{21} E_1^{-1} D_{21}^T)^{-1} y(t) - (D_{21} E_1^{-1} D_{21}^T)^{-1}$$
$$D_{21} E_1^{-1} \left(D_{11}^T C_1 x(t) + D_{11}^T D_{12} u(t) + B_1^T \lambda(t+1) \right). \tag{A.21}$$

Substitution of (A.21) of (A.19) results in an expression for $w(t)$ as function of states $x(t)$ and $\lambda(t+1)$ and measured signal $y(t)$:

$$w(t) = E_2 \left(D_{11}^T C_1 x(t) + D_{11}^T D_{12} u(t) + B_1^T \lambda(t+1) \right)$$
$$+ E_1^{-1} D_{21}^T (D_{21} E_1^{-1} D_{21}^T)^{-1} y(t), \tag{A.22}$$

with $E_2 := E_1^{-1} - E_1^{-1} D_{21}^T (D_{21} E_1^{-1} D_{12}^T)^{-1} D_{21} E_1^{-1}$.

By combining (A.16) and (A.22), we find the expression for $u(t)$ as function of $x(t)$, $\lambda(t+1)$, and $y(t)$

$$u(t) = -E_3^{-1}(D_{12}^T C_1 + D_{12}^T D_{11} E_2 D_{11}^T C_1)x(t)$$
$$- E_3^{-1}(D_{12}^T D_{11} E_2 B_1^T + B_2^T)\lambda(t+1)$$
$$- E_3^{-1} D_{12}^T D_{11} E_1^{-1} D_{21}^T (D_{21} E_1^{-1} D_{21}^T)^{-1} y(t), \tag{A.23}$$

with $E_3 = D_{12}^T D_{12} + D_{12}^T D_{11} E_2 D_{11}^T D_{12}$.

To find $x(t+1)$, we first substitute (A.22) in (A.17):

$$x(t+1) = (A + B_1 E_2 D_{11}^T C_1)x(t) + (B_1 E_2 D_{11}^T D_{12} + B_2)u(t)$$
$$+ B_1 E_2 B_1^T \lambda(t+1) + B_1 E_1^{-1} D_{21}^T (D_{21} E_1^{-1} D_{21}^T)^{-1} y(t). \tag{A.24}$$

Substitution of (A.23) in (A.24) yields the expression for $x(t)$ as given in (6.16).

To find $\lambda(t)$, we combine (A.14) and (A.22):

$$\lambda(t) = (C_1^T C_1 + C_1^T D_{11} E_2 D_{11}^T C_1)x(t) + (C_1^T D_{12} + C_1^T D_{11} E_2 D_{11}^T D_{12})u(t)$$
$$+ (A^T + C_1^T D_{11} E_2 B_1^T)\lambda(t+1) + C_1^T D_{11} E_1^{-1} D_{21}^T (D_{21} E_1^{-1} D_{21}^T)^{-1} y(t). \tag{A.25}$$

Finally, substitution of (A.23) in (A.25) gives $\lambda(t)$ of (6.16).

A.6.5   Derivation of (6.21) and (6.22)

The matrices in (6.21) and (6.22) are obtained using the matrices

$$E_1 = \begin{bmatrix} \gamma^2 I - W_i^2 & W_i^2 & -W_i & 0 \\ W_i^2 & \gamma^2 I - W_i^2 & W_i & 0 \\ -W_i & W_i & \gamma^2 - I & 0 \\ 0 & 0 & 0 & \gamma^2 I - R - D_w^T D_w \end{bmatrix}$$

$$E_1^{-1} D_{21}^T (D_{21} E_1^{-1} D_{21}^T)^{-1} = \begin{bmatrix} \frac{W_i}{\gamma^2 - 2W_i^2} I & 0 \\ \frac{-W_i}{\gamma^2 - 2W_i^2} I & 0 \\ I & 0 \\ 0 & I \end{bmatrix}$$

$$E_2 = \begin{bmatrix} \frac{\gamma^2 - W_i^2}{\gamma^2(\gamma^2 - 2W_i^2)} I & \frac{-W_i^2}{\gamma^2(\gamma^2 - 2W_i^2)} I & 0 & 0 \\ \frac{-W_i^2}{\gamma^2(\gamma^2 - 2W_i^2)} I & \frac{\gamma^2 - W_i^2}{\gamma^2(\gamma^2 - 2W_i^2)} I & 0 & 0 \\ 0 & 0 & 0 & 0 \\ 0 & 0 & 0 & 0 \end{bmatrix}$$

$$D_{12}^T D_{11} E_2 = \begin{bmatrix} 0 & 0 & 0 & 0 \end{bmatrix}$$

$$E_3 = D_w^T D_w + R$$

and

$$D_{12}^T D_{11} E_1^{-1} D_{21}^T (D_{21} E_1^{-1} D_{21}^T)^{-1} = \begin{bmatrix} 0 & -R \end{bmatrix}.$$

A.6.6   Derivation of (6.24)

Given the general solution for the R-ILC controller

$$\begin{bmatrix} x(t+1) \\ \lambda(t) \end{bmatrix} = \begin{bmatrix} A_h & -B_h R_h^{-1} B_h^T \\ C_h^T Q_h C_h & A_h^T \end{bmatrix} \begin{bmatrix} x(t) \\ \lambda(t+1) \end{bmatrix} + \begin{bmatrix} F_1 \\ F_2 \end{bmatrix} y(t)$$

$$u(t) = \begin{bmatrix} G_1 & G_2 \end{bmatrix} \begin{bmatrix} x(t) \\ \lambda(t+1) \end{bmatrix} + H_y y(t),$$

$$\begin{bmatrix} x(0) \\ \lambda(N) \end{bmatrix} = \begin{bmatrix} x_0 \\ 0 \end{bmatrix},$$

and the similarity transformation $x(t) = g(t) - Y(t)\lambda(t)$. Then substitution of $x(t)$ in the expression for $\lambda(t)$ yields

$$\lambda(t) = \left(I + C_h^T Q_h C_h Y(t) \right)^1 \left(C_h^T Q_h C_h g(t) + A_h^T \lambda(t+1) + F_2 y(t) \right).$$

Subsequent substitution $x(t + 1) = g(t + 1) - Y(t + 1)\lambda(t + 1)$ and $\lambda(t)$ in the expression for $x(t + 1)$ gives

$$g(t+1) = \left(A_h - A_h Y(t)(I + C_h^T Q_h C_h Y(t))^{-1} C_h^T Q_h C_h\right) g(t)$$
$$+ \left(F_1 - A_h Y(t)(I + C_h^T Q_h C_h Y(t))^{-1} F_2\right) y(t)$$
$$+ \left[Y(t+1) - A_h Y(t)(I + C_h^T Q_h C_h Y(t))^{-1} A_h^T\right.$$
$$\left. - B_h R_h^{-1} B_h^T\right] \lambda(t+1).$$

Removal of the influence of $\lambda(t + 1)$ on $g(t + 1)$ requires

$$0 = Y(t+1) - A_h Y(t)(I + C_h^T Q_h C_h Y(t))^{-1} A_h^T - B_h R_h^{-1} B_h^T$$
$$Y(t+1) = A_h Y(t)(I + C_h^T Q_h C_h Y(t))^{-1} A_h^T + B_h R_h^{-1} B_h^T.$$

It can be shown, e.g., see Appendix C of [37], that this expression equals a time varying Riccati equation.

A.6.7   Derivation of (6.30)

Given the time invariant version of (6.24)

$$\begin{bmatrix} g(t+1) \\ \lambda(t) \end{bmatrix} = \begin{bmatrix} A_{T1} & 0 \\ A_{T2} & A_{T1}^T \end{bmatrix} \begin{bmatrix} g(t) \\ \lambda(t+1) \end{bmatrix} + \begin{bmatrix} F_{T1} \\ F_{T2} \end{bmatrix} y(t),$$
$$u(t) = \begin{bmatrix} G_1 & G_2 \end{bmatrix} \begin{bmatrix} g(t) \\ \lambda(t+1) \end{bmatrix} - G_1 Y \lambda(t) + H_y y(t),$$
$$\begin{bmatrix} g(0) \\ \lambda(N) \end{bmatrix} = \begin{bmatrix} x_0 \\ 0 \end{bmatrix},$$

and the similarity transformation $\lambda(t) = \zeta(t) - Xg(t)$. Then substitution of $\lambda(t)$ by $\zeta(t)$ yields

$$\zeta(t) = (X + A_{T2} - A_{T1}^T X A_{T1})g(t) + A_{T1}^T \zeta(t+1) + (F_{T2} - A_{T1}^T X F_{T1})y(t).$$

Removal of the influence of $g(t)$ on $\zeta(t)$ requires

$$0 = X + A_{T2} - A_{T1}^T X A_{T1}.$$

Under the assumption that A_{T1} is of full rank, this equation can be written as the Sylvester equation

$$(A_{T1}^T)^{-1} X - X A_{T1} = -(A_{T1}^T)^{-1} A_{T2}.$$

Appendix B

Example: Allowable uncertainty for RC and RMC

To illustrate the difference in allowable Δ for RC and RMC, consider the following simple example: Given an uncertain system with input multiplicative uncertainty $J(I + \Delta)$, and ILC controller $(\mathcal{Q}, L_o, L_c) = (I, gJ^{-1}, I)$ with $g > 0$. Then for RMC, we need $\|(1 - g)I - g\Delta\|_{i2} < 1$, resulting in $\|\Delta\|_{i2} < 1$.

On the other hand, for RC, we require

$$|\lambda_i(I - g(I + \Delta))| < 1 \Leftrightarrow |1 - g - g\lambda_i(\Delta)| < 1.$$

With $\lambda_i(\Delta) =: \lambda_{re} + i\lambda_{im}$, RC requires $\lambda_{re} > -1$, independent of the value for g. Furthermore, if $\lambda_{re} > -1$, we find that RC can be achieved for

$$g < \frac{2 + 2\lambda_{re}}{1 + 2\lambda_{re} + \lambda_{re}^2 + \lambda_{im}^2}.$$

Hence, for $\lambda_{re} > -1$, there always exists a learning gain $g > 0$ such that the ILC controlled system is RC. In contrast, RMC does not depend on the value for g.

The difference in allowable uncertainty for RC and RMC for scalar Δ is depicted in Figure B.1. As can be seen, the demand of monotonic convergence can restrict the allowable uncertainty set considerably.
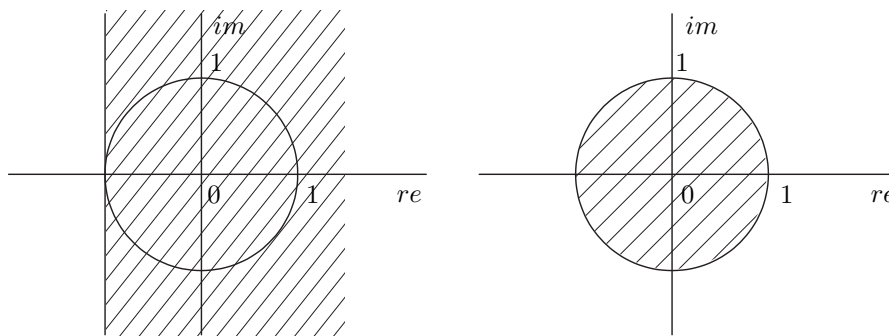
Figure B.1: Graphical representation of the uncertainty region for scalar Δ for which the ILC controlled system is RC (left) and RMC (right).

Appendix C

Flexible two-inertia setup

In this Appendix, we discuss modeling and time domain feedback control design of the flexible two-inertia system presented in Figure C.1. This system is a mass produced mechanical SISO system showing production tolerances. The system is driven by a DC motor which is connected to the first mass m_1. The input of the amplifier connected to the motor is limited to [-2.5,2.5] volt. The second mass m_2 is connected to the first with a poorly damped shaft. Although the angular position of both m_1 and m_2 can be measured by encoders with a resolution of $\pi \cdot 10^{-3}$ radians, we only consider the output of m_2.

Figure C.1: Two-inertia setup used for the experiments.

A model of the two-inertia system, see Figure C.2, includes the inertia of the

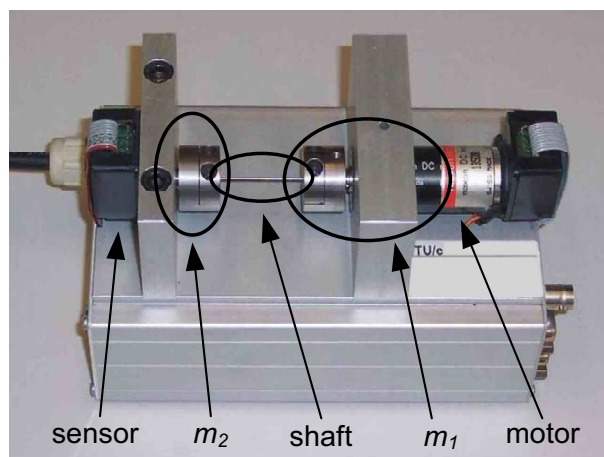masses and the flexibility and damping of the shaft, but leaves out cogging effects of the motor and the small amount of friction in the bearings.
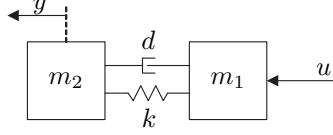
Figure C.2: Model P of the two-inertia setup.

The corresponding continuous time model is given by

$$P(s) = \frac{ds + k}{m_1 m_2 s^4 + (m_1 + m_2)ds^3 + (m_1 + m_2)ks^2}.$$

The system parameters are determined experimentally, and are given by

$$m_1 = 2 \cdot 10^{-4}, \quad m_2 = 1.6 \cdot 10^{-4}, \quad d = 5.66 \cdot 10^{-4}, \quad k = 9.8.$$

A discrete time equivalent of this model is obtained by using a "zero-order-hold" approximation with a sampling frequency of 1 kHz, see Figure C.3.
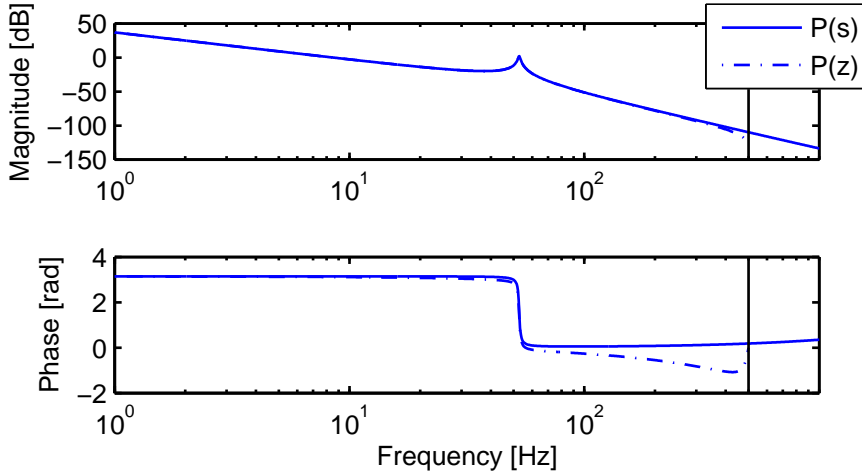
Figure C.3: Bode plot of continuous time system $P(s)$ and discrete time system $P(z)$.

Since without feedback controller the system is marginally stable, we choose to stabilize the system using time domain feedback controller $C(s)$. This controller consists of a notch filter at 52 Hz, a lead filter and additional gain. Subsequently, this continuous time controller is implemented in discrete time using a Tustin approximation with a prewarp frequency of 52 Hz.

$$C(s) = 0.2 \frac{\frac{1}{2\pi 3}s + 1}{\frac{1}{2\pi 20}s + 1} \frac{\frac{1}{(2\pi 52)^2}s^2 + \frac{0.02}{2\pi 52}s + 1}{\frac{1}{(2\pi 52)^2}s^2 + \frac{2}{2\pi 52}s + 1}.$$
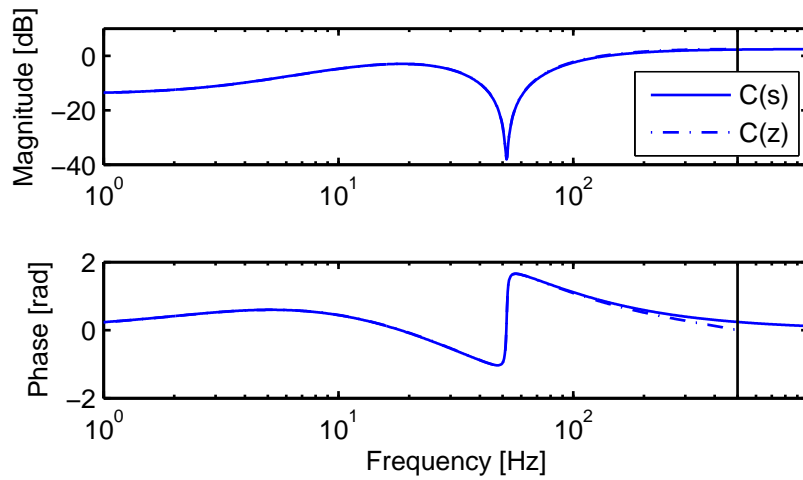
Figure C.4: Bode plot of continuous time controller $C(s)$ and discrete time controller $C(z)$.

The system $J(z)$ used for ILC control is given by $J(z) = (1 + P(z)C(z))^{-1}P(z)$, see Figure C.5 for the Bode plot and Figure C.6 for the impulse response.
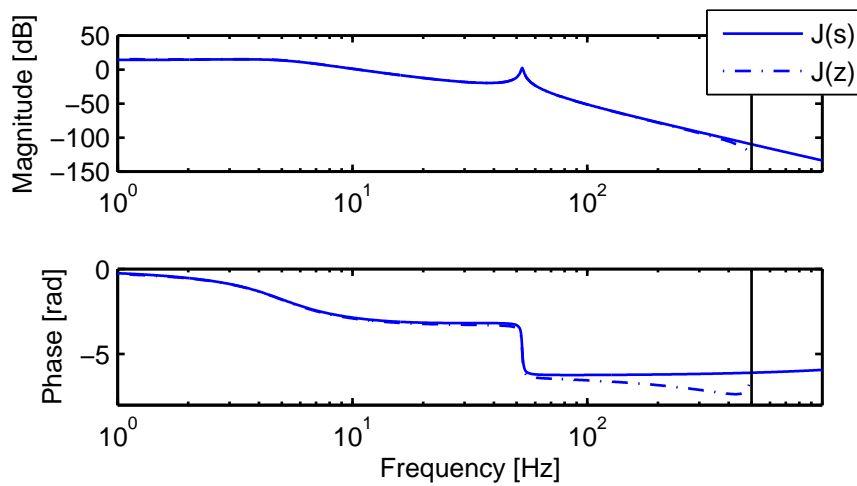
Figure C.5: Bode plot of continuous time system $J(s)$ and discrete time system $J(z)$.
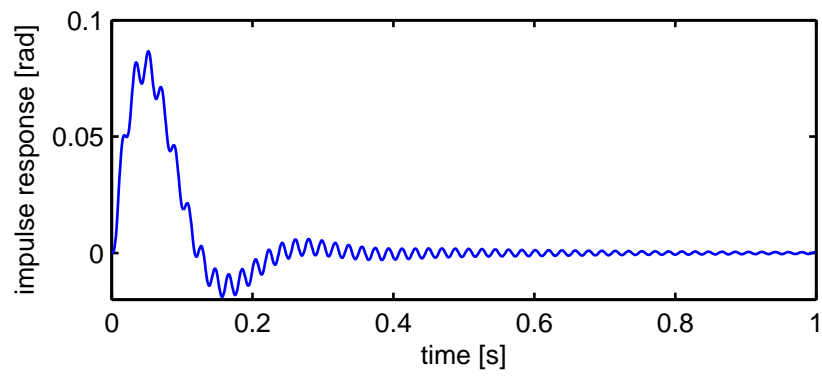
Figure C.6: Impulse response of $J(z)$.

Appendix D

Flexible beam setup

In this Appendix, we discuss the modeling and control of the flexible beam setup presented in Figure D.1. The steel beam (500mm × 20mm × 2mm) is fixed to the environment by five leaf springs, which remove four degrees of freedom (DOF). The two remaining DOFs consist of a translation in x direction and rotation around φ.
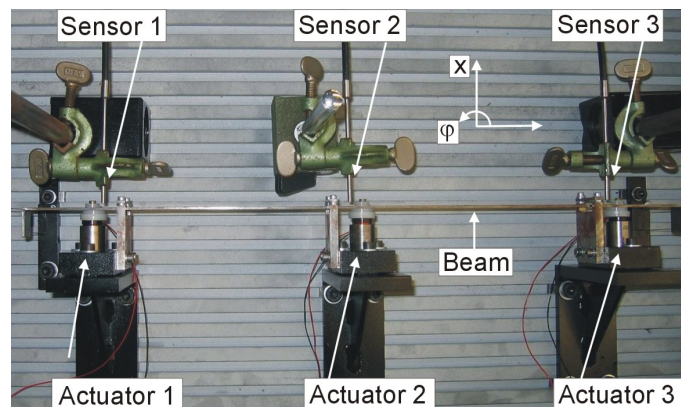
Figure D.1: The flexible beam setup used for the experiments.

The system is actuated by three current driven Lorentz' voice coil actuators. Two actuators are required to control the two DOFs, while the third actuator can be used to suppress flexible modes in the beam. The input of an actuator is provided by an amplifier (voltage-to-current converter) with an input voltage approximately proportional to the output current. The input of the amplifier is limited to [-2.5, 2.5] volt.

The position of the beam is measured with fiberoptic sensors. These sensors perform non-contact measurements of the displacement of the beam by transmitting light and measuring the intensity of the reflected light. In our range of operation, the displacement-to-intensity ratio is approximately constant. The experimentally determined noise level, i.e., standard deviation of the measured output, is 0.35 μm.

For control implementation on the flexible beam, we use a rapid prototyping environment. It consists of real-time hardware which is connected to the amplifiers and sensors, in combination with Matlab Simulink. All experiments are performed with a sample time T_s of 1 ms.

For ILC to be implementable on the experimental setup, the ILC control problem and setup should satisfy the following conditions [17].

- A trial has a fixed and finite time span.

- Repetition of initial time domain state for each trial, i.e., $x_k(0) = x_0$.

- Invariance of the system dynamics is ensured throughout all trials.

With the reference signal known, we satisfy the first condition. To meet the second condition, we have developed a homing procedure which brings the system within 0.4 μm of the desired initial position.

The third condition provides more difficulties. When repeatedly applying a pulse with an amplitude of 1 volt to the three actuators (20 trials with a trial length of 1 second), the three measured outputs vary much more than 0.4 μm, Table D.1 second column. Without knowing the exact source for the non-repetitiveness of the outputs, spectral analysis of the outputs reveals that the non-repetitiveness is dominated by the low frequent rigid body frequencies.

Table D.1: Repetitiveness of the systems dynamics, (standard deviation in [μm]).

noise	open loop	closed loop	closed loop with integrator
0.35	3.53	0.95	0.85

To improve the repetitiveness of our system, we introduce feedback control into the time domain loop. With the variances in the outputs dominated by the two *rigid body* frequencies, we use time domain feedback control to control these two rigid body modes. The outputs y^1 and y^3 are first transformed to the rigid body coordinates $y^{1,rb}$ (translations) and $y^{2,rb}$ (rotation), using matrix D_y. Matrix D_y

is determined based on the geometry of the system, resulting in (D.1).

$$D_y = \begin{bmatrix} \frac{1}{\sqrt{2}} & \frac{1}{\sqrt{2}} \\ \frac{1}{\sqrt{2}} & -\frac{1}{\sqrt{2}} \end{bmatrix}. \tag{D.1}$$

In this coordinate system, a diagonal controller is designed consisting of a lead filter with a zero at 10 Hz, a pole at 90 Hz, and a gain of 0.15, in series with a low pass filter with a cut-off frequency of 400 Hz. Subsequently, the feedback controller outputs $u^{1,rb}$ and $u^{3,rb}$ are transformed back to u^1 and u^3, using matrix D_f. With the positions of the actuators and sensors approximately equal, we choose $D_f = D_y^{-1} = D_y$.

The time domain closed loop system is shown in Figure D.2. Note that, since the second actuator and output are not used in the feedback loop, the system in Figure D.2 is partly open loop, partly closed loop. If we again apply the pulse of 1 volt to the three actuators, the repetitiveness of the output after 20 trials is significantly improved, Table D.1 third column.
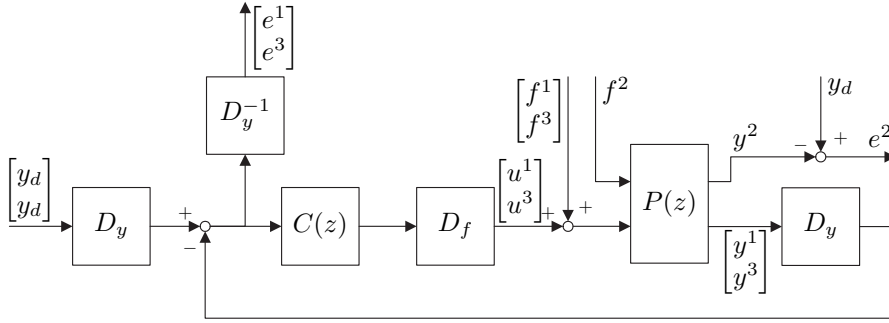
Figure D.2: Partial feedback controlled system in time domain.

In an attempt to further improve the invariance of the dynamics, we introduce an integrator in each of the two diagonal entries with a gain of 0.5. The result in repetitiveness is indeed improved, Table D.1 fourth column. A closer look at the error signals of the closed loop system with and without the integrator reveals, however, that for the integrator case the non-repetitiveness during the transient time interval is larger, but that the steady state offset is smaller.

Looking at the results of Table D.1, the closed loop system including the integrator outperforms the closed loop system without the integrator. Based on this, and the fact that the applied reference signal contains relatively long constant outputs which require small steady state errors, we decide to perform ILC and Hankel ILC to the closed loop system with feedback control including the integrator action.

To apply ILC to the flexible beam, we require the impulse response of the system. This impulse response of the system is obtained by separately applying a pulse with an amplitude of 2 volt to each of the actuators and measure the response

of all three outputs. These experiments are repeated 20 times for each actuator. Afterwards, the measurements are averaged and divided by 2, to correct for the pulse amplitude. The resulting impulse response of the time domain system is presented in Figure D.3.
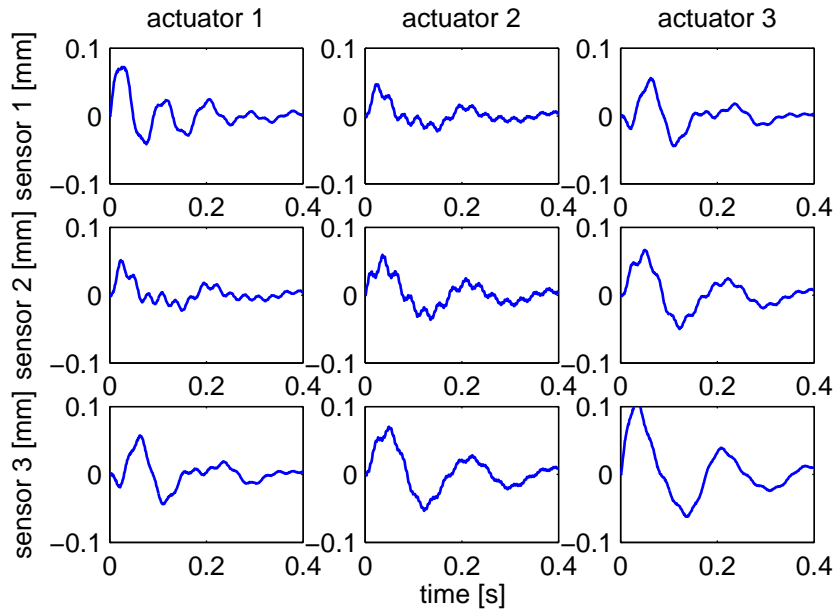
Figure D.3: Impulse response of the MIMO flexible beam, for $t = [0, 0.4]$s.

Bibliography

[1] H.-S. Ahn, K.L. Moore, and Y.-Q. Chen. Monotonic convergent Iterative Learning Controller design based on interval model conversion. *IEEE Transactions on Automatic Control*, 51(2):366–371, February 2006.

[2] H.-S. Ahn, Y.-Q. Chen, and K.L. Moore. Iterative Learning Control: brief survey and categorization. *IEEE Transactions on Systems, Man, and Cybernetics*, 37(6):1099–1121, November 2007. Part C: Applications and Reviews.

[3] H.-S. Ahn, K.L. Moore, and Y.-Q. Chen. *Iterative Learning Control: Robustness and monotonic convergence for interval systems.* Springer-Verlag, 2007. ISBN: 978-1-84628-846-3.

[4] H.-S. Ahn, K.L. Moore, and Y.-Q. Chen. Stability analysis of discrete-time Iterative Learning Control systems with interval uncertainty. *Automatica*, 43:892–902, 2007.

[5] N. Amann, D.H. Owens, and E. Rogers. New results in Iterative Learning Control. In *Int. Conference on Control*, volume 1, pages 640–645, Coventry, UK, 21-24 March 1994.

[6] N. Amann, D.H. Owens, and E. Rogers. Robustness of norm-optimal Iterative Learning Control. In *UKACC International Conference on Control*, number 427, pages 1119–1124, UK, September 2-5 1996.

[7] N. Amann, D.H. Owens, and E. Rogers. Iterative Learning Control for discrete-time systems with exponential rate of convergence. In *IEE Proc. Control Theory Applications*, volume 143, pages 217–224, March 1996.

[8] N. Amann, D.H. Owens, E. Rogers, and A. Wahl. An H_∞ approach to linear Iterative Learning Control design. *Int. Journal of Adaptive Control and Signal Processing*, 10:767–781, 1996.

[9] E.H. Anderson and J.P. How. Active vibration isolation using adaptive feedforward control. In *Proc. of the American Control Conference*, pages 1783–1788, Albuquerque, New Mexico USA, June 1997.

[10] S. Arimoto, S. Kawamura, and F. Miyazaki. Bettering operation of robots by learning. *Journal of Robotic Systems*, 1(2):123–140, 1984.

[11] S. Arimoto, S. Kawamura, and F. Miyazaki. Iterative Learning Control for robot systems. In *Proc. of IECON*, Tokyo, Japan, October 22-26 1984.

[12] K.E. Avrachenkov and R.W. Longman. Iterative Learning Control for over-determined, under-determined, and ill-conditioned systems. *International Journal of Applied Mathematics and Computer Science*, 13(1):113–122, 2003.

[13] M. Baggen, M. Heertjes, and R. Kamidi. Data–based feed–forward control in MIMO motion systems. In *Proc. of the American Control Conference*, pages 3011–3016, Seattle, WA USA, June 2008.

[14] K.L. Barton, J.J.M. van de Wijdeven, A.G. Alleyne, O.H. Bosgra, and M. Steinbuch. Norm optimal cross–coupled Iterative Learning Control. In *Proc. 47th IEEE Conference on Decision and Control (accepted)*, Cancun, Mexico, December 9-11 2008.

[15] T. Başar and P. Bernhard. H_∞–*Optimal control and related minimax design problems: a dynamic game approach.* Birkhäuser, 1991. ISBN: 0-8176-3554-8.

[16] A. Ben-Israel and T.N.E. Greville. *Generalized Inverses: Theory and Applications.* Wiley-Interscience, 1974.

[17] Z. Bien and J. Xu. *Iterative Learning Control: Analysis, Design, Integration, and Applications.* Kluwer Academic Publishing, Norwell, MA USA, 1998. ISBN: 0-7923-8213-7.

[18] M. Boerlage. MIMO jerk derivative feedforward for motion systems. In *Proc. of the American Control Conference*, pages 3892–3897, Minneapolis, MN USA, June 14-16 2006.

[19] A. Böttcher and S.M. Grudsky. *Toeplitz matrices, asymptotic linear algebra, and functional analysis.* Birkhäuser Verlag, 2000. ISBN: 3-7643-6290-1.

[20] A. Böttcher and B. Silbermann. *Introduction to large truncated Toeplitz matrices.* Springer-Verlag, 1999. ISBN: 0-387-98570-0.

[21] D.A. Bristow. Frequency domain analysis and design of Iterative Learning Control for systems with stochastic disturbances. In *Proc. of the American Control Conference*, pages 3901–3907, Seattle, WA USA, June 11-13 2008.

[22] D.A. Bristow, M. Tharayil, and A.G. Alleyne. A survey of Iterative Learning Control – a learning–based method for high–performance tracking control. *Control Systems Magazine*, 26(3):96–114, June 2006.

[23] B. Bukkems, D. Kostić, B. de Jager, and M. Steinbuch. Learning–based identification and Iterative Learning Control of direct–drive robots. *IEEE Transaction on Control Systems Technology*, 13(4):537–549, July 2005.

[24] J.B. Burl. *Linear optimal control: H_2 and H_∞ methods.* Addison-Wesley, 1999. ISBN: 0-201-80868-4.

[25] G. Casalino and G. Bartolini. A learning procedure for the control of movements of robotic manipulators. In *Proc. IASTED Symposium on Robotics and Automation*, pages 108–111, Amsterdam, The Netherlands, 1984.

[26] Y.-Q. Chen and K.L. Moore. PI–type Iterative Learning Control revisited. In *Proc. of the American Control Conference*, pages 2138–2143, Anchorage, AK USA, May 8-10 2002.

[27] Y.-Q. Chen, J.-X. Xu, and T.H. Lee. An Iterative Learning Controller using current iteration tracking error information and initial state learning. In *Proc. of the 35th Conference on Decision and Control*, pages 3064–3069, Kobe, Japan, December 1996.

[28] Y.-Q. Chen, C. Wen, H. Dou, and M. Sun. Iterative learning identification of aerodynamic drag curve from tracking radar measurements. *Control Engineering Practice*, 5(1):1543–1553, 1997.

[29] Y.-Q. Chen, J.-X. Xu, and C. Wen. A high–order terminal Iterative Learning Control scheme. In *Proc. of the 36th Conference on Decision and Control*, pages 3771–3772, San Diego, CA USA, December 1997.

[30] I. Chin, S.J. Qin, K.S. Lee, and M. Cho. A two–stage Iterative Learning Control technique combined with a real–time feedback for independent disturbance rejection. *Automatica*, 40:1913–1922, 2004.

[31] J.J. Craig. Adaptive control of manipulators through repeated trials. In *Proc. of the American Control Conference*, pages 1566–1573, San Diego, CA USA, 1984.

[32] C.F. Cutforth and L.Y. Pao. Adaptive command shaping for maneuvering flexible structures. *Automatica*, 40:685–693, 2004.

[33] D. de Roover. *Motion control of a wafer stage.* PhD thesis, Delft University of Technology, 1997. ISBN: 90-47-1562-9.

[34] D. de Roover and O.H. Bosgra. Synthesis of robust multivariable Iterative Learning Controllers with application to a wafer stage motion system. *Int. Journal of Control*, 73(10):968–979, 2000.

[35] D. de Roover, O.H. Bosgra, and M. Steinbuch. Internal model based design of repetitive and Iterative Learning Controllers for linear multivariable systems. *Int. Journal of Control*, 73(10):929–941, 2000.

[36] S. Devasia. Should model–based inverse commands be used as feedforward under plant uncertainty? *IEEE Transactions on Automatic Control*, 47 (11):1865–1871, November 2002.

[37] B. Dijkstra. *Iterative Learning Control, with application to a wafer stage.* PhD thesis, Delft University of Technology, 2004. ISBN: 90-370-0209-9.

[38] B.G. Dijkstra and O.H. Bosgra. Extrapolation of optimal lifted system ILC solution, with application to a waferstage. In *Proc. of the American Control Conference*, pages 2595–2600, Anchorage, AK USA, May 8-10 2002.

[39] B.G. Dijkstra and O.H. Bosgra. Convergence design considerations of low order Q-ILC for closed loop systems, implemented on a high precision wafer stage. In *Proc. of the 41st IEEE Conference on Decision and Control*, pages 2494–2499, Las Vegas, NV USA, December 2002.

[40] B.G. Dijkstra and O.H. Bosgra. Exploiting Iterative Learning Control for command shaping with application to a wafer stage. In *Proc. of the American Control Conference*, pages 4811–4815, Denver, CO USA, June 4-6 2003.

[41] T.-Y. Doh, J.-H. Moon, and M.J. Chung. An Iterative Learning Control for uncertain systems using structured singular value. *Journal of Dynamic Systems, Measurement, and Control*, 121:660–667, December 1999.

[42] T.-Y. Doh, J.-H. Moon, K.B. Jin, and M.J. Chung. Robust Iterative Learning Control with current feedback for uncertain linear systems. *International Journal of Systems Science*, 30(1):39–47, 1999.

[43] T. Donkers, J.J.M. van de Wijdeven, and O.H. Bosgra. Robustness against model uncertainties of norm optimal Iterative Learning Control. In *Proc. of the American Control Conference*, pages 4561–4566, Seattle, WA, USA, June 11-13 2008.

[44] T. Donkers, J.J.M. van de Wijdeven, and O.H. Bosgra. A design approach for noncausal robust Iterative Learning Control using worst case disturbance optimisation. In *Proc. of the American Control Conference*, pages 4567–4572, Seattle, WA, USA, June 11-13 2008.

[45] J.C. Doyle. Analysis of feedback systems with structured uncertainties. *IEE proceedings*, 129(6):242–250, November 1982.

[46] Y Fang and T.W.S. Chow. 2-D analysis for Iterative Learning Controller for discrete-time systems with variable initial conditions. *Transactions on Circuits and Systems–I: Fundamental Theory and Applications*, 50(5):722–727, May 2003.

[47] B.A. Francis and W.M. Wonham. The internal model principle of control theory. *Automatica*, 12:457–465, 1976.

[48] C. Freeman, P. Lewin, and E. Rogers. Experimental evaluation of Iterative Learning Control algorithms for non-minimum phase plants. *Int. Journal of Control*, 78(11):826–846, July 20 2005.

[49] M. French, G. G. Munde, E. Rogers, and D.H. Owens. Recent developments in adaptive Iterative Learning Control. In *Proc. of the 38th IEEE Conference on Decision and Control*, pages 264–269, Phoenix,Az USA, December 1999.

[50] J.A. Frueh and M.Q. Phan. Linear quadratic optimal Learning Control (LQL). *Int. Journal of Control*, 73(10):832–839, 2000.

[51] K. Galkowski, J. Lam, E. Rogers, S. Xu, B. Sulikowski, W. Paszke, and D.H. Owens. LMI based stability analysis and robust controller design for discrete linear repetitive processes. *Int. Journal of Robust and Nonlinear Control*, 13:1195–1211, 2003.

[52] F. Gao, Y. Yang, and C. Shao. Robust Iterative Learning Control with applications to injection molding process. *Chemical Engineering Science*, 56:7025–7034, 2001.

[53] M. Garden. *Learning control of actuators in control systems*. US patent 03555252, Philadelphia, PA USA, January 1971. Leeds & Northrup Company.

[54] G. Gauthier and B. Boulet. Convergence analysis of terminal ILC in the z–domain. In *Proc. of the American Control Conference*, pages 184–189, Portland, OR USA, June 8-10 2005.

[55] J. Ghosh and B. Paden. Pseudo–inverse based Iterative Learning Control for linear nonminimum phase plants with unmodeled dynamics. *Journal of Dynamic Systems, Measurement, and Control*, 126:661–665, September 2004.

[56] D. Gorinevsky. Loop shaping for Iterative Control of batch processes. *IEEE Control Systems Magazine*, (6):55–65, December 2002.

[57] M.B. Groot Wassink. *Inkjet printhead performance enhancement by feed-forward command design based on two–port modeling*. PhD thesis, Delft University of Technology, 2007. ISBN: 978-90-9021484-9.

[58] S. Gunnarsson and M. Norrlöf. On the design of ILC algorithms using optimization. *Automatica*, 37:2011–2016, 2001.

[59] S. Gunnarsson and M. Norrlöf. On the disturbance properties of high order Iterative Learning Control algorithms. *Automatica*, 42:20312034, 2006.

[60] W.B.J. Hakvoort, R.G.K.M. Aarts, J. van Dijk, and J.B. Jonker. Lifted system Iterative Learning Control applied to an industrial robot. *Control Engineering Practice*, 16:377391, 2008.

[61] K. Hamamoto and T. Sugie. An Iterative Learning Control algorithm within prescribed command–output subspace. *Automatica*, 37(11):1803–1809, 2001.

[62] K. Hamamoto and T. Sugie. Iterative Learning Control for robot manipulators using the finite dimensional command subspace. *IEEE Transactions on Robotics and Automation*, 18(4):632–635, August 2002.

[63] S. Hara, Y. Yamamoto, T. Omata, and M. Nakano. Repetitive control system: A new type servo system for periodic exogenous signals. *IEEE Transactions on Automatic Control*, 33(7):659–668, July 1988.

[64] T.J. Harte, J. Hätönen, and D.H. Owens. Discrete-time inverse model–based Iterative Learning Control: stability, monotonicity and robustness. *Int. Journal of Control*, 78(8):577–586, May 2005.

[65] J. Hätönen, D.H. Owens, and K.L. Moore. An algebraic approach to Iterative Learning Control. *Int. Journal of Control*, 77(1):45–54, January 2004.

[66] J. Hätönen, D.H. Owens, and K. Feng. Basis functions and parameter optimisation in high–order Iterative Learning Control. *Automatica*, 42(2):287–294, February 2006.

[67] M. Heertjes and T. Tso. Robustness, convergence, and Lyapunov stability of a nonlinear Iterative Learning Control applied at a wafer scanner. In *Proc. of the American Control Conference*, pages 5490–5495, New York, NY USA, July 11-13 2007.

[68] S. Hillenbrand and M. Pandit. A discrete–time Iterative Learning Control law with exponential rate of convergence. In *Proc. of the 38th Conference on Decision and Control*, pages 1575–1580, Phoenix, AZ USA, December 1999.

[69] T.-H. Kim, X. Zheng, and T. Sugie. Noise tolerant Iterative Learning Control and identification for continuous–time systems with unknown bounded command disturbances. *Journal of Dynamic Systems, Measurement, and Control*, 129:825–836, November 2007.

[70] J.H. Lee, K. S. Lee, and W.C. Kim. Model–based Iterative Learning Control with a quadratic criterion for time–varying linear systems. *Automatica*, 36(5):641–657, May 2000.

[71] K.H. Lee and Z. Bien. Initial condition problem of Learning Control. In *IEE Proceedings–D*, volume 138, pages 525–528, November 1991.

[72] P.A. LeVoci and R.W. Longman. Intersample error in discrete time learning and repetitive control. In *Proc. of the AIAA/AAS Astrodynamics Specialist Conference*, pages 1–24, Providence, RI USA, August 16-19 2004.

[73] X.-D. Li, T.W.S. Chow, and J.K.L. Ho. 2-D system theory based Iterative Learning Control for linear continuous systems with time delays. *IEEE Transactions on Circuits and Systems*, 52(7):1421–1430, July 2005.

[74] Y. Li and R. Horowitz. Active suspension vibration control with dual stage actuators in hard disk drives. In *Proc. of the American Control Conference*, pages 2786–2791, Arlington, VA USA, June 25-27 2001.

[75] D.J.N. Limebeer, M. Green, and D. Walker. Discrete time H_∞ control. In *Proc. of the 28th IEEE Conference on Decision and Control*, pages 392–396, Tampa, FL USA, December 1989.

[76] R.W. Longman. Iterative Learning Control and repetitive control for engineering practise. *Int. Journal of Control*, 73(10):930–954, 2000.

[77] R.W. Longman and C.-P. Lo. Generalized holds, ripple attenuation, and tracking additional outputs in learning control. *Journal of Guidance, Control, and Dynamics*, 20(6):1207–1214, November-December 1997.

[78] P. Lucibello. Output zeroing with internal stability by learning. *Automatica*, 31(11):1665–1672, 1995.

[79] P. Lucibello, S. Panzieri, and G. Ulivi. Repositioning control of a two–link flexible arm by learning. *Automatica*, 33(4):579–590, 1997.

[80] D.G. Luenberger. *Linear and nonlinear programming.* Springer, 2003. ISBN: 978-14020-7593-3.

[81] J.M. Maciejowski. *Multivariable feedback control.* Addison-Wesley Publishing Company Inc., 1989. ISBN:0-201-18243-2.

[82] A. Madady. Self tuning Iterative Learning Control systems. In 5th *Asian Control Conference*, pages 1786–1792, Melbourne, Australia, July 20-23 2004.

[83] O. Markusson, H. Hjalmarsson, and M. Norrlöf. Iterative Learning Control of nonlinear non-minimum phase systems and its application to system and model inversion. In *Proc. of the 40th IEEE Conference on Decision and Control*, pages 4481–4482, Orlando, FL USA, December 2001.

[84] S. Mishra and M. Tomizuka. An optimization–based approach for design of Iterative Learning Controllers with accelerated rates of convergence. In *Proc. of the 44th IEEE Conference on Decision and Control, and the European Control Conference 2005*, pages 2427–2432, Seville, Spain, December 12-15 2005.

[85] S. Mishra, J. Coaplen, and M. Tomizuka. Precision positioning of wafer scanners segmented Iterative Learning Control for nonrepetitive disturbances. *Control Systems Magazine*, 27(4):20–25, August 2007.

[86] K.L. Moore. An observation about monotonic convergence in discrete–time, P–type Iterative Learning Control. In *Proc. of the 2001 IEEE International Symposium on Intelligent Control*, pages 45–49, México City, México, September 5-7 2001.

[87] K.L. Moore. *Iterative Learning Control for deterministic systems.* Springer-Verlag, London, 1993. ISBN: 3-540-19707-9.

[88] K.L. Moore. Iterative Learning Control - an expository overview. *Applied and Computational Controls, Signal Processing, and Circuits*, 1:151–214, 1999.

[89] K.L. Moore, H.-S. Ahn, and Y.-Q. Chen. Iteration domain $\mathcal{H}_\infty$-optimal Iterative Learning Controller design. *Int. Journal of Robust and Nonlinear Control*, 18(10):1001–1017, July 2008.

[90] D.S. Naidu. *Optimal control systems.* CRC Press, 2003. ISBN: 0-8493-0892-5.

[91] M. Norrlöf. Comparative study on first and second order ilc – frequency domain analysis and experiments. In *Proc. of the 39th IEEE Conference on Decision and Control*, pages 3415–3420, Sydney, Australia, December 2000.

[92] M. Norrlöf. An adaptive Iterative Learning Control algorithm with experiments on an industrial robot. *IEEE Transactions on Robotics and Automation*, 18(2):245–251, April 2002.

[93] M. Norrlöf. *Iterative Learning Control, analysis, design and experiments.* PhD thesis, Linköping university, Linköping, Sweden, 2000. ISBN: 91-7219-837-0.

[94] M. Norrlöf and S. Gunnarsson. Disturbance aspects of Iterative Learning Control. *Engineering Applications of Artificial Intelligence*, 14:87–94, 2001.

[95] M. Norrlöf and S. Gunnarsson. Time and frequency domain convergence properties in Iterative Learning Control. *Int. Journal of Control*, 75(14):1114–1126, 2002.

[96] M. Norrlöf and S. Gunnarsson. Experimental comparison of some classical Iterative Learning Control algorithms. *IEEE Transactions on Robotics and Automation*, 18(4):636–641, August 2002.

[97] M. Norrlöf and S. Gunnarsson. A note on causal and CITE Iterative Learning Control algorithms. *Automatica*, 41:345–350, 2005.

[98] T.A.E. Oomen, J.J.M. van de Wijdeven, and O.H. Bosgra. Suppressing intersample behavior in Iterative Learning Control. *(submitted).*

[99] T.A.E. Oomen, J.J.M. van de Wijdeven, and O.H. Bosgra. Suppressing intersample behavior in Iterative Learning Control. In *Proc. 47th IEEE Conference on Decision and Control (accepted)*, 2008.

[100] D.H. Owens and K. Feng. Parameter optimization in Iterative Learning Control. *Int. Journal of Control*, 76(11):1059–1069, 2003.

[101] D.H. Owens and E. Rogers. Boundary conditions and the stability of a class of 2D continuous–discrete linear systems. In *Proc. of the American Control Conference*, pages 2076–2081, Portland, OR USA, June 8-10 2005.

[102] D.H. Owens, E. Rogers, and K.L. Moore. Analysis of linear Iterative Learning Control schemes using repetitive process theory. *Asian Journal of Control*, 4(1):68–89, March 2002.

[103] A. Packard and J. Doyle. The complex structured singular value. *Automatica*, 29(1):71–109, 1993.

[104] K.-H. Park and Z. Bien. Intervalized Iterative Learning Control control for monotonic convergence in the sense of sup–norm. *Int. Journal of Control*, 78(15):1218–1227, October 2005.

[105] M. Phan and R.W. Longman. A mathematical theory of Learning Control for linear discrete multivariable systems. In *Proc. of the AIAA/AAS Astrodynamics Specialist Conference*, pages 740–746, Minneapolis, MN USA, August 5-17 1988.

[106] M.Q. Phan and H. Rabitz. Learning control of quantum–mechanical systems by laboratory identification of effective command–output maps. *Chemical Physics*, 217:389–400, May 1997.

[107] M.Q. Phan and H. Rabitz. A self–guided algorithm for learning control of quantum–mechanical systems. *Journal of Chemical Physics*, 110(1):34–41, January 1 1999.

[108] S. Rhim and W.J. Book. Adaptive time-delay command shaping filter for flexible manipulator control. *IEEE/ASME Transactions on Mechatronics*, 9(4):619–626, December 2004.

[109] E. Rogers, K. Galkowski, and D.H. Owens. *Control Systems Theory and Applications for Linear Repetitive Processes*. Springer-Verlag, 2007. ISBN:978-3-540-42663-9.

[110] W.J. Rugh. *Linear system theory*. Englewood Cliffs : Prentice Hall, 1993. ISBN: 0-13-555038-6.

[111] S.S. Saab. Optimality of First–Order ILC among higher order ILC. *IEEE Transactions on Automatic Control*, 51(8):1332–1336, August 2006.

[112] F. Sakai and T. Sugie. $\mathcal{H}_2$–suboptimal Iterative Learning Control for continuous–time system identification. In *Proc. of the American Control Conference*, pages 946–951, Minneapolis, MN USA, June 14-16 2006.

[113] J.S. Shamma. Robust stability with time–varying structured uncertainty. *IEEE Transactions on Automatic Control*, 39(4):714–724, April 1994.

[114] J. Shi, F. Gao, and T.-J. Wu. Robust design of integrated feedback and Iterative Learning Control of a batch process based on a 2D Roesser system. *Journal of Process Control*, 15:907–924, 2005.

[115] N. Singer, W. Singhose, and W. Seering. Comparison of filtering methods for reducing residual vibration. *European Journal of Control*, 5:208–218, 1999.

[116] T. Singh and W. Singhose. Tutorial on command shaping/time delay control of maneuvering flexible structures. In *Proc. of the American Control Conference*, pages 1717–1731, Anchorage, AK, USA, May 8-10 2002.

[117] S. Skogestad and I. Postlethwaite. *Multivariable feedback control*. John Wiley & Sons Ltd., 2005. ISBN: 0-470-01168-8.

[118] M. Steinbuch, S. Weiland, and T. Singh. Design of noise and period–time robust high–order repetitive control, with application to optical storage. *Automatica*, 43:2086–2095, 2007.

[119] K.M. Tao, R.L. Kosut, and G. Aral. Learning feedforward control. In *Proc. of the American Control Conference*, pages 2575–2579, Baltimore, MD USA, June 1994.

[120] A. Tayebi and M.B. Zaremba. Robust Iterative Learning Control design is straightforward for uncertain LTI systems satisfying the robust performance condition. *IEEE Transactions on Automatic Control*, 48(1):101–106, January 2003.

[121] A. Tayebi, S. Abdul, and M.B. Zaremba. Robust Iterative Learning Control design via μ-synthesis. In *Proc. of the 2005 IEEE Int. Conference on Control Applications*, pages 416–421, Toronto, Canada, August 2005.

[122] R. Tousain and D. van Casteren. Iterative Learning Control in a mass product: light on demand in DLP projection systems. In *Proc. of the American Control Conference*, pages 5478–5483, New York City, USA, July 11-13 2007.

[123] R. Tousain, E. van der Meché, and O. Bosgra. Design strategy for Iterative Learning Control based on optimal control. In *Proc. 40th IEEE Conference on Decision and Control*, pages 4463–4468, Orlando, FL USA, December 4-7 2001.

[124] T.-C. Tsao and M. Tomizuka. Robust adaptive and repetitive digital tracking control and application to a hydraulic servo for noncircular machining. *Journal of Dynamic Systems, Measurement, and Control*, 116:24–32, March 1994.

[125] A. Tzes and S. Yurkovich. An adaptive command shaping control scheme for vibration suppression in slewing flexible structures. *IEEE Transaction on Control Systems Technology*, 1(2):114–121, June 1993.

[126] M. Uchiyama. Formulation of high–speed motion pattern of a mechanical arm by trial (in japanese). *Transactions of the Society for Instrumentation and Control Engineers*, 14(6):706–712, 1978.

[127] J.J.M. van de Wijdeven and O.H. Bosgra. Residual vibration suppression using Hankel Iterative Learning Control. In *Proc. of the American Control Conference*, pages 1778–1783, Minneapolis, MN USA, June 14-16 2006.

[128] J.J.M. van de Wijdeven and O.H. Bosgra. Stabilizability, performance, and the choice of actuation and observation time windows in Iterative Learning Control. In *Proc. 45th IEEE Conference on Decision and Control*, pages 5042–5047, San Diego, CA USA, December 13-15 2006.

[129] J.J.M. van de Wijdeven and O.H. Bosgra. Residual vibration suppression using Hankel Iterative Learning Control. *Int. Journal of Robust and Nonlinear Control*, 18(10):1034–1051, July 2008.

[130] J.J.M. van de Wijdeven and O.H. Bosgra. Hankel Iterative Learning Control for residual vibration suppression with MIMO flexible structure experiments. In *Proc. of the American Control Conference*, pages 4993–4998, New York, NY USA, July 11-13 2007.

[131] J.J.M. van de Wijdeven and O.H. Bosgra. Noncausal finite–time robust Iterative Learning Control. In *Proc. 46th IEEE Conference on Decision and Control*, pages 258–263, New Orleans, LA USA, December 12-14 2007.

[132] S.H. van der Meulen, R.L. Tousain, and O.H. Bosgra. Fixed structure feedforward controller design exploiting iterative trials: Application to a wafer stage and a desktop printer. *Journal of Dynamic Systems, Measurement, and Control*, 130(5):051006, September 2008.

[133] C.L. van Oosten, O.H. Bosgra, and B.G. Dijkstra. Reducing residual vibrations through Iterative Learning Control, with application to a wafer stage. In *Proc. of the American Control Conference*, pages 5150–5155, Boston, MA USA, June 30 - July 2 2004.

[134] M. Vidyasagar. Optimal rejection of persistent bounded disturbances. *IEEE Transactions on Automatic Control*, 31(6):527–534, June 1986.

[135] J. Xu, M. Sun, and L. Yu. LMI-based robust Iterative Learning Controller design for discrete linear uncertain systems. *Journal of Control Theory and Applications*, 3:259–265, 2005.

[136] J.-X. Xu and Y. Tan. *Linear and Nonlinear Iterative Learning Control*. Springer-Verlag, 2003. ISBN: 3-540-40173-3.

[137] J.-X. Xu, Y.-Q. Chen, T. H. Lee, and S. Yamamoto. Terminal Iterative Learning Control with an application to RTPCVD thickness control. *Automatica*, 35(9):1535–1542, 1999.

[138] Y. Ye and D. Wang. DCT basis function Learning Control. *IEEE/ASME Transactions on Mechatronics*, 10(4):449–454, August 2005.

[139] Y. Ye and D. Wang. Clean system inversion learning control law. *Automatica*, 41:1549–1556, 2005.

[140] Y. Ye and D. Wang. Learning more frequency components using P–type ILC with negative learning gain. *IEEE Transactions on Industrial Electronics*, 53(2):712–716, April 2006.

[141] P.M. Young and J.C. Doyle. Properties of the mixed μ problem and its bounds. *IEEE Transactions on Automatic Control*, 41(1):155–159, January 1996.

[142] B. Zhang, D. Wang, K. Zhou, Y. Ye, and Y. Wang. Pseudo–downsampled Iterative Learning Control. *Int. Journal of Robust and Nonlinear Control*, 18(10):1072–1088, July 2008.

[143] K. Zhou, J.C. Doyle, and K. Glover. *Robust and optimal control.* Prentice Hall, 1996. ISBN: 0-13-456567-3.

Summary

Iterative Learning Control design for uncertain and time-windowed systems

Iterative Learning Control (ILC) is a control strategy capable of dramatically increasing the performance of systems that perform batch repetitive tasks. This performance improvement is achieved by iteratively updating the command signal, using measured error data from previous trials, i.e., by learning from past experience.

This thesis deals with ILC for time-windowed and uncertain systems. With the term "time-windowed systems", we mean systems in which actuation and measurement time intervals differ. With "uncertain systems", we refer to systems whose behavior is represented by incomplete or inaccurate models.

To study the ILC design issues for time-windowed systems, we consider the task of residual vibration suppression in point-to-point motion problems. In this application, time windows are used to modify the original system to comply with the task. With the properties of the time-windowed system resulting in non-converging behavior of the original ILC controlled system, we introduce a novel ILC design framework in which convergence can be achieved. Additionally, this framework reveals new design freedom in ILC for point-to-point motion problems, which is unknown in "standard" ILC. Theoretical results concerning the problem formulation and control design for these systems are supported by experimental results on a SISO and MIMO flexible structure.

The analysis and design results of ILC for time-windowed systems are subsequently extended to the whole class of linear systems whose input and output are filtered with basis functions (which include time windows). Analysis and design theory of ILC for this class of systems reveals how different ILC objectives can be reached by design of separate parts of the ILC controller.

Our research on ILC for uncertain systems is divided into two parts. In the first part, we formulate an approach to analyze the robustness properties of existing

ILC controllers, using well developed μ theory. To exemplify our findings, we analyze the robustness properties of linear quadratic (LQ) norm optimal ILC controllers. Moreover, we show that the approach is applicable to the class of linear trial invariant ILC controlled systems with basis functions.

In the second part, we present a finite time interval robust ILC control strategy that is robust against model uncertainty as given by an additive uncertainty model. For that, we exploit $\mathcal{H}_\infty$ control theory, however, modified such that the controller is not restricted to be causal and operates on a finite time interval. Furthermore, we optimize the robust controller so as to optimize performance while remaining robustly monotonically convergent. By means of experiments on a SISO flexible system, we show that this control strategy can indeed outperform LQ norm optimal ILC and causal robust ILC control strategies.

Samenvatting

Iteratief Lerend Regelen (ILC) is een regel strategie die de prestaties van een batch repeterend systeem dramatisch kan verbeteren. Deze verbetering in prestatie wordt bereikt door bij het bepalen van een nieuw stuur signaal gebruik te maken van kennis (meetdata) van eerdere experimenten, oftewel, door te leren van eerdere ervaringen.

Dit proefschrift richt zich op ILC voor onzekere en tijd gewogen systemen. Met de term "tijd gewogen systeem" wordt een systeem bedoeld waarbij het aansturen en meten van het systeem op verschillende tijdsintervallen plaatsvindt. Met een "onzeker systeem" wordt een systeem bedoeld wiens gedrag door een onvolledig of onnauwkeurig model wordt beschreven.

Het voorbeeld van onderdrukking van rest trillingen in point-to-point bewegingen is gebruikt om de ontwerpaspecten van ILC voor tijd gewogen systemen te onderzoeken. De verschillende stappen in ILC voor point-to-point bewegingen zijn besproken: het formuleren van de vraagstelling, het afleiden van een tijd gewogen systeem beschrijving, het ontwerp van ILC regelaars, de analyse van het ILC geregelde systeem, en de implementatie van ILC voor point-to-point bewegingen op een SISO en MIMO systeem. Daarbij hebben we een nieuw ILC raamwerk geïntroduceerd, en bewezen dat er ontwerp vrijheid in ILC voor point-to-point bewegingen aanwezig is waarmee de amplitude van het stuursignaal geminimaliseerd kan worden.

De analyse en ontwerp resultaten van tijd gewogen ILC zijn vervolgens uitgebreid naar de klasse van lineaire systemen met in- en uitgangen die bewerkt kunnen zijn met basis functies. Een analyse en ontwerp theorie van ILC voor deze klasse van systemen heeft uitgewezen dat verschillende ILC doelstellingen kunnen worden bereikt door ontwerp van afzonderlijke delen van de ILC regelaar.

Het onderzoek naar ILC voor onzekere systemen bestaat uit twee delen. In het eerste deel zijn resultaten uit μ theorie gebruikt om robuuste monotone convergentie condities af te leiden voor lineaire, batch invariante ILC regelaars. Deze vindingen zijn toegelicht door de robuustheid eigenschappen van lineair kwadratische (LQ) norm optimale ILC regelaars te analyseren. Daarnaast is aangetoond

dat de behaalde resultaten ook toepasbaar zijn op de klasse van lineaire batch invariante ILC geregelde systemen met basis functies.

In het tweede deel is een robuuste regelstrategie ontworpen, die gebaseerd is op $\mathcal{H}_\infty$ theorie. Het robuuste synthese probleem is zo gedefinieerd, dat de gevonden regelaar niet causaal hoeft te zijn en opereert in het eindige tijdsinterval van een experiment. De ontworpen regelaar is vervolgens geoptimaliseerd om de prestaties te verbeteren terwijl robuuste monotone convergentie gegarandeerd blijft. Experimenten tonen aan dat de regelaar betere prestaties kan leveren dan LQ norm optimale ILC regelaars en causale robuuste regelaars.

Dankwoord

Met het schrijven van dit dankwoord komt het einde van mijn promotie in zicht. Terugkijkend op de afgelopen vier jaar, kan ik niet anders zeggen dan dat ik het zeer getroffen heb met mijn collega's. Alle mensen die deze vier jaar tot een waar genoegen hebben gemaakt, wil ik daarom ook erg bedanken.

Ten eerste wil ik Okko Bosgra bedanken voor de mogelijkheid die hij me heeft geboden om onder zijn leiding te promoveren. Het gemak waarmee jij tot de kern van een vraagstuk weet door te dringen, jouw scherpe opmerkingen, immense hoeveelheid parate kennis, en motiverende gesprekken in moeilijke perioden, zijn een drijvende kracht geweest achter mijn promotieonderzoek.

Ook wil ik Maarten Steinbuch bedanken voor zijn bijdrage aan het verfijnen van het proefschrift, en niet te vergeten, voor de vrijheid die hij mij geboden heeft om conferenties en summer schools bij te wonen. De ILC summer school in Logan, waar ik als student van jou naar toe mocht (als broekie tussen de goeroe's), heeft de basis gelegd voor mijn promotie op het gebied van ILC.

Verder heb ik het geluk gehad om tijdens mijn promotie Tijs Donkers en Michael Ronde te mogen begeleiden. Tijs, al ben jij mijn enige afstudeerder geweest, je hebt werk verzet voor twee. Daarnaast heeft jouw kritische en nuchtere houding een grote invloed gehad op de scherpte van de resultaten. Michael, de mooie resultaten die jij in de korte periode van jouw stage hebt behaald, zijn de puntjes op de i.

Natuurlijk wil ik ook alle DCT collega's bedanken voor jullie hulp en gezelligheid, zowel tijdens werktijd als daarbuiten.

Oh ja, en mijn kamergenoten ook bedankt.

Oke, zonder gekheid, ik heb het getroffen met mijn roomie's Matthijs Boerlage, Michiel Koot, Maurice Schneiders, Dennis van Raaij, Chris Criens, Kira Barton, Schnautzie, en zo-goed-als roomie Tom Oomen. Het was mij een waar genoegen om jullie als sparring partners te hebben, maar ook als gesprekspartners over de minder serieuze zaken des levens. De gezellige afleiding op zijn tijd heeft mijn

promotie goed gedaan. Kira, it has been a pleasure working with you.

Buiten de werkkring wil ik ten eerste mijn vrienden bedanken. De avonden stappen, de filmpjes, spellen, festivals, gezamenlijke vakanties, maar ook serieuze gesprekken, hebben me de broodnodige afleiding gegeven.

Ook ben ik mijn familie erg dankbaar voor hun getoonde interesse in mijn werk. In het bijzonder wil ik papa en mama bedanken voor hun onvoorwaardelijk steun. Zonder jullie zou ik nooit zo ver gekomen zijn. En Sander, je kan zo veel ontkennen als je wilt, ik kan me geen betere broer voorstellen. Thanks voor de morele steun en vertrouwen.

En tenslotte, mijn liefdevolle dank aan Suzanne. Bij tegenslagen vind ik bij jou een luisterend oor, bij doorbraken kan ik mijn vreugde met jou delen. Thuiskomen bij jou geeft me de rust die ik tijdens mijn promotie soms zo hard nodig had. Suuz, dank je wel voor alles!

Jeroen van de Wijdeven
September, 2008

Curriculum Vitae

November 21, 1977	Born in Veghel, The Netherlands
1990-1996	Secondary school (VWO), Kandinsky college in Nijmegen (*Cum Laude*)
1996-2004	MSc study Mechanical Engineering at Eindhoven University of Technology (*Cum Laude*)
	Master's project: "*Shape change of tensegrity structures*" at Eindhoven University of Technology Internship: "*Pulse Width Pulse Amplitude Control of systems with Coulomb friction and viscous damping*" at University at Buffalo, Buffalo NY USA
2004-2008	PhD student Mechanical Engineering at Eindhoven University of Technology, in the Control Systems Technology group.
	The PhD research focussed on analysis and design issues in Iterative Learning Control for uncertain and time-windowed systems.